Study and Application of Intelligent Control to Power System Scheduling

Thesis Submitted by

JAGAT KISHORE PATTANAIK

Doctor of Philosophy (Engineering)

Department of Power Engineering
Faculty Council of Engineering & Technology
Jadavpur University
Kolkata- India
2018

CERTIFICATE FROM THE SUPERVISORS

This is to certify that the thesis entitled "***Study and Application of Intelligent Control to Power System Scheduling***" submitted by Shri **Jagat Kishore Pattanaik** who got his name registered on 2012 for the award of Ph. D. (Engineering) degree of Jadavpur University is absolutely based upon his own work under the supervision of Prof.(Dr.) Mousumi Basu and Prof.(Dr.) Deba Prasad Dash and that neither his thesis nor any part of the thesis has been submitted for any degree or any other academic award anywhere before.

Prof.(Dr.) Mousumi Basu
Department of Power Engineering
Jadavpur University, Kolkata – 700 098

Prof.(Dr.) Deba Prasad Dash
Department of Electrical Engineering
Government College of Engineering,
Kalahandi, Odisha – 766002

JADAVPUR UNIVERSITY

KOLKATA- 700032, INDIA

INDEX NO. 85/12/E

1. **Title of the Thesis:** Study and Application of Intelligent Control to Power System Scheduling.

2. **Name , Designation & Institutions of the Supervisors:**
   (I) Prof.(Dr.) Mousumi Basu, Professor, Department of Power Engineering, Jadavpur University, Salt Lake Campus, Kolkata-700098.
   (II) Prof.(Dr.) Deba Prasad Dash, Associate Professor & Head, Department of Electrical Engineering, Government College of Engineering, Kalahandi, Odisha-766002, India.

3. **List of Publication:**

Research Article:

1. **Jagat Kishore Pattanaik**, Mousumi Basu, Deba Prasad Dash, "Improved Real Coded Genetic Algorithm for Dynamic Economic Dispatch", Journal of Electrical Systems and Information Technology, Volume-5, Issue-3, December 2018, pp-349-362, **ELSEVIER PUBLISHER.**

2. **Jagat Kishore Pattanaik**, Mousumi Basu, Deba Prasad Dash, "Modified Teaching-Learning-Based Optimization for Combined Heat and Power Economic Dispatch", International Journal of Emerging Electric Power Systems, Volume-18, Issue-5, October 2017, **DE-GRUYTER PUBLISHER.**

3. **Jagat Kishore Pattanaik**, Mousumi Basu, Deba Prasad Dash, "Opposition-based Differential Evolution for Hydrothermal Power System", Protection and Control of Modern Power System, Volume-2, 2017, **SPRINGER PUBLISHER.**

4. **Jagat Kishore Pattanaik**, Mousumi Basu, Deba Prasad Dash, "Review on Application and Comparison of Metaheuristic Techniques to Multi-area Economic Dispatch Problem", Protection and Control of Modern Power System, Volume-2, 2017, **SPRINGER PUBLISHER.**

5. **Jagat Kishore Pattanaik**, Mousumi Basu, Deba Prasad Dash, "Dynamic Economic Dispatch: A Comparative Study for Differential Evolution, Particle Swarm Optimization, Evolutionary Programming, Genetic Algorithm and Simulated Annealing" **accepted for publication in the Journal of Electrical Systems and Information Technology, ELSEVIER PUBLISHER.**

6. D. P. Dash, S. Das, **J. Pattanaik**, "Multiarea Environmental Dispatch with Emission Constraints using Hybrid Intelligence Algorithm", International Journal of Engineering Research and Development, Volume-10, Issue-6, Jan2014, pp-52-59.

Under Review:

1. **Jagat Kishore Pattanaik**, Mousumi Basu, Deba Prasad Dash, "Heat transfer search algorithm for Combined Heat and Power Economic Dispatch" under review in the Electric Power Components and Systems, Taylor & Francis Publisher.

2. **Jagat Kishore Pattanaik**, Mousumi Basu, Deba Prasad Dash, "Improved Real Coded Genetic Algorithm for fixed head hydrothermal power system" under review in the IETE Journal of Research, Taylor & Francis Publisher.

3. **Jagat Kishore Pattanaik**, Mousumi Basu, Deba Prasad Dash, "Improved Real Coded Genetic Algorithm for Reactive Power Dispatch" under review in the IETE Journal of Research, Taylor & Francis Publisher.

4. **Jagat Kishore Pattanaik**, Mousumi Basu, Deba Prasad Dash, "Quasi-oppositional differential evolution for solution of optimal power flow" under review in the Journal of Electrical Systems and Information Technology, Elsevier Publisher.

5. **Jagat Kishore Pattanaik**, Mousumi Basu, Deba Prasad Dash, "Heat transfer search algorithm for solution of optimal power flow problems" under review in the International Journal of Electrical Power and Energy Systems, Elsevier Publisher.

4. List of Patents: Nil

5. List of Presentations in International Conferences:

1. **Jagat Kishore Pattanaik**, Mousumi Basu, Deba Prasad Dash, "Optimal Power Flow with FACTS Devices using Artificial Immune Systems", **2017 IEEE International Conference on Technological Advancements in Power and Energy (TAP Energy)**, Pages.1-6, 2017.

2. D. P. Dash, M. Basu, **J. Pattanaik** "A New Approach for Dynamic Economic Dispatch Using Improved Bacterial Foraging Algorithm**", 2012 IEEE International Conference on Communications, Devices and Intelligent Systems (CODIS)**, Pages.330-332, 2012.

DECLARATION

I, Shri Jagat Kishore Pattanaik, hereby certify that the work "**Study and Application of Intelligent Control to Power System Scheduling**" submitted by me to Jadavpur University, Kolkata, India for the award of Doctor of Philosophy (Engineering) degree, has not been submitted previously in this university or any other University for the degree of Ph. D./D.Litt./D.Sc.

Jagat Kishore Pattanaik

ACKNOWLEDGEMENTS

It is a pleasant task to express my gratitude to all those who have accompanied and helped me in my project work.

First and foremost, I really take this opportunity to express my deep sense of gratitude to my guide, **Prof. Mousumi Basu**, Department of Power Engineering, Jadavpur University, Kolkata for her invaluable guidance, suggestions and encouragement throughout the project, which helped me a lot to improve this project work. It has been very nice to be under her guidance. His appreciation during the good times has been boosting my morals and confidence.

I am also thankful to my co-guide **Prof. Deba Prasad Dash,** Department of Electrical Engineering, Government College of Engineering, Kalahandi, Odisha for his guidance, encouragement and valuable suggestions in the course of this work.

I am also indebted to Head and all staffs of department of Power Engineering, Jadavpur University, for his kind help during this project work. And I am also thankful to Dean Faculty of Engineering and Technology for their kind help and co-operation during this project work.

I would also like to convey my gratitude to my wife **Mrs. Prerana Pattanaik,** for her valuable suggestions and co-operation for completion of this thesis work.

Last, but not the least, I would like to thank my batch-mates and my parents who have directly or indirectly helped me in this work.

Jagat Kishore Pattanaik
Jadavpur University
Kolkata-700032

Abbreviations and Notations

Symbol	Description
P_{it}:	real power output of i th unit during time interval t
$\mathrm{P}_i^{\min}$, $\mathrm{P}_i^{\max}$:	lower and upper generation limits of i th unit
P_{Dt}:	load demand at the time interval t
P_{Lt}:	transmission line losses at time t
a_i, b_i, c_i, d_i, e_i:	cost coefficients of i th unit
$F_{it}(\mathrm{P}_{it})$:	cost of producing real power output P_{it} at time t
UR_i, DR_i:	ramp-up and ramp-down rate limits of the i th generator
N:	number of generating units
T:	number of intervals in the scheduled horizon
P_{ti}:	power output of i th conventional thermal generating unit
$\mathrm{P}_{ti}^{\min}$, $\mathrm{P}_{ti}^{\max}$:	lower and upper power capacity limits of i th conventional thermal generating unit .
P_{ci}, H_{ci}:	power output and heat output of i th cogeneration unit.
H_{hi}:	heat output of i th heat-only unit
$\mathrm{H}_{hi}^{\min}$, $\mathrm{H}_{hi}^{\max}$:	lower and upper heat production limits of the i th heat-only unit
C_{T} :	total production cost
C_{ti}, C_{ci}, C_{hi}:	fuel cost characteristics of the conventional thermal generating unit, cogeneration unit and heat-only unit respectively
a_i, b_i, d_i, e_i, f_i:	cost coefficients of i th conventional thermal generating unit
$\alpha_i, \beta_i, \gamma_i, \delta_i, \varepsilon_i, \xi_i$:	cost coefficients of i th cogeneration unit
$\varphi_i, \eta_i, \lambda_i$:	cost coefficients of i th heat-only unit
H_D:	system heat demand
P_D:	system power demand
P_L:	transmission loss
N_t, N_c, N_h:	numbers of conventional thermal generating units, cogeneration units and heat-only units respectively
a_{si}, b_{si}, c_{si}, d_{si}, e_{si}:	cost curve coefficients of i th thermal unit

P_{sim}:	power output of i th thermal generator during subinterval m
$P_{si}^{\min}$, $P_{si}^{\max}$:	lower and upper generation limits for i th thermal unit
t_m:	duration of subinterval m.
P_{hjm}:	power output of j th hydro unit during subinterval m
P_{Dm}:	load demand during subinterval m
P_{Lm}:	transmission loss during subinterval m
B_{lr}:	loss formula coefficients.
a_{0hj}, a_{1hj}, and a_{2hj}:	coefficients for water discharge rate function of j th hydro generator
W_{hj}:	prespecified volume of water available for generation by j th hydro unit during the scheduling period.
$P_{hj}^{\min}$, $P_{hj}^{\max}$:	lower and upper generation limits for j th hydro unit
P_{sit}:	output power of i th thermal unit at time t
P_{Dt}:	load demand at time t
P_{Lt}:	transmission loss at time t
P_{hjt}:	output power of j th hydro unit at time t
C_{1j}, C_{2j}, C_{3j}, C_{4j}, C_{5j}, C_{6j}:	power generation coefficients of j th hydro unit
Q_{hjt}:	water discharge rate of j th reservoir at time t
V_{hjt}:	storage volume of j th reservoir at time t
$Q_{hj}^{\min}$, $Q_{hj}^{\max}$:	minimum and maximum water discharge rate of j th reservoir
$Q_{hj,k}^{L}$, $Q_{hj,k}^{U}$:	lower and upper bounds of k th prohibited zones of hydro unit j
$V_{hj}^{\min}$, $V_{hj}^{\max}$:	minimum and maximum storage volume of j th reservoir
I_{hjt}:	inflow rate of j th reservoir at time t
R_{uj}:	number of upstream units directly above j th hydro plant
S_{hjt}:	spillage of j th reservoir at time t
τ_{lj}:	water transport delay from reservoir l to j
t, T:	time index and scheduling period
N_s:	number of thermal generating units
N_h:	number of hydro generating units
n_j:	number of prohibited zones for hydro unit j
k:	index of prohibited zones of a hydro unit

EXECUTIVE SUMMARY

The present work is the study and application of intelligent control to power system scheduling. Here, the work focuses on different optimization techniques for power system scheduling. Intelligent control such as evolutionary algorithm, differential evolution, evolutionary programming, genetic algorithm, artificial immune system, simulated annealing, teaching learning based optimization, modified teaching learning based optimization , quasi oppositional differential algorithm ,heat transfer search algorithm are used to optimize the power system for economic dispatch, dynamic economic dispatch, multi area economic dispatch, reactive power dispatch, combined heat and power economic dispatch and hydrothermal system etc. Also the study carried out on optimal scheduling of generation for fixed and variable head hydrothermal system using both opposition-based differential evolution and heat transfer search algorithm. The proposed method is validated by applying it to two test problems, two fixed head hydrothermal test systems and three hydrothermal multi-reservoir cascaded hydroelectric test systems having prohibited operating zones and thermal units with valve point loading. The modified teaching learning based optimization method has been applied to solve the non-smooth/non-convex combined heat and power economic dispatch problem. Here modified teaching-learning-based optimization where gaussian random variables are introduced in the 'Teacher phase' and 'Learner phase' which improves search efficiency and guarantees a high probability of obtaining the global optimum without significantly impairing the speed of convergence and the simplicity of the structure of teaching learning based optimization. Also the present work describes on optimal power flow (OPF) which optimizes the fuel, emission minimization, reduction of voltage deviation and improvement of voltage stability. The effectiveness of the proposed algorithm for OPF is tested on IEEE 30-bus, 57-bus and 118-bus test systems for four objective problems. Different test systems are used for the above intelligent techniques for optimization of power system. Here two different optimization technique like heat transfer search and quasi-oppositional differential evolution has been applied to solve optimal power flow problem. Test results obtained from the proposed algorithm for three different test systems are compared with other optimization techniques suggested in literature.

Table of Contents

CHAPTER 1

Introduction

1.1. General Introduction

The word “scheduling” means “to plan”, “to arrange”, “to organize”, or “to take place” at a particular time. Power system scheduling is an important aspect both from the economic and environmental safety viewpoints. The scheduling involves decisions with regards to the units start-up and shut-down times and to the assignment of the load demands to the committed generating units for minimizing the system operation costs and the emission of atmospheric pollutants. As many other real-world engineering problems, power system generation scheduling involves multiple, conflicting optimization criteria for which there exists no single best solution with respect to all criteria considered. Mathematical optimization methods have been used over the years for many power systems planning, operation, and control problems. Mathematical formulations of real-world problems are derived under certain assumptions and even with these assumptions; the solution of large-scale power systems is not simple. On the other hand, there are many uncertainties in power system problems because power systems are large, complex, and geographically widely distributed. An optimization problem is a mathematical model where main objective is to minimize undesirable things i.e. cost, energy loss, errors, etc. or maximize desirable things i.e. profit, quality, efficiency, etc. subject to some constraints.

To handle complex power system problems, researchers have been looking into nature for years both as model and as metaphor for inspiration. Optimization is at the heart of many natural processes like Darwinian evolution itself. Through millions of years, everyone had to adapt physical structure to fit to the environment. A keen observation of the underlying relation between optimization and biological evolution led to the development of an important paradigm of computational intelligence known as evolutionary computing techniques for performing very complex search and optimization.

Evolutionary programming (EP) was introduced by Lawrence J.Fogel in the USA, while almost simultaneously I. Rechenberg and H.-P. Schwefel introduced evolution strategies (ESs) in Germany. Almost a decade later, John Henry Holland from University of Michigan, devised an independent method of simulating the Darwinian evolution to solve practical optimization problems and called it the genetic algorithm (GA). These areas developed separately for about 15 years. From the early 1990s on they are unified as different representatives of one technology, called evolutionary computing. Since the mid-eighties several multi-objective EAs have been developed and capable of searching for multiple pareto-optimal solutions concurrently in a single run. After the first studies on evolutionary multi-objective optimization in the mid-eighties, a number of Pareto-based techniques were proposed in 1993 and 1994, e.g., multi-objective genetic algorithm, niched pareto genetic algorithm and non-dominated sorting genetic algorithm which demonstrated the capability of EMO algorithms to approximate the set of optimal trade-offs in a single optimization run. These approaches did not incorporate elitism explicitly, but a few years later the importance of this concept in multi-objective search was recognized and supported experimentally. A couple of elitist multi-objective evolutionary algorithms were presented at this time, e.g., strength pareto evolutionary algorithm and pareto archived evolution strategy. Strength pareto evolutionary algorithm2 is developed later which outperforms. It provides good performance in terms of convergence and diversity. In artificial intelligence, an Evolutionary Algorithm (EA) is a subset of evolutionary computation i.e. generic population-based metaheuristic optimization algorithm. An EA uses mechanisms inspired by biological evolution, such as reproduction, mutation, recombination, and selection. Evolutionary algorithms often perform well approximating solutions to all types of problems because they ideally do not make any assumption about the underlying fitness landscape. Techniques from evolutionary algorithms applied to the modeling of biological evolution are generally limited to explorations of micro-evolutionary processes and planning models based upon cellular processes. In most real applications of EAs, computational complexity is a prohibiting factor. In fact, this computational complexity is due to fitness function evaluation. Fitness approximation is one of the solutions to overcome this difficulty. EA can solve many complex problems of Artificial Intelligence system.

The immune system of vertebrates including human is composed of cells, molecules and organs in the body which protect the body against infectious diseases caused by foreign pathogens such

as viruses, bacteria, etc. To perform these functions, the immune system has to be able to distinguish between the body's own cells as the self cells and foreign pathogens as the non-self cells or antigens. After distinguishing between self and non-self cells, the immune system has to perform an immune response in order to eliminate non-self cell or antigen. Antigens are further categorized in order to activate the suitable defense mechanism and at the same time, the immune system also developed a memory to enable more efficient responses in case of further infection by the similar antigen. Artificial immune system (AIS) mimics these biological principles of clone generation, proliferation and maturation. The main steps of AIS based on clonal selection principle are activation of antibodies, proliferation and differentiation on the encounter of cells with antigens, maturation by carrying out affinity maturation process, eliminating old antibodies to maintain the diversity of antibodies and to avoid premature convergence, selection of those antibodies whose affinities with the antigen are greater. In order to emulate AIS in optimization, the antibodies and affinity are taken as the feasible solutions and the objective function respectively.

Economic dispatch is an important optimization task in power system operation for allocating generation among the committed units. Its objective is to minimize the total generation cost of units, while satisfying the various physical constraints. Static economic dispatch (SED) allocates the load demand for a given interval of time among the committed generating units economically while fulfilling various constraints. Dynamic economic dispatch (DED) which is an extension of static economic dispatch, determines the optimal sharing of time varying load demand among the committed units. Power plant operators try to keep gradients for temperature and pressure inside the boiler and turbine within safe limits to avoid shortening the life of the equipment. This mechanical constraint imposes limit on the rate of increase or decrease of the electrical power output. This limit is called ramp rate limit which differentiates DED from SED problem. Thus, in DED, the dispatch decision at one time period affects those at later time periods. DED is the most accurate formulation of the economic dispatch problem but it is the most difficult to solve because of its large dimensionality. Here improved real coded genetic algorithm (IRCGA) has been developed for solving dynamic economic dispatch problem with non-smooth fuel cost function in view of one-to-one competition to boost convergence speed and solution quality.

Multi-area economic dispatch (MAED) is an extension of economic dispatch. MAED determines the generation level and interchange power between areas such that total fuel cost in all areas is minimized while satisfying power balance constraints, generating limits constraints and tie-line capacity constraints.

Non-linear optimization methods, such as dual and quadratic programming and gradient descent approaches, such as Lagrangian relaxation, have been applied for solving combined heat and power economic dispatch (CHPED). However, these methods cannot handle non-convex fuel cost functions of the generating units. The advent of teaching-learning-based optimization (TLBO), a teaching-learning process where Gaussian random variables are introduced in the 'Teacher phase' and 'Learner phase' which improves search efficiency and guarantees a high probability of obtaining the global optimum without significantly impairing the speed of convergence and the simplicity of the structure of TLBO.

Optimal scheduling of power plant generation is of great importance to electric utility systems. Because of insignificant marginal cost of hydroelectric power, the problem of minimizing the operational cost of hydrothermal system essentially reduces to that of minimizing the fuel cost of thermal plants under the various constraints on the hydraulic, thermal and power system network. Here, opposition-based differential evolution (ODE) for optimal scheduling of generation in a hydrothermal system have been applied to optimize the operational cost of hydrothermal system.

Reactive power dispatch (RPD) minimizes active power transmission loss and perks up voltage profile and voltage stability by adjusting control variables such as generator voltages, transformer tap settings, reactive power output of shunt VAR compensators etc. at the same time satisfying several equality and inequality constraints.

Optimal power flow (OPF) is an important tool for power system operators both in power system planning and operation for many years. The OPF minimizes the power system operating objective problems like fuel cost minimization, emission minimization, voltage deviation minimization and enhancement of voltage stability while satisfying a set of equality and inequality constraints. The equality constraints are power flow equations and inequality constraints are the limits on control variables and functional operating constraints. Here two different intelligent methods i.e. heat transfer search algorithm and quasi oppositional differential evolution have been applied to solve optimal power flow problems.

1.2. Literature Survey

Evolutionary algorithms (EA) [1]-[2] are search algorithms based on the simulated evolutionary process of natural selection and genetics. Genetic algorithm (GA) [3] belongs to a class of evolutionary computation techniques [4]-[5] based on models of biological evolution. The main difficulty of GA is its binary representation which arises when dealing with continuous search space with large dimensions. Evolutionary Programming (EP) [4] is a technique in the field of evolutionary computation. It seeks the optimal solution by evolving a population of candidate solutions over a number of generations or iterations. Differential evolution (DE) is a very simple and robust method originally proposed by Price and Stron [5] for optimization problem over a continuous domain. The basic idea of DE is to adapt the search during the evolutionary process. At the start of the evolution, the perturbations are large since parent populations are far away from each other. Simulated annealing [6] is a powerful optimization technique which exploits the resemblance between a minimization process and the cooling of molten metal. The physical annealing process is simulated in the simulated annealing (SA) technique for the determination of global or near-global optimum solutions for optimization problems.

Economic dispatch (ED) is one of the important optimization problems in power system operation. ED allocates the load demand among the committed generators most economically while satisfying the physical and operational constraints in a single area. The economic dispatch problem is frequently solved without considering transmission constraints. However, some researchers have taken transmission capacity constraints into account. Shoults et al. [7] solved economic dispatch problem considering import and export constraints between areas. This study provides a complete formulation of multi-area generation scheduling, and a framework for multi-area studies. Romano et al. [8] presented the Dantzig–Wolfe decomposition principle to the constrained economic dispatch of multi-area systems. An application of linear programming to transmission constrained production cost analysis was proposed in [9]. Helmick et al. [10] solved multi-area economic dispatch with area control error. Wang and Shahidehpour [11] proposed a decomposition approach for solving multi-area generation scheduling with tie-line constraints using expert systems. Network flow models for solving the multi-area economic dispatch problem with transmission constraints have been proposed by Streiffert [12]. An algorithm for multi-area economic dispatch and calculation of short range margin cost based prices has been

presented by Wernerus and Soder [13], where the multi-area economic dispatch problem was solved via Newton–Raphson's method. Yalcinoz and Short [14] solved multi-area economic dispatch problems by using Hopfield neural network approach. Jayabarathi et al. [15] solved multi-area economic dispatch problems with tie line constraints using evolutionary programming. The direct search method for solving economic dispatch problem considering transmission capacity constraints was presented in Ref. [16]. Since generators are practically supplied with multi-fuel sources by Chiang [17]. Evolutionary Programming (EP) [18] is a technique in the field of evolutionary computation. It seeks the optimal solution by evolving a population of candidate solutions over a number of generations or iterations. Gaing[19] defines the modified generator data and each area consists of three generators with prohibited operating zones. The initial temperature of SA algorithm has been determined by using the procedures described by Wong and Fung [20].

Static economic dispatch (SED) allocates the load demand for a given interval of time among the committed generating units economically while fulfilling various constraints. Dynamic economic dispatch (DED) which is an extension of static economic dispatch, determines the optimal sharing of time varying load demand among the committed units. DED is the most accurate formulation of the economic dispatch problem but it is the most difficult to solve because of its large dimensionality. Since the DED was introduced, several classical methods [23]–[28] have been employed for solving this problem. Yao et al. defines the evolutionary programming and have been pertained for solving 15 benchmark functions [29]. However, all of these methods may not be able to find an optimal solution and usually stuck at a local optimum solution. Classical calculus-based methods address DED problem with convex cost function. But in reality large steam turbines have a number of steam admission valves, which contribute nonconvexity in the fuel cost function of the generating units. Dynamic programming (DP) can solve such type of problems but it suffers from the curse of dimensionality. Recently, stochastic search algorithms such as simulated annealing (SA) [30], tabu search [31], differential evolution (DE) [32] have been successfully used to solve dynamic economic dispatch problem due to their ability to find the near global solution of a nonconvex optimization problem. Recently, stochastic search algorithms such as differential evolution (DE) [32],[35], harmony search algorithm [33], particle swarm optimization (PSO) [34] have been successfully used to solve dynamic economic dispatch problem due to their ability to find the near global solution of a nonconvex optimization

problem. Due to difficulties of binary representation when dealing with continuous search space with large dimensions, real-coded genetic algorithm (RCGA) [36]-[37] has been employed. The Simulated Binary Crossover (SBX) and polynomial mutation have been applied in this work.

Non-linear classical optimization methods, such as quadratic programming [38], Lagrangian relaxation [39] and semi-definite programming approach [40] have been pertained to solve combined heat and power economic dispatch (CHPED). However, these methods cannot handle non-convex fuel cost function of the conventional thermal generating units. The foreword of heuristic search algorithms has given alternative approaches for solving CHPED problem. Improved ant colony search algorithm [41], evolutionary programming [42], genetic algorithm [43], harmonic search algorithm [44]-[45], multi-objective particle swarm optimization [46], self adaptive real-coded genetic algorithm [47], novel selective particle swarm optimization [48], mesh adaptive direct search algorithm [49], particle swarm optimization with time varying acceleration coefficients [50] and oppositional teaching learning based optimization [51] have been pertained for solving CHPED problem. Teaching-learning-based optimization (TLBO), a teaching-learning process inspired algorithm recently proposed by Rao et al. [52], [53] and Rao and Patel [54] is based on the effect of influence of a teacher on the output of learners in a class. It is a population-based method and does not require any algorithm-specific control parameters. The main advantage of TLBO is that it requires only common controlling parameters like population size and number of generations for its working. Javadi, et al. [55] define the harmonic search algorithm (HS) have been proposed for solving the CHPED problem. The improved HS methods have obtained better solution quality than the original one. However, the convergence characteristic of the HS has revealed that the method is still slow for obtaining optimal solution. Many meta-heuristic and artificial intelligent algorithms like genetic algorithm (GA) [56], opposition-based group search optimization (OGSO) [57], group search optimization (GSO) [58], cuckoo search algorithm (CSA) [59], integrated civilized swarm optimization (CSO) and Powell's pattern search (PPS) method [60] have been used for solving the CHPED problem.

Very recently, V. K. Patel and V. J. Savsani has pioneered heat transfer search (HTS) algorithm [61], based on the edict of thermodynamics and heat transfer. The searching procedure of HTS mulls over three components namely 'conduction phase', 'convection phase' and 'radiation phase'. The HTS algorithm imitates the thermal balance manners of any system. The HTS algorithm replicates the thermal equilibrium behavior of any system. The thermal equilibrium

can be achieved when molecules of the system, transfer heat in the form of conduction, convection and radiation. Each phase of the proposed algorithm is executed with equal probability during an entire search process. The search processes of all three phases are calculated in such a manner that during the first half each phase explores search space while in the second half each phase exploits the search space. The feasible operating regions of a conventional thermal generator with prohibited operating zones define by Pereira-Neto et al. [62].

Optimal scheduling of power plant generation is of great importance to electric utility systems. Because of insignificant marginal cost of hydroelectric power, the problem of minimizing the operational cost of hydrothermal system essentially reduces to that of minimizing the fuel cost of thermal plants under the various constraints on the hydraulic, thermal and power system network. The hydrothermal scheduling problem has been the subject of investigation for several decades. Several classical methods such as Newton's method [63], mixed integer programming [65], [79] dynamic programming (DP) [66], etc. have been widely used to solve hydrothermal scheduling problem. Among these methods, DP appears to be the most popular. However, major disadvantages of DP method are computational and dimensional requirements which grow drastically with increasing system size and planning horizon. Recently, stochastic search algorithms such as simulated annealing (SA) [67], evolutionary programming (EP) [68], genetic algorithm (GA) [69]-[70], evolutionary programming technique [71], differential evolution (DE) [72]-[74], particle swarm optimization [75], artificial immune system [76], clonal selection algorithm [77] and teaching learning based optimization [78] have been successfully used to solve hydrothermal scheduling problem. Since the mid 1990s, many techniques originated from Darwin's natural evolution theory have emerged. These techniques are usually termed by "evolutionary computation methods" including evolutionary algorithms (EAs), swarm intelligence and artificial immune system. Differential evolution (DE) [80]-[82], a relatively new member in the family of evolutionary algorithms, first proposed over 1995-1997 by Storn and Price at Berkeley is a novel approach to numerical optimization. It is a population-based stochastic parallel search evolutionary algorithm which is very simple yet powerful. Price and Storn describe the technique of differential evolution in optimizing the hydrothermal system. The main advantages of DE are its capability of solving optimization problems which require minimization process with nonlinear, non-differentiable and multi-modal objective functions.

Oppositional based learning (OBL) was first utilized to improve learning and back propagation in neural networks and since then, it has been applied to many EAs such as particle swarm optimization define by Wang et al [83]. The basic concept of opposition-based learning [84]-[86] was originally introduced by Tizhoosh. The main idea behind OBL is for finding a better candidate solution and the simultaneous consideration of an estimate and its corresponding opposite estimate (i.e., guess and opposite guess) which is closer to the global optimum. OBL was first utilized to improve learning and back propagation in neural networks by Ventresca and Tizhoosh [87], and since then, it has been applied to many EAs, such as differential evolution [88] and ant colony optimization [89]. Opposition-based harmony search algorithm [90] has been applied to solve combined economic and emission dispatch problems. In [91] oppositional real coded chemical reaction optimization has been used for solving economic dispatch problems. Opposition-based gravitational search algorithm has been applied for solving reactive power dispatch problem. The maximization and minimization problem in optimizing fixed head hydrothermal system define by Michalewicz [92].

Reactive power dispatch (RPD) perks up power system economy and security. Reactive power generation has no production cost but in general it has an effect on the production cost related with active power transmission loss. RPD minimizes active power transmission loss and perks up voltage profile and voltage stability by adjusting control variables such as generator voltages, transformer tap settings, reactive power output of shunt VAR compensators etc. at the same time satisfying several equality and inequality constraints.A variety of classical optimization techniques [93]–[96] such as Newton method, linear programming, quadratic programming and interior point method have been pertained to solve RPD problem. RPD is a mixture of discrete and continuous variables with multiple local optima. So it is exigent to acquire global optima by using classical optimization techniques. In recent times nature-inspired metaheuristics such as quasi-oppositional differential evolution [97], evolutionary programming (EP) [98], novel teaching–learning-based optimization algorithm [99] quantum-inspired evolutionary algorithm (QEA) [100], comprehensive learning particle swarm optimization (CLPSO) [101], hybrid shuffled frog leaping algorithm (HSFLA) modified teaching learning algorithm and double differential evolution algorithm [102], and have been pertained to solve RPD problem. Voltage stability is the capacity of a power system to keep up suitable voltages at all bus bars beneath normal operating condition and even after disturbances such as change in load demand or system

configuration. In recent times a number of major network collapses [103] have been taken place due to voltage instability. Improvement of voltage stability has been acquired by minimizing voltage stability indicator define by Kessel and Glavitsch [104]. Multi-area dynamic economic dispatch (MADED) is an extension of multi-area static economic dispatch problem. It schedules the online generator outputs, and interchange power between areas with the predicted load demands over a certain period of time so as to operate an electric power system most economically. The algorithm is based on iterative method, proposed by Metropolis et al. [105], which simulates the transition of atoms in equilibrium at a given temperature

Optimal power flow (OPF) is an important tool for power system operators both in power system planning and operation for many years. The OPF minimizes the power system operating objective function while satisfying a set of equality and inequality constraints. The equality constraints are power flow equations and inequality constraints are the limits on control variables and functional operating constraints. The OPF is a highly non-linear, non-convex, large scale static optimization problem. Several optimization techniques have emerged so far and have been applied to solve OPF problem. Earlier, OPF algorithms were based on classical mathematics-based on differential evolution (QODE) [106], Gradient based method [107], quadratic programming (QP) [108], Newton-based method [109], linear programming (LP) [110], and interior point methods (IPMs) [111]-[112] have been successfully applied to solve OPF problems. The problem of OPF was originally formulated in 1962 by Carpentier [107] and he solved the OPF problem by using reduced gradient method. In the following years, a lot of research took place to improve the quality of OPF solution. These classical optimization techniques have been widely applied to varieties of OPF problems. However, these techniques fail to deal with systems having complex non-smooth, non-convex and non-differentiable objective functions and constraints. Due to tremendous improvement in capability of computers in recent years, evolutionary algorithms, such as genetic algorithm (GA) [112], evolutionary programming (EP) [113], particle swarm optimization (PSO) [114]-[115], simulated annealing (SA) [116], differential evolution (DE) [117], biogeography-based optimization (BBO) [118], faster evolutionary algorithm [119], particle swarm optimization (PSO) [120] have been applied for solving various complex OPF problems to overcome the drawbacks of classical techniques. Earlier, OPF algorithms were based on classical mathematics-based methods. Tinney and Hart describes the Newton-based method [121] was successfully applied to solve OPF problems.

The line data, bus data, generator data and the minimum and maximum limits for the control variables have been adapted from [122]. Due to tremendous improvement in capability of computers in recent years, evolutionary algorithms, such as improved evolutionary programming [123], enhanced genetic algorithm [124], differential evolution (DE) [125] and particle swarm optimization (PSO) [126] have been applied for solving various complex OPF problems to overcome the drawbacks of classical techniques. Yokoyama and Bae[127] defines the objective for comparison purposes i.e. the total emission of these pollutants which is the sum of a quadratic and an exponential function. For IEEE 57 test bus system, the system line data, bus data, generator data and the minimum and maximum limits for the control variables have been adapted from [128] and [130]. The upper and lower limits of reactive power sources and transformer tap settings are taken from [129]. To test optimal power flow, system line data, bus data, generator data and the minimum and maximum limits for the control variables have been adapted for IEEE 57-bus and for IEEE 118-bus test system the system line data, bus data, generator data and the minimum and maximum limits for the control variables have been adapted from [130]-[132].

1.3. Motivation behind the work

The valve-point loading, prohibited operating zones, ramp-rate limits and other constraints turn the decision space into disjoint subsets, transforming the most of the power system problems into difficult non-smooth, non-convex optimization problems. The calculus-based methods fail to address these types of problems. The dynamic programming method has no restrictions on the shape of the objective function and can solve these types of problems. However, this method suffers from the curse of dimensionality or local optimality. Modern Intelligent algorithms are promising alternatives for the solution of complex power system optimization problems. Keeping this in mind, this work mainly focuses on complex power system optimization by using various intelligent control methods.

1.4. Organization of Thesis

The layout of Thesis is as follows.

Chapter: 1

This chapter describes the general introduction to all intelligent control methods. Also it describes the Literature Survey and motivation towards this present work. It presents the earlier works done on different optimization technique like differential evolution, opposition based differential evolution, quasi-oppositional differential evolution, evolutionary algorithm, genetic algorithm, improved real coded genetic algorithm, simulated annealing, teaching-learning based optimization, modified teaching-learning based optimization, heat transfer search algorithm.

Chapter: 2

This chapter describes about different metaheuristic techniques like differential evolution, evolutionary programming, genetic algorithm, and simulated annealing and application of this metaheuristic techniques to multi-area economic dispatch problem (MAED). The proposed methods have been validated by application of three types of MAED problems i.e. test system 1: MAED with quadratic cost function prohibited operating zones and transmission losses, test system2: with valve point loading and test system3: with valve point loading multiple fuel sources and transmission losses.

Chapter: 3

This chapter describes about dynamic economic dispatch. Here improved real coded genetic algorithm (IRCGA) has been developed in view of one-to-one competition to boost convergence speed and solution quality. IRCGA has been pertained for solving dynamic economic dispatch problem with nonsmooth fuel cost function. Two test systems and 15 benchmark functions are exploited here. Test results are matched up to those acquired by real coded genetic algorithm (RCGA).

Chapter: 4

This chapter describes about combined heat and power economic dispatch (CHPED) problem. Also intelligent control methods like modified teachning learning based optimization and heat

transfer search algorithm have been applied to CHEPD problem and 15 benchmark functions. Test results are compared with those acquired by other evolutionary techniques.

Chapter: 5

This chapter describes about fixed-head hydrothermal system. Also it describes the application of opposition-based differential equation and improved real coded genetic algorithm to fixed head hydrothermal system.

Chapter: 6

This chapter describes about variable-head hydrothermal system. Also it describes the application of opposition-based differential equation to variable head hydrothermal system, multi-reservoir cascaded hydro plants having prohibited operating zones and thermal units with valve point loading.

Chapter: 7

This chapter describes about reactive power dispatch. Also in this study it describes application of improved real coded genetic algorithm to reactive power dispatch problem. The developed IRCGA and RCGA have been pertained to solve different types of RPD problems and three different test systems with three different objective functions and 15 benchmark functions.

Chapter: 8

This chapter describes about Optimal Power Flow problems. Two different intelligent control methods like, heat transfer search (HTS) algorithm and quasi-oppositional differential evolution (QODE) have been successfully applied to solve optimal power flow problems. The performance of the proposed algorithm has been assessed on IEEE 30-bus, 57-bus and 118-bus test systems to demonstrate its effectiveness.

At end of this thesis, conclusion form all chapters have been presented and future work also described. The references and appendices are included in the end of this thesis.

CHAPTER-2

Multi-area Economic Dispatch

2.1. Introduction:

Economic dispatch (ED) is one of the important optimization problems in power system operation. ED allocates the load demand among the committed generators most economically while satisfying the physical and operational constraints in a single area. Generally, the generators are divided into several generation areas interconnected by tie-lines. Multi-area economic dispatch (MAED) is an extension of economic dispatch. MAED determines the generation level and interchange power between areas such that total fuel cost in all areas is minimized while satisfying power balance constraints, generating limits constraints and tie-line capacity constraints.

With the emergence of metaheuristic techniques, attention has been gradually shifted to applications of such technology-based approaches to handle the complexity involved in real world problems. Metaheuristic techniques have been given much attention by many researchers due their ability to seek for the near global optimal solution.

Here four different metaheuristic techniques have been applied in the MAED problem to investigate the applicability of this technique. These are, differential evolution (DE), evolutionary programming (EP), genetic algorithm (GA), and simulated annealing (SA).

The proposed methods have been validated by application of three types of MAED problems. These are A) multi area economic dispatch with quadratic cost function prohibited operating zones and transmission losses (MAEDQCPOZTL) B) multi area economic dispatch with valve point loading (MAEDVPL) C) multi area economic dispatch with valve point loading multiple fuel sources and transmission losses (MAEDVPLMFTL).

The metaheuristic techniques are evaluated against three different test systems for comparison with each other.

2.2. Problem Formulation:

The objective of MAED is to minimize the total cost of supplying loads to all areas while satisfying power balance constraints, generating limits constraints and tie-line capacity constraints.

Three different types of MAED problems have been considered.

2.2.1. MAEDQCPOZTL

The objective function F_t, total cost of committed generators of all areas, of MAED problem may be written as

$$F_t = \sum_{i=1}^{\mathrm{N}} \sum_{j=1}^{\mathrm{M}_i} F_{ij}\left(\mathrm{P}_{ij}\right) = \sum_{i=1}^{\mathrm{N}} \sum_{j=1}^{\mathrm{M}_i} a_{ij} + b_{ij}\mathrm{P}_{ij} + c_{ij}\mathrm{P}_{ij}^2 \tag{2.1}$$

where $F_{ij}\left(\mathrm{P}_{ij}\right)$ is the cost function of jth generator in area i and is usually expressed as a quadratic polynomial; a_{ij}, b_{ij} and c_{ij} are the cost coefficients of jth generator in area i; N is the number of areas, M_i is the number of committed generators in area i; P_{ij} is the real power output of jth generator in area i. The MAED problem minimizes F_t subject to the following constraints.

2.2.1.1. Real power balance constraint:

$$\sum_{j=1}^{\mathrm{M}_i} \mathrm{P}_{ij} = \mathrm{P}_{Di} + \mathrm{P}_{Li} + \sum_{k,k\neq i} \mathrm{T}_{ik} \qquad i \in \mathrm{N} \tag{2.2}$$

The transmission loss P_{Li} of area i may be expressed by using B-coefficients as

$$\mathrm{P}_{Li} = \sum_{l=1}^{\mathrm{M}_i} \sum_{j=1}^{\mathrm{M}_i} \mathrm{P}_{ij}\mathrm{B}_{ilj}\mathrm{P}_{il} + \sum_{j=1}^{\mathrm{M}_i} \mathrm{B}_{0ij}\mathrm{P}_{ij} + \mathrm{B}_{00i} \tag{2.3}$$

Where P_{Di} is the real power demand of area i; T_{ik} is the tie line real power transfer from area i to area k. T_{ik} is positive when power flows from area i to area k and T_{ik} is negative when power flows from area k to area i.

2.2.1.2. Tie line capacity constraints

The tie line real power transfer T_{ik} from area i to area k should not exceed the tie line transfer capacity for security consideration.

$$-T_{ik}^{\max} \le T_{ik} \le T_{ik}^{\max} \tag{2.4}$$

where $T_{ik}^{\max}$ is the power flow limit from area i to area k and $-T_{ik}^{\max}$ is the power flow limit from area k to area i.

2.2.1.3. Real power generation capacity constraints

The real power generated by each generator should be within its lower limit $P_{ij}^{\min}$ and upper limit $P_{ij}^{\max}$, so that

$$P_{ij}^{\min} \le P_{ij} \le P_{ij}^{\max} \qquad i \in N \text{ and } j \in M_i \tag{2.5}$$

2.2.1.4. Prohibited Operating Zone

The prohibited operating zones are the range of power output of a generator where the operation causes undue vibration of the turbine shaft bearing caused by opening or closing of the steam valve. Normally operation is avoided in such regions. The feasible operating zones of unit can be described as follows:

$$P_{ij}^{\min} \le P_{ij} \le P_{ij,1}^{l}$$

$$P_{ij,m-1}^{u} \le P_{ij} \le P_{ij,m}^{l} \;\; ; \;\; m = 2,3,...,n_{ij} \tag{2.6}$$

$$P_{ij,n_{ij}}^{u} \le P_{ij} \le P_{ij}^{\max}$$

where m represents the number of prohibited operating zones of j the generator in area i. $\mathrm{P}^{u}_{ij,m-1}$ is the upper limit of $(m-1)$ th prohibited operating zone of j the generator in area i. $\mathrm{P}^{l}_{ij,m}$ is the lower limit of m th prohibited operating zone of j the generator in area i. Total number of prohibited operating zone of j the generator in area i is n_{ij}.

2.2.2. MAEDVPL

To model the effect of valve-points, a recurring rectified sinusoid contribution is added to the quadratic function [22]. The fuel cost function considering valve-point loadings of the generator is given as

$$F_t = \sum_{i=1}^{\mathrm{N}} \sum_{j=1}^{\mathrm{M}_i} F_{ij}\left(\mathrm{P}_{ij}\right) = \sum_{i=1}^{\mathrm{N}} \sum_{j=1}^{\mathrm{M}_i} a_{ij} + b_{ij}\mathrm{P}_{ij} + c_{ij}\mathrm{P}_{ij}^2 + \left| d_{ij} \times \sin\left\{ e_{ij} \times \left(\mathrm{P}_{ij}^{\min} - \mathrm{P}_{ij}\right)\right\}\right| \tag{2.7}$$

where d_{ij} and e_{ij} are cost coefficients of j th generator in area i due to valve-point effect. The objective of MAEDVPL is to minimize F_t subject to the constraints given in (2.2), (2.4) and (2.5). Here transmission loss (P_L) is not considered.

2.2.3. MAEDVPLMFTL

Since generators are practically supplied with multi-fuel sources [17], each generator should be represented with several piecewise quadratic functions superimposed sine terms reflecting the effect of fuel type changes and the generator must identify the most economical fuel to burn. The fuel cost function of the j th generator in area i with N_F fuel types considering valve-point loading is expressed as

$$F_{ij}\left(\mathrm{P}_{ij}\right) = a_{ijm} + b_{ijm}\mathrm{P}_{ij} + c_{ijm}\mathrm{P}_{ij}^2 + \left| d_{ijm} \times \sin\left\{ e_{ijm} \times \left(\mathrm{P}_{ijm}^{\min} - \mathrm{P}_{ij}\right)\right\}\right| \tag{2.8}$$

if $\mathrm{P}_{ijm}^{\min} \le \mathrm{P}_{ij} \le \mathrm{P}_{ijm}^{\max}$ for fuel type m and $m = 1,2,...,\mathrm{N}_F$

The objective function F_t is given by

$$F_t = \sum_{i=1}^{N} \sum_{j=1}^{M_i} F_{ij}\left(P_{ij}\right) \tag{2.9}$$

The objective function F_t is to be minimized subject to the constraints given in (2.2), (2.4) and (2.5).

2.3. Determination of Generation Level of slack generator

M_i committed generators in area i deliver their power output subject to the power balance constraint (2.2), tie line capacity constraints (2.4) and the respective generation capacity constraints (2.5). Assuming the power loading of first $(M_i - 1)$ generators are known, the power level of the M_i th generator (i.e. the slack generator) is given by

$$P_{iM_i} = P_{Di} + P_{Li} + \sum_{k,k\neq i} T_{ik} - \sum_{j=1}^{M_i-1} P_{ij} \tag{2.10}$$

The transmission loss P_{Li} is a function of all generator outputs including the slack generator and it is given by

$$P_{Li} = \sum_{l=1}^{M_i-1}\sum_{j=1}^{M_i-1} P_{ij} B_{ilj} P_{il} + 2P_{iM_i}\left(\sum_{j=1}^{M_i-1} B_{iM_i j} P_{ij}\right) + B_{iM_iM_i} P_{iM_i}^2 + \sum_{j=1}^{M_i-1} B_{0ij} P_{ij} + B_{0iM_i} P_{iM_i} + B_{00i} \tag{2.11}$$

Expanding and rearranging, equation (2.10) becomes

$$B_{iM_iM_i} P_{iM_i}^2 + \left(2\sum_{j=1}^{M_i-1} B_{iM_i j} P_{ij} + B_{0iM_i} - 1\right) P_{iM_i} + \left(P_{Di} + \sum_{k,k\neq i} T_{ik} + \sum_{j=1}^{M_i-1}\sum_{l=1}^{M_i-1} P_{ij} B_{ilj} P_{il} + \sum_{j=1}^{M_i-1} B_{0ij} P_{ij}\right.$$

$$\left. - \sum_{j=1}^{M_i-1} P_{ij} + B_{00i}\right) = 0 \tag{2.12}$$

The loading of the slack generator (i.e. M_i th) can then be found by solving equation (2.12) using standard algebraic method

2.4. Overview of Metaheuristic Techniques

Several metaheuristic techniques have evolved in recent past that facilitate to solve optimization problems which were previously difficult or impossible to solve. These techniques include evolutionary programming, differential evolution, genetic algorithm, simulated annealing, etc.

2.4.1. Evolutionary Programming

Evolutionary Programming (EP) [18] is a technique in the field of evolutionary computation. It seeks the optimal solution by evolving a population of candidate solutions over a number of generations or iterations. During each iteration, a second new population is formed from an existing population through the use of a mutation operator. This operator produces a new solution by perturbing each component of an existing solution by a random amount. The degree of optimality of each of the candidate solutions or individuals is measured by their fitness, which can be defined as a function of the objective function of the problem. Through the use of a competition scheme, the individuals in each population compete with each other. The winning individuals form a resultant population, which is regarded as the next generation. For optimization to occur, the competition scheme must be such that the more optimal solutions have a greater chance of survival than the poorer solutions. Through this the population evolves towards the global optimal point. The algorithm is described as follows:

i) Initialization: The initial population of control variables is selected randomly from the set of uniformly distributed control variables ranging over their upper and lower limits. The fitness score f_i is obtained according to the objective function and the environment.

ii) Statistics: The maximum fitness $f_{\max}$, minimum fitness $f_{\min}$, the sum of fitness $\sum f$, and average fitness f_{avg} of this generation are calculated.

iii) Mutation: Each selected parent, for example X_i, is mutated and added to its population with the following rule:

$$\mathrm{X}_{i+m,j} = \mathrm{X}_{ij} + N\left(0, \beta\left(\bar{x}_j - \underline{x}_j\right)\frac{f_i}{f_{\max}}\right), \qquad j \in n, i \in \mathrm{N_P} \tag{2.13}$$

where n is the number of decision variables in an individual, $\mathrm{N_P}$ is the population size, X_{ij} denotes the j th element of the i th individual; $N(\mu,\sigma^2)$ represents a Gaussian random variable with mean μ and variance σ^2; $f_{\max}$ is the maximum fitness of the old generation which is obtained in statistics; $\overline{x}_j$ and $\underline{x}_j$ are respectively maximum and minimum limits of the j th element; and β is the mutation scale, $0 < \beta \le 1$, that could be adaptively decreased during generations. If any mutated value exceeds its limit, it will be given the limit value. The mutation process allows an individual with larger fitness to produce more offspring for the next generation.

iv) Competition: Several individuals (k) which have the best fitness are kept as the parents for the next generation. Other individuals in the combined population of size ($2\mathrm{N_P} - k$) have to compete with each other to get their chances for the next generation. A weight value w_i of the i th individual is calculated by the following competition:

$$w_i = \sum_{t=1}^{\mathrm{N}_t} w_{i,t} \tag{2.14}$$

where N_t is the competition number generated randomly; $w_{i,t}$ is either 0 for loss or 1 for win as the i th individual competes with a randomly selected (r th) individual in the combined population. The value of $w_{i,t}$ is given in the following equation:

$$w_{i,t} = \begin{cases} 1 & \text{, if } f_i < f_r \\ 0 & \text{, otherwise} \end{cases} \tag{2.15}$$

where f_r is the fitness of randomly selected r th individuals, and f_i is the fitness of the i th individual. When all $2\mathrm{N_P}$ individuals, get their competition weights, they will be ranked in a descending order according to their corresponding value w_i. The first m individuals are selected along with their corresponding fitness f_i to be the bases for the next generation. The maximum, minimum and the average fitness and the sum of the fitness of the current generation are then calculated in the statistics.

v) Convergence test: If the convergence condition is not met, the mutation and competition will run again. The maximum generation number can be used for convergence condition. Other criteria, such as the ratio of the average and the maximum fitness of the population is computed and generations are repeated until

$$\{f_{avg} / f_{\max}\} \geq \delta \tag{2.16}$$

where δ should be very close to 1, which represents the degree of satisfaction. If the convergence has reached a given accuracy, an optimal solution has been found for an optimization problem.

2.4.2. Differential Evolution

Differential Evolution (DE) [82] is a type of evolutionary algorithm originally proposed by Price and Storn [5] for optimization problems over a continuous domain. DE is exceptionally simple, significantly faster and robust. The basic idea of DE is to adapt the search during the evolutionary process. At the start of the evolution, the perturbations are large since parent populations are far away from each other. As the evolutionary process matures, the population converges to a small region and the perturbations adaptively become small. As a result, the evolutionary algorithm performs a global exploratory search during the early stages of the evolutionary process and local exploitation during the mature stage of the search. In DE the fittest of an offspring competes one-to-one with that of corresponding parent which is different from other evolutionary algorithms. This one-to-one competition gives rise to faster convergence rate. Price and Storn gave the working principle of DE with simple strategy in [82]. Later on, they suggested ten different strategies of DE [5]. Strategy-7 (DE/rad/1/bin) is the most successful and widely used strategy. The key parameters of control in DE are population size ($\mathrm{N_P}$), scaling factor (F) and crossover constant (C_R). The optimization process in DE is carried out with three basic operations: mutation, crossover and selection. The DE algorithm is described as follows:

Initialization

The initial population of $\mathrm{N_P}$ vectors is randomly selected based on uniform probability distribution for all variables to cover the entire search uniformly. Each individual $\mathbf{X}_i$ is a vector that contains as many parameters as the problem decision variables D. Random values are assigned to each decision parameter in every vector according to:

$$\mathrm{X}_{ij}^{0} \sim U\left(\mathrm{X}_{j}^{\min}, \mathrm{X}_{j}^{\max}\right) \tag{2.17}$$

where $i = 1, \ldots, \mathrm{N_P}$ and $j = 1, \ldots, D$; $\mathrm{X}_{j}^{\min}$ and $\mathrm{X}_{j}^{\max}$ are the lower and upper bounds of the j th decision variable; $U\left(\mathrm{X}_{j}^{\min}, \mathrm{X}_{j}^{\max}\right)$ denotes a uniform random variable ranging over $\left[\mathrm{X}_{j}^{\min}, \mathrm{X}_{j}^{\max}\right]$. X_{ij}^{0} is the initial j th variable of i th population. All the vectors should satisfy the constraints. Evaluate the value of the cost function $f\left(\mathrm{X}_{i}^{0}\right)$ of each vector.

Mutation

DE generates new parameter vectors by adding the weighted difference vector between two population members to a third member. For each target vector X_{i}^{g} at g th generation the noisy vector $\mathrm{X}_{i}^{/g}$ is obtained by

$$\mathrm{X}_{i}^{/g} = \mathrm{X}_{a}^{g} + S_F\left(\mathrm{X}_{b}^{g} - \mathrm{X}_{c}^{g}\right), \qquad i \in \mathrm{N_P} \tag{2.18}$$

where X_{a}^{g}, X_{b}^{g} and X_{c}^{g} are selected randomly from $\mathrm{N_P}$ vectors at g th generation and $a \neq b \neq c \neq i$. The scaling factor (S_F), in the range $0 < S_F \leq 1.2$, controls the amount of perturbation added to the parent vector. The noisy vectors should satisfy the constraint.

Crossover

Perform crossover for each target vector X_{i}^{g} with its noisy vector $\mathrm{X}_{i}^{/g}$ and create a trial vector $\mathrm{X}_{i}^{//g}$ such that

$$\mathrm{X}_{i}^{//g} = \begin{cases} \mathrm{X}_{i}^{/g} & \text{, if } \quad \rho \leq C_R \\ \mathrm{X}_{i}^{g} & \text{, otherwise} \end{cases} \qquad , \qquad i \in \mathrm{N_P} \tag{2.19}$$

where ρ is an uniformly distributed random number within [0, 1]. The crossover constant (C_R), in the range $0 \leq C_R \leq 1$, controls the diversity of the population and aids the algorithm to escape from local optima.

Selection

Perform selection for each target vector, X_i^g by comparing its cost with that of the trial vector, $\mathrm{X}_i^{//g}$. The vector that has lesser cost of the two would survive for the next generation.

$$\mathrm{X}_i^{g+1} = \begin{cases} \mathrm{X}_i^{//g} , & \text{if} \quad f\left(\mathrm{X}_i^{//g}\right) \le f\left(\mathrm{X}_i^{g}\right) \\ \mathrm{X}_i^{g} , & \text{otherwise} \end{cases} , \qquad i \in \mathrm{N_P} \tag{2.20}$$

The process is repeated until the maximum number of iterations or no improvement is seen in the best individual after many iterations.

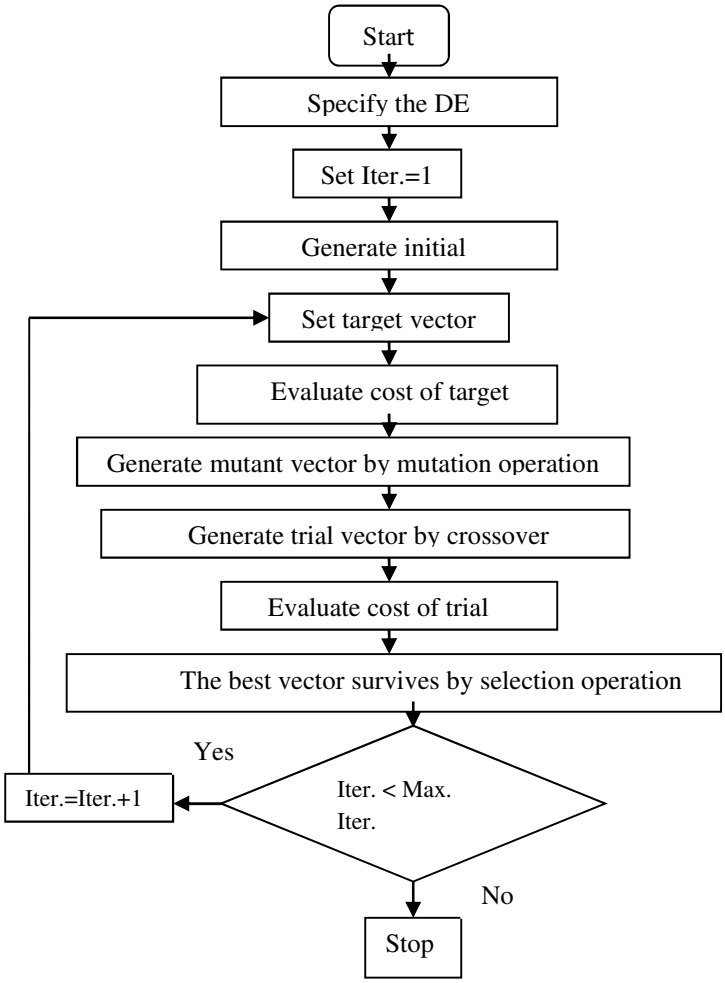

Fig. 2.1. Flowchart of Differential Evolution

2.4.3. Genetic Algorithm

Genetic algorithm [3] is based on the mechanics of natural selection. An initial population of candidate solutions is created randomly. Each of these candidate solutions is termed as individual. Each individual is assigned a fitness, which measures its quality. During each generation of the evolutionary process, individuals with higher fitness are favored and more probabilities to be selected as parents. After parents are selected for reproduction, they produce children via the processes of crossover and mutation. The individuals formed during reproduction explore different areas of the solution space. These new individuals replace lesser-fit individuals of the existing population.

Due to difficulties of binary representation when dealing with continuous search space with large dimensions, the proposed approach has been implemented using real-coded genetic algorithm (RCGA) [36]. The simulated Binary Crossover (SBX) and polynomial mutation are explained as follows.

Simulated Binary Crossover (SBX) operator

The procedure of computing child populations c_1 and c_2 from two parent populations y_1 and y_2 under SBX operator as follows:

1. Create a random number *u* between 0 and 1.

2. Find a parameter γ using a polynomial probability distribution as follows:

$$\gamma = \begin{cases} (u\alpha)^{1/(\eta_c+1)} , & \text{if } u \le \dfrac{1}{\alpha} \\ (1/(2-u\alpha))^{1/(\eta_c+)} , & \text{otherwise} \end{cases} \tag{2.21}$$

where $\alpha = 2-\beta^{-(\eta_c+1)}$ and $\beta = 1+\dfrac{2}{y_2-y_1}\min[(y_1-y_l),(y_u-y_2)]$

Here, the parameter y is assumed to vary in $[y_l, y_u]$. Here, the parameter η_c is the distribution index for SBX and can take any non-negative value. A small value of η_c allows the creation of

child populations far away from parents and a large value restricts only near-parent populations to be created as child populations.

3. The intermediate populations are calculated as follows:

$$c_{p1} = 0.5\left[(y_1 + y_2) - \gamma(|y_2 - y_1|)\right]$$

$$c_{p2} = 0.5\left[(y_1 + y_2) + \gamma(|y_2 - y_1|)\right] \tag{2.22}$$

Each variable is chosen with a probability p_c and the above SBX operator is applied variable-by-variable.

Polynomial Mutation Operator

A polynomial probability distribution is used to create a child population in the vicinity of a parent population under the mutation operator. The following procedure is used:

1. Create a random number *u* between 0 and 1.

2. Calculate the parameter δ as follows:

$$\delta = \begin{cases} \left[2u + (1-2u)(1-\phi)^{(\eta_m+1)}\right]^{\frac{1}{(\eta_m+1)}} - 1 & \text{, if } u \le 0.5 \\ 1 - \left[2(1-u) + 2(u-0.5)(1-\phi)^{(\eta_m+1)}\right]^{\frac{1}{(\eta_m+1)}} & \text{, otherwise} \end{cases} \tag{2.23}$$

where $\varphi = \dfrac{\min\left[(c_p - y_l), (y_u - c_p)\right]}{(y_u - y_l)}$

The parameter η_m is the distribution index for mutation and takes any non-negative value.

3. Calculate the mutated child as follows:

$$c_1 = c_{p1} + \delta(y_u - y_l) \tag{2.24}$$

$$c_2 = c_{p2} + \delta(y_u - y_l) \tag{2.25}$$

The perturbance in the population can be adjusted by varying η_m and p_m with generations as given below:

$$\eta_m = \eta_{m\min} + gen \tag{2.26}$$

$$p_m = \frac{1}{n} + \frac{gen}{gen_{\max}}\left(1 - \frac{1}{n}\right) \tag{2.27}$$

where $\eta_{m\min}$ is the user defined minimum value for η_m, p_m is the probability of mutation, and n is the number of decision variables

2.4.4 Simulated Annealing

The Simulated Annealing algorithm simulates the procedure of gradually cooling a metal, until the energy of the system reaches the globally minimum value. Beginning with a high temperature, a metal is slowly cooled, so that the system is in thermal equilibrium at every stage. At high temperatures, the metal is in liquid phase and the atoms of the system are randomly arranged. By gradually cooling the metal, the system becomes more organized, until it finally reaches a "frozen" ground state, where the energy of the system has reached the globally minimum value [6]. Metropolis et al. [105] proposed an iterative method to simulate the evolution of thermal equilibrium of a metal for a fixed value of temperature. In each trial, the state of an atom is randomly perturbed, resulting in a change of energy (ΔE) of the system. If $\Delta E \le 0$, the perturbation results in a lower energy of the system and the change is accepted. The new configuration of the system constitutes the starting point for the next trial. If $\Delta E > 0$, the proposed change is accepted with a probability given by Boltzmann distribution

$$P(\Delta) = 1/\{1 + \exp(\Delta E / K_{\mathrm{B}}\mathrm{T})\} \tag{2.28}$$

where K_{B} is Boltzmann's constant and T corresponds to the current value of temperature. The acceptance of the new state with higher energy level is determined by comparing a random number generated from a uniform distribution on the interval between 0 and 1. If the random number is less than the value of $P(\Delta)$, the new state is accepted as the current state. This acceptance rule for new state is referred to as the "Metropolis criterion".

At each temperature, the “Metropolis criterion” is applied for a sequence of trials, where the outcome of each trial depends only on the outcome of the previous one. This procedure is mathematically described by means of a Markov chain, where the length of each chain is equal to a specific number of iterations performed at each temperature. As the temperature decreases, the Boltzmann distribution concentrates on the states with lower energy and finally, when the temperature approaches asymptotically to zero, only the minimum energy states have a nonzero probability of appearance. The above procedure is modeled through (2.28), due to which the probability of acceptance of higher energy configurations is large in high temperatures, whereas it becomes smaller as the temperature decreases. The flow chart of simulated annealing technique is shown in Fig. 2.2.

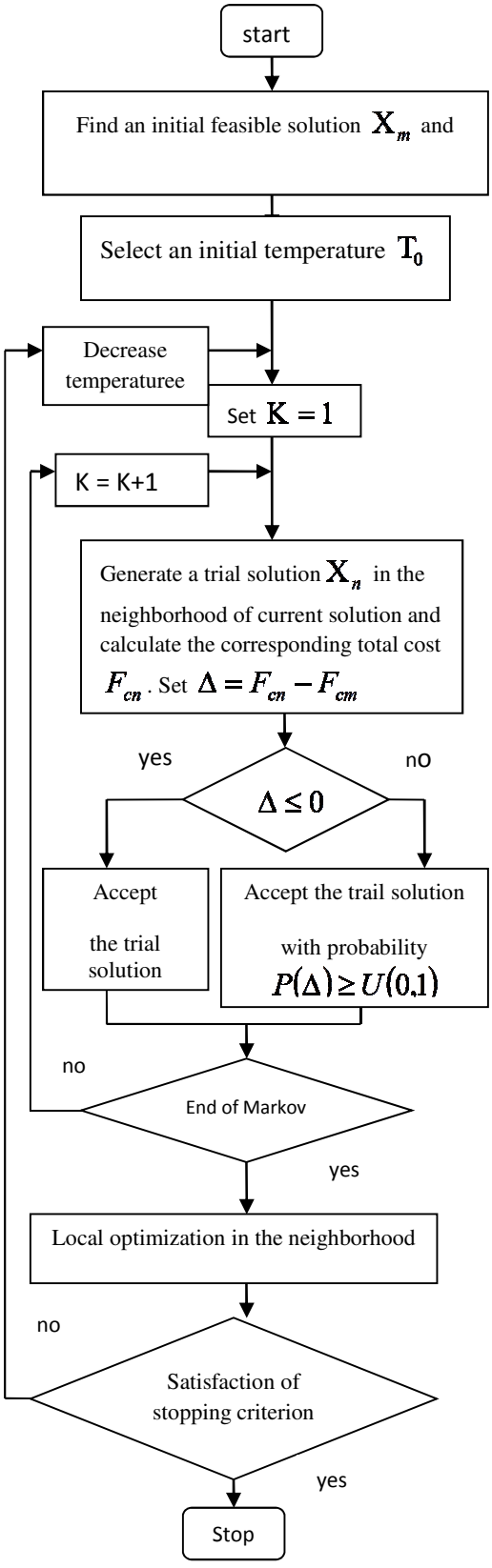

Fig. 2.2. Flow chart of simulated annealing

2.5. Simulation and Results of Metaheuristic technique

A comparative study is performed for the four metaheuristic techniques by solving the MAED problem for three different test systems. All metaheuristic techniques for the MAED problems are implemented by using MATLAB 7.0 on a PC (Pentium-IV, 80 GB, 3.0 GHz).

The initial temperature (T_0) of SA algorithm has been determined by using the procedures described in [20]. As per guideline [6], the value of r lies in the range from 0.80 to 0.99. For seeking the optimal solution, the value of r is required to be set close to 0.99 so that a slow cooling process is simulated. The appropriate setting of r is set by experimenting with its value in the range from 0.95 to 0.99, and this value is found to be 0.98. Number of trials at each temperature has been taken 30. In this paper, iterative process is terminated when the maximum number of iterations is reached.

2.5.1. Test System 1: This system consists of two areas. Each area consists of three generators with prohibited operating zones. Transmission loss is considered here. The generator data has modified from [19]. The generator data and B-coefficients are given in the appendices Table A.1. The percentage of the total load demand in area 1 is 60% and 40% in area 2. The total load demand is 1263 MW and power flow limit of the system is 100 MW.

The problem is solved by using DE, EP, RCGA, and SA. In case of DE, the population size, scaling factor, and crossover rate have been selected as 100, 0.75, and 1.0 respectively for the test system under consideration. The population size and scaling factor have been selected as 100, and 0.1 respectively in case of EP. In case of RCGA, the population size, crossover and mutation probabilities have been selected as 100, 0.9 and 0.2 respectively.

Maximum number of generations has been selected 100 for all the four metaheuristic techniques discussed in this paper.

Results obtained from the four metaheuristic techniques i.e. DE, EP, RCGA, and SA have been summarized in Table 2.1. Fig. 2.3. gives the comparison of convergence of minimum total cost obtained by DE, EP, RCGA, and SA.

Table 2.1: Simulation results for test system 1

	DE	SA	EP	RCGA
$P_{1,1}$ (MW)	500.0000	500.0000	500.0000	500.0000
$P_{1,2}$ (MW)	200.0000	200.0000	200.0000	200.0000
$P_{1,3}$ (MW)	150.0000	150.0000	149.9919	149.6328
$P_{2,1}$ (MW)	204.3341	204.2157	206.4493	205.9398
$P_{2,2}$ (MW)	154.7048	155.0575	154.8892	155.8322
$P_{2,3}$ (MW)	67.5770	67.3516	65.2717	65.2209
T_{12} (MW)	82.7731	82.7731	82.7652	82.4135
P_{L1} (MW)	9.4269	9.4269	9.4267	9.4193
P_{L2} (MW)	4.1890	4.1979	4.1754	4.2064
Cost ($/h)	12255.39	12255.39	12255.43	12256.23
CPU time (second)	17.6875	14.7656	21.3281	24.2031

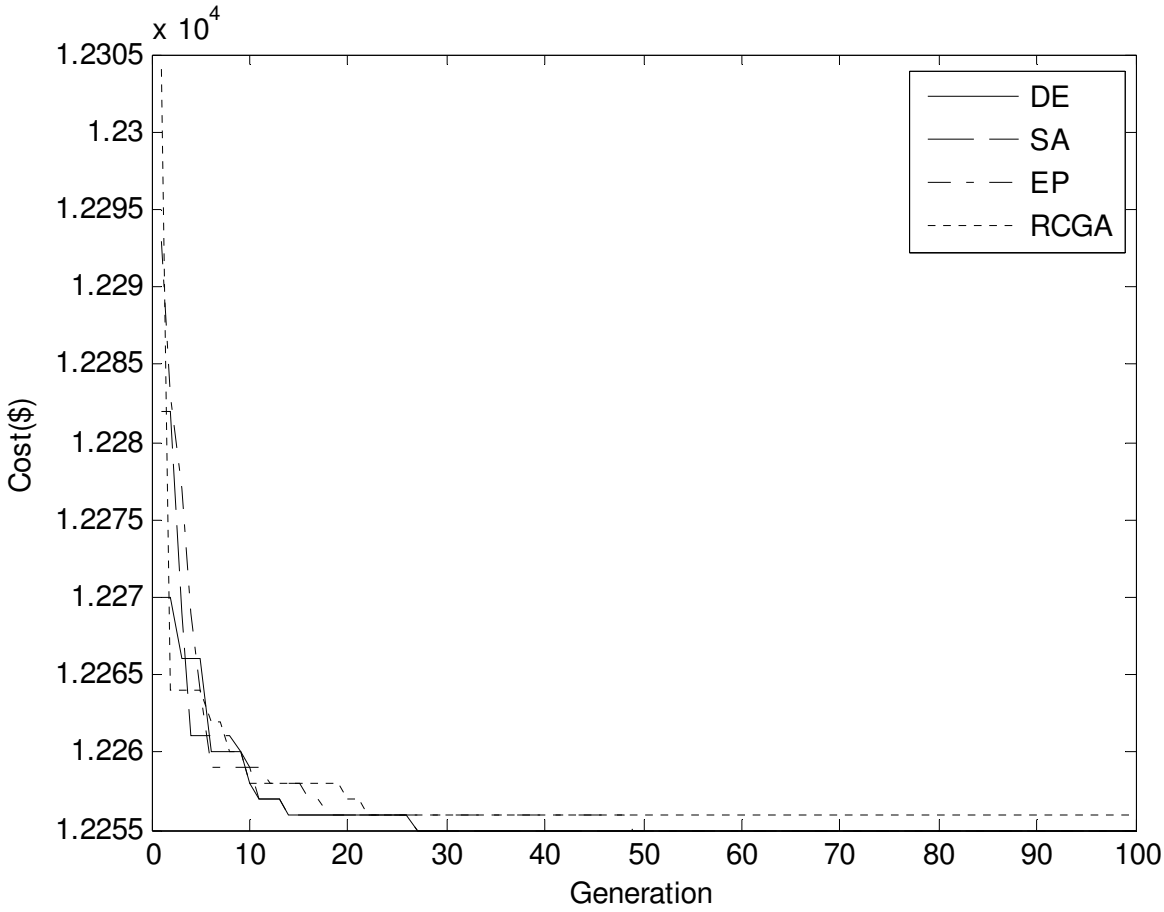

Fig. 2.3. Cost convergence characteristic of DE, SA, EP, RCGA of test system 1

2.5.2. Test System 2: This system comprises ten generators with valve-point loading and multi-fuel sources having three fuel options. Transmission loss is considered here. The generator data has been taken from [17]. The total load demand is 2700 MW. The ten generators are divided into three areas. Area 1 consists of the first four units; area 2 includes the next three units and area 3 includes the last three units. The load demand in area 1 is assumed as 50 % of the total demand. The load demand in area 2 is assumed as 25 % and in area 3 is taken as 25 % of the total demand. The power flow limit from area 1 to area 2 or from area 2 to area 1 is 100 MW. The power flow limit from area 1 to area 3 or from area 3 to area 1 is 100 MW. Also the power flow limit from area 2 to area 3 or from area 3 to area 2 is 100 MW. The B-coefficients are given in the appendices Table A.2. The problem is solved by using four metaheuristic techniques i.e. DE, EP, RCGA, and SA.

In case of DE, the population size, scaling factor, and crossover rate have been selected as 200, 0.75, and 1.0 respectively for the test system under consideration. The population size and scaling factor have been selected as 100, and 0.1 respectively in case of EP. In case of RCGA, the population size, crossover and mutation probabilities have been selected as 100, 0.9 and 0.2 respectively. Maximum number of generations has been selected 300 for DE, EP, RCGA, and SA.

Results obtained from DE, EP, RCGA and RCGA have been presented in Table 2.2. The cost convergence characteristic of this test system obtained from DE, EP, RCGA and SA is shown in Fig. 2.4.

Table 2.2: Simulation results for test system 2

Power (MW)	DE		SA		EP		RCGA	
		Fuel		Fuel		Fuel		Fuel
$P_{1,1}$ (MW)	225.9431	2	228.1730	2	223.8491	2	239.0958	2
$P_{1,2}$ (MW)	211.1594	1	213.3402	1	209.5759	1	216.1166	1
$P_{1,3}$ (MW)	489.9216	2	482.8722	2	496.0680	2	484.1506	2
$P_{1,4}$ (MW)	240.6232	3	242.6425	3	237.9954	3	240.6228	3
$P_{2,1}$ (MW)	254.0397	1	253.505s9	1	259.4299	1	259.6639	1
$P_{2,2}$ (MW)	235.4927	3	236.5760	3	228.9422	3	219.9107	3
$P_{2,3}$ (MW)	263.8837	1	266.6356	1	264.1133	1	254.5140	1
$P_{3,1}$ (MW)	237.0006	3	234.3130	3	238.2280	3	231.3565	3
$P_{3,2}$ (MW)	328.7373	1	325.9516	1	331.2982	1	341.9624	1
$P_{3,3}$ (MW)	248.8607	1	251.4034	1	246.6025	1	248.2782	1
T_{21} (MW)	99.8288		100		100		93.1700	
T_{31} (MW)	99.7334		99.8797		100		93.8739	
T_{32} (MW)	31.2615		28.1853		32.5231		43.7824	
P_{L1} (MW)	17.2095		16.9000		17.4884		17.0297	
P_{L2} (MW)	9.8488		9.9028		10.0085		9.7010	
P_{L3} (MW)	8.6037		8.6030		8.6056		8.9408	
Cost ($/h)	653.9995		654.0916		655.1716		657.3325	
CPU time (second)	95.0351		10.0156		108.0625		133.8438	

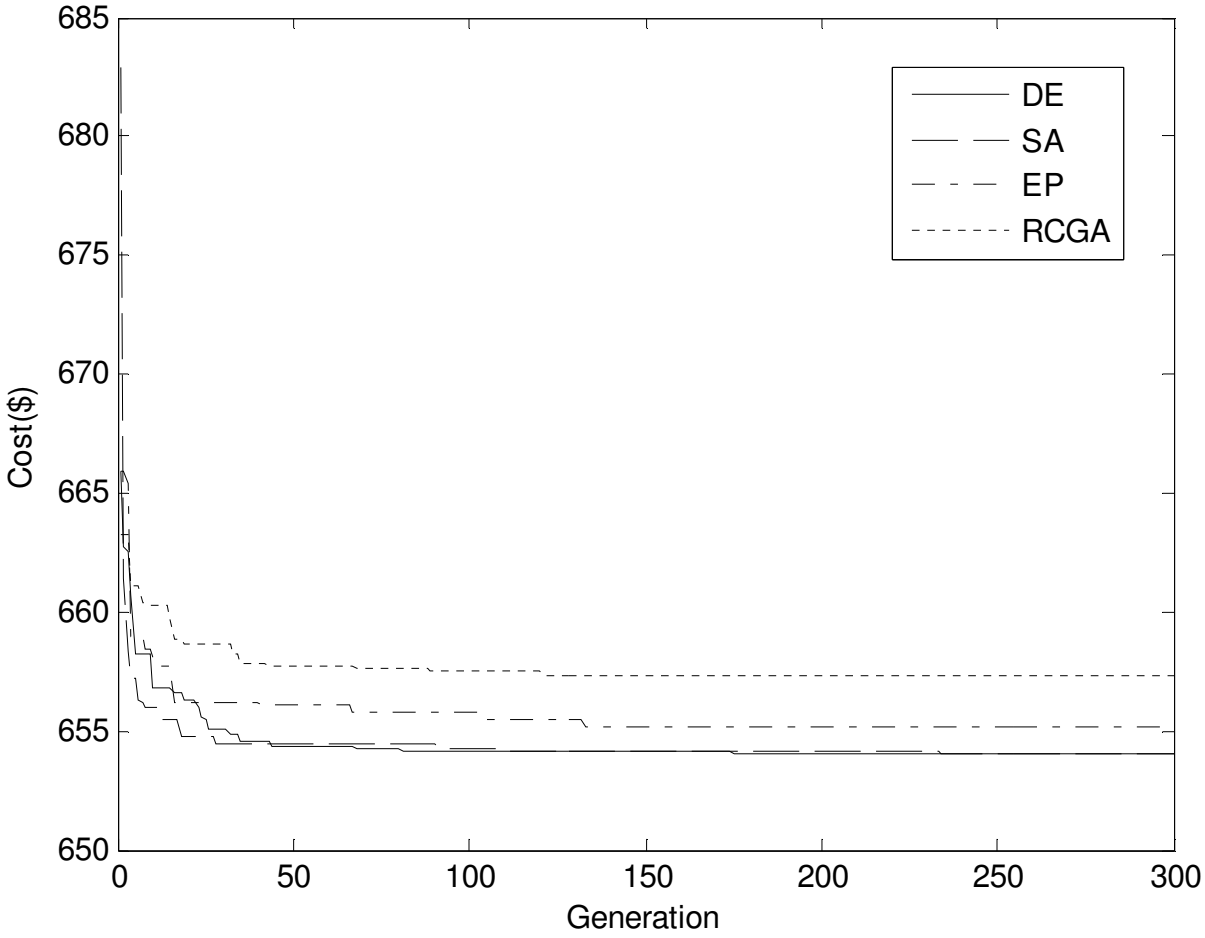

Fig. 2.4. Cost convergence characteristic of DE, SA, EP, RCGA of test system 2

2.5.3. Test System 3: This system comprises forty generators with valve-point loading. The generator data has been taken from [21]. The total load demand is 10500 MW. The forty generators are divided into four areas. Area 1 includes first ten units and 15 % of the total load demand. Area 2 has second ten generators and 40 % of the total load demand. Area 3 consists of third ten generators and 30 % of the total load demand. Area four includes last ten generators and 15 % of the total load demand. The power flow limit from area 1 to area 2 or from area 2 to area 1 is 200 MW. The power flow limit from area 1 to area 3 or from area 3 to area 1 is 200 MW. The power flow limit from area 2 to area 3 or from area 3 to area 2 is 200 MW. The power flow limit from area 4 to area 1 or from area 1 to area 4 is 100 MW. The power flow limit from area 4 to area 2 or from area 2 to area 4 is 100 MW. The power flow limit from area 4 to area 3 or from area 3 to area 4 is 100 MW. Transmission loss is neglected here.

Four metaheuristic techniques i.e. DE, EP, RCGA, and SA have been used to solve the problem. The population size, scaling factor, and crossover rate have been been selected as 400, 0.75 and 1.0 respectively in case of DE. In EP, the population size and scaling factor have been selected 200 and 0.1 respectively. In case of RCGA, the population size, crossover and mutation probabilities have been selected as 200, 0.9 and 0.2 respectively. Maximum number of generations has been selected 500 for DE, EP, RCGA and SA.

Results obtained from DE, EP, RCGA and SA has been depicted in Table 2.3. The cost convergence characteristic of this test system obtained from DE, EP, RCGA and SA is shown in Fig. 2.5.

From Tables 1, 2 and 3, it can be inferred that, the lowest minimum total cost amongst the four is achieved by DE, followed by SA. Minimum total cost obtained by EP is more than DE and SA. RCGA is the worst performer. The CPU time requirement is least in case of SA and highest in the case of RCGA amongst the four metaheuristic techniques discussed in the paper.

Table 2.3: Simulation results for test system 3

Power (MW)	DE	SA	EP	RCGA	**Power** (MW)	DE	SA	EP	RCGA
$P_{1,1}$	111.5448	110.9120	107.6644	95.7552	$P_{3,4}$	523.4073	523.3366	525.7752	518.1120
$P_{1,2}$	111.7092	111.8740	12.0673	88.5828	$P_{3,5}$	523.7703	525.5247	531.2092	538.1994
$P_{1,3}$	98.2429	110.2589	91.8132	97.6063	$P_{3,6}$	523.5424	523.2794	513.5659	527.4775
$P_{1,4}$	179.8834	179.7351	175.3171	126.4966	$P_{3,7}$	10.1621	10.0002	11.3612	24.4133
$P_{1,5}$	95.9500	88.8739	92.4242	71.0127	$P_{3,8}$	10.1326	10.0006	10.0000	28.9856
$P_{1,6}$	139.3533	68.0000	112.5634	116.3866	$P_{3,9}$	10.6366	10.0006	10.0000	28.8571
$P_{1,7}$	259.3395	184.9322	257.5370	244.5857	$P_{3,10}$	88.1189	93.2065	78.3523	87.9016
$P_{1,8}$	285.3569	285.0432	297.3619	210.6920	$P_{4,1}$	161.2220	190.0000	162.4480	159.7482
$P_{1,9}$	284.9627	284.6015	285.2035	236.1685	$P_{4,2}$	189.5668	189.9990	166.3508	153.6255
$P_{1,10}$	130.2217	130.0008	134.5862	130.1286	$P_{4,3}$	189.9240	159.7546	190.0000	160.4706
$P_{2,1}$	243.6005	168.6194	162.4313	367.4862	$P_{4,4}$	165.6621	165.6736	178.4541	169.9359
$P_{2,2}$	95.3890	318.3986	217.8387	297.9501	$P_{4,5}$	165.4321	164.8248	168.0752	168.5220
$P_{2,3}$	214.5171	304.5197	125.0000	394.9246	$P_{4,6}$	164.9868	196.1794	174.4529	172.2638
$P_{2,4}$	394.0808	394.2792	384.0187	370.3473	$P_{4,7}$	109.8137	89.1143	77.3875	91.2423
$P_{2,5}$	394.2481	469.0618	397.6902	455.7123	$P_{4,8}$	109.7935	89.1147	90.1059	86.4778
$P_{2,6}$	394.4360	304.5195	407.4993	393.9673	$P_{4,9}$	90.1543	104.7206	109.5654	88.3627
$P_{2,7}$	489.9552	489.2801	500.0000	424.1994	$P_{4,10}$	459.1140	458.7992	549.0335	279.2691
$P_{2,8}$	488.8885	489.2803	480.8874	484.5498	T_{12}	172.0652	192.6532	200	-71.7855
$P_{2,9}$	511.4713	511.2790	524.8487	528.4148	T_{31}	-36.3060	160.6028	17.5885	161.9336
$P_{2,10}$	511.4125	511.2805	499.7857	511.3403	T_{32}	191.1128	-46.9736	200	95.2833
$P_{3,1}$	523.2896	524.8208	523.4522	525.4497	T_{41}	86.8070	52.8188	90.8733	-76.1340
$P_{3,2}$	523.2950	523.2802	526.5051	510.7391	T_{42}	98.8231	93.8021	100	-52.3900
$P_{3,3}$	523.4129	433.6204	537.3675	533.6399	T_{43}	45.0391	86.5590	100	83.4418
Total cost ($/h)						121794.8	123337.1	123591.9	128046.5
CPU time (second)						134.8125	29.2813	144.5000	160.5313

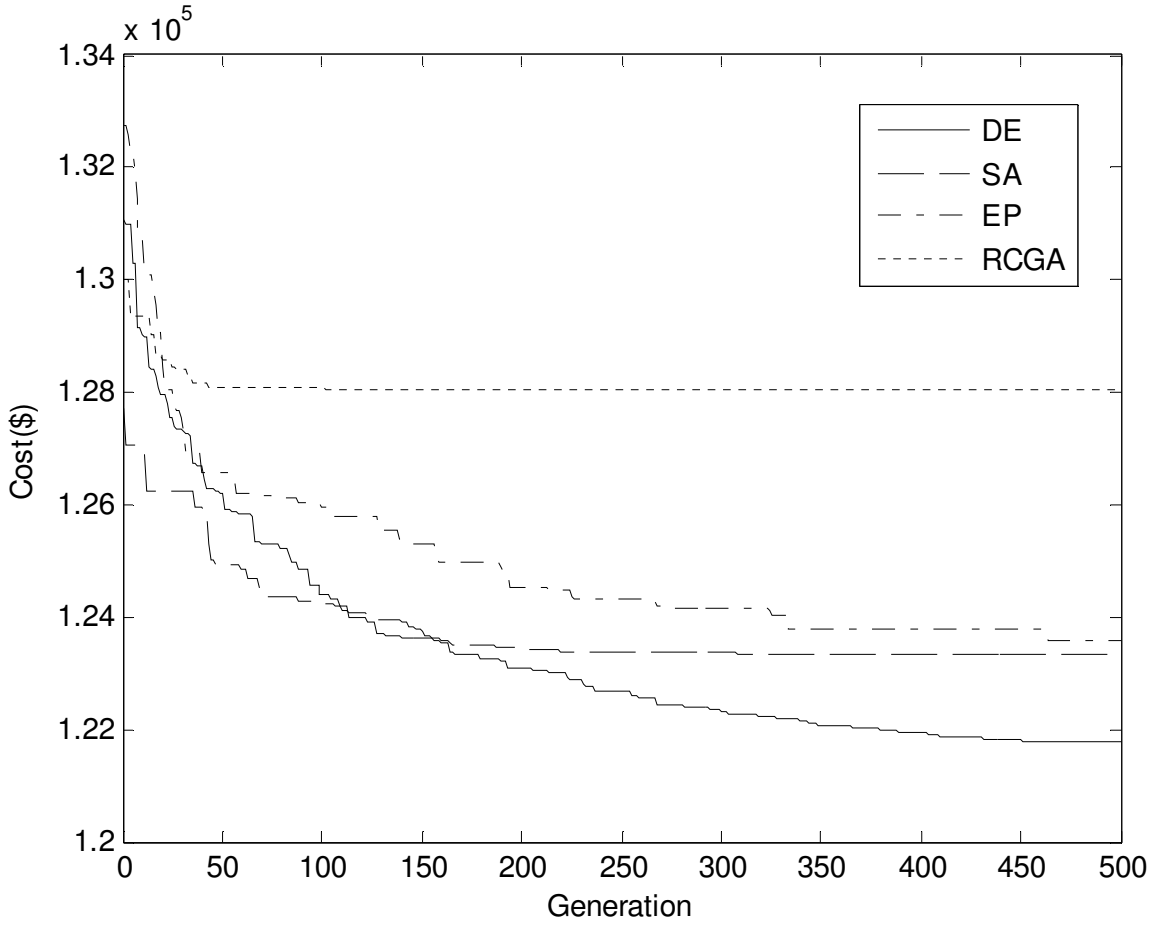

Fig. 2.5. Cost convergence characteristic of DE, SA, EP, RCGA of test system 3

2.6. Conclusion

Here, a comparison analysis has been done for the four metaheuristic techniques viz., differential evolution, evolutionary programming, real coded genetic algorithm and simulated annealing technique for multi-area economic dispatch problem considering transmission losses, multiple fuels, valve-point loading and prohibited operating zones with respect to minimum cost and CPU time. Differential evolution achieves the lowest minimum cost and SA requires least CPU time amongst the four metaheuristic techniques.

CHAPTER-3
Dynamic Economic Dispatch

3.1. Introduction.

Static economic dispatch (SED) allocates the load demand for a given interval of time among the committed generating units economically while fulfilling various constraints. Dynamic economic dispatch (DED) which is an extension of static economic dispatch, determines the optimal sharing of time varying load demand among the committed units. Power plant operators try to keep gradients for temperature and pressure inside the boiler and turbine within safe limits to avoid shortening the life of the equipment. This mechanical constraint imposes limit on the rate of increase or decrease of the electrical power output. This limit is called ramp rate limit which differentiates DED from SED problem. Thus, in DED the dispatch decision at one time period affects those at later time periods.

Dynamic economic dispatch (DED) is one of the main functions of power system operation and control. DED is a real time power system problem. It determines the optimal operation of units with predicted load demands over a certain period of time with an objective to minimize total production cost while the system is operating within its ramp rate limits. DED is the most accurate formulation of the economic dispatch problem but it is the most difficult to solve because of its large dimensionality. As competition is increasingly introduced into the wholesale generation markets, there is a need to understand the incremental cost burden imposed on the system operation by the generator ramping rate limitations.

Here improved real coded genetic algorithm (IRCGA) has been developed in view of one-to-one competition to boost convergence speed and solution quality.

IRCGA has been pertained for solving dynamic economic dispatch problem with nonsmooth fuel cost function. Two test systems and 15 benchmark functions are exploited here. Test results are matched up to those acquired by real coded genetic algorithm (RCGA). It has been observed that the developed IRCGA offers superior solution.

3.2. Problem Formulation

Normally, the DED problem minimizes the following total production cost of committed units:

$$F = \sum_{t=1}^{\mathrm{T}} \sum_{i=1}^{\mathrm{N}} F_{it}(\mathrm{P}_{it}) \tag{3.1}$$

The fuel cost function of each unit considering valve-point effect [22] can be expressed as

$$F_{it}(\mathrm{P}_{it}) = a_i + b_i \mathrm{P}_{it} + c_i \mathrm{P}_{it}^2 + \left| d_i \sin\left(e_i \left(\mathrm{P}_i^{\min} - \mathrm{P}_{it}\right)\right)\right| \tag{3.2}$$

Subject to the following equality and inequality constraints for the t th interval in the scheduled horizon

3.2.1. Real power balance

The total power generated must be equal the total load demand plus transmission losses.

$$\sum_{i=1}^{\mathrm{N}} \mathrm{P}_{it} - \mathrm{P}_{Dt} - \mathrm{P}_{Lt} = 0 \qquad t \in \mathrm{T} \tag{3.3}$$

3.2.2. Real power operating limits

The power generated by each generator is constrained between its lower and upper limits as follows:

$$\mathrm{P}_i^{\min} \le \mathrm{P}_{it} \le \mathrm{P}_i^{\max} \qquad i \in \mathrm{N},\ t \in \mathrm{T} \tag{3.4}$$

3.2.3. Generator ramp rate limits

The rate of output power change of thermal generator must be within an acceptable range to avoid undue stresses on the boiler and combustion equipment. The ramp rate limits of thermal generator can be mathematically expressed as follows:

$$\mathrm{P}_{it} - \mathrm{P}_{i(t-1)} \le UR_i\ , \qquad i \in \mathrm{N},\ t \in \mathrm{T} \tag{3.5}$$

$$\mathrm{P}_{i(t-1)} - \mathrm{P}_{it} \le DR_i\ , \qquad i \in \mathrm{N},\ t \in \mathrm{T} \tag{3.6}$$

3.3. Determination of Generation Levels

In this approach, the power loading of first $(N-1)$ generators are specified. From the equality constraints in equation (3.3) the power level of the Nth generator (i.e. the slack generator) is given by

$$P_{Nt} = P_{Dt} + P_{Lt} - \sum_{i=1}^{N-1} P_{it} \qquad t \in T \tag{3.7}$$

The transmission loss P_{Lt} is a function of all the generators including that of the dependent generator and it is given by

$$P_{Lt} = \sum_{i=1}^{N-1}\sum_{j=1}^{N-1} P_{it} B_{ij} P_{jt} + 2P_{Nt}\left(\sum_{i=1}^{N-1} B_{Ni} P_{it}\right) + B_{NN} P_{Nt}^2 \qquad t \in T \tag{3.8}$$

Expanding and rearranging, equation (3.6) becomes

$$B_{NN} P_{Nt}^2 + \left(2\sum_{i=1}^{N-1} B_{Ni} P_{it} - 1\right) P_{Nt} + \left(P_{Dt} + \sum_{i=1}^{N-1}\sum_{j=1}^{N-1} P_{it} B_{ij} P_{jt} - \sum_{i=1}^{N-1} P_{it}\right) = 0 \qquad t \in T \tag{3.9}$$

The loading of the dependent generator (i.e. Nth) can then be found by solving equation (3.9) using standard algebraic method.

3.4. Overview of Improved Real Coded Genetic Algorithm

Genetic algorithm [2] pioneered in the early 1970s at the University of Michigan by John Holland and his students, engenders the global or close to the global optima of a minimization problem by creating a number of populations over a number of iterations. Genetic algorithm [2] is inspired from Darwinian evolution theory "the survival of the fittest". An initial population of candidate solutions is generated randomly. The capability of the global or close to the global optima of each of the new population is assessed by its fitness which can be stated by a function of the objective function. After parents are selected for reproduction, they produce offspring via the processes of crossover and mutation. The individuals formed during reproduction explore different areas of the solution space.

Due to difficulties of binary representation when dealing with continuous search space with large dimensions, real-coded genetic algorithm (RCGA) [36] [37] has been employed. The Simulated Binary Crossover (SBX) [36] and polynomial mutation have been applied in this work.

In case of improved real coded genetic algorithm (IRCGA), one-to-one challenge is pioneered in real coded genetic algorithm (RCGA) to boost the convergence speed and solution quality. Here, an offspring contends one-to-one with that of matching parent. Initialization, selection of parent population, crossover, mutation and selection between parent and offspring are the five stages of IRCGA stated as:

3.4.1. Initialization: The initial population (X_i) of control variables chosen randomly from the set of uniformly distributed control variables ranging over their maximum and minimum limits has been stated as:

$$x_{i,j}^{0} \sim U\left(x_j^{\min}, x_j^{\max}\right), \quad j \in n, i \in \mathrm{N_P} \tag{3.10}$$

where n is the number of decision variables in an individual, $\mathrm{N_P}$ is the population size; $x_{i,j}^{0}$ signifies the initial j th variable of the i th population ; $x_j^{\min}$ and $x_j^{\max}$ are the minimum and maximum limits of the j th decision variable; $U\left(x_j^{\min}, x_j^{\max}\right)$ signifies a uniform random variable ranging over $\left[x_j^{\min}, x_j^{\max}\right]$. Compute the objective function value f_i of each population.

3.4.2. Selection of parent population

The binary tournament selection method is utilized for choosing the parents in the mating pool. Two chromosomes are haphazardly chosen from the population, and their objective function values are compared and the chromosome with lower objective function value i.e. winner chromosome is set aside in the mating pool. This process is repetitive until the mating pool is full by the chromosomes.

3.4.3. Simulated Binary Crossover (SBX)

The process of computing offsprings $x_1^{/}$ and $x_2^{/}$ from two parents x_1 and x_2 by utilizing SBX operator as follows:

1. Generate a random number *u* between 0 and 1.

2. Get a parameter γ by utilizing a polynomial probability distribution as follows:

$$\gamma = \begin{cases} (u\alpha)^{1/(\eta_c+1)} & , \text{ if } u \le 1/\alpha \\ (1/(2-u\alpha))^{1/(\eta_c+1)} & , \text{ otherwise} \end{cases} \tag{3.11}$$

where $\alpha = 2-\beta^{-(\eta_c+1)}$ and β is computed as follows:

$$\beta = 1+\frac{2}{x_2-x_1}\min\left[(x_1-x^{\min}),(x^{\max}-x_2)\right]$$

The parameter η_c is the distribution index for SBX and can obtain any non-negative value. A minute value of η_c permits the formation of offsprings far-off from parents and a great value confines only close to-parent populations to be generated as offsprings.

3. The intermediate populations are computed as follows:

$$x_{p1} = 0.5\left[(x_1+x_2)-\gamma(|x_2-x_1|)\right] \tag{3.12}$$

$$x_{p2} = 0.5\left[(x_1+x_2)+\gamma(|x_2-x_1|)\right] \tag{3.13}$$

3.4.4. Polynomial Mutation

The polynomial probability distribution is utilized to generate an offspring in the neighborhood of a parent population underneath the mutation operator. This is stated as follows:

1. Generate a random number *u* between 0 and 1.

2. Compute the parameter σ as follows:

$$\sigma = \begin{cases} \left[2u+(1-2u)(1-\phi)^{(\eta_m+1)}\right]^{\frac{1}{(\eta_m+1)}}-1 & , \text{ if } u \le 0.5 \\ 1-\left[2(1-u)+2(u-0.5)(1-\phi)^{(\eta_m+1)}\right]^{\frac{1}{(\eta_m+1)}} & , \text{ otherwise} \end{cases} \tag{3.14}$$

where $\varphi = \dfrac{\min\left[\left(x_p - x^{\min}\right), \left(x^{\max} - x_p\right)\right]}{\left(x^{\max} - x^{\min}\right)}$

The parameter η_m is the distribution index for mutation and obtains any non-negative value.

3.4.5. Compute the mutated offspring as follows:

$$x_1^{/} = x_{p1} + \sigma\left(x^{\max} - x^{\min}\right) \tag{3.15}$$

$$x_2^{/} = x_{p2} + \sigma\left(x^{\max} - x^{\min}\right) \tag{3.16}$$

The perturbation can be changed by varying η_m and p_m with iterations as follows:

$$\eta_m = \eta_{m\min} + iter \tag{3.17}$$

$$p_m = \frac{1}{n} + \frac{iter}{iter_{\max}}\left(1 - \frac{1}{n}\right) \tag{3.18}$$

where $\eta_{m\min}$ is the abuser definite lowest value for η_m, p_m is the probability of mutation, and n is the number of choice variables.Compute the objective function value of each offspring.

3.4.6. Selection between parent and offspring:

Carry out assortment for each parent $\left(\mathrm{X}_i\right)$ by comparing its objective function value with that of the matching offspring $\left(\mathrm{X}_i^{/}\right)$. The population that has lower objective function value between parent and offspring, carries on for the next iteration.

$$\mathrm{X}_i = \begin{cases} \mathrm{X}_i^{/} & , \text{ if } f\left(\mathrm{X}_i^{/}\right) \le f\left(\mathrm{X}_i\right) \\ \mathrm{X}_i & , \text{ otherwise} \end{cases} \quad , i \in \mathrm{N_P} \tag{3.19}$$

The procedure is replicated till the maximum number of iterations is arrived at. Fig. 3.1. portrays the flowchart of improved real coded genetic algorithm (IRCGA).

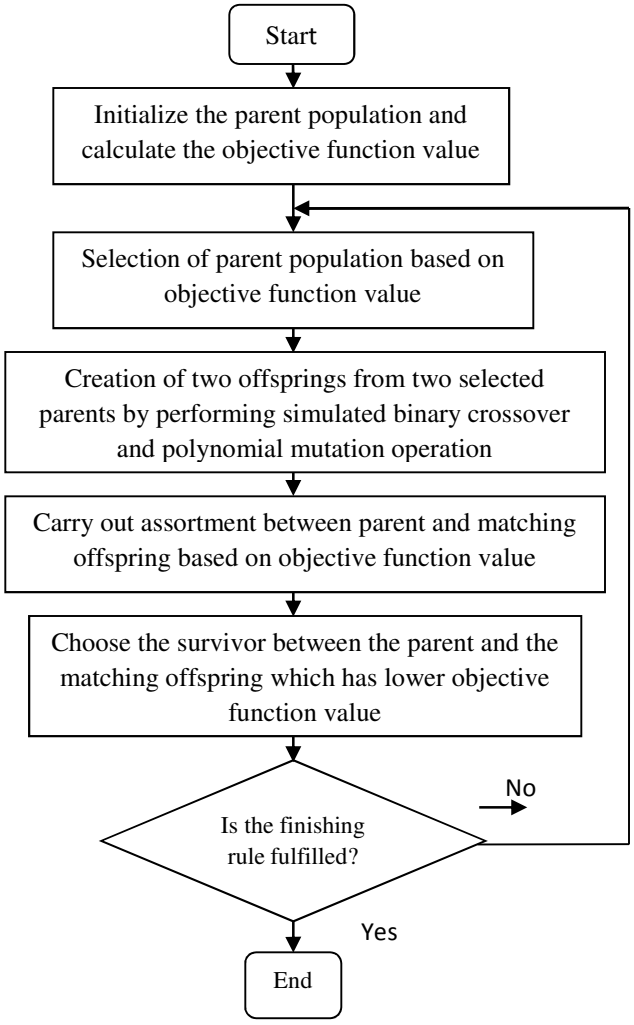

Fig. 3.1. Flowchart of improved real coded genetic algorithm

3.5. Simulation and Results of IRCGA algorithm

The developed improved real coded genetic algorithm (IRCGA) and real coded genetic algorithm (RCGA) have been pertained for solving two different test systems and 15 benchmark functions. IRCGA and RCGA techniques have been realized by using MATLAB 7.0 on a PC (Pentium-IV, 80 GB, 3.0 GHz).

3.5.1. Test System 1

This system comprises a five-unit test system with non-smooth fuel cost function**.** The demand of the system has been divided into 24 intervals. Unit data and load demands can be found in the

appendices Table.A.3 and Table.A.4 respectively. The transmission loss coefficients are also found in the appendices.

The problem is solved by using IRCGA and RCGA. Here, maximum number of iterations, population size, crossover and mutation probabilities have been chosen as 200, 50, 0.9 and 0.2, respectively for IRCGA and RCGA.

Test results acquired from the best fuel cost among 100 runs of solutions by using developed IRCGA and RCGA are summed up in Table 3.1 and Table 3.2 respectively.

The cost convergence characteristic acquired from developed IRCGA and RCGA has been portrayed in Fig. 3.2. It has been observed from Table 3.1 and Table 3.2 that the total production cost acquired from IRCGA is the less than RCGA.

Table 3.1: Hourly generation (MW) schedule, cost ($\times 10^4$ \$) and CPU time (second) of dynamic economic dispatch obtained from IRCGA for test system 1

Hour	P_1	P_2	P_3	P_4	P_5	Cost	CPU time
1	11.3164	94.4161	34.8735	146.6867	126.5497	4.7185	70.35
2	23.1813	90.1666	73.7201	113.5044	138.4590		
3	11.9324	93.9033	108.5855	115.6246	149.7128		
4	27.1539	112.3399	129.1379	127.4656	139.8012		
5	33.0977	105.1074	119.7769	157.6852	148.8756		
6	34.2727	113.1852	118.1478	198.1880	152.0965		
7	21.0618	95.2011	126.5935	200.9683	190.5027		
8	13.2336	84.1612	124.7809	210.7558	230.2387		
9	15.4049	111.9255	114.6057	206.1754	252.2273		
10	38.1468	102.8138	112.3537	228.4493	232.9199		
11	22.9734	115.6917	116.1610	245.6676	230.8052		
12	22.6146	100.7327	131.6335	217.3580	279.4648		
13	17.1397	101.0136	130.8908	230.8320	234.7908		
14	14.4215	125.0000	116.7502	208.0259	236.1501		
15	27.3155	102.7837	132.0737	186.6684	214.2108		
16	10.0000	88.8931	112.6023	143.4474	232.2756		
17	29.3193	75.7853	115.8604	111.6682	231.9894		
18	10.9216	98.6467	128.8807	155.2371	222.1789		
19	10.0000	97.3583	116.4014	204.7380	234.7459		
20	21.3901	101.9513	111.1422	249.0230	231.3192		
21	41.8179	92.4563	124.0882	204.4698	226.9759		
22	26.2425	83.8814	120.7969	168.0922	213.7139		
23	27.0398	93.6921	111.9390	124.6404	175.5184		
24	13.9996	97.5889	112.7651	112.7183	130.4413		

Table 3.2: Hourly generation (MW) schedule, cost ($\times 10^4$ \$) and CPU time (second) of dynamic economic dispatch obtained from RCGA for test system 1

Hour	P_1	P_2	P_3	P_4	P_5	Cost	CPU time
1	13.1295	83.5304	30.0000	131.5777	155.5877	4.7564	63.41
2	20.7587	103.9699	47.7241	121.1508	145.5922		
3	30.0888	96.8590	39.0542	121.3086	192.7561		
4	34.6016	120.1340	45.9461	99.9179	235.8191		
5	11.1545	99.4230	79.6158	127.7968	246.9099		
6	38.5179	103.8989	104.0526	114.2895	255.2500		
7	10.0000	112.3671	121.8815	162.0736	228.0966		
8	12.1923	94.8772	114.6329	200.1064	241.4309		
9	40.3314	92.0681	109.8161	227.9227	230.1095		
10	51.9218	99.9601	123.7857	204.9619	233.8897		
11	67.8766	104.7002	116.5753	219.9124	221.9794		
12	68.0362	104.4624	141.4227	222.6975	214.9175		
13	39.2518	107.5492	115.4971	210.8340	241.5070		
14	15.9646	110.7312	140.0208	212.6738	220.7837		
15	15.6750	95.3407	106.4133	202.2451	243.6056		
16	10.0000	99.2551	69.7553	184.2966	224.1859		
17	25.4383	100.0201	35.7367	202.2340	201.7308		
18	54.1205	96.0491	31.3978	205.6964	229.1920		
19	54.9027	109.0564	61.4139	212.5498	225.5727		
20	67.8133	98.9348	96.8481	219.0149	232.0707		
21	64.1935	97.1720	105.7931	192.3558	230.3411		
22	59.0403	96.4422	112.5213	160.1490	184.5178		
23	51.9522	97.0567	99.1880	138.5687	146.0497		
24	28.7679	100.1259	71.3424	135.5410	131.8331		

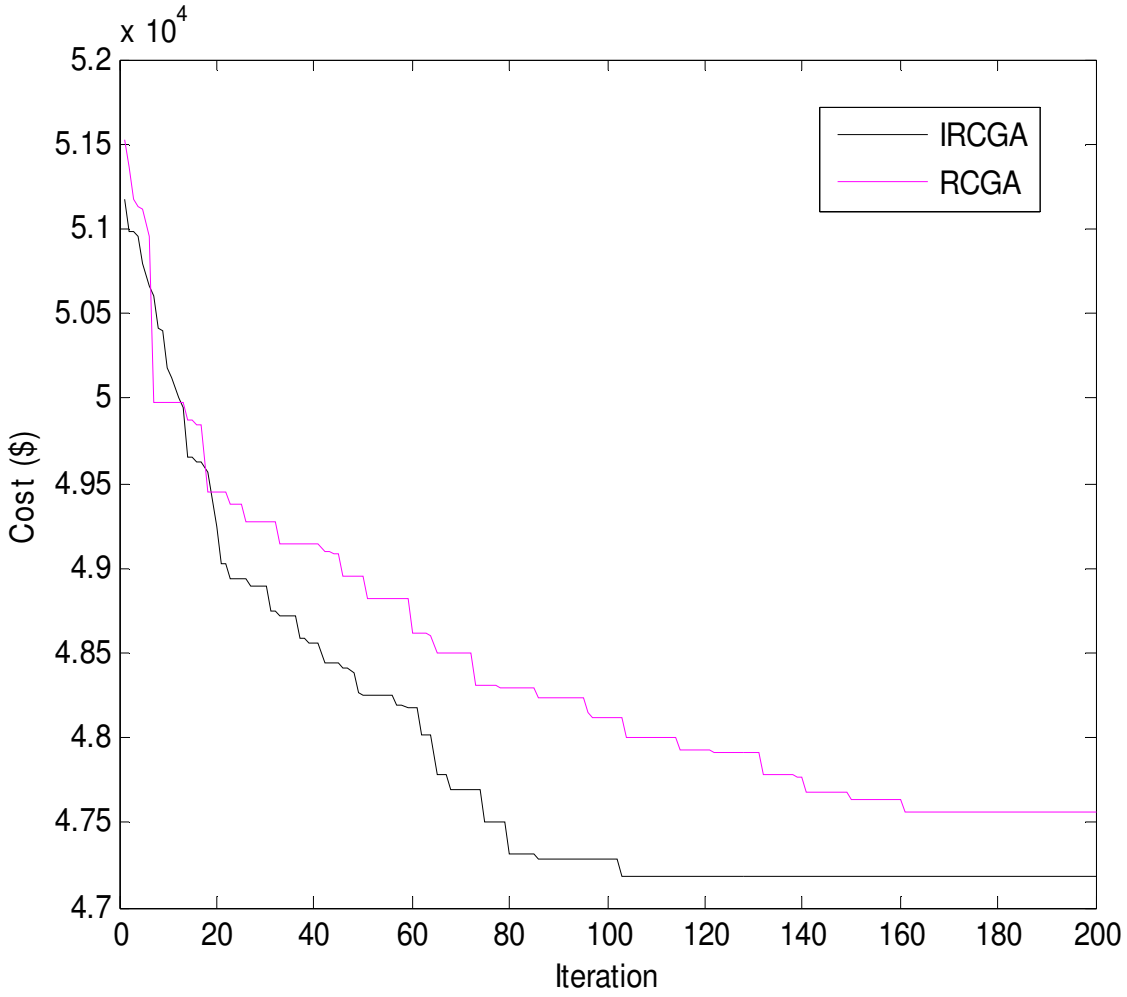

Fig. 3.2. Cost convergence characteristic for test system 1

3.5.2. Test System 2

This system comprises a ten-unit test system with non-smooth fuel cost function**.** The demand of the system has been divided into 24 intervals. Unit data and load demands can be found in Table.A.5 and Table.A.6 respectively in the appendices. The transmission loss coefficients are also found in the appendices.

The problem is solved by using IRCGA and RCGA. Here, maximum number of iterations, population size, crossover and mutation probabilities have been chosen as 300, 100, 0.9 and 0.2, respectively for IRCGA and RCGA.

Test results acquired from the best fuel cost among 100 runs of solutions by using developed IRCGA and RCGA are summed up in Table 3.3 and Table 3.4 respectively.

The cost convergence characteristic acquired from developed IRCGA and RCGA has been portrayed in Fig. 3.3. It has been observed from Table 3.3 and Table 3.4 that the total production cost acquired from IRCGA is the less than RCGA.

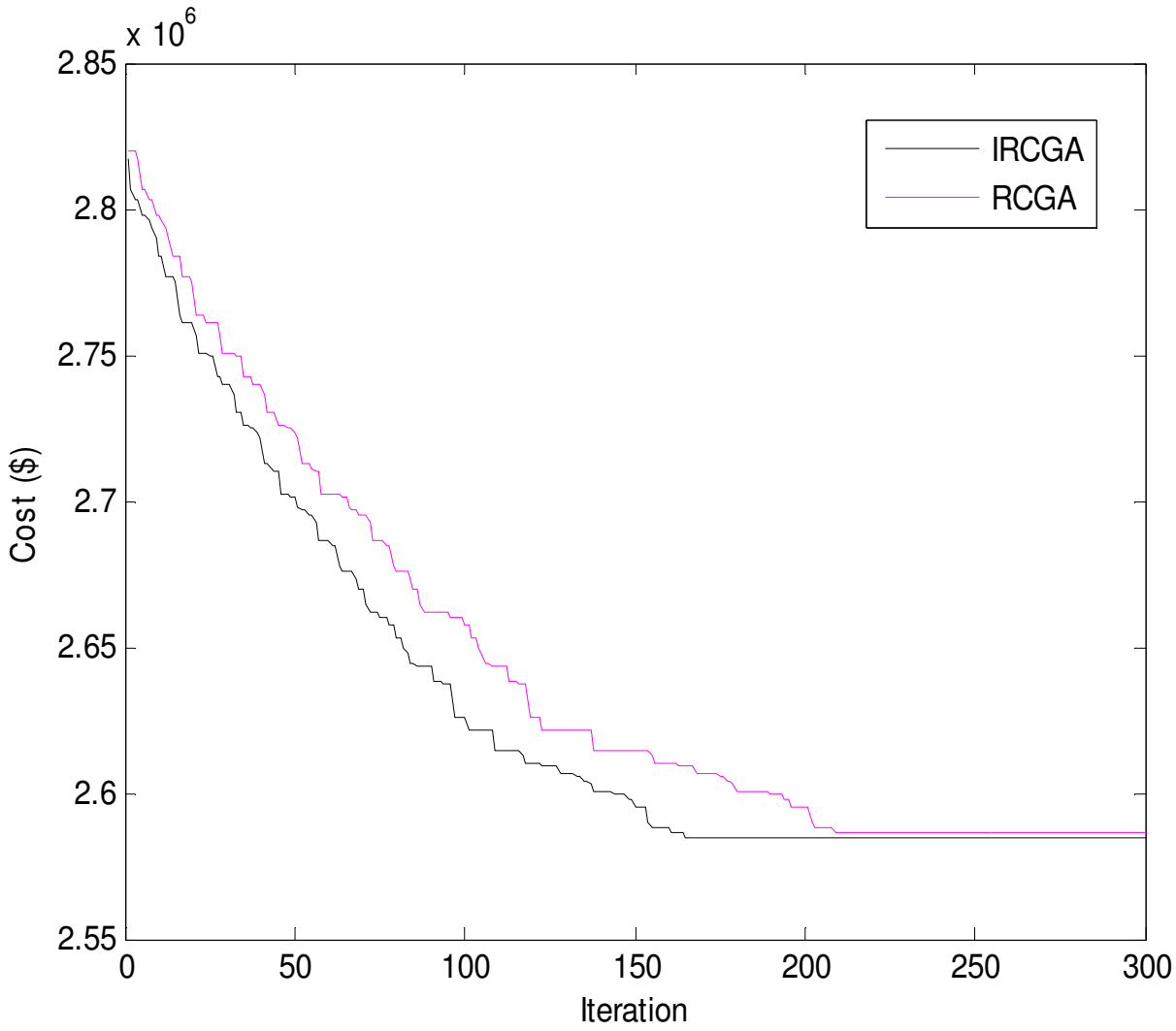

Fig. 3.3. Cost convergence characteristic for test system 2

Table 3.3: Hourly generation (MW) schedule, cost ($\times 10^6$ \$) and CPU time (second) of dynamic economic dispatch obtained from IRCGA for test system 2

Hour	P_1	P_2	P_3	P_4	P_5	P_6	P_7	P_8	P_9	P_{10}	Cost	CPU time
1	170.0479	135.0000	192.6901	80.8424	73.0000	154.3788	130.0000	52.8560	22.8966	44.2913	2.5846	98.35
2	162.4527	157.4800	208.9139	63.4751	101.8075	152.6401	125.3130	68.0419	38.1231	54.7364		
3	171.7873	175.3694	232.5499	138.1431	151.7197	137.6965	95.6378	66.6527	63.6616	54.0304		
4	209.3238	135.0000	328.5352	156.7839	207.8623	120.6867	122.8788	78.2603	45.5571	38.0044		
5	167.1108	174.8619	304.4829	207.4663	243.0000	144.5933	122.1273	79.1574	28.5795	48.8394		
6	150.5984	274.5884	331.7668	270.4349	223.2717	148.4555	97.3318	102.6412	36.2662	42.3119		
7	183.9816	312.5799	294.9857	293.5312	210.8582	160.0000	97.7485	113.9463	53.4248	35.7131		
8	282.2848	254.1162	339.2119	284.8594	243.0000	144.2156	86.1617	113.0337	38.6628	50.7865		
9	344.2388	322.0815	306.1054	300.0000	236.0309	158.0670	111.8435	118.3255	53.0498	46.4289		
10	349.0350	417.7704	335.8070	289.4027	219.6325	141.6536	130.0000	113.6310	58.5891	47.9318		
11	342.2568	469.3050	326.2087	293.1140	243.0000	160.0000	116.6308	111.4778	79.1320	53.8436		
12	435.1132	454.7974	337.1691	286.6126	227.0852	159.6202	130.0000	112.6503	57.8492	43.2443		
13	370.2295	397.4357	331.5782	284.8071	240.3289	160.0000	126.9121	120.0000	77.8540	48.0171		
14	280.5887	332.6855	319.5450	299.8766	243.0000	150.8031	127.4609	112.0207	76.5221	52.7926		
15	228.2424	242.9967	306.8294	300.0000	234.8736	152.9236	128.6402	115.0161	75.3307	50.1898		
16	150.0000	250.9624	253.5642	293.2289	210.3790	128.0041	106.1838	95.5585	71.2451	39.8182		
17	159.2353	205.9445	192.7515	290.4024	243.0000	155.2386	111.3697	65.9490	42.4189	54.0599		
18	252.6480	152.6482	286.6603	300.0000	227.0753	129.6603	129.8947	93.2049	63.6187	42.0691		
19	243.8322	220.8389	340.0000	269.1818	240.2404	154.2803	116.7962	119.6214	80.0000	50.3610		
20	321.1724	317.3856	335.7388	300.0000	243.0000	153.0017	130.0000	116.0057	78.8976	52.0603		
21	311.4281	335.2963	323.1403	282.4210	240.2808	157.3177	122.9299	115.3374	79.7618	27.8216		
22	215.9857	235.3213	232.5551	293.7490	237.9273	139.2567	100.7775	97.3881	75.8539	48.8466		
23	150.0000	164.9318	242.8354	228.0769	201.6605	114.1467	98.0189	95.4461	47.1013	22.1347		
24	152.5138	144.3522	181.9009	170.7653	196.5345	104.1802	107.8064	104.0548	36.1573	11.1460		

Table 3.4: Hourly generation (MW) schedule, cost ($\times 10^6$ \$) and CPU time (second) of dynamic economic dispatch obtained from RCGA for test system 2

Hour	P_1	P_2	P_3	P_4	P_5	P_6	P_7	P_8	P_9	P_{10}	Cost	CPU time
1	169.6782	135.0000	215.3823	62.5555	88.2848	159.9788	128.0962	49.7207	25.2229	22.1714	2.5862	90.04
2	150.0000	158.2374	210.7686	75.4813	117.2002	154.8310	112.5570	75.1567	44.4317	34.0486		
3	168.1968	149.8369	229.0087	151.0554	167.0417	148.2731	95.9306	66.1359	60.0834	51.3607		
4	185.7484	135.0000	324.1029	193.3018	205.4031	107.8792	122.7947	85.3723	43.1031	39.8648		
5	158.4763	149.3037	340.0000	232.8472	241.0500	132.4656	114.0782	80.8442	28.6401	42.5392		
6	172.5213	242.3215	334.0163	261.6742	239.2640	152.8587	95.7984	109.8432	37.9905	31.0766		
7	185.9565	302.6341	312.4701	293.5866	188.5660	154.8110	94.1240	120.0000	58.0830	46.5614		
8	279.5536	281.5387	327.5860	268.0157	227.9288	141.4513	109.0384	116.9311	42.9092	41.4668		
9	349.1114	304.4209	323.5911	300.0000	242.0828	158.0591	101.6306	108.6452	56.2897	52.3394		
10	336.8889	402.0839	338.2607	295.8877	243.0000	154.4746	130.0000	118.6656	51.5046	31.9295		
11	361.4835	470.0000	331.3869	293.4665	235.6580	159.5167	123.0234	96.7633	70.4333	53.6632		
12	434.2881	462.7087	340.0000	290.4506	239.3750	151.1169	129.4341	111.9401	55.5505	29.4622		
13	371.7406	412.8996	330.0234	289.8269	243.0000	152.5171	114.8754	111.5222	76.3217	54.9619		
14	286.1102	350.6039	313.6475	297.7600	241.8185	160.0000	130.0000	115.7702	59.8236	39.9652		
15	236.1590	283.7791	330.7395	252.8145	239.2359	155.3320	115.1991	120.0000	80.0000	22.4301		
16	150.0000	282.0557	265.0021	276.8190	212.3728	114.7462	108.6983	90.4793	64.4079	34.8455		
17	151.6128	213.8723	217.5640	284.8984	218.3762	153.0215	129.0562	72.9735	42.9939	35.8299		
18	211.9547	182.2002	302.8357	279.4265	243.0000	125.2994	123.2188	91.3917	71.5106	46.4008		
19	222.3904	249.0910	340.0000	272.1415	237.8443	152.2739	124.5323	109.4703	78.3633	49.0821		
20	311.6497	344.2860	335.5613	282.3693	243.0000	154.9173	130.0000	120.0000	74.9944	50.6934		
21	277.5024	334.1937	337.5220	296.2484	240.6938	156.9802	115.2833	105.1382	79.1628	52.6521		
22	211.6221	235.9096	250.4202	291.2272	243.0000	125.1411	90.7778	118.8654	65.2889	45.4533		
23	151.4487	158.2970	204.1604	214.2778	203.6673	128.2102	118.1466	96.5378	63.2699	26.0850		
24	159.6004	143.2313	148.0736	188.7526	189.1664	106.5601	107.4814	113.5277	36.5113	16.5484		

3.6. Benchmark Functions

The developed IRCGA and RCGA have been pertained for solving 15 benchmark functions [29]. These test functions are revealed in Table 3.5. All other data is taken from [29]. The population size, crossover and mutation probabilities have been chosen as 100, 0.9 and 0.2 respectively for IRCGA and RCGA.

To verify the performance of the proposed IRCGA technique, these 15 test functions are repeatedly tested by using the IRCGA. Each test is repeated 100 times. Mean results of 15 test functions acquired from 100 runs are summarized in Table 3.6. Table 3.7 summarizes best optimum values and the variables corresponding to the best optimum value, number of iterations and CPU time of all 15 benchmark functions in 100 runs acquired from IRCGA.

These 15 test functions are also tested by using RCGA technique. Table 3.8 shows best optimum values, number of iterations and CPU time acquired from RCGA.

Table 3.6: **Mean optimum value, number of iterations and mean CPU time acquired from IRCGA**

Function	Mean Optimum Value	Number of Iterations	Mean CPU time (sec)
f_1	1.6703e-22	200	27.5631
f_2	8.6875e-18	200	28.6573
f_3	7.0153e-17	300	38.9348
f_4	1.2035e-17	300	37.9738
f_5	3.0151e-17	300	39.0571
f_6	9.4572e-18	300	41.3401
f_7	22.324e-17	300	38.0479
f_8	6.8957e-18	300	40.9752
f_9	-186.7307	100	1.5042
f_{10}	0.00030763	200	5.9033
f_{11}	-1.031642	50	0.7047
f_{12}	0.397733	50	0.6981
f_{13}	3	50	0.6348
f_{14}	-3.8626	50	0.9015
f_{15}	-3.319	50	1.7748

Table 3.5: Test Functions

Mathematical representation	Domain	Optimum
$f_1(x)=\sum_{i=1}^{30} x_i^2$	[-100,100]	0
$f_2(x)=\sum_{i=1}^{30}\lvert x_i\rvert+\prod_{i=1}^{30}\lvert x_i\rvert$	[-10,10]	0
$f_3(x)=\sum_{i=1}^{30}\left(\sum_{j=1}^{i} x_j\right)^2$	[-100,100]	0
$f_4(x)=\max_i\{\lvert x_i\rvert, 1\le i\le 30\}$	[-100,100]	0
$f_5(x)=\sum_{i=1}^{29}\left[100\left(x_{i+1}-x_i^2\right)^2+(x_i-1)^2\right]$	[-30,30]	0
$f_6(x)=\sum_{i=1}^{30}\left[x_i^2-10\cos(2\pi x_i)+10\right]$	[-5.12,5.12]	0
$f_7(x)=-20\exp\left(-0.2\sqrt{\frac{1}{30}\sum_{i=1}^{30}x_i^2}\right)-\exp\left(\frac{1}{30}\sum_{i=1}^{30}\cos 2\pi x_i\right)+20+e$	[-32,32]	0
$f_8(x)=\frac{1}{4000}\sum_{i=1}^{30}x_i^2-\prod_{i=1}^{30}\cos\left(\frac{x_i}{\sqrt{i}}\right)+1$	[-600,600]	0
$f_9(x)=\sum_{i=1}^{5} i\cos[(i+1)x_1+i]\sum_{i=1}^{5} i\cos[(i+1)x_2+i]$	[-10,10]	-186.73
$f_{10}(x)=\sum_{i=1}^{11}\left[a_i-\frac{x_1\left(b_i^2+b_i x_2\right)}{b_i^2+b_i x_3+x_4}\right]$	[-5,5]	0.0003075
$f_{11}(x)=4x_1^2-2.1x_1^4+\frac{1}{3}x_1^6+x_1x_2-4x_2^2+4x_2^4$	[-5,5]	-1.0316285
$f_{12}(x)=\left(x_2-\frac{5.1}{4\pi^2}x_1^2+\frac{5}{\pi}x_1-6\right)^2+10\left(1-\frac{1}{8\pi}\right)\cos x_1+10$	[-5,10], [0,15]	0.398
$f_{13}(x)=[1+(x_1+x_2+1)^2(19-14x_1+3x_1^2-14x_2+6x_1x_2+3x_2^2)]$ $\times[30+(2x_1-3x_2)^2\times(18-32x_1+12x_1^2+48x_2-36x_1x_2+27x_2^2)]$	[-2,2]	3
$f_{14}(x)=-\sum_{i=1}^{4}c_i\exp\left[-\sum_{j=1}^{3}a_{ij}\left(x_j-p_{ij}\right)^2\right]$	[0,1]	-3.86
$f_{15}(x)=-\sum_{i=1}^{4}c_i\exp\left[-\sum_{j=1}^{6}a_{ij}\left(x_j-p_{ij}\right)^2\right]$	[0,1]	-3.32

Table 3.7: Best Optimum value, the variables corresponding to the best optimum value, number of iterations and CPU time acquired from IRCGA

Function	x^*	$f(x^*)$	Number of Iterations	CPU time (sec)
f_1	[0,0,…….,0]	1.6701e-24	200	25.5788
f_2	[0,0,…….,0]	7.7935e-18	200	26.9347
f_3	[0,0,…….,0]	5.8031e-17	300	37.7409
f_4	[0,0,…….,0]	1.3135e-17	300	36.7092
f_5	[1,1,…….,1]	2.6149e-17	300	37.5872
f_6	[0,0,…….,0]	8.9901e-18	300	40.8805
f_7	[0,0,…….,0]	2.1067e-17	300	37.7943
f_8	[0,0,…….,0]	6.3568e-18	300	39.9052
f_9	[4.8581, 5.4829] , [-7.0835, -7.7083], [-0.8003, -7.7083]	-186.7309	100	1.6325
f_{10}	[0.1928, 0.1909, 0.1231, 0.1358]	0.0003075	200	5.8807
f_{11}	[0.089842, -0.712654], [-0.089842, 0.712655],	-1.0316285	50	0.6183
f_{12}	[-3.1416, 12.272], [3.1416, 2.276]	0.397725	50	0.5996
f_{13}	[0, -1]	3	50	0.6074
f_{14}	[0.1146, 0.5556, 0.8525]	-3.86	50	0.8807
f_{15}	[0.2017, 0.1468, 0.4767, 0.2753, 0.3117, 0.6573]	-3.32	50	1.6038

Table 3.8: Best optimum value, number of iterations and CPU time acquired from RCGA

Function	RCGA		
	$f(x^*)$	Number of Iterations	CPU time (sec)
f_1	6.0739e-019	200	25.7905
f_2	1.6857e-005	300	39.6358
f_3	0.26796	500	62.7043
f_4	0.05389	500	64.9351
f_5	71.7808	400	54.9532
f_6	33.8247	300	40.8562
f_7	1.5308e-005	300	37.7794
f_8	4.9494	300	39.8093
f_9	-186.7308	100	1.3835
f_{10}	0.0003077	200	5.8774
f_{11}	-1.0316273	50	0.6058
f_{12}	0.397728	50	0.5495
f_{13}	3	50	0.6015
f_{14}	-3.8621	50	0.8795
f_{15}	-3.3214	50	1.49752

3.7. Conclusion

Here, improved real coded genetic algorithm (IRCGA) has been developed and pertained for solving dynamic economic dispatch problem with non-smooth fuel cost function and 15 benchmark functions. Test results have been matched up to those acquired from real coded genetic algorithm. It has been observed from the comparison that the developed improved real coded genetic algorithm has the capability to offer superior solution and quick convergence. Due to these properties, improved real coded genetic algorithm can be utilized for solving complicated power system problems.

CHAPTER-4
Combined Heat & Power Economic Dispatch

4.1. Introduction

The conversion of fossil fuel into electricity takes place inefficiently. Most of the energy desecrated in the process of conversion is heat. Cogeneration gets better this heat and makes use of it usefully. On the whole, the efficiency of the conversion is moved up. Comparing with the other form of power suppliers, cogeneration such as heat and power generation is more energy efficient and lower green house gas emission power supplier.

Even the energy efficiency of the most modern combined cycle plants is less than 60%. Most of the energy wasted in the conversion process is heat. But the fuel efficiency of combined heat and power generation unit can be as much as 90%. Also combined heat and power generation unit has less green house gas emission as compared with the other forms of energy supply. The principle of combined heat and power, known as cogeneration, is to recover and make beneficial use of this heat and as a result the overall efficiency of the conversion process is increased. Cogeneration units play an increasingly important role in the utility industry. For most cogeneration units, the heat production capacity depends on the power generation and vice versa. This introduces complexity due to the non-separable nature of electrical power and heat in the combined heat and power unit. The mutual dependencies of heat and power generation initiate a complication in the incorporation of cogeneration units into the power economic dispatch. Non-linear optimization methods, such as dual and quadratic programming and gradient descent approaches, such as Lagrangian relaxation, have been applied for solving combined heat and power economic dispatch (CHPED). However, these methods cannot handle non-convex fuel cost functions of the generating units.

The advent of Teaching-learning-based optimization (TLBO), a teaching-learning process inspired algorithm recently proposed by Rao et al. [52], [53] and Rao and Patel [54] is based on the effect of influence of a teacher on the output of learners in a class. It is a population-based

method and does not require any algorithm-specific control parameters. The main advantage of TLBO is that it requires only common controlling parameters like population size and number of generations for its working.

Here modified teaching-learning-based optimization (MTLBO) where Gaussian random variables are introduced in the 'Teacher phase' and 'Learner phase' which improves search efficiency and guarantees a high probability of obtaining the global optimum without significantly impairing the speed of convergence and the simplicity of the structure of TLBO.

In this study, MTLBO has been applied to solve the non-smooth/non-convex combined heat and power economic dispatch (CHPED) problem and 15 benchmark functions. The valve-point loading and forbidden working regions of conventional thermal generators and transmission loss are taken into consideration. Three test systems are exploited here. Test results are compared with those acquired by other evolutionary techniques. It has been observed that the developed MTBLO offers superior solution.

4.2. Problem Formulation

The system under consideration has conventional thermal generators, cogeneration units and heat-only units. The heat-power feasible operating region of a combined cycle co-generation unit is portrayed in Fig. 4.1. The heat and power outputs of this type of unit are inseparable and one output varies with the other. The heat-power feasible operating region is enclosed by the boundary curve ABCDEF.

The power output of the conventional thermal generators and the heat output of heat units are confined by their own maximum and minimum limits. The power is created by conventional thermal generators and combined heat and power units and the heat is created by combined heat and power units and heat-only units. The CHPED problem determines the unit power and heat production so that the system production cost is minimized at the same time satisfying the power and heat demands and other constraints. The objective function and constraints of CHPED problem can be stated as:

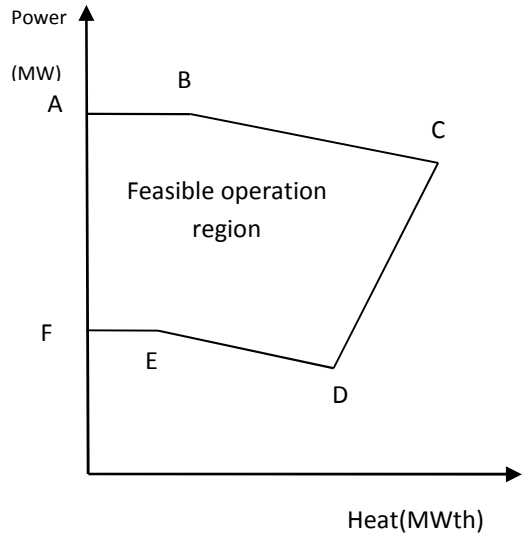

Fig. 4.1. Heat-Power Feasible Operation Region for a cogeneration unit

4.2.1. Objective

The cost function of conventional thermal generator is acquired when the unit output is slowly varied throughout its workable region. The valve point effect takes place due to the aperture of each steam admission valve in a turbine. The valve point effect is modeled as a summation of recurring rectified sinusoid and quadratic function [22].

The total heat and power production cost can be stated as

$$C_{\mathrm{T}} = \sum_{i=1}^{\mathrm{N}_t} C_{ti}\left(\mathrm{P}_{ti}\right) + \sum_{i=1}^{\mathrm{N}_c} C_{ci}\left(\mathrm{P}_{ci}, \mathrm{H}_{ci}\right) + \sum_{i=1}^{\mathrm{N}_h} C_{hi}\left(\mathrm{H}_{hi}\right)$$

$$= \sum_{i=1}^{\mathrm{N}_t} \left[a_i + b_i \mathrm{P}_{ti} + d_i \mathrm{P}_{ti}^2 + \left| e_i \sin\left\{ f_i \left(\mathrm{P}_{ti}^{\min} - \mathrm{P}_{ti} \right) \right\} \right| \right]$$

$$+ \sum_{i=1}^{\mathrm{N}_c} \left[\alpha_i + \beta_i \mathrm{P}_{ci} + \gamma_i \mathrm{P}_{ci}^2 + \delta_i \mathrm{H}_{ci} + \varepsilon_i \mathrm{H}_{ci}^2 + \xi_i \mathrm{P}_{ci} \mathrm{H}_{ci} \right] + \sum_{i=1}^{\mathrm{N}_h} \left[\varphi_i + \eta_i \mathrm{H}_{hi} + \lambda_i \mathrm{H}_{hi}^2 \right] \quad (4.1)$$

4.2.2. Constraints:

Two types of constraints i.e. equality and inequality constraints are taken into account. Equality constraints are the power and heat balance constraints. Inequality constraints are the capacity limits on heat and power generated by each unit and the forbidden working regions of conventional thermal generator.

4.2.2.1. Power balance constraint

$$\sum_{i=1}^{N_t} P_{ti} + \sum_{i=1}^{N_c} P_{ci} = P_D + P_L \tag{4.2}$$

Transmission loss P_L is a function of power of all generating units and can be stated as:

$$P_L = \sum_{i=1}^{N_t}\sum_{j=1}^{N_t} P_{ti} B_{ij} P_{tj} + \sum_{i=1}^{N_t}\sum_{j=1}^{N_c} P_{ti} B_{ij} P_{cj} + \sum_{i=1}^{N_c}\sum_{j=1}^{N_c} P_{ci} B_{ij} P_{cj} \tag{4.3}$$

where B_{ij} is the loss coefficient for a network branch connected between units i and j.

4.2.2.2. Heat balance constraint

$$\sum_{i=1}^{N_c} H_{ci} + \sum_{i=1}^{N_h} H_{hi} = H_D \tag{4.4}$$

The heat demand is used within a short distance of cogeneration units and so the heat loss is insignificant.

4.2.2.3. Capacity limits of conventional thermal generating units

$$P_{ti}^{\min} \le P_{ti} \le P_{ti}^{\max} \qquad i \in 1,2,...,N_t \tag{4.5}$$

4.2.2.4. Capacity limits of cogeneration units

The heat and power outputs of the cogeneration units are inseparable and one output affects the other. $P_c^{\min}(H_c), P_c^{\max}(H_c)$, $H_c^{\min}(P_c)$ and $H_c^{\max}(P_c)$ are the linear inequalities that define the feasible operating region of the cogeneration units

$$P_{ci}^{\min}(H_{ci}) \le P_{ci} \le P_{ci}^{\max}(H_{ci}), \qquad i \in 1,2,...,N_c \tag{4.6}$$

$$H_{ci}^{\min}(P_{ci}) \le H_{ci} \le H_{ci}^{\max}(P_{ci}), \qquad i \in 1,2,...,N_c \tag{4.7}$$

4.2.2.5. Production limits of heat-only units

$$H_{hi}^{\min} \le H_{hi} \le H_{hi}^{\max} \qquad i \in 1,2,...,N_h \tag{4.8}$$

where $H_{hi}^{\min}$ and $H_{hi}^{\max}$ are heat production limits of the ith heat-only unit.

4.3. Forbidden working region

Shaft bearing tremor caused by the steam admission valve or the machine fault or the associated auxiliary equipment fault can produce forbidden working regions in the input-output curve of a conventional thermal generator. The greatest achievable saving is achieved by circumventing operation in these areas. The feasible working regions of a conventional thermal generator with forbidden working regions can be stated as:

$$\begin{aligned} & P_{ti}^{\min} \le P_{ti} \le P_{ti,1}^{l} \\ & P_{ti,j-1}^{u} \le P_{ti} \le P_{ti,j}^{l} \quad , \quad j = 2,3,...,n_i \\ & P_{ti,n_i}^{u} \le P_{ti} \le P_{ti}^{\max} \quad , \quad i \in N_t \end{aligned} \tag{4.9}$$

where j represents the number of forbidden working regions of i the conventional thermal generator. $P_{ti,j-1}^{u}$ is the upper limit of $(j-1)$th forbidden working region of i the conventional thermal generator. $P_{ti,j}^{l}$ is the lower limit of j th forbidden working region of i the conventional thermal generator. Total number of forbidden working region of i the conventional thermal generator is n_i.

4.4. Overview of Modified Teaching Learning Based Optimization algorithm

4.4.1. Teaching–learning-based optimization

Teaching–learning-based optimization (TLBO) is a teaching–learning process inspired algorithm recently proposed by Rao et al. [52], [53] and Rao and Patel [54] based on the effect of influence of a teacher on the output of learners in a class. The algorithm mimics teaching–learning ability of teacher and learners in a classroom. Teacher and learners are the two vital components of the algorithm. The algorithm describes two basic modes of the learning: (i) through teacher (known as teacher phase) and (ii) interacting with the other learners (known as learner phase). The output in TLBO algorithm is considered in terms of results or grades of the learners which depend on the quality of teacher. A high quality teacher is usually considered as a highly learned person who trains learners so that they can have better results in terms of their marks or grades. Learners also learn from the interaction among themselves which also helps in improving their results.

TLBO is population based method. In this optimization algorithm a group of learners are considered as population and different subjects offered to the learners are considered as different design parameters and a learner's result is analogous to the 'fitness' value of the optimization problem. The best solution in the entire population is considered as the teacher. The design variables are actually the parameters involved in the objective function of the given optimization problem and the best solution is the best value of the objective function. The working of TLBO is divided into two parts, 'Teacher phase' and 'Learner phase'.

4.4.1.1. Teacher phase

It is the first part of the optimization algorithm where learners learn through the teacher. During this phase a teacher tries to improve the mean result of the class in the subject taught by him or her depending on his or her capability. At any iteration i, assume that there are 'm' number of subjects (i.e. design variables), 'n' number of learners (i.e. population size, $k = 1,2,.....,\mathrm{N_P}$) and $L_{i,j}$ be the mean result of the learners in a particular subject' j' ($j = 1,2,.....,l$). The best overall result $\mathrm{X}_{total\_kbest,i}$, obtained in the entire population of learners considering all the subjects together can be considered as the result of best learner $kbest$. However, as the teacher is usually considered as a highly learned person who trains learners so that they can have better results. The best learner identified is considered by the algorithm as the teacher. The difference between the existing mean result of each subject and the corresponding result of the teacher for each subject is given by:

$$Difference\_Mean_{i,j,k} = r_i \times \left(\mathrm{X}_{i,j,kbest} - L_{i,j}\right) \tag{4.10}$$

where $\mathrm{X}_{i,j,kbest}$ is the result of the best learner (i.e. teacher) in subject j and r_i is the random number in the range [0, 1].

Based on the $Difference\_Mean_{i,j,k}$, the existing solution is updated in the teacher phase according to the following expression.

$$\mathrm{X}'_{i,j,k} = \mathrm{X}_{i,j,k} + Difference\_mean_{i,j,k} \tag{4.11}$$

where $\mathrm{X}'_{i,j,k}$ is the updated value of $\mathrm{X}_{i,j,k}$. Accept $\mathrm{X}_{i,j,k}$ if it gives better function value.

All the accepted function values at the end of the teacher phase are maintained and these values become the input to the learner phase.

4.4.1.2. Learner phase

The learner phase depends upon the teacher phase. It is the second part of the algorithm where learners increase their knowledge by interaction among themselves. A learner interacts randomly with other learners for enhancing his or her knowledge. A learner learns new things if the other learner has more knowledge than him or her. Considering a population size of 'N_P', the learning phenomenon of this phase is expressed below.

Randomly select two learners P and Q such that $X'_{i,total-P} \neq X'_{i,total-Q}$ where $X'_{i,total-P}$ and $X'_{i,total-Q}$ are the updated values of $X_{i,total-P}$ and $X_{i,total-Q}$ respectively at the end of the teacher phase.

$$X''_{i,j,P} = X'_{i,j,P} + r'_i \left(X'_{i,j,P} - X'_{i,j,Q}\right), \text{ if } X'_{i,total-P} < X'_{i,total-Q} \tag{4.12}$$

$$X''_{i,j,P} = X'_{i,j,P} + r'_i \left(X'_{i,j,Q} - X'_{i,j,P}\right), \text{ if } X'_{i,total-Q} < X'_{i,total-P} \tag{4.13}$$

where r'_i is the random number in the range [0, 1]. Accept $X''_{i,j,P}$ if it gives a better function value. Repeat the procedure of teacher phase and learner phase till the termination criterion is met.

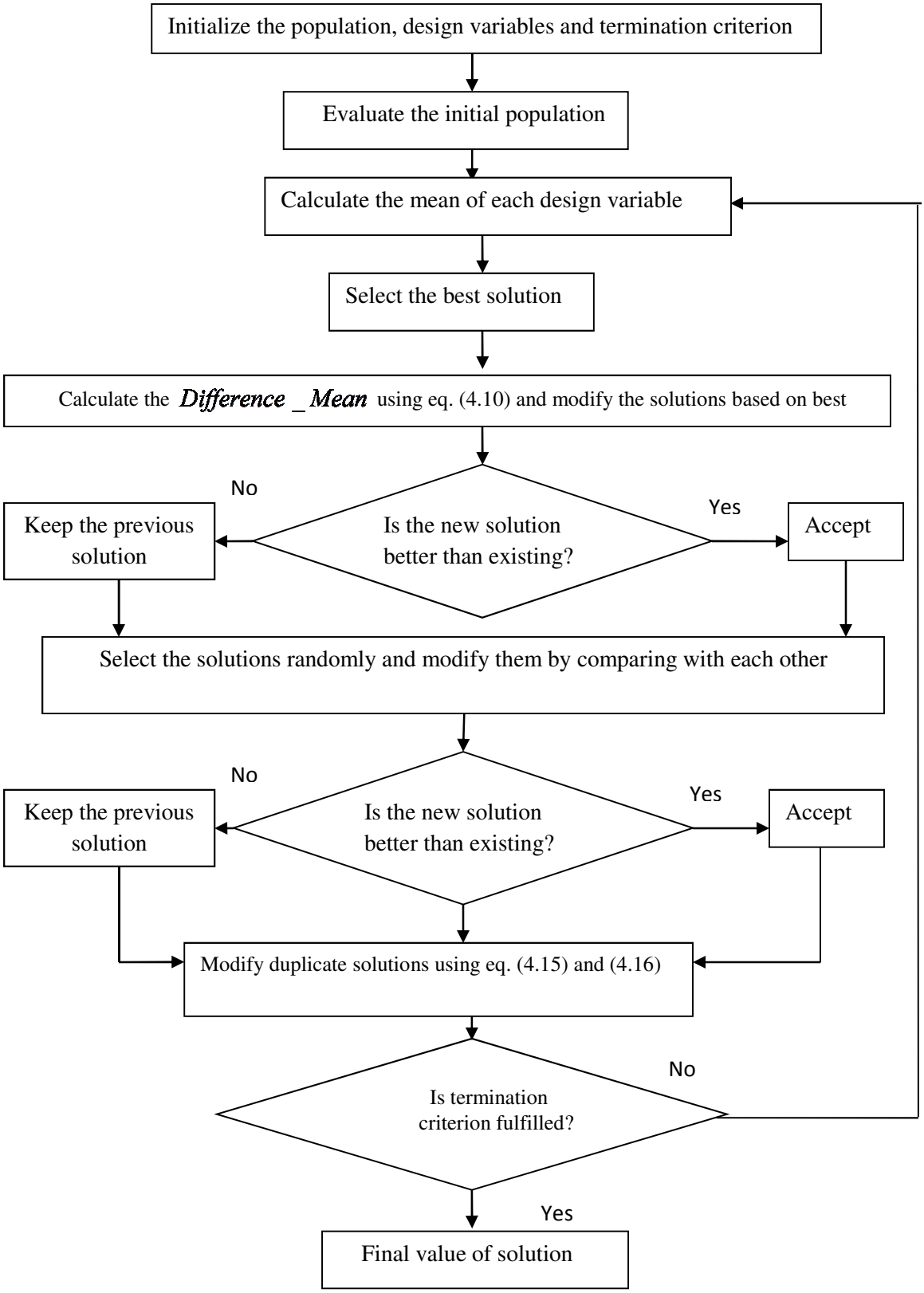

Fig. 4.2. Flowchart of TLBO algorithm

4.4.2. Modified Teaching–learning-based optimization

In modified teaching–learning-based optimization (MTLBO), Gaussian random variables are introduced in the 'Teacher phase' and 'Learner phase' which improves search efficiency and guarantees a high probability of obtaining the global optimum without significantly impairing the speed of convergence and the simplicity of the structure of TLBO. Accordingly the difference between the existing mean result of each subject and the corresponding result of the teacher for each subject is thus modified to

$$Difference\_Mean_{i,j,k} = N(0,1)\times\left(\mathrm{X}_{i,j,kbest} - L_{i,j}\right) \tag{4.14}$$

where $\mathrm{X}_{i,j,kbest}$ is the result of the best learner (i.e. teacher) in subject j and $N(0,1)$ represents a Gaussian random variable with mean zero and standard deviation 1.

Accordingly randomly select two learners P and Q such that $\mathrm{X}'_{i,total-\mathrm{P}} \neq \mathrm{X}'_{i,total-Q}$ where $\mathrm{X}'_{i,total-\mathrm{P}}$ and $\mathrm{X}'_{i,total-Q}$ are the updated values of $\mathrm{X}_{i,total-\mathrm{P}}$ and $\mathrm{X}_{i,total-Q}$ respectively at the end of the teacher phase is thus modified to.

$$\mathrm{X}''_{i,j,\mathrm{P}} = \mathrm{X}'_{i,j,\mathrm{P}} + N(0,1)\times\left(\mathrm{X}'_{i,j,\mathrm{P}} - \mathrm{X}'_{i,j,Q}\right), \text{ if } \mathrm{X}'_{i,total-\mathrm{P}} < \mathrm{X}'_{i,total-Q} \tag{4.15}$$

$$\mathrm{X}''_{i,j,\mathrm{P}} = \mathrm{X}'_{i,j,\mathrm{P}} + N(0,1)\times\left(\mathrm{X}'_{i,j,Q} - \mathrm{X}'_{i,j,\mathrm{P}}\right), \text{ if } \mathrm{X}'_{i,total-Q} < \mathrm{X}'_{i,total-\mathrm{P}} \tag{4.16}$$

where $N(0,1)$ represents a Gaussian random variable with mean zero and standard deviation 1.

The Gaussian random variables control the amount of perturbation added to the 'Teacher phase' and 'Learner phase' and aids the method to escape from local optima. This maintains the diversity of the population throughout iterative process which guarantees a high probability of achieving the global optimum.

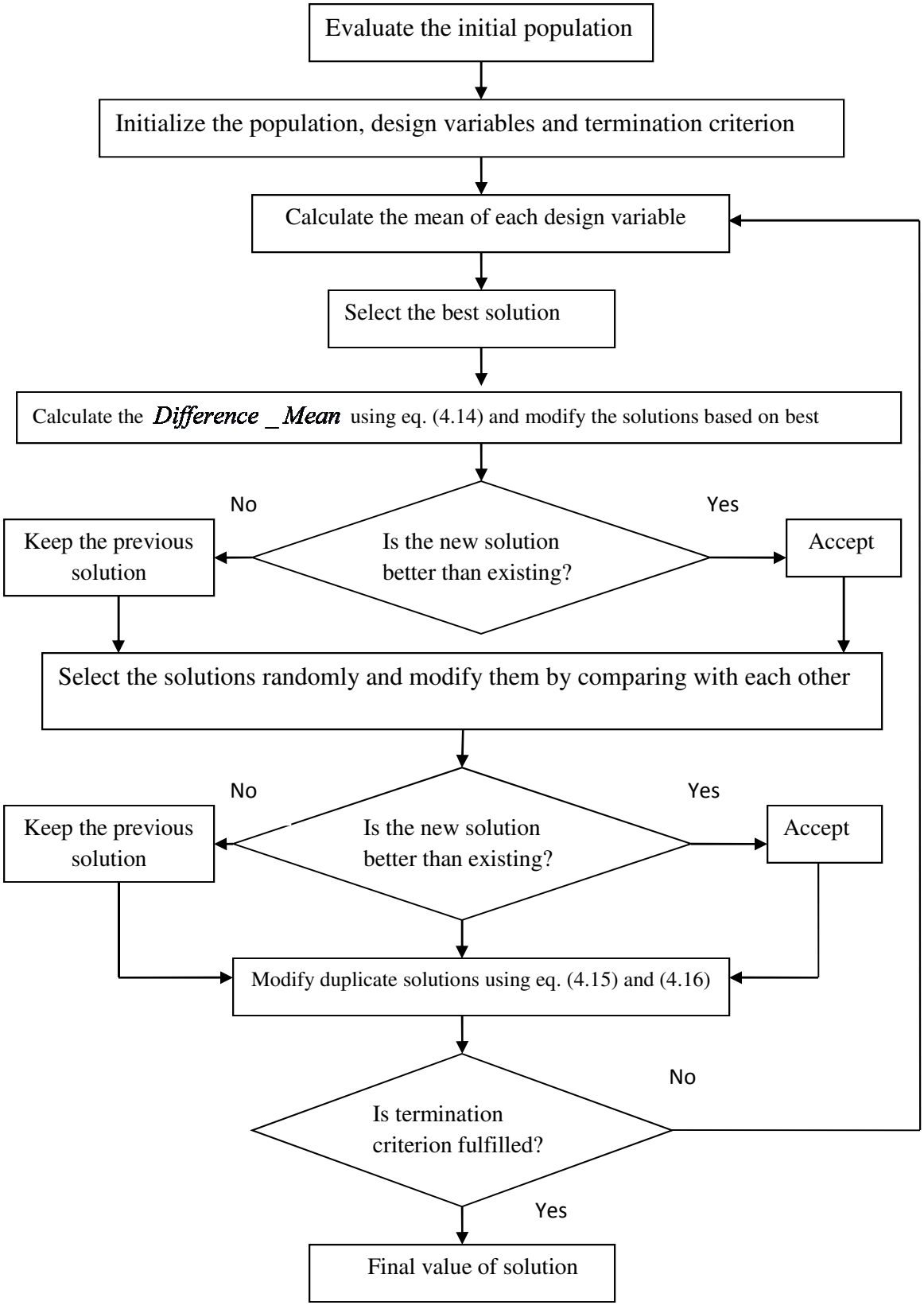

Fig. 4.3. Flowchart of MTLBO algorithm

4.5. Simulation and Results of MTLBO algorithm

The developed MTLBO has been pertained to solve three test systems and 15 benchmark functions. Computational results of three test systems have been used to compare the efficacy of the developed MTLBO approach with that of other evolutionary techniques suggested in the literature. The developed MTLBO is utilized by using MATLAB 7.0 on a PC (Pentium-IV, 80 GB, 3.0 GHz).

4.5.1. Test System 1

This system comprises four conventional thermal generators, two cogeneration units and a heat-only unit. Here, transmission loss is taken into account. Unit data has been modified from [39]. System data containing coefficients of fuel cost equations, prohibited operating zones, B loss coefficients and heat-power feasible regions are given in the Appendix. The power and heat demand of the test system are 600 MW and 150 MWth respectively. Here, two cases are chosen.

Case 1

Here, only valve point loading of conventional thermal generators has been considered. The problem is solved by using the developed MTLBO. Here, the population size (N_P) and the maximum iteration number (N_{max}) have been selected as 50 and 100 respectively for the test system under consideration. The power and heat generations corresponding to best cost obtained from proposed MTLBO is summarized in Table 4.1. The best, average and worst cost and average CPU time among 100 runs of solutions obtained from developed MTLBO are summarized in Table 4.2. The cost acquired from classical PSO (CPSO) [50], time varying acceleration coefficients PSO (TVAC-PSO) [50], teaching learning-based optimization (TLBO) [51] and oppositional teaching learning based optimization (OBTLBO) [51] are also shown in Table 4.2.

The cost convergence characteristic acquired from developed MTLBO is portrayed in Fig. 4.4. It is observed from Table 4.2 that the cost found by using MTLBO is the lowest among all other techniques.

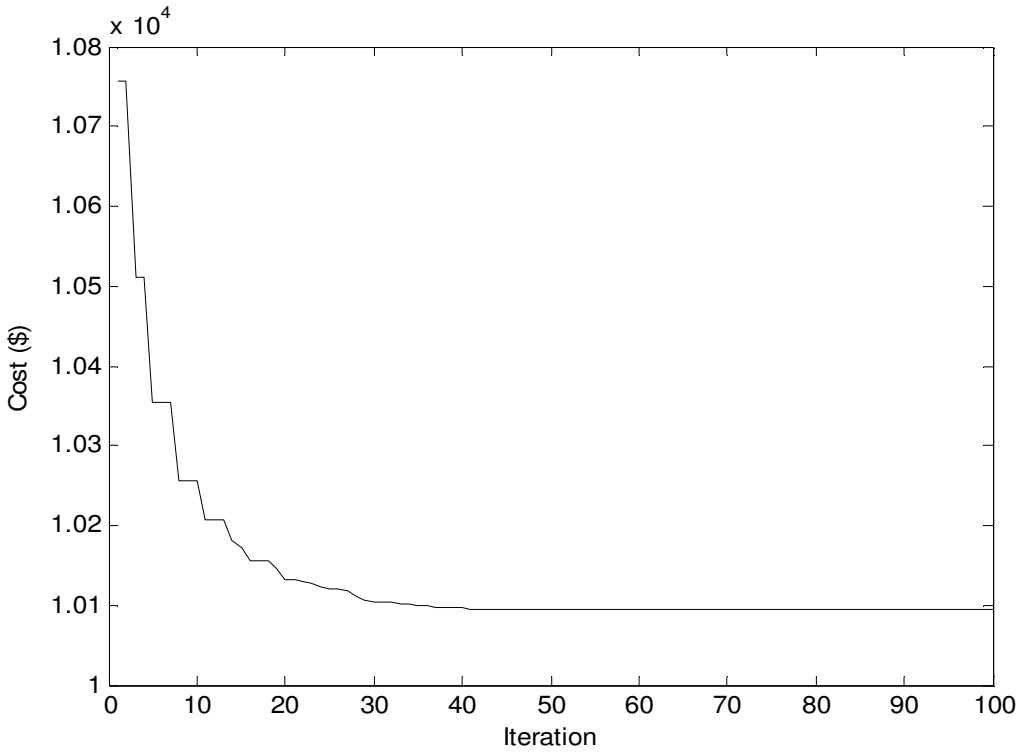

Fig. 4.4. Cost convergence characteristics for case 1 of test system 1

Table 4.1: Power generation (MW) and heat generation (MWth) for case 1 of Test System 1

P_1	45.6342	P_4	209.8158	H_5	27.7500	Ploss	0.7499
P_2	98.5397	P_5	94.0869	H_6	74.9991		
P_3	112.6732	P_6	40.0001	H_7	47.2509		

Table 4.2: Comparison of performance for case 1 of Test System 1

Techniques	Best cost ($)	Average cost ($)	Worst cost ($)	CPU time (s)
MTLBO	10094.25	10094.34	10094.47	2.25
TVAC-PSO [50]	10100.31	-	-	-
CPSO [50]	10325.33	-	-	-
OBTLBO [51]	10094.35	10099.40	10106.83	3.06
TLBO [51]	10094.83	10114.15	10133.61	2.86

Case 2

Here, valve point loading of conventional thermal generators and prohibited operating zones of conventional thermal generators have been considered. The data of conventional thermal generator is same as in [50] except the following modifications in Table A.1 which lists the prohibited zones of conventional thermal generating units. These forbidden regions result in three disjoint feasible sub-regions for each of the conventional thermal generators. Hence, those zones result in a non-convex decision space which consists of 81 convex sub-spaces for this system. The problem is solved by using the developed MTLBO. Here, the population size (N_P) and the maximum iteration number (N_{max}) have been selected as 50 and 100 respectively for the test system under consideration.

The power and heat generations corresponding to best cost acquired from developed MTLBO is summarized in Table 4.3. The best, average and worst cost and average CPU time among 100 runs of solutions obtained from developed MTLBO are summarized in Table 4.4. The cost convergence characteristic acquired from developed MTLBO is portrayed in Fig. 4.5.

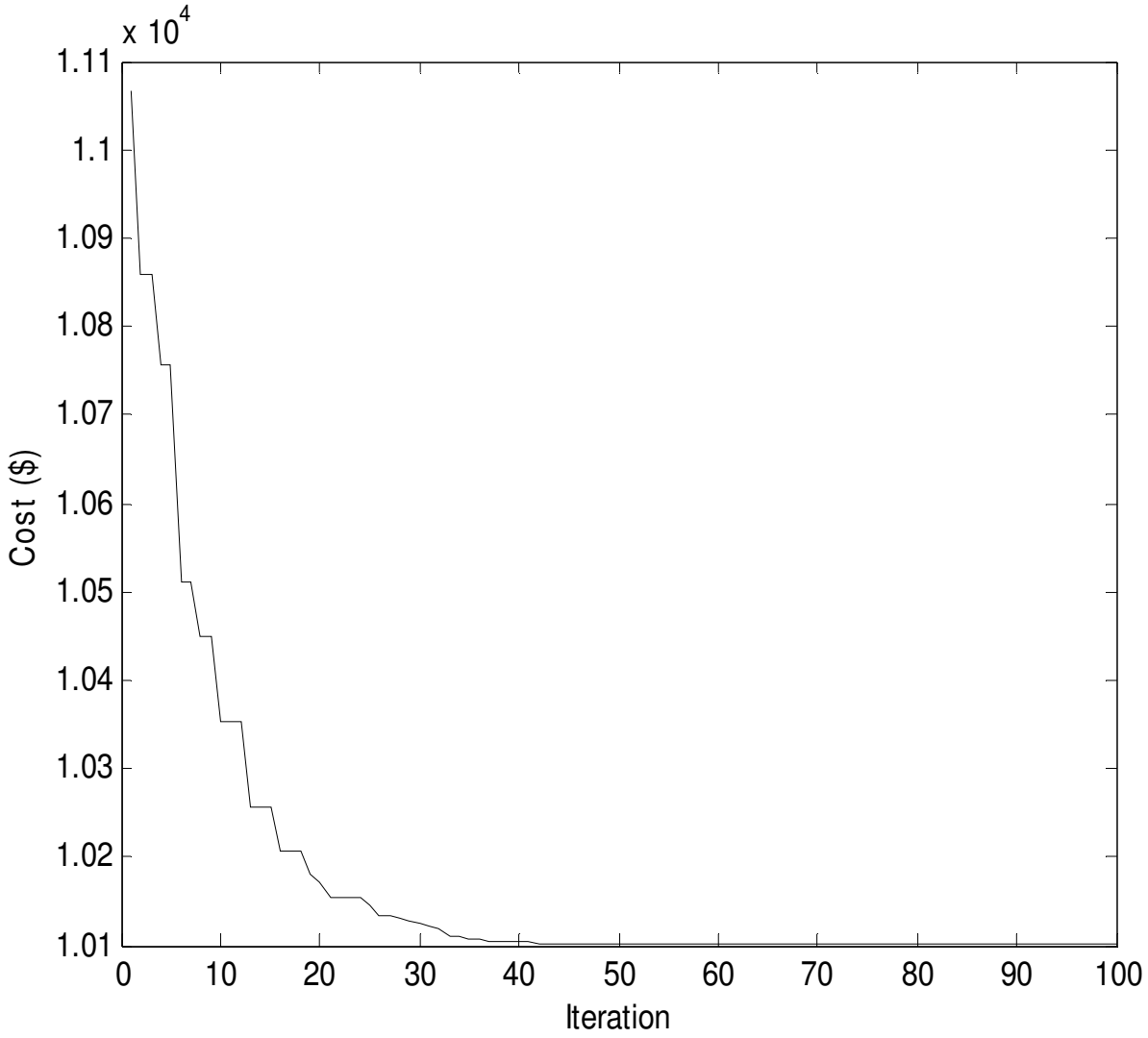

Fig. 4.5. Cost convergence characteristics for case 2 of test system 1

Table 4.3: Power generation (MW) and heat generation (MWth) for case 2 of Test System 1

P_1	44.1501	P_4	209.8158	H_5	27.6123	Ploss	0.7511
P_2	100.0015	P_5	94.1101	H_6	74.9999		
P_3	112.6736	P_6	40.0000	H_7	47.3878		

Table 4.4: Comparison of performance for case 2 of Test System 1

Techniques	MTLBO
Best cost ($)	10101.29
Average cost ($)	10101.44
Worst cost ($)	10101.71
CPU time (s)	2.5656

4.5.2. Test System 2

The system consists of thirteen conventional thermal generators having prohibited operating zones and valve-point effect, six cogeneration units and five heat-only units. System data containing coefficients of fuel cost equations, prohibited operating zones, and heat-power feasible regions are given in the Appendix. The power and heat demands of the test system are 2350 MW and 1250 MWth respectively. Here, two cases are chosen.

Case 1

Here, only valve point loading of conventional thermal generators has been considered. The problem is solved by using the proposed MTLBO. Here, the population size (N_P) and the maximum iteration number (N_{max}) have been selected as 100 and 100 respectively for the test system under consideration. The power and heat generations corresponding to best cost acquired from developed MTLBO is summarized in Table 4.5.

The best, average and worst cost and average CPU time among 100 runs of solutions obtained from developed MTLBO are summarized in Table 4.6. The cost obtained from classical PSO (CPSO) [50], time varying acceleration coefficients PSO (TVAC-PSO) [50], teaching learning based optimization (TLBO) [51] and oppositional teaching learning based optimization (OBTLBO) [51] are also summarized in Table 4.6. The cost convergence characteristic acquired from developed MTLBO is portrayed in Fig. 4.6. It has been observed seen from Table 4.6 that the cost found by using MTLBO is the lowest among all other techniques.

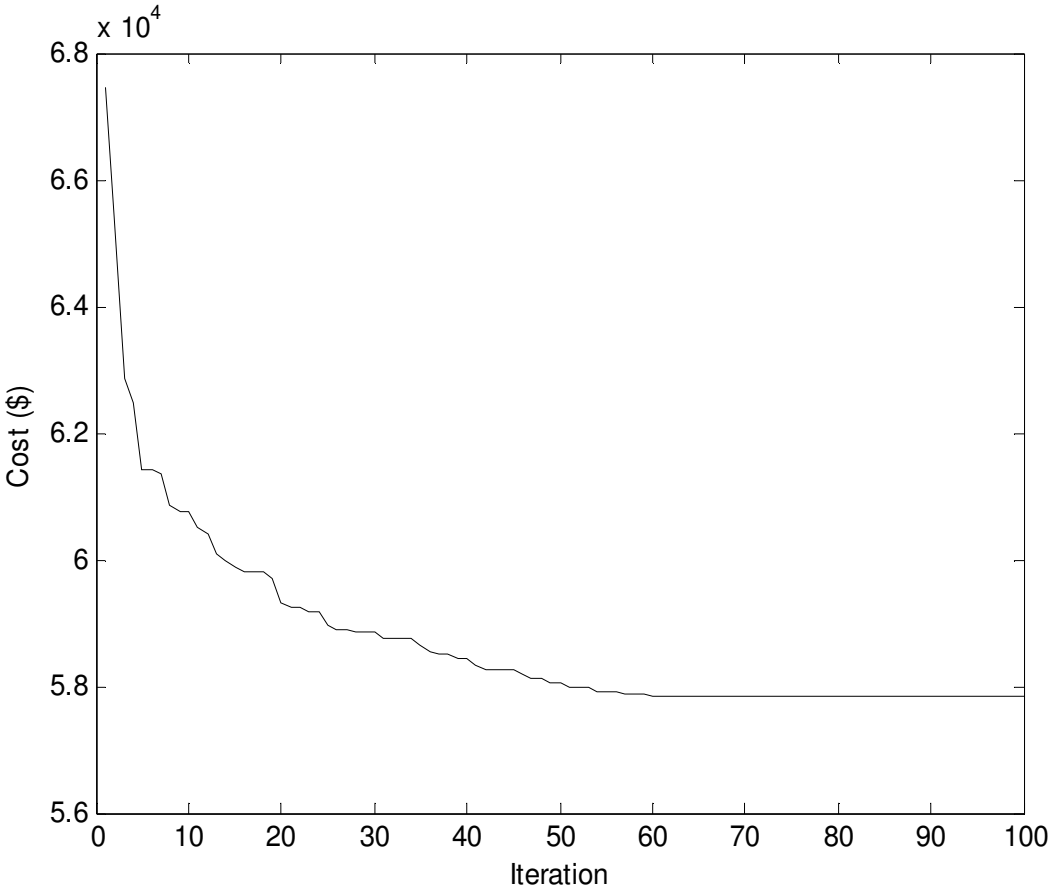

Fig. 4.6. Cost convergence characteristics for case 1 of test system 2

Table 4.5: Power generation (MW) and heat generation (MWth) for case 1 of Test System 2

P_1	538.5724	P_{11}	77.8364	H_{15}	76.5205
P_2	298.6487	P_{12}	55.0023	H_{16}	105.5142
P_3	298.9085	P_{13}	55.0109	H_{17}	75.4833
P_4	110.2820	P_{14}	81.0524	H_{18}	39.9999
P_5	110.2645	P_{15}	40.0015	H_{19}	18.3944
P_6	110.3381	P_{16}	81.0030	H_{20}	468.9043
P_7	110.2745	P_{17}	40.0009	H_{21}	59.9994
P_8	110.2452	P_{18}	10.0002	H_{22}	59.9999
P_9	110.1592	P_{19}	35.0001	H_{23}	119.9854
P_{10}	77.3992	H_{14}	105.2219	H_{24}	119.9768

Table 4.6: Comparison of performance for case 1 of Test System 2

Techniques	Best cost ($)	Average cost ($)	Worst cost ($)	CPU time (s)
MTLBO	57829.49	57830.21	57830.95	5.19
TVAC-PSO [50]	58122.74	58198.31	58359.55	7.84
CPSO [50]	59736.26	59853.47	60076.69	8.00
OBTLBO [51]	57856.26	57883.21	57913.77	5.82
TLBO [51]	58006.99	58014.36	58038.52	5.67

Case 2

Here, valve point loading of conventional thermal generators and prohibited operating zones of conventional thermal generators have been considered. The data of conventional thermal generator is same as in [50] except the following modifications in Table A.2 which lists the prohibited zones of conventional thermal generating units 1, 2, 3, 10 and 11. These forbidden regions result in four disjoint feasible sub-regions for each of conventional thermal generators 1, 2, and 3 and three disjoint feasible sub-regions for each of the conventional thermal generators 10 and 11. Hence, those zones result in a non-convex decision space which consists of 576 convex sub-spaces for this system.

The problem is solved by using the developed MTLBO. Here, the population size (N_P) and the maximum iteration number (N_{max}) have been selected as 100 and 100 respectively for the test system under consideration.

The power and heat generations corresponding to best cost obtained from proposed MTLBO is summarized in Table 4.7. The best, average and worst cost and average CPU time among 100 runs of solutions acquired from developed MTLBO are given in Table 4.8. The cost convergence characteristic acquired from developed MTLBO is portrayed in Fig. 4.7.

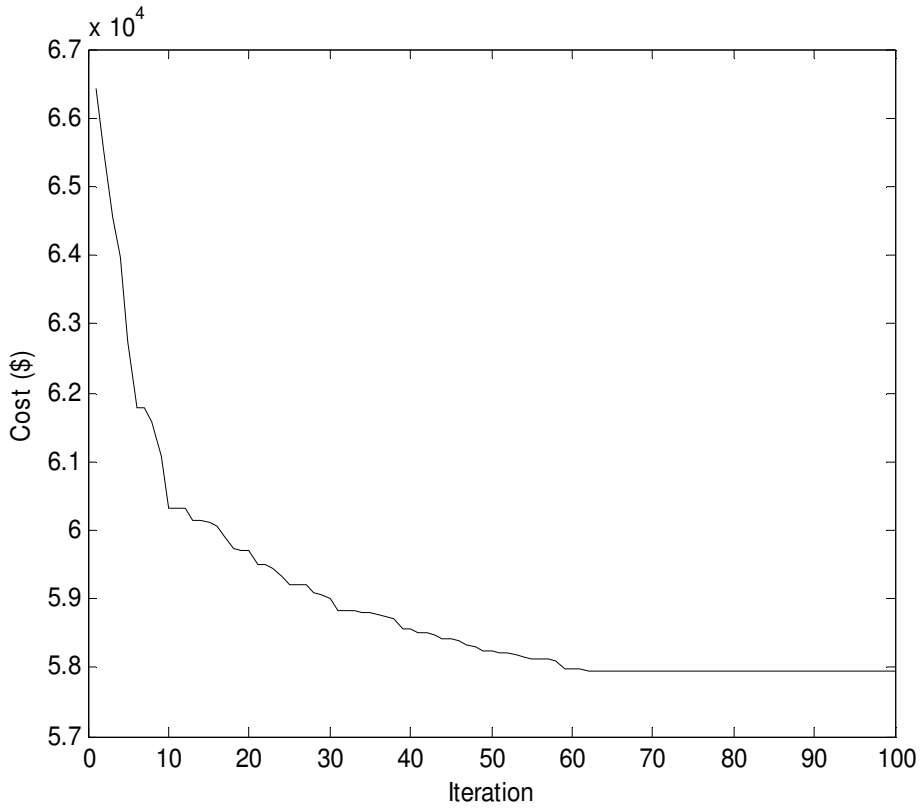

Fig. 4.7. Cost convergence characteristics for case 2 of test system 2

Table 4.7: Power generation (MW) and heat generation (MWth) for case 2 of Test System 2

P_1	628.3185	P_{11}	40.0000	H_{15}	79.2433
P_2	299.2051	P_{12}	55.0000	H_{16}	107.7938
P_3	224.4078	P_{13}	92.3999	H_{17}	80.1432
P_4	60.0000	P_{14}	89.3203	H_{18}	40.0006
P_5	159.7331	P_{15}	44.8825	H_{19}	20.0013
P_6	60.0000	P_{16}	86.3330	H_{20}	453.3426
P_7	159.7331	P_{17}	45.9304	H_{21}	60.0000
P_8	60.0000	P_{18}	10.0000	H_{22}	60.0000
P_9	159.7331	P_{19}	35.0029	H_{23}	120.0000
P_{10}	40.0000	H_{14}	109.4702	H_{24}	120.0000

Table 4.8: Comparison of performance for case 2 of Test System 2

Techniques	MTLBO
Best cost ($)	57942.33
Average cost ($)	57943.05
Worst cost ($)	57943.86
CPU time (s)	5.8787

4.5.3. Test System 3

This system consists of twenty six conventional thermal generators, twelve cogeneration units and ten heat-only units. Data of this test system is obtained by duplicating data of test system 3. Characteristics of conventional thermal generators 1-13 and 14-26 in this test system are same as units 1-13 in test system 3. Characteristics of cogeneration units 27-32 and 33-38 are same as units 14-19 in case of test system 3. Also characteristics of heat-only units 39-43 and 44-48 are same as units 19-24 in case of test system 3. The power and heat demands of this test system are 4700 MW and 2500 MWth respectively. Total number of decision variables is sixty. Here, two cases are considered.

Case 1

Here, only valve point loading of conventional thermal generators has been considered. The problem is solved by using the developed MTLBO. Here, the population size (N_P) and the maximum iteration number (N_{max}) have been selected as 200 and 200 respectively for the test system under consideration. The power and heat generations corresponding to best cost acquired from proposed MTLBO is summarized in Table 4.9. The best, average and worst cost and average CPU time among 100 runs of solutions acquired from developed MTLBO are summarized in Table 4.10. The cost obtained from classical PSO (CPSO) [50], time varying acceleration coefficients PSO (TVAC-PSO) [50], teaching learning based optimization (TLBO) [51] and oppositional teaching learning based optimization (OBTLBO) [51] are also summarized in Table 4.10. The cost convergence characteristic acquired from developed MTLBO is

portrayed in Fig. 4.8. It has been observed from Table 4.10 that the cost found by using MTLBO is the lowest among all other techniques.

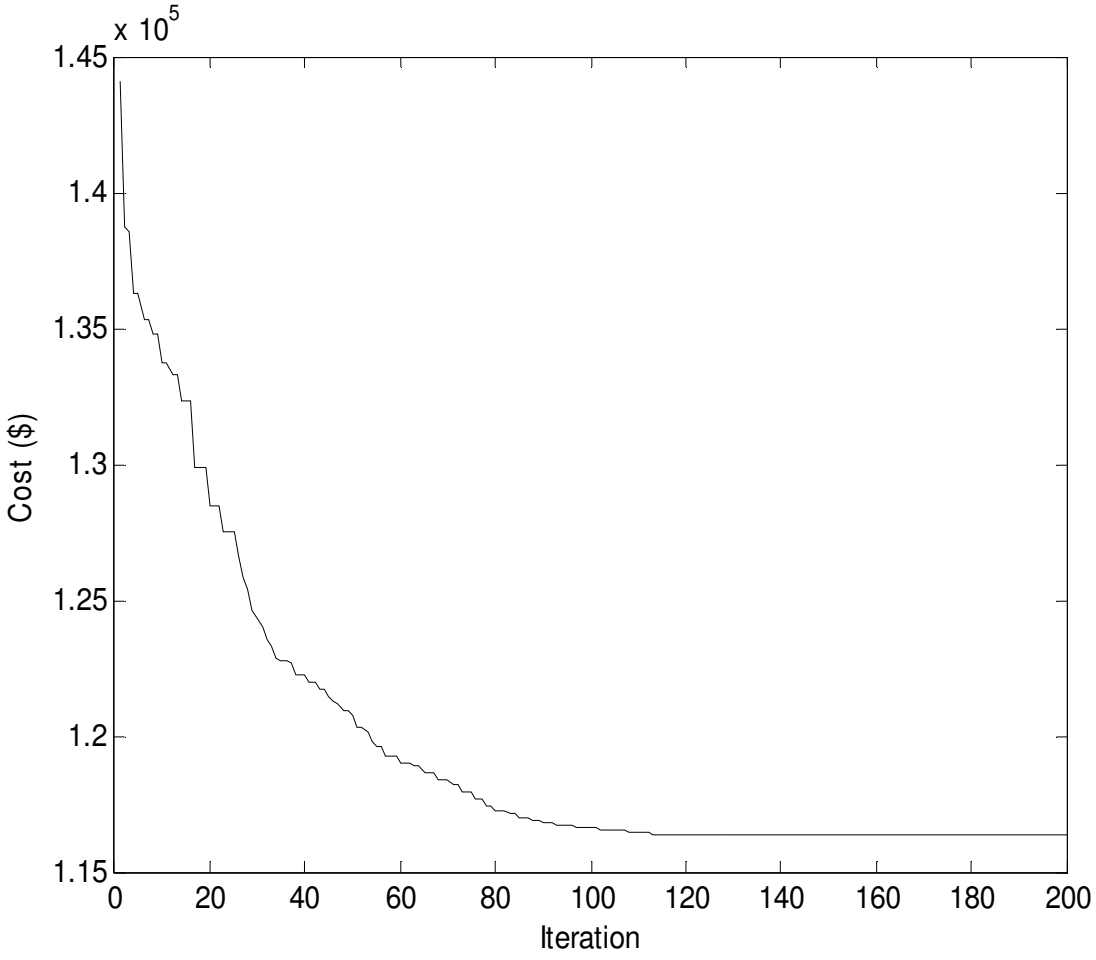

Fig. 4.8. Cost convergence characteristics for case 1 of test system 3

Table 4.9: Power generation (MW) and heat generation (MWth) for case 1of Test System 3

P_1	628.3190	P_{16}	299.2444	P_{31}	10.0001	H_{34}	85.8329
P_2	153.5074	P_{17}	60.0003	P_{32}	35.2279	H_{35}	108.9109
P_3	225.6470	P_{18}	109.8680	P_{33}	84.3575	H_{36}	85.8975
P_4	159.7349	P_{19}	60.0000	P_{34}	52.5133	H_{37}	40.0019
P_5	60.0002	P_{20}	159.7331	P_{35}	88.3237	H_{38}	22.8867
P_6	159.7332	P_{21}	159.7332	P_{36}	52.5881	H_{39}	461.4128
P_7	159.7331	P_{22}	159.7333	P_{37}	10.0031	H_{40}	60.0000
P_8	60.0000	P_{23}	40.0772	P_{38}	41.3508	H_{41}	60.0000
P_9	159.7336	P_{24}	114.8015	H_{27}	110.0761	H_{42}	120.0000
P_{10}	114.7999	P_{25}	92.4022	H_{28}	80.5508	H_{43}	120.0000
P_{11}	114.8010	P_{26}	119.9999	H_{29}	105.5007	H_{44}	423.9202
P_{12}	55.0001	P_{27}	90.3999	H_{30}	88.2204	H_{45}	60.0000
P_{13}	55.0055	P_{28}	46.3967	H_{31}	40.0006	H_{46}	60.0000
P_{14}	269.2799	P_{29}	82.2470	H_{32}	20.1036	H_{47}	120.0000
P_{15}	300.4257	P_{30}	55.2780	H_{33}	106.6851	H_{48}	120.0000

Table 4.10: Comparison of performance for case 1 of Test System 3

Techniques	Best cost ($)	Average cost ($)	Worst cost ($)	CPU time (s)
MTBLO	116402.48	116403.17	116403.75	6.32
TVAC-PSO [50]	117824.89	-	-	-
CPSO [50]	119708.88	-	-	-
OBTLBO [51]	116579.23	116613.65	116649.44	10.9
TLBO [51]	116739.36	116756.00	116825.82	10.3

Case 2

Here, valve point loading of conventional thermal generators and prohibited operating zones of conventional thermal generators have been considered. The data of conventional thermal generator is same as in case 1 except the following modifications in Table A.3 which lists the forbidden regions of conventional thermal generators 1, 2, 3, 10, 11, 14, 15, 16, 23 and 24. These prohibited zones result in four disjoint feasible sub-regions for each of conventional thermal generators 1, 2, 3, 14, 15 and 16 and three disjoint feasible sub-regions for each of the conventional thermal generators 10, 11, 23 and 24. Hence, those zones result in a non-convex decision space which consists of 331776 convex sub-spaces for this system.

The problem is solved by using the developed MTLBO. Here, the population size (N_P) and the maximum iteration number (N_{max}) have been selected as 200 and 200 respectively for the test system under consideration. The power and heat generations corresponding to best cost obtained from developed MTLBO is summarized in Table 4.11.

The best, average and worst cost and average CPU time among 100 runs of solutions acquired from developed MTLBO are summarized in Table 4.12. The cost convergence characteristic acquired from proposed MTLBO is portrayed in Fig. 4.9.

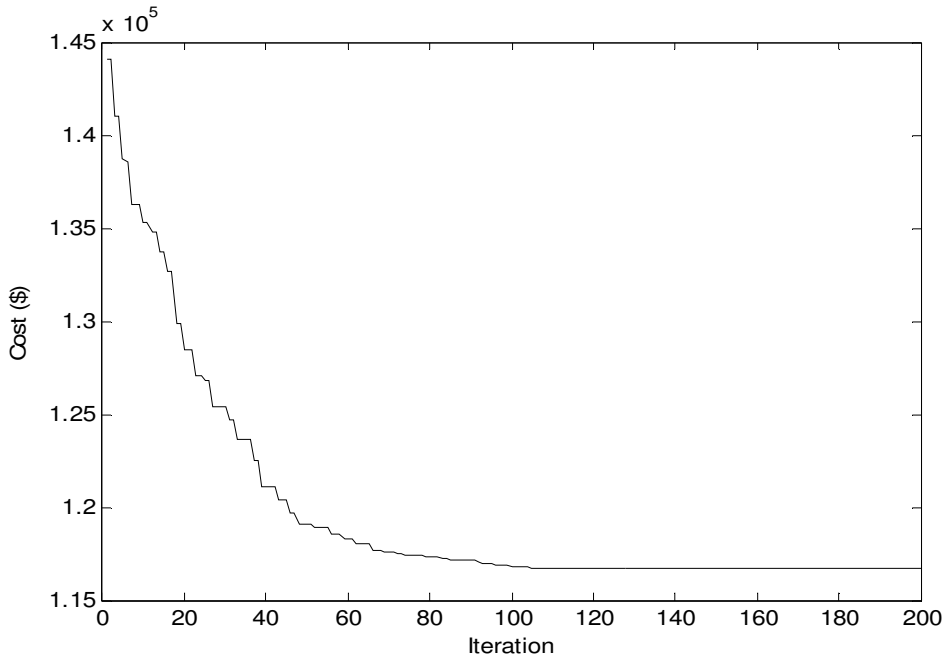

Fig. 4.9. Cost convergence characteristics for case 2 of test system 3

Table 4.11: Power generation (MW) and heat generation (MWth) for case 2 of Test System 3

P_1	628.4322	P_{16}	152.6009	P_{31}	10.0213	H_{34}	81.3596
P_2	225.2795	P_{17}	159.7504	P_{32}	45.0196	H_{35}	108.4749
P_3	360.0000	P_{18}	159.9559	P_{33}	81.0331	H_{36}	89.0333
P_4	159.7473	P_{19}	159.7512	P_{34}	47.3354	H_{37}	40.0626
P_5	159.8316	P_{20}	159.8017	P_{35}	87.6543	H_{38}	20.2502
P_6	159.7316	P_{21}	159.9887	P_{36}	56.2196	H_{39}	448.2178
P_7	160.0075	P_{22}	159.7755	P_{37}	10.2250	H_{40}	60.0000
P_8	159.7481	P_{23}	114.8030	P_{38}	35.5826	H_{41}	60.0000
P_9	109.9707	P_{24}	115.2846	H_{27}	115.5509	H_{42}	119.9999
P_{10}	40.0307	P_{25}	55.0887	H_{28}	83.6316	H_{43}	119.9994
P_{11}	40.0046	P_{26}	119.9971	H_{29}	.105.9947	H_{44}	438.7974
P_{12}	119.9529	P_{27}	100.2425	H_{30}	79.3812	H_{45}	59.9972
P_{13}	55.1176	P_{28}	50.0101	H_{31}	39.9999	H_{46}	60.0000
P_{14}	0	P_{29}	83.2744	H_{32}	24.5086	H_{47}	119.9998
P_{15}	153.6658	P_{30}	45.0643	H_{33}	104.7422	H_{48}	119.9988

Table 4.12: Comparison of performance for case 2 of Test System 3

Techniques	MTLBO
Best cost ($)	116669.57
Average cost ($)	116670.34
Worst cost ($)	116671.77
CPU time (s)	7.9805

4.6. Benchmark Functions

The developed MTLBO and TLBO have been pertained for solving 15 benchmark functions. These test functions are revealed in Table 4.13. The first five functions $f_1 - f_5$ are unimodal high-dimensional functions. The next four functions $f_6 - f_9$ are multimodal functions and the number of local minima raises exponentially with the problem dimension. Functions $f_{10} - f_{15}$ are low-dimensional functions and have only a few local minima. Table 4.14 shows the coefficients of function f_{10}. Table 4.15 and Table 4.16 show the coefficients of f_{14} and f_{15}.

To verify the performance of the proposed technique, these 15 test functions are repeatedly tested by using the MTLBO. In MTLBO, the population size (N_P) is taken as 50. Each test is repeated 100 times. Mean results of 15 test functions acquired from 100 runs are summarized in Table 4.15. Table 4.16 summarizes best optimum values and the variables corresponding to the best optimum value, number of iterations and CPU time of all 15 benchmark functions in 100 runs acquired from MTLBO.

These 15 test functions are also tested by using TLBO technique. In TLBO, the population size (N_P) is taken as 50. Table 4.17 shows best optimum values, number of iterations and CPU time acquired from TLBO.

Table 4.14: Function f_{10}

i	a_i	b_i^{-1}
1	0.1957	0.25
2	0.1947	0.5
3	0.1735	1
4	0.1600	2
5	0.0844	4
6	0.0627	6
7	0.0456	8
8	0.0342	10
9	0.0323	12
10	0.0235	14
11	0.0246	16

Table 4.13: Test Functions

Mathematical representation	Domain	Optimum
$f_1(x)=\sum_{i=1}^{30} x_i^2$	[-100,100]	0
$f_2(x)=\sum_{i=1}^{30}\lvert x_i\rvert+\prod_{i=1}^{30}\lvert x_i\rvert$	[-10,10]	0
$f_3(x)=\sum_{i=1}^{30}\left(\sum_{j=1}^{i} x_j\right)^2$	[-100,100]	0
$f_4(x)=\max_i\{\lvert x_i\rvert,1\le i\le 30\}$	[-100,100]	0
$f_5(x)=\sum_{i=1}^{29}\left[100\left(x_{i+1}-x_i^2\right)^2+\left(x_i-1\right)^2\right]$	[-30,30]	0
$f_6(x)=\sum_{i=1}^{30}\left[x_i^2-10\cos\left(2\pi x_i\right)+10\right]$	[-5.12,5.12]	0
$f_7(x)=-20\exp\left(-0.2\sqrt{\frac{1}{30}\sum_{i=1}^{30}x_i^2}\right)-\exp\left(\frac{1}{30}\sum_{i=1}^{30}\cos 2\pi x_i\right)+20+$	[-32,32]	0
$f_8(x)=\frac{1}{4000}\sum_{i=1}^{30}x_i^2-\prod_{i=1}^{30}\cos\left(\frac{x_i}{\sqrt{i}}\right)+1$	[-600,600]	0
$f_9(x)=\sum_{i=1}^{5} i\cos[(i+1)x_1+i]\sum_{i=1}^{5} i\cos[(i+1)x_2+i]$	[-10,10]	-186.73
$f_{10}(x)=\sum_{i=1}^{11}\left[a_i-\frac{x_1\left(b_i^2+b_i x_2\right)}{b_i^2+b_i x_3+x_4}\right]$	[-5,5]	0.0003075
$f_{11}(x)=4x_1^2-2.1x_1^4+\frac{1}{3}x_1^6+x_1x_2-4x_2^2+4x_2^4$	[-5,5]	-1.0316285
$f_{12}(x)=\left(x_2-\frac{5.1}{4\pi^2}x_1^2+\frac{5}{\pi}x_1-6\right)^2+10\left(1-\frac{1}{8\pi}\right)\cos x_1+10$	[-5,10] ,[0,15]	0.398
$f_{13}(x)=[1+(x_1+x_2+1)^2(19-14x_1+3x_1^2-14x_2+6x_1x_2+3x_2^2)]$ $\times[30+(2x_1-3x_2)^2\times(18-32x_1+12x_1^2+48x_2-36x_1x_2+27x_2^2)]$	[-2,2]	3
$f_{14}(x)=-\sum_{i=1}^{4}c_i\exp\left[-\sum_{j=1}^{3}a_{ij}\left(x_j-p_{ij}\right)^2\right]$	[0,1]	-3.86
$f_{15}(x)=-\sum_{i=1}^{4}c_i\exp\left[-\sum_{j=1}^{6}a_{ij}\left(x_j-p_{ij}\right)^2\right]$	[0,1]	-3.32

Table 4.15: Function f_{14}

i	a_{ij}, j=1,2,3			c_i	p_{ij}, j=1,2,3		
1	3	10	30	1	0.36890	0.1170	0.2673
2	0.1	10	35	1.2	0.46990	0.4387	0.7470
3	3	10	30	3	0.10910	0.8732	0.5547
4	0.1	10	35	3.2	0.03815	0.5743	0.8828

Table 4.16: Function f_{15}

i	a_{ij}, j = 1,....,6						c_i	p_{ij}, j = 1,....,6					
1	10	3	17	3.5	1.7	8	1	0.1312	0.1696	0.5569	0.0124	0.8283	0.5886
2	0.05	10	17	0.1	8	14	1.2	0.2329	0.4135	0.8307	0.3736	0.1004	0.9991
3	3	3.5	1.7	10	17	8	3	0.2348	0.1415	0.3522	0.2883	0.3047	0.6650
4	17	8	0.05	10	0.1	14	3.2	0.4047	0.8828	0.8732	0.5743	0.1091	0.0381

Table 4.17: Best optimum value, number of iterations and CPU time acquired from TLBO

Function	TLBO		
	$f(x^*)$	Number of Iterations	CPU time (sec)
f_1	5.4739e-019	200	25.1875
f_2	1.6653e-005	300	39.40625
f_3	0.26788	500	62.6406
f_4	0.05381	500	64.5156
f_5	71.7587	400	54.7812
f_6	33.8118	300	40.6718
f_7	1.5218e-005	300	37.7656
f_8	4.9450	300	39.4531
f_9	-186.7309	100	1.3750
f_{10}	0.0003075	200	5.8751
f_{11}	-1.0316275	50	0.6250
f_{12}	0.397726	50	0.6406
f_{13}	3	50	0.6093
f_{14}	-3.8623	50	0.8751
f_{15}	-3.3219	50	1.4375

4.7. Overview of Heat Transfer Search algorithm

In a Heat Transfer Search (HTS) algorithm [61], a population is analogous to groups of molecules that participate in a heat transfer process attaining different temperature echelons. Here, the different design variables correspond to different temperature of molecules. Further, the energy level of the molecules denotes the objective function value of the problem. The best solution is considered as the surrounding and the remaining solutions as the system. Now, in order to visualize the procedure followed by the HTS algorithm, we need to see the case of thermal imbalance in a system i.e. if a thermal imbalance exists between a system and its surroundings (or within the system itself), the former always tries to reduce this imbalance in order to attain thermal equilibrium. Similarly, during optimization in the Heat transfer search (HTS) algorithm, which is a population based algorithm, if the difference in the solution exists within the population, the solution tries to improve its value. This improvement can be made by taking into account the difference between the present solution and either of the best solution, other random solution from the population or the mean value of the solution from the population.

The HTS algorithm method can be considered to be of three parts namely, 'conduction phase', radiation phase' and convection phase', which oppose the thermal imbalance of the system by conduction, radiation and convection modes of heat transfer respectively. All three modes happen with equal probability, which is managed by the parameter 'R' in each iteration. 'R' is a uniformly random number which varies between 0 and 1. During optimization, as R varies between 0 and 1, for equal probability, each phase must share the equal proportion of R .According to the value of R, any one of the three phases can be applied to update the solution in that iteration as follows:

Value of R	Phase
0-0.3333	Conduction
0.3333-0.6666	Radiation
0.6666-1	Convection

The HTS algorithm starts with a random initial population of n solutions, where n is the size of population. Each solution is an m dimensional vector and m is the number of optimization parameters or design variables. At first the population is initialized and then its value is updated

in each iteration g (g = 1, 2, ….,Gmax) by the search procedure of conduction, convection or radiation phase. Moreover, the selection procedure here is called the greedy selection technique which allows the modernized solution in HTS algorithm only if it creates better objective function value. After selection, the worst solutions of the population are replaced by the best solutions and finally any existing duplicate solution is replaced by a randomly generated solution. The operational procedure of all three phases is brought below to minimize a function $f(x)$, which is the objective function for an optimization problem.

The Conduction Phase

The conduction phase is the part of the algorithm where the system tries to attain thermal balance by conduction heat transfer. Energy is transferred from higher energetic molecules to lower energetic molecules. As declared earlier, if the number of molecules of the system i.e. population be n and the different temperature levels of the molecules i.e. design variables be m, then during the first conduction phase where generation $g \leq$ Gmax/CDF (where CDF is the conduction factor), the solutions are updated as follows:

$$x_{j,i}^{new} = x_{k,i}^{old} + CDS_1 \qquad \text{if } f(x_j) > f(x_k) \tag{4.17}$$

$$x_{k,i}^{new} = x_{j,i}^{old} + CDS_1 \qquad \text{if } f(x_k) > f(x_j) \tag{4.18}$$

where $j = 1,2,.....,n$, $k \in (1,2,.....,n)$, $j \neq k$ and k is a randomly selected solution from the population, $i \in (1,2,...,m)$ and i is a randomly selected design variables. CDS_1 and CDS_2 are the conduction steps stated as follows:

$$CDS_1 = -R^2 x_{k,i}^{old} \tag{4.19}$$

$$CDS_2 = -R^2 x_{j,i}^{old} \tag{4.20}$$

(R = value of probability for the selection of conduction phase)

Here, R^2 is matched up to the conductance of the Fourier's equation and $x_{k,i}$, $x_{j,i}$ are matched up to the temperature gradient. The conductance of any system depends on the thermal conductivity which in turn is a function of temperature. During heat transfer, the temperature of

the system and hence its thermal conductivity and conductance are varying constantly. Thus, to replicate this temperature dependent behavior of conductance, it is represented by variable R which can attain any value between 0 and 0.33333 at the starting of iteration in the conduction phase. Moreover, to use the search space, this random variable is represented by squaring its value so that it can pursue a fine search.

In the second part of the conduction phase where g ≥ Gmax/CDF, the solution are brought up to date as

$$x_{j,i}^{new} = x_{k,i}^{old} + CDS_3 \quad ; \qquad \text{if} \quad f(x_j) > f(x_k) \tag{4.21}$$

$$x_{k,i}^{new} = x_{j,i}^{old} + CDS_4 \quad ; \qquad \text{if} \quad f(x_k) > f(x_j) \tag{4.22}$$

CDS_3 and CDS_4 are the conduction steps stated as follows:

$$CDS_3 = -rx_{k,i}^{old} \tag{4.23}$$

$$CDS_4 = -rx_{j,i}^{old} \tag{4.24}$$

Where r is a random number in the range [0, 1]. In Eqs. (9.16) and (9.17), r matches up to the conductance of the Fourier's equation and $x_{k,i}$ and $x_{j,i}$ are matched up to the temperature gradient. The value of CDF is taken 2 for the conduction phase.

The Convection Phase

The convection phase is the part of the algorithm where the system tries to attain thermal balance by convection heat transfer. Here, the mean temperature of the system interacts with the surrounding temperature to find a thermal balance between the system and the surrounding. The surrounding is considered as the best solution. At any iteration g (where g <Gmax/COF and COF is a convection factor), x_s be the temperature of the surrounding, x_{ms} be the mean temperature of the system. When the energy of the system is higher than that of the surrounding i.e. $f(x_s) < f(x_{ms})$, the solution is updated as follows:

$$x_{j,i}^{new} = x_{j,i}^{old} + \text{COS} \tag{4.25}$$

Where $j = 1,2,...,n$, $i = 1,2,...,m$. Each design variable of the population is updated in the conduction phase. COS is the convection step stated as follows:

$$\text{COS} = R\left(x_s - x_{ms} * TCF\right) \tag{4.26}$$

(R = value of probability for the selection of convection phase)

R becomes equal to the convection element of the Newton's law of cooling and x_s , x_{ms} the temperature of the surrounding and the mean temperature of the system respectively. The system temperature constantly changes during the heat transfer process. The surrounding becomes the heat sink or heat source, so its temperature remains constant. To account this effect, temperature change factor (TCF) is initiated. Thus, TCF is the temperature change factor based on which the mean temperature of the system can be varied. The value of TCF is determined as follows:

$$TCF = abs\left(R - r\right) \quad , \quad \text{if g} \le \text{Gmax/COF} \tag{4.27}$$

$$TCF = round\left(1 + r\right) \quad , \quad \text{if g} \ge \text{Gmax/COF} \tag{4.28}$$

Where r is a random number in the range [0, 1]. The value of TCF changes randomly between 0 and 1 in the first part of the conduction phase. In the second part of the conduction phase, the value of TCF is either 1 or 2. The different value of TCF in the proposed algorithm is to balance the exploration and exploitation. The value of COF is set to 10 for this phase.

The Radiation Phase

The radiation phase is the part of the algorithm where the system tries to attain thermal balance by radiation heat transfer. Here, the system interacts with the surrounding (i.e. best solution) or within the system (i.e. other solution) to achieve thermal balance. In the first part of the radiation phase, where g ≤ Gmax/RDF (where RDF is the radiation factor) the solution is updated (i.e. energy reduction of the system) as follows:

$$x_{j,i}^{new} = x_{j,i}^{old} + RDS_1 \quad , \quad \text{if } f\left(x_j\right) > f\left(x_k\right) \tag{4.29}$$

$$x_{j,i}^{new} = x_{j,i}^{old} + RDS_2 \quad , \quad \text{if } f\left(x_k\right) > f\left(x_j\right) \tag{4.30}$$

Where $j = 1,2,.....,n$, $k \in (1,2,.....,n)$, $j \neq k$ and k is a randomly selected solution from the population, $i \in (1,2,...,m)$. All design variables of the solution is brought up to date during each iteration of the radiation phase. RDS_1 and RDS_2 are radiation step stated as follows:

$$RDS_1 = R\left(x_{k,i}^{old} - x_{j,i}^{old}\right) \tag{4.31}$$

$$RDS_2 = R\left(x_{j,i}^{old} - x_{k,i}^{old}\right) \tag{4.32}$$

(R = the value of probability for the selection of radiation phase)

R matches up to the radiation element of the Stefan-Boltzmann law and x_k, x_j matches up to the system and the surrounding temperature respectively.

In the second part of radiation phase where g ≥Gmax/RDF, the solution is brought up to date as follows:

$$x_{j,i}^{new} = x_{j,i}^{old} + RDS_3, \quad \text{if } f\left(x_j\right) > f\left(x_k\right) \tag{4.33}$$

$$x_{j,i}^{new} = x_{j,i}^{old} + RDS_4, \quad \text{if } f\left(x_k\right) > f\left(x_j\right) \tag{4.34}$$

Where RDS_3 and RDS_4 are radiation step stated as follows:

$$RDS_3 = r\left(x_{k,i}^{old} - x_{j,i}^{old}\right) \tag{4.35}$$

$$RDS_4 = r\left(x_{j,i}^{old} - x_{k,i}^{old}\right) \tag{4.36}$$

Where r is a random number in the range [0, 1] and RDF is the radiation factor which finds out the exploration and exploitation tendency in this phase. In radiation phase, the value of RDF is set to 2.

Fig. 4.10 portrays the flow chart of heat transfer search algorithm.

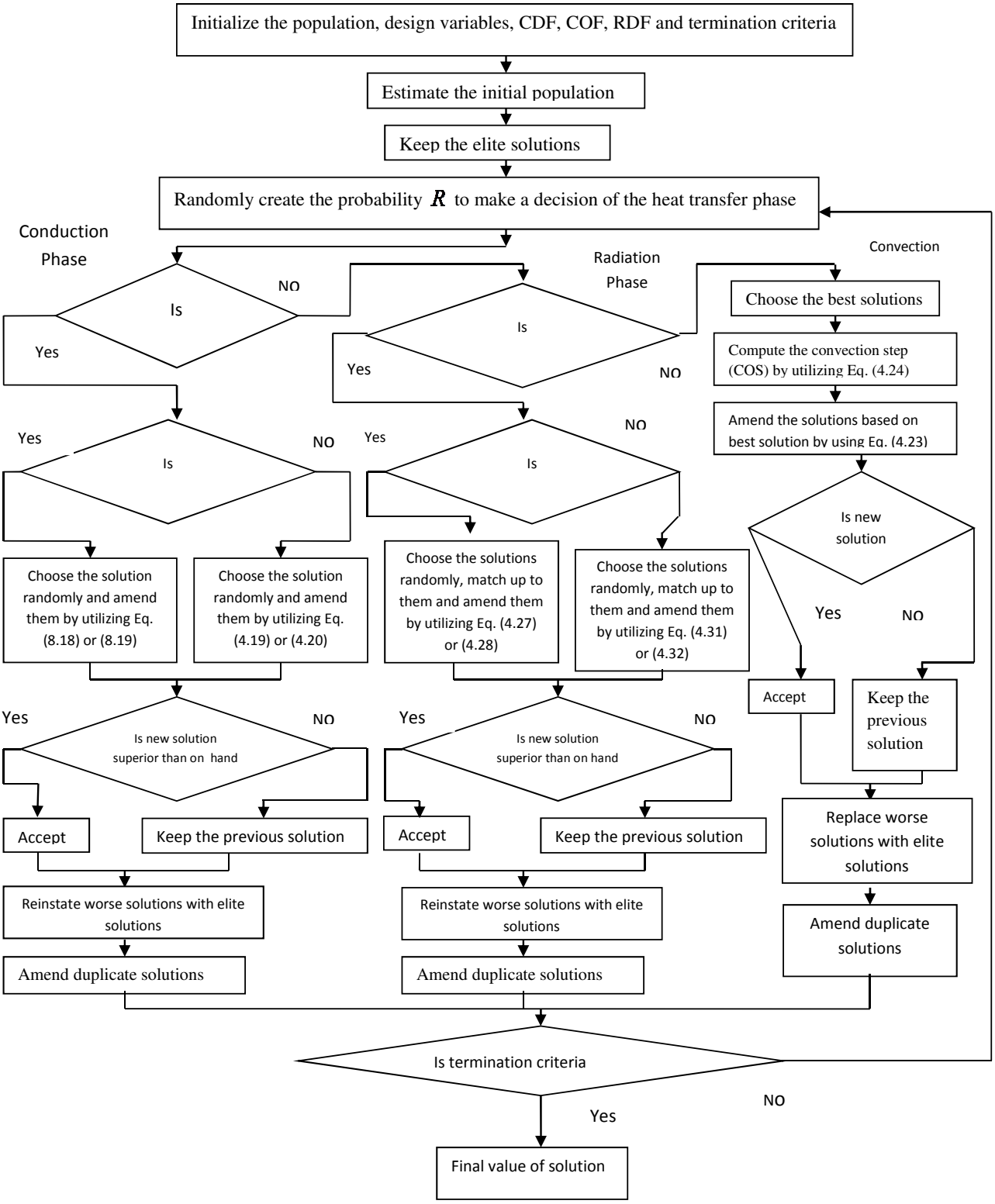

Fig. 4.10. Flow chart of heat transfer search algorithm

4.8. Application of Heat Transfer Search Algorithm for CHPED

The Heat Transfer Search (HTS) algorithm includes three phases each of which is divided in two parts whose activation is based on the current number of iterations and depends on the conduction, convection and radiation factors. Iteration is completed when the randomly selected phase is performed. The HTS algorithm repeats the search process until the predetermined total number of iterations is performed.

The HTS algorithm for solving CHPED problem is described below.

Step 1: Initialize the HTS algorithm parameters: population size (N_P), elite solution size (N_E), conduction factor (*CDF*), convection factor (*COF),* radiation factor (*RDF*). Set the iteration counter: *it*=0.

Step 2: Let $p_k = \begin{bmatrix} P_1, P_2, ..., P_{N_t}, P_{N_t+1}, P_{N_t+2} ..., P_{N_t+N_c}, \\ H_{N_t+1}, H_{N_t+2}, ..., H_{N_t+N_c}, H_{N_t+N_c+1}, \\ H_{N_t+N_c+2}, ..., H_{N_t+N_c+N_h} \end{bmatrix}^T$

be the k th vector of a population to be evolved and $k = 1,2,..., N_P$. The elements of p_k should satisfy the constraints given by equations (4.2)-(4.9). Production cost of each vector p_k is calculated.

Step 3: Increase the iteration counter, *it*=*it*+1. Generate a uniformly distributed random number *R* between 0 and 1 in order to decide which heat transfer phase should be performed.

Step 4: If $0 \le R \le 0.3333$, perform the conduction phase by using Eqs. (4.17-4.24).

Step 5: If $0.3333 < R < 0.6666$, perform the radiation phase by using Eqs (4.29-4.36).

Step 6: If $0.6666 \le R \le 1.0$, perform convection phase by using Eqs. (4.25-4.28).

Step 7: Obtain a new vector. The new vector should satisfy the constraints given by equations (4.2)-(4.9). Calculate the production cost of the new vector. If the production cost of the new vector is less than the previous one, replace them. Otherwise leave the original vector unchanged. Repeat this process until all vectors in the population are updated.

Step 8: Replace the worst solutions of the current iteration with the elite solutions of previous iteration.

Step 9: Stop the search process if the termination criterion is satisfied i.e. maximum number of iterations is reached. Otherwise, go to step 3.

4.9. Prohibited operating zones

Shaft bearing shaking due to steam admission valve opening or the machine and associated auxiliary equipment fault can produce prohibited operating zones in the input-output curve of a conventional thermal generator. The greatest achievable saving is achieved by circumventing operation in these areas. The feasible operating regions of a conventional thermal generator with prohibited operating zones [62] can be stated as:

$$\mathrm{P}_{ti}^{\min} \le \mathrm{P}_{ti} \le \mathrm{P}_{ti,1}^{l}$$

$$\mathrm{P}_{ti,j-1}^{u} \le \mathrm{P}_{ti} \le \mathrm{P}_{ti,j}^{l} \quad , \quad j = 2,3,...,n_i \tag{4.37}$$

$$\mathrm{P}_{ti,n_i}^{u} \le \mathrm{P}_{ti} \le \mathrm{P}_{ti}^{\max} \quad , \quad i \in \mathrm{N}_t$$

where j represents the number of prohibited operating zones of i the conventional thermal generator. $\mathrm{P}_{ti,j-1}^{u}$ is the upper limit of $(j-1)$th prohibited operating zones of i the conventional thermal generator. $\mathrm{P}_{ti,j}^{l}$ is the lower limit of j th prohibited operating zones of i th conventional thermal generator. Total number of prohibited operating zones of i th conventional thermal generator is n_i.

4.10. Simulation and Results of HTS algorithm

The suggested (HTS) has been applied to four different test systems. Computational results have been used to compare the efficacy of the suggested HTS with that of other evolutionary techniques suggested in the literature. The suggested HTS is utilized by using MATLAB 7.0 on a PC (Pentium-IV, 80 GB, 3.0 GHz).

4.10.1. Test System 1

This test system comprises one conventional thermal generator and two cogeneration units and a heat-only unit. Unit data has been adopted from [50]. The power and heat demands of the test system are 200 MW and 115 MWth respectively. Here, two cases are chosen.

Case 1

Firstly, only valve point loading of conventional thermal generator has been reflected on. The problem is pertained to solve by utilizing HTS. Here, the population size (N_P), elite size (N_E) and the maximum iteration number (N_{max}) have been chosen as 50, 5, 100 respectively.

The power and heat generations matching to best cost acquired from the suggested HTS is revealed in Table 4.18. The best, average and worst cost and average CPU time among 100 runs of solutions acquired from suggested HTS are summed up in Table 4.19. The cost acquired from classical PSO (CPSO) [50] and time varying acceleration coefficients PSO (TVAC-PSO) [50] are also summed up in Table 4.19. The cost convergence characteristic acquired from the suggested HTS is portrayed in Fig. 4.11. It has been observed from Table 4.19 that the cost acquired by utilizing HTS is the lowest among all other techniques.

Table 4.18: Power generation (MW) and heat generation (MWth) for case 1 of Test System 1

P_1	0.00039	P_3	40.0000	H_3	75.0058
P_2	159.9996	H_2	39.9911	H_4	0.0031

Table 4.19: Comparison of performance for case 1 of Test System 1

Techniques	HTS	TVAC-PSO [50]	CPSO [50]
Best cost ($)	9256.95	9257.07	9257.08
Average cost ($)	9257.06	-	-
Worst cost ($)	9257.10	-	-
CPU time (s)	1.3897	-	-

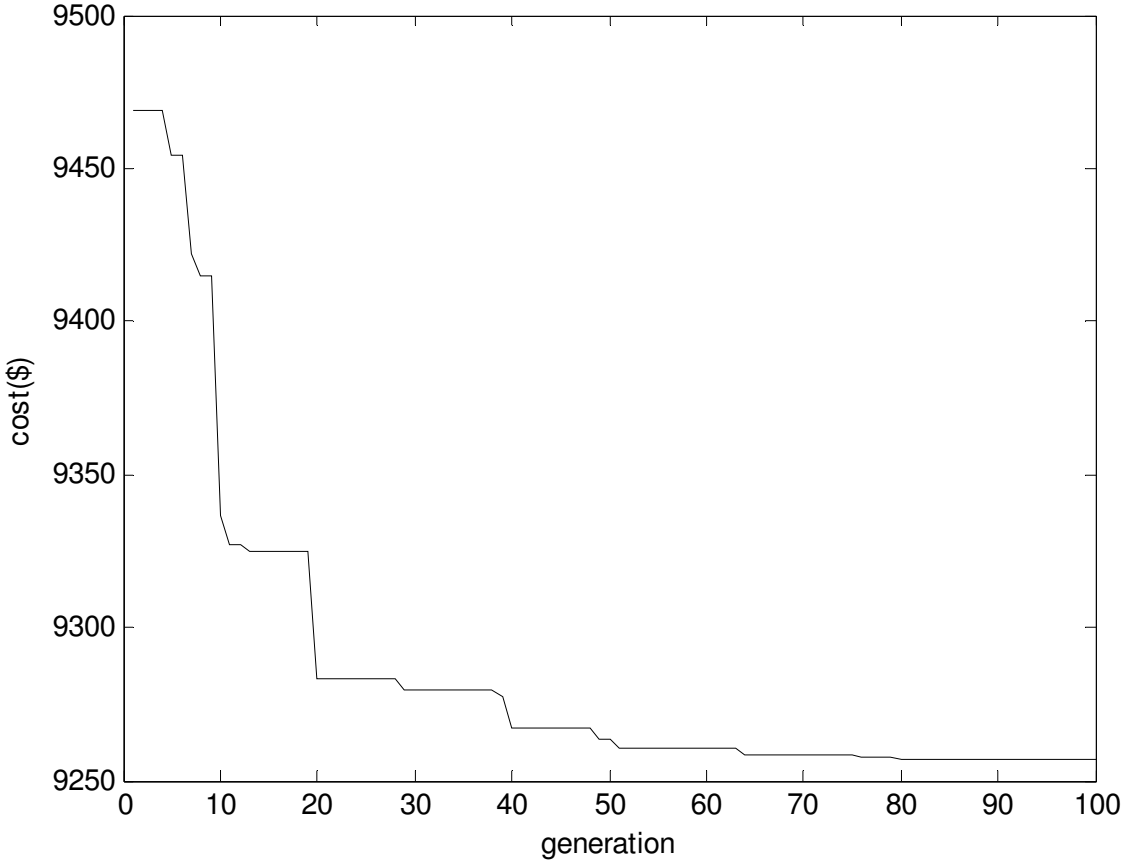

Fig. 4.11. Cost convergence characteristics for case 1 of test system 1

Case 2

Here, valve point loading of conventional thermal generator and prohibited operating zones of conventional thermal generator have been reflected on. The data of conventional thermal generator is similar as in [50].

The problem is pertained to solve by utilizing HTS. Here, the population size (N_P), elite size (N_E) and the maximum iteration number (N_{max}) have been chosen as 50, 5 and 100 respectively. The power and heat generations matching to best cost acquired from the suggested HTS is revealed in Table 4.20. The best, average and worst cost and average CPU time among 100 runs of solutions acquired from suggested HTS are summed up in Table 4.21. The cost convergence characteristic obtained from suggested HTS is portrayed in Fig. 4.12.

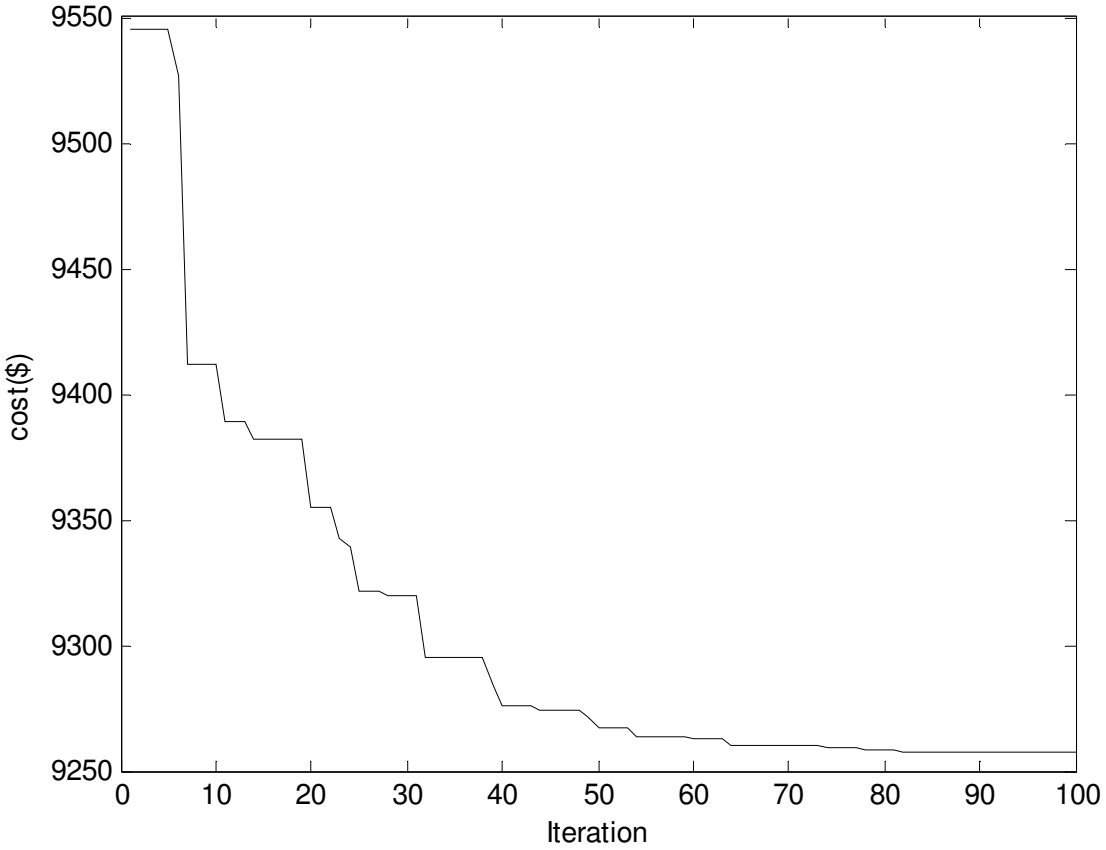

Fig. 4.12. Cost convergence characteristics for case 2 of test system 1

Table 4.20: Power generation (MW) and heat generation (MWth) for case 2 of Test System 1

P_1	0.0012	P_3	40.0000	H_3	75.0005
P_2	159.9988	H_2	39.9908	H_4	0.0086

Table 4.21: Comparison of performance for case 2 of Test System 1

Techniques	HTS
Best cost ($)	9257.04
Average cost ($)	9257.07
Worst cost ($)	9257.12
CPU time (s)	1.6513

4.10.2. Test System 2

This system comprises four conventional thermal generators, two cogeneration units and a heat-only unit. Here, transmission loss is reflected on. Unit data has been adopted from [50]. The power and heat demands of this test system are 600 MW and 150 MWth respectively. Here, two cases are chosen.

Case 1

Firstly, only valve point loading of conventional thermal generators has been reflected on. The problem is pertained to solve by utilizing HTS. Here, the population size (N_P), elite size (N_E) and the maximum iteration number (N_{max}) have been chosen as 50, 5 and 100 respectively.

The power and heat generations matching to best cost acquired from suggested HTS is revealed in Table 4.22. The best, average and worst cost and average CPU time among 100 runs of solutions acquired from suggested HTS are summed up in Table 4.23. The cost acquired from classical PSO (CPSO) [50], time varying acceleration coefficients PSO (TVAC-PSO) [50], teaching learning based optimization (TLBO) [51] and oppositional teaching learning based optimization (OBTLBO) [51] are also summed up in Table 4.23. The cost convergence characteristic acquired from suggested HTS is portrayed in Fig. 4.13. It has been observed from Table 4.23 that the cost acquired by utilizing HTS is the lowest among all other techniques.

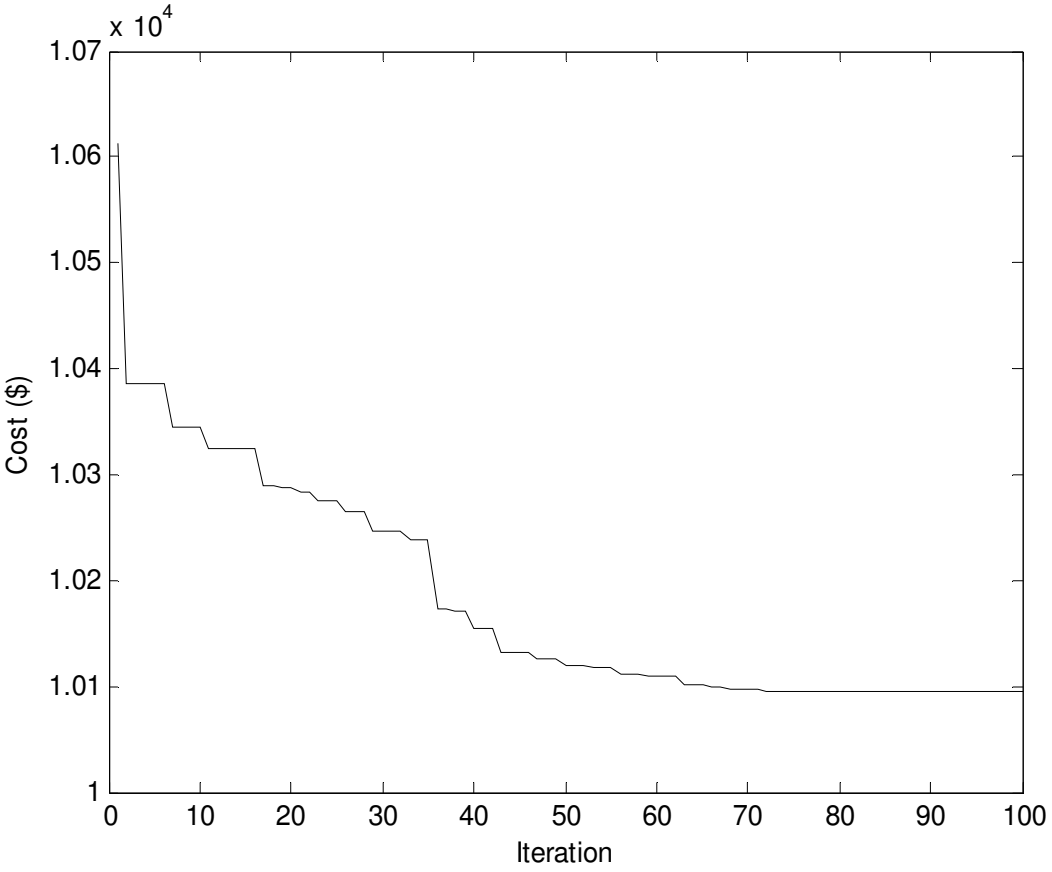

Fig. 4.13. Cost convergence characteristics for case 1 of test system 2

Table 4.22: Power generation (MW) and heat generation (MWth) for case 1 of Test System 2

P_1	45.5410	P_3	112.6714	P_5	94.1215	H_5	27.5498	H_7	47.4842
P_2	98.5905	P_4	209.8220	P_6	40.0035	H_6	74.9660	Ploss	0.7499

Table 4.23: Comparison of performance for case 1 of Test System 2

Techniques	Best cost ($)	Average cost ($)	Worst cost ($)	CPU time(s)
HTS	10094.7109	10094.8512	10094.9743	2.0153
TVAC-PSO [50]	10100.3124	-	-	-
CPSO [50]	10325.3339	-	-	-
OBTLBO [51]	10094.3529	10099.4057	10106.8314	3.06
TLBO [51]	10094.8384	10114.1539	10133.6130	2.86
GSO [58]	10094.2670	10095.6615	10097.2406	2.4203

Case 2

Here, valve point loading of conventional thermal generators and prohibited operating zones of conventional thermal generators have been reflected on. The data of conventional thermal generator is similar as in [50].

The problem is pertained to solve by utilizing HTS. Here, the population size (N_P), elite size (N_E) and the maximum iteration number (N_{max}) have been chosen as 50, 5 and 100 respectively.

The power and heat generations matching to best cost acquired from suggested HTS is summed up in Table 4.24. The best, average and worst cost and average CPU time among 100 runs of solutions acquired from suggested HTS are revealed in Table 4.25. The cost convergence characteristic acquired from suggested HTS is portrayed in Fig. 4.14.

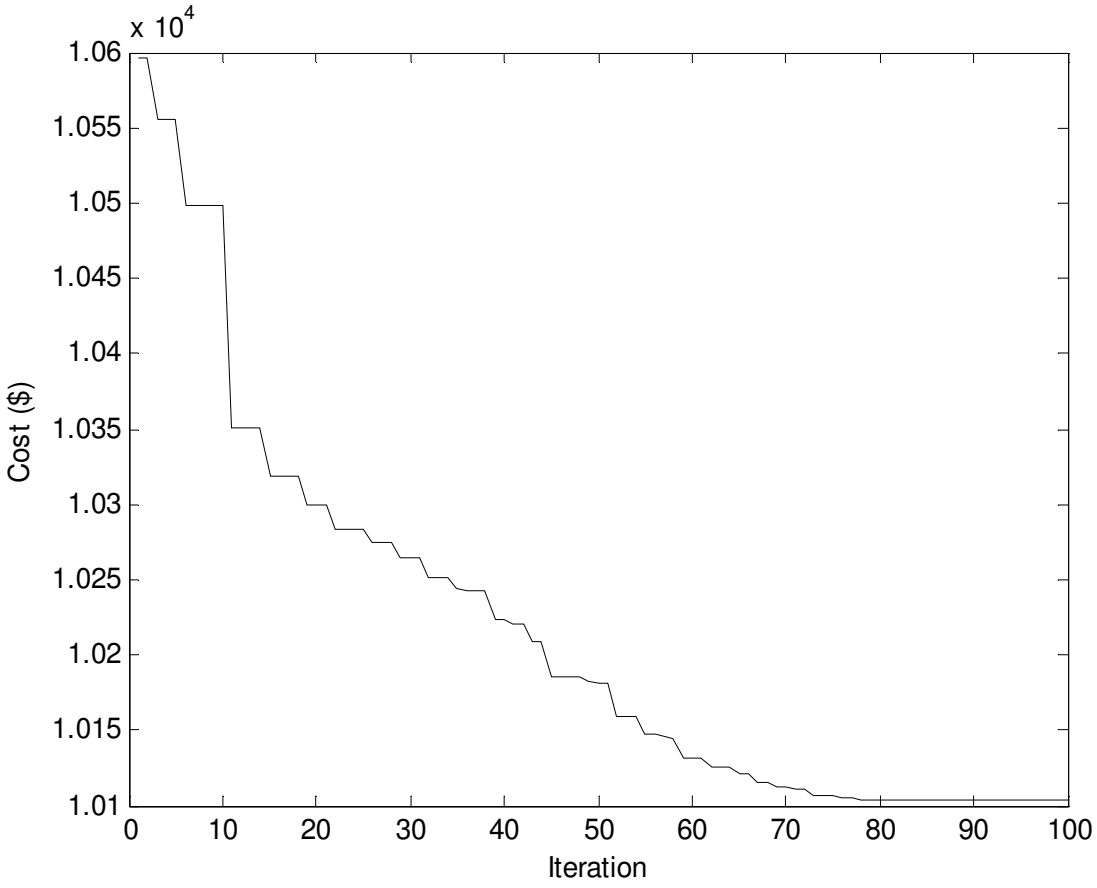

Fig. 4.14. Cost convergence characteristics for case 2 of test system 2

Table 4.24: Power generation (MW) and heat generation (MWth) for case 2 of Test System 2

P_1	44.2825	P_3	112.6214	P_5	94.0105	H_5	28.2620	H_7	46.9948
P_2	100.1107	P_4	209.7009	P_6	40.0235	H_6	74.7432	Ploss	0.7495

Table 4.25: Comparison of performance for case 2 of Test System 2

Techniques	HTS
Best cost ($)	10104.2707
Average cost ($)	10104.4054
Worst cost ($)	10104.7031
CPU time (s)	2.4405

4.10.3. Test System 3

This system comprises thirteen conventional thermal generators, six cogeneration units and five heat-only units. Unit data has been adopted from [58]. The power and heat demands of the test system are 2350 MW and 1250 MWth respectively. Here, two cases are chosen.

Case 1

Here, only valve point loading of conventional thermal generators has been reflected on. The problem is pertained to solve by utilizing HTS. Here, the population size (N_P), elite size (N_E) and the maximum iteration number (N_{max}) have been chosen as 100, 10 and 200 respectively.

The power and heat generations matching to the best cost acquired from the suggested HTS is revealed in Table 4.26. The best, average and worst cost and average CPU time among 100 runs of solutions acquired from suggested HTS are summed up in Table 4.27. The cost acquired from classical PSO (CPSO) [50], time varying acceleration coefficients PSO (TVAC-PSO) [50], teaching learning based optimization (TLBO) [51] and oppositional teaching learning based optimization (OBTLBO) [51] are also revealed in Table 4.27. The cost convergence characteristic acquired from suggested HTS is portrayed in Fig. 4.15. It has been observed from Table 4.27 that the cost acquired by utilizing HTS is the lowest among all other techniques.

Table 4.26: Power generation (MW) and heat generation (MWth) for case 1 of Test System 3

P_1	539.5724	P_{11}	77.8364	H_{15}	76.5205
P_2	298.9487	P_{12}	55.0023	H_{16}	105.5142
P_3	297.9085	P_{13}	55.0109	H_{17}	75.4833
P_4	110.0820	P_{14}	81.0524	H_{18}	39.9999
P_5	110.2645	P_{15}	40.0015	H_{19}	18.3944
P_6	110.2381	P_{16}	81.0030	H_{20}	468.9043
P_7	110.2745	P_{17}	40.0009	H_{21}	59.9994
P_8	110.2452	P_{18}	10.0002	H_{22}	59.9999
P_9	110.1592	P_{19}	35.0001	H_{23}	119.9854
P_{10}	77.3992	H_{14}	105.2219	H_{24}	119.9768

Table 4.27: Comparison of performance for case 1 of Test System 3

Techniques	Best cost ($)	Average cost ($)	Worst cost ($)	CPU time (s)
HTS	57842.99	57843.15	57843.77	5.47
TVAC-PSO [50]	58122.74	58198.31	58359.55	7.84
CPSO [50]	59736.26	59853.47	60076.69	8.00
OBTLBO [51]	57856.26	57883.21	57913.77	5.82
TLBO [51]	58006.99	58014.36	58038.52	5.67
GSO [58]	57843.51	57849.30	57857.79	5.41

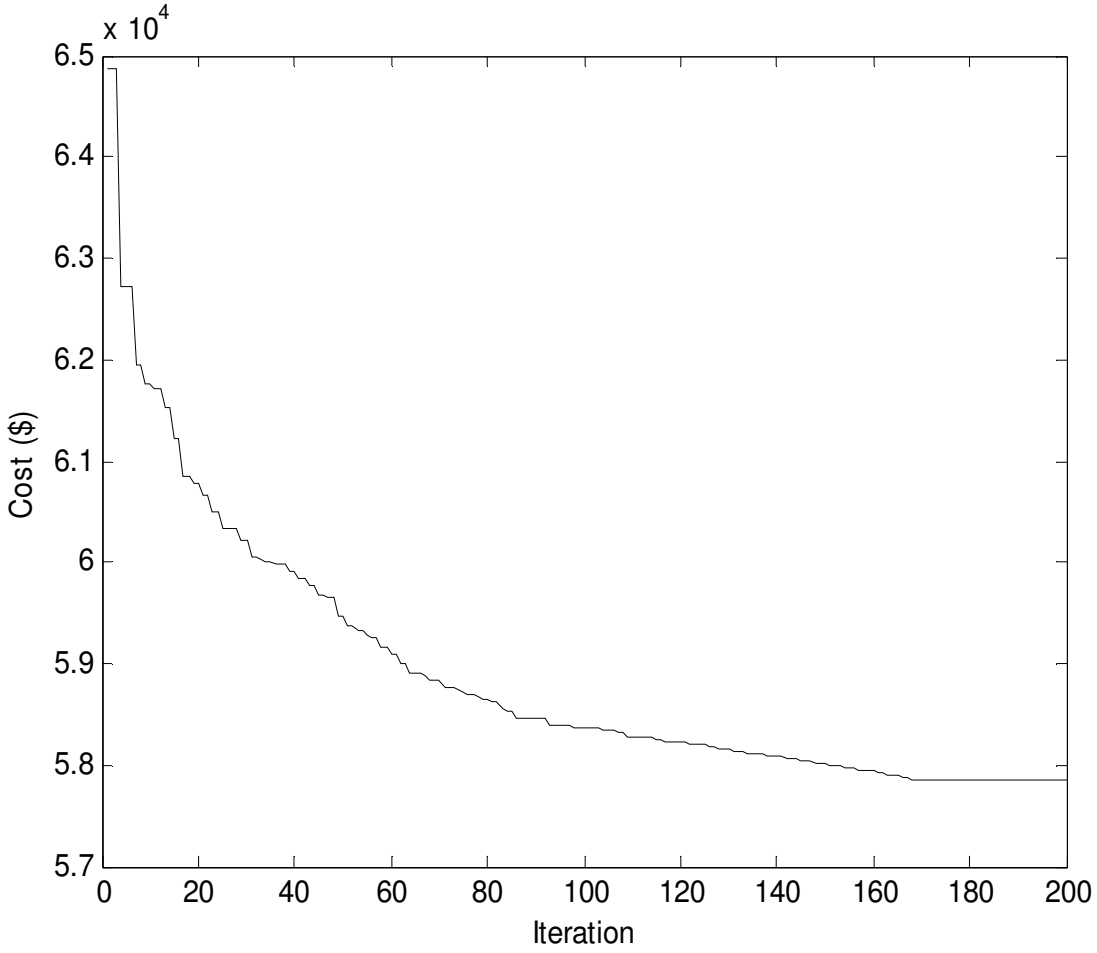

Fig. 4.15. Cost convergence characteristics for case 1 of test system 3

Case 2

Here, valve point loading of conventional thermal generators and prohibited operating zones of conventional thermal generators have been reflected on. The data of conventional thermal generator is similar as in [58]. The problem is pertained to solve by utilizing HTS. Here, the population size (N_P), elite size(N_E) and the maximum iteration number (N_{max}) have been chosen as 100, 10 and 200 respectively. The power and heat generations matching to best cost acquired from suggested HTS is revealed in Table 4.28. The best, average and worst cost and average CPU time among 100 runs of solutions acquired from suggested HTS are summed up in Table 4.29. The cost convergence characteristic acquired from the suggested HTS has been portrayed in Fig. 4.16.

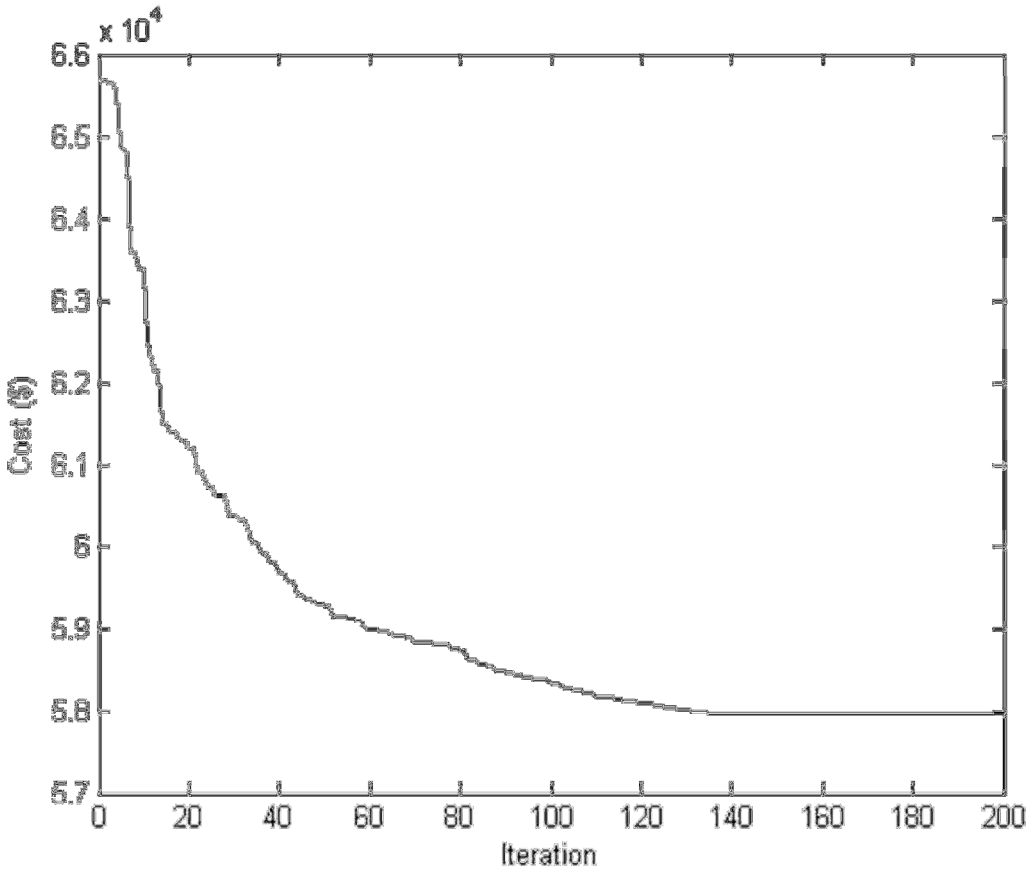

Fig. 4.16. Cost convergence characteristics for case 2 of test system 3

Table 4.28: Power generation (MW) and heat generation (MWth) for case 2 of Test System 3

P_1	628.3185	P_{11}	40.0000	H_{15}	79.2433
P_2	298.9051	P_{12}	55.0000	H_{16}	107.7938
P_3	224.4078	P_{13}	92.3999	H_{17}	80.1432
P_4	60.0000	P_{14}	89.3203	H_{18}	40.0006
P_5	159.1331	P_{15}	44.8825	H_{19}	20.0013
P_6	60.0000	P_{16}	86.3330	H_{20}	453.3426
P_7	159.6331	P_{17}	45.9304	H_{21}	60.0000
P_8	60.0000	P_{18}	10.0000	H_{22}	60.0000
P_9	159.7331	P_{19}	35.0029	H_{23}	120.0000
P_{10}	40.0000	H_{14}	109.4702	H_{24}	20.0000

Table 4.29: **Comparison of performance for case 2 of Test System 3**

Techniques	HTS
Best cost ($)	57959.41
Average cost ($)	57959.92
Worst cost ($)	57960.73
CPU time (s)	6.6877

4.10.4. Test System 4

This system comprises twenty six conventional thermal generators, twelve cogeneration units and ten heat-only units. Data of this test system is acquired by duplicating data of test system 3. The power and heat demands of this test system are 4700 MW and 2500 MWth respectively. Here, two cases are chosen.

Case 1

Firstly, only valve point loading of conventional thermal generators has been reflected on. The problem is pertained to solve by utilizing HTS. Here, the population size (N_P), elite size (N_E) and the maximum iteration number (N_{max}) have been chosen as 150, 15 and 300 respectively.

The power and heat generations matching to best cost acquired from the suggested HTS is revealed in Table 4.30. The best, average and worst cost and average CPU time among 100 runs of solutions acquired from the suggested HTS are summed up in Table 4.31. The cost acquired from classical PSO (CPSO) [50], time varying acceleration coefficients PSO (TVAC-PSO) [50], teaching learning based optimization (TLBO) [51] and oppositional teaching learning based optimization (OBTLBO) [51] are also revealed in Table 4.31. The cost convergence characteristic acquired from the suggested HTS has been portrayed in Fig. 4.17. It has been observed from Table 4.31 that the cost acquired by utilizing HTS is the lowest among all other techniques.

Table 4.30: Power generation (MW) and heat generation (MWth) for case 1 of Test System 4

P_1	538.5705	P_{16}	224.2057	P_{31}	10.0002	H_{34}	78.4853
P_2	224.5205	P_{17}	159.8062	P_{32}	48.6396	H_{35}	105.7117
P_3	229.6394	P_{18}	60.2947	P_{33}	86.0222	H_{36}	83.7420
P_4	159.8146	P_{19}	109.8813	P_{34}	44.0049	H_{37}	40.0004
P_5	60.0409	P_{20}	109.9534	P_{35}	82.6239	H_{38}	22.2596
P_6	159.7333	P_{21}	109.8681	P_{36}	50.0926	H_{39}	514.5539
P_7	159.7483	P_{22}	159.7347	P_{37}	10.0004	H_{40}	60.0000
P_8	60.3910	P_{23}	77.4085	P_{38}	39.9712	H_{41}	60.0000
P_9	159.7346	P_{24}	77.4089	H_{27}	108.4796	H_{42}	120.0000
P_{10}	77.8308	P_{25}	92.4043	H_{28}	78.5030	H_{43}	119.9997
P_{11}	77.4274	P_{26}	55.0095	H_{29}	106.4777	H_{44}	389.4737
P_{12}	92.4412	P_{27}	87.5554	H_{30}	78.4939	H_{45}	59.9999
P_{13}	55.0051	P_{28}	44.0256	H_{31}	40.0006	H_{46}	59.9999
P_{14}	628.3214	P_{29}	83.9878	H_{32}	26.1998	H_{47}	120.0000
P_{15}	149.6676	P_{30}	44.0149	H_{33}	107.6192	H_{48}	120.0000

Table 4.31: Comparison of performance for case 1 of Test System 4

Techniques	Best cost ($)	Average cost ($)	Worst cost ($)	CPU time (s)
HTS	116362.50	116369.06	116385.37	6.0035
TVAC-PSO [50]	117824.89	-	-	-
CPSO [50]	119708.88	-	-	-
OBTLBO [51]	116579.23	116613.65	116649.44	10.93
TLBO [51]	116739.36	116756.00	116825.82	10.38
GSO [58]	116457.95	116463.65	116473.21	9.51

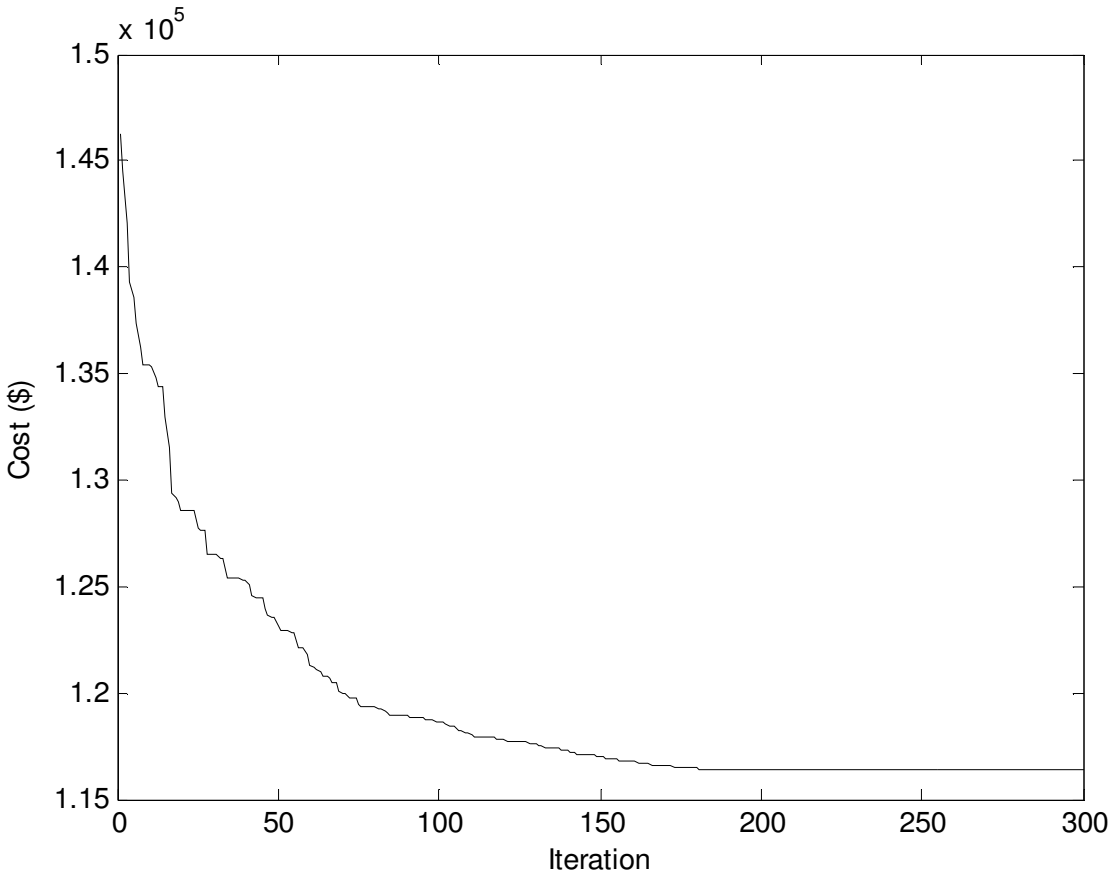

Fig. 4.17. Cost convergence characteristics for case 1 of test system 4

Case 2

Here, valve point loading of conventional thermal generators and prohibited operating zones of conventional thermal generators have been reflected on. The data of conventional thermal generator is similar as in case [58]. The problem has been pertained to solve by utilizing HTS. Here, the population size (N_P), elite size (N_E) and the maximum iteration number (N_{max}) have been chosen as 150, 15 and 300 respectively. The power and heat generations matching to best cost acquired from the suggested HTS is revealed in Table 4.32. The best, average and worst cost and average CPU time among 100 runs of solutions acquired from the suggested HTS are summed up in Table 4.33. The cost convergence characteristic acquired from the suggested HTS has been portrayed in Fig. 4.18.

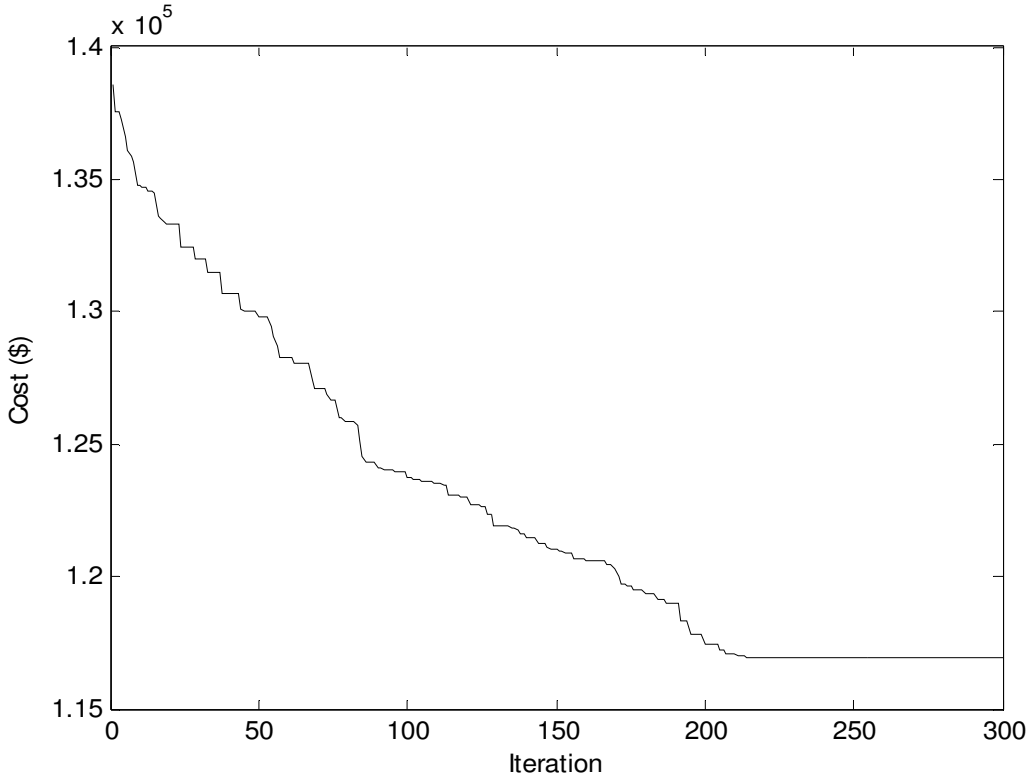

Fig. 4.18. Cost convergence characteristics for case 2 of test system 4

Table 4.32: Power generation (MW) and heat generation (MWth) for case 2 of Test System 4

P_1	259.9998	P_{16}	299.2020	P_{31}	10.0000	H_{34}	78.8757
P_2	299.2292	P_{17}	174.3803	P_{32}	35.8856	H_{35}	113.0611
P_3	293.0285	P_{18}	159.7327	P_{33}	85.7164	H_{36}	81.5086
P_4	109.8682	P_{19}	111.5855	P_{34}	44.4571	H_{37}	40.0004
P_5	108.6801	P_{20}	159.9501	P_{35}	95.7190	H_{38}	20.4882
P_6	159.7799	P_{21}	159.7332	P_{36}	47.5058	H_{39}	508.5805
P_7	109.8663	P_{22}	159.7331	P_{37}	10.0000	H_{40}	59.9999
P_8	109.8662	P_{23}	114.7999	P_{38}	36.0743	H_{41}	60.0000
P_9	159.7325	P_{24}	114.8014	H_{27}	106.1234	H_{42}	120.0000
P_{10}	64.6775	P_{25}	119.8199	H_{28}	78.4828	H_{43}	119.9999
P_{11}	77.4946	P_{26}	92.4016	H_{29}	108.3679	H_{44}	395.3627
P_{12}	119.9999	P_{27}	83.3573	H_{30}	81.2992	H_{45}	60.0000
P_{13}	55.0048	P_{28}	44.0020	H_{31}	40.0006	H_{46}	59.9999
P_{14}	179.5202	P_{29}	87.3568	H_{32}	20.4024	H_{47}	119.9998
P_{15}	299.7767	P_{30}	47.2635	H_{33}	107.4477	H_{48}	119.9995

Table 4.33: Comparison of performance for case 2 of Test System 4

Techniques	HTS
Best cost ($)	116918.90
Average cost ($)	116924.75
Worst cost ($)	116935.38
CPU time (s)	6.9056

4.11. Conclusion

Modified teaching-learning-based optimization (MTLBO) has been developed and pertained to solve three different complex combined heat and power economic dispatch problems and 15 benchmark functions. Test results acquired from three different complex combined heat and power economic dispatch problems have been compared with those acquired by other evolutionary techniques suggested in the literature. A comparison has been observed for both test cases i.e. a valve point loading of conventional thermal generator and valve point loading of conventional thermal generators and prohibited operating zones of conventional thermal generators in MTLBO gives better result for minimum cost and good performance.

Heat transfer search (HTS) algorithm has been pertained to solve four different complex combined heat and power economic dispatch problems. Test results have been matched up to those acquired by other evolutionary techniques suggested in literature. A comparison of performance for different test system has been observed and found that the best cost, average cost, worst cost and CPU time gives better result in HTS algorithm.

CHAPTER-5

Short-term Scheduling of Fixed Head Hydrothermal Power System

5.1. Introduction:

Optimal scheduling of power plant generation is of great importance to electric utility systems. Because of insignificant marginal cost of hydroelectric power, the problem of minimizing the operational cost of hydrothermal system essentially reduces to that of minimizing the fuel cost of thermal plants under the various constraints on the hydraulic, thermal and power system network. Since the mid1990s, many techniques originated from Darwin's natural evolution theory have emerged. These techniques are usually termed by "evolutionary computation methods" including evolutionary algorithms (EAs), swarm intelligence and artificial immune system.

In this study, opposition-based differential evolution (ODE) for optimal scheduling of generation in a hydrothermal system has been applied to a fixed head hydrothermal power system. This paper considers a fixed head hydrothermal system. Here the system with fixed head hydro plants, water discharge rate curves are modeled as a quadratic function of the hydropower generation and thermal units with non-smooth fuel cost function. Here, scheduling period is divided into a number of subintervals each having a constant load demands. In case of variable head hydrothermal system, multi-reservoir cascaded hydro plants having prohibited operating zones and thermal units with valve point loading are used. The proposed method is validated by applying it to two test problems, two fixed head hydrothermal test systems and three hydrothermal multi-reservoir cascaded hydroelectric test systems having prohibited operating zones and thermal units with valve point loading. The test results are compared with those obtained by other evolutionary methods like differential evolution (DE), particle swarm optimization (PSO) and evolutionary programming (EP) techniques.

5.2. Problem Formulation

Fixed head hydrothermal scheduling problem with N_h hydro units and N_s thermal units over M time subintervals is described as follows:

5.2.1. Objective function

The fuel cost function of each thermal generator, considering valve-point effect, is expressed as a sum of quadratic and sinusoidal function. The superimposed sine components represent rippling effect produced by steam admission valve opening.

The problem minimizes following total fuel cost

$$f_{FH} = \sum_{m=1}^{M}\sum_{i=1}^{N_s} t_m \left[a_{si} + b_{si}P_{sim} + c_{si}P_{sim}^2 + d_{si} \times \sin\left\{e_{si} \times \left(P_{si}^{\min} - P_{sim}\right)\right\}\right] \tag{5.1}$$

5.2.2. Constraints

(i) Power balance constraints:

$$\sum_{i=1}^{N_s} P_{sim} + \sum_{j=1}^{N_h} P_{hjm} - P_{Dm} - P_{Lm} = 0 \qquad m \in M \tag{5.2}$$

and

$$P_{Lm} = \sum_{l=1}^{N_h+N_s}\sum_{r=1}^{N_h+N_s} P_{lm}B_{lr}P_{rm} \qquad m \in M \tag{5.3}$$

(ii) Water availability constraints:

$$\sum_{m=1}^{M}\left[t_m\left(a_{0hj} + a_{1hj}P_{hjm} + a_{2hj}P_{hjm}^2\right)\right] - W_{hj} = 0 \qquad j \in N_h \tag{5.4}$$

(iii) Generation limits:

$$P_{hj}^{\min} \le P_{hjm} \le P_{hj}^{\max} \qquad j \in N_h,\ m \in M \tag{5.5}$$

and $$P_{si}^{\min} \le P_{sim} \le P_{si}^{\max} \qquad i \in N_s,\ m \in M \tag{5.6}$$

5.3. Determination of Generation Level of Slack Generator

Thermal generators and hydro generators deliver their power output subject to the power balance constraint (5.2), water availability constraint (5.4) and respective capacity constraints (5.5) and (5.6). Assuming the power loading of N_P and first (N_s - 1) generators are known, the power

level of the N_s th generator (i.e. the slack generator) is given by

$$P_{N_s m} = P_{Dm} + P_{Lm} - \sum_{l=1}^{N_h+N_s-1} P_{lm} \qquad m \in M \tag{5.7}$$

The transmission loss P_{Lm} is a function of all the generators including the slack generator and it is given by

$$P_{Lm} = \sum_{l=1}^{N_h+N_s-1} \sum_{r=1}^{N_h+N_s-1} P_{lm} B_{lr} P_{rm} + 2P_{N_s m}\left(\sum_{l=1}^{N_h+N_s-1} B_{N_s l} P_{lm} \right) + B_{N_s N_s} P_{N_s m}^2 \qquad m \in M \tag{5.8}$$

Expanding and rearranging, equation (5.7) becomes

$$B_{N_s N_s} P_{N_s m}^2 + \left(2 \sum_{l=1}^{N_h+N_s-1} B_{N_s l} P_{lm} - 1 \right) P_{N_s m} + P_{Dm} + \sum_{l=1}^{N_h+N_s-1} \sum_{r=1}^{N_h+N_s-1} P_{lm} B_{lr} P_{rm} - \sum_{l=1}^{N_h+N_s-1} P_{lm} = 0 \tag{5.9}$$

$$m \in M$$

The loading of the slack generator (i.e. N_s th) can then be found by solving equation (5.9) using standard algebraic method.

5.4. Overview of Opposition based Differential Evolution method

Opposition-based learning (OBL) was developed by Tizhoosh to improve candidate solution by considering current population as well as its opposite population at the same time.

Evolutionary optimization methods start with some initial population and try to improve them toward some optimal solution. The process of searching terminates when some predefined criteria are satisfied. The process is started with random guesses in the absence of prior information about the solution. The process can be improved by starting with a closer i.e. fitter solution by simultaneously checking the opposite solution. By doing this, the fitter one (guess or opposite guess) may be chosen as an initial solution. According to the theory of probability, 50% of the time, a guess is further from the solution than its opposite guess. Therefore, process starts with the closer of the two guesses. The same approach can be applied not only to the initial solution but also continuously to each solution in the current population.

5.4.1. Definition of opposite number

If x be a real number between $[lb, ub]$, its opposite number is defined as

$$\bar{x} = lb + lu - x \tag{5.10}$$

Similarly, this definition can be extended to higher dimensions [84] as stated in the next sub-section.

5.4.2. Definition of opposite point

Let $X = (x_1, x_2, ..., x_n)$ be a point in n- dimensional space where $x_i \in [lb_i, ub_i]$ and $i \in 1,2,..., n$ .The opposite point $\overline{X} = (\overline{x_1}, \overline{x_2}, ..., \overline{x_n})$ is completely defined by its components as in

$$\overline{x_i} = lb_i + ub_i - x_i \tag{5.11}$$

By employing the definition of opposite point, the opposition-based optimization is defined in the following sub-section.

5.4.3. Opposition-based optimization

Let $X = (x_1, x_2, ..., x_n)$ be a point in n- dimensional space i.e. a candidate solution. Assume $f = (\bullet)$ is a fitness function which is used to measure the candidate's fitness. According to the definition of the opposite point, $\overline{X} = (\overline{x_1}, \overline{x_2}, ..., \overline{x_n})$ is the opposite of $X = (x_1, x_2, ..., x_n)$. Now, if $f(\overline{X}) < f(X)$ (for a minimization problem), then point X can be replaced with $\overline{X}$; otherwise, the process is continued with X . Hence, the point and its opposite point are evaluated simultaneously in order to continue with the fitter one.

5.4.4. Opposition-based Differential evolution

Here, the concept of the opposition-based learning [84] is incorporated in differential evolution. The original DE is chosen as a parent algorithm and the opposition-based ideas are embedded in DE.

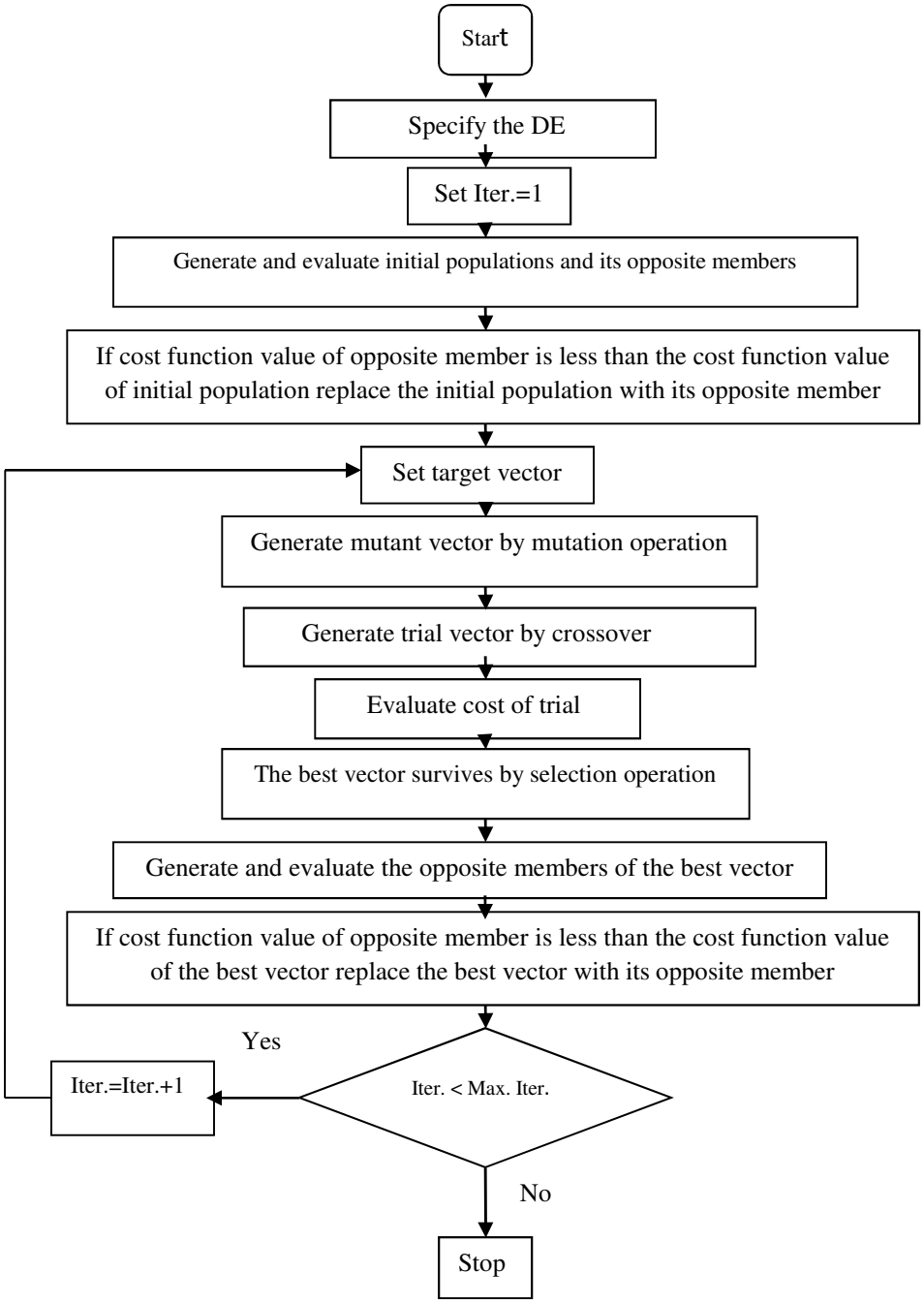

Fig. 5.1. Flowchart of ODE

5.5. Simulation Results of ODE and DE algorithm

Two test problems, two fixed head hydrothermal systems and three hydrothermal multi-reservoir cascaded hydroelectric test systems having prohibited operating zones and thermal units with valve point loading are investigated. The computational results have been used to compare the performance of the proposed ODE method with that of other evolutionary methods. The proposed ODE algorithm and DE algorithm used in this paper are implemented by using MATLAB 7.0 on a PC (Pentium-IV, 80 GB, 3.0 GHz).

5.5.1. Example1: Consider the maximization problem [92].

$$\max_{x_1,x_2} f(x_1, x_2) = 21.5 + x_1 \sin(4\pi x_1) + x_2 \sin(20\pi x_2) \tag{5.12}$$

where $-3.0 \le x_1 \le 12.1$ and $4.1 \le x_2 \le 5.8$

This function is multimodal. The problem is solved by using ODE. .

Here, the population size (N_P), scaling factor (F), crossover constant (C_R) and maximum iteration number have been selected 10, 0.3, 1.0 and 50 respectively. The best optimum value, the variables corresponding to the best optimum value, average and worst value and average CPU time among 100 runs of solutions obtained from proposed ODE and DE for example 1 have been shown in Table 5.1. Figure 5.2 shows the nature of convergence obtained from ODE and DE for example 1

Table 5.1: Best optimum value, the variables corresponding to the best optimum value, average value, worst value and average CPU time for example 1

Method	x^*	$f(x^*)$	Average value	Worst value	CPU time(sec)
ODE	[12.1000, 5.7227]	38.9377	38.9377	38.9377	0.0473
DE	[12.1000, 5.7228]	38.9375	38.9373	38.9371	0.0469

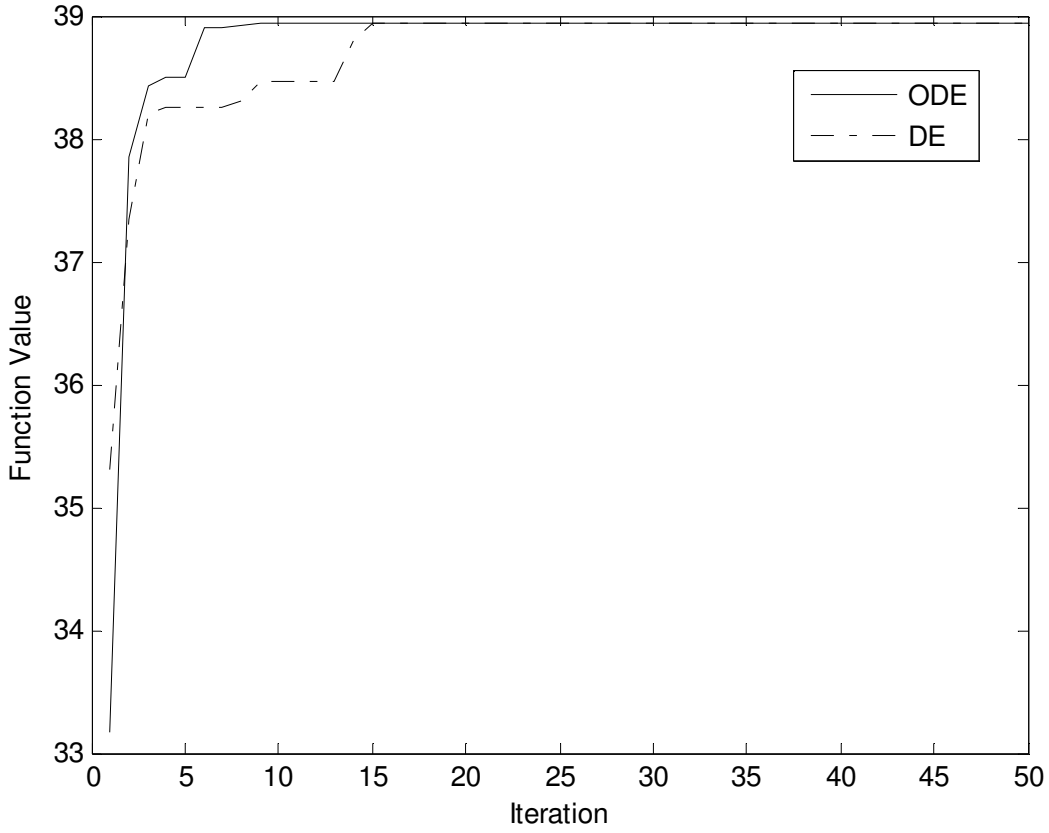

Fig. 5.2. Convergence characteristic of example 1

5.5.2. Example 2: Consider the minimization problem [92].

$$\min_{x_1,x_2} f(x_1,x_2) = \sum_{i=1}^{5} i\cos[(i+1)x_1 + i]\sum_{i=1}^{5} i\cos[(i+1)x_2 + i] \tag{5.13}$$

where $-10 \le x_1 \le 10$ and $-10 \le x_2 \le 10$

This function has 760 local minima, 18 of which are global minima with -186.73. The problem is solved by using ODE. . Here, the population size (N_P), scaling factor (F), crossover constant (C_R) and maximum iteration number have been selected 10, 0.3, 1 and 100 respectively for the example under consideration.

To validate the proposed ODE based approach, the same example is solved by using DE.

In case of DE, the population size (N_P), scaling factor (F), crossover constant (C_R) and maximum iteration number have been selected as 10, 0.3, 1.0 and 100 respectively. Table 5.2 summarizes the best optimum value, the variables corresponding to the best optimum value, average and worst value and average CPU time among 100 runs of solutions obtained from

proposed ODE and DE for example 2. Figure 5.3 depicts the nature of convergence obtained from ODE and DE for example 2.

Figure 5.3 depicts the nature of convergence obtained from ODE and DE for example 2.

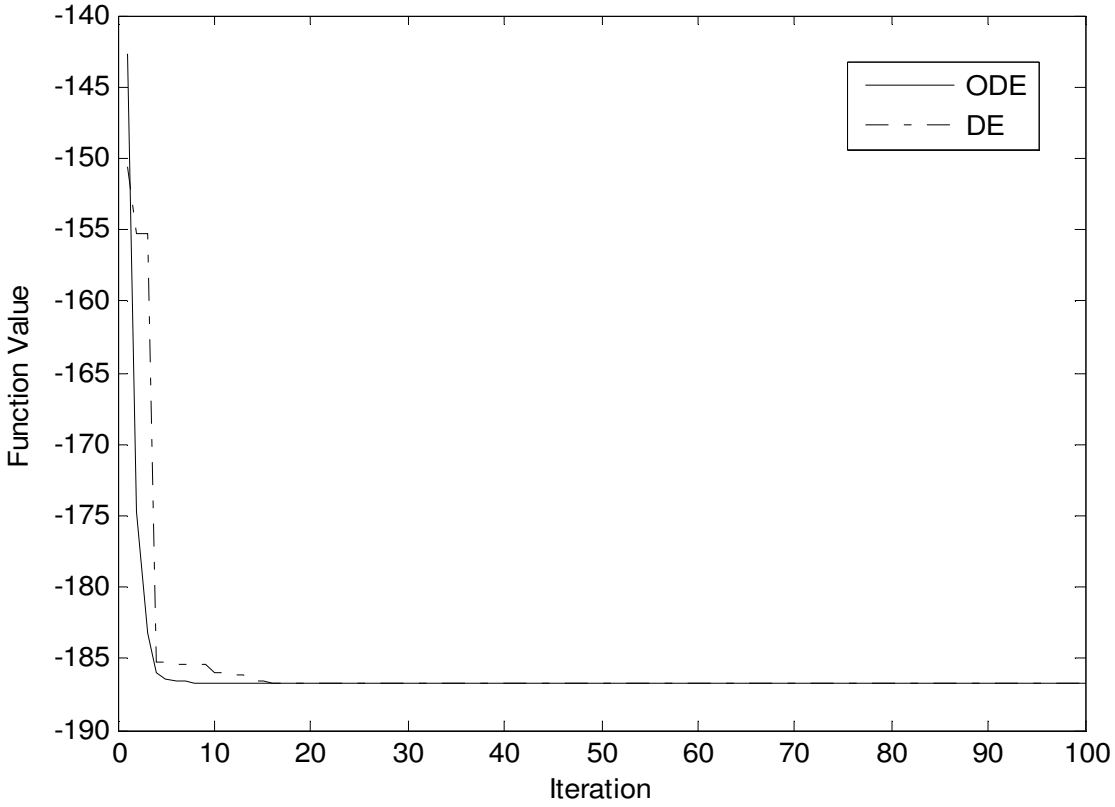

Fig. 5.3. Convergence characteristic of example 2

Table 5.2: Best optimum value, the variables corresponding to the best optimum value, average value, worst value and average CPU time for example 2

Method	x^*	$f(x^*)$	Average value	Worst value	CPU time (sec)
ODE	[5.4830, 4.8581]	-186.7309	-186.7309	-186.7309	0.0625
DE	[-7.7084, -7.0834]	-186.7308	-186.7307	-186.7303	0.0781

5.6. Case Study of Fixed Head Hydrothermal System

5.6.1. Test System 1

This system consists of two hydro plants and two thermal plants whose characteristics and load demands are given in Table A-9, Table A-10 and Table A-11 respectively in appendices. Transmission loss formula coefficients are also given in the appendix. Hydro plant data is taken from [64].

The problem is solved by using both the proposed ODE and DE. Here, the population size (N_P), scaling factor (F), crossover rate (C_R) and the maximum iteration number (N_{max}) have been selected as 100, 1.0, 1.0 and 100 respectively for the test system under consideration.

The optimal hydrothermal generation obtained by the proposed ODE and DE are provided in Table 5.3 and Table 5.4 respectively. The best, average and worst cost and average CPU time among 100 runs of solutions obtained from proposed ODE and DE method are summarized in Table 5.5. The cost obtained from artificial immune system (AIS) [76], particle swarm optimization (PSO) [76] and evolutionary programming (EP) [76] are also shown in Table 5.5. The cost convergence characteristic obtained from proposed ODE and DE is shown in Fig. 5.4. It is seen from Table 5.5 that the cost found by using ODE is the lowest among all other methods.

Table 5.3: Results obtained from ODE of test system 1 of fixed head hydrothermal system

Sub-interval	P_{h1} (MW)	P_{h2} (MW)	P_{s1} (MW)	P_{s2} (MW)
1	244.5860	90.7689	179.4953	424.9773
2	307.3581	163.3383	228.7850	570.1572
3	285.4852	139.2931	211.2739	522.5895

Table 5.4: Results obtained from DE for test system 1 of fixed head hydrothermal system

Sub-interval	P_{h1} (MW)	P_{h2} (MW)	P_{s1} (MW)	P_{s2} (MW)
1	240.3807	85.6583	206.3934	407.6673
2	310.1176	167.5754	206.3934	585.2895
3	286.6845	139.7912	206.3934	525.7479

Table 5.5: Comparison of performance for Test System 1 of fixed head hydrothermal system

Techniques	Best cost ($)	Average cost ($)	Worst cost ($)	CPUtime (s)
ODE	66030.85	66031.68	66032.46	40.31
DE	66060.74	66061.44	66064.14	36.01
AIS [74]	66117	-	-	53.43
PSO [74]	66166	-	-	71.62
EP [74]	66198	-	-	75.48

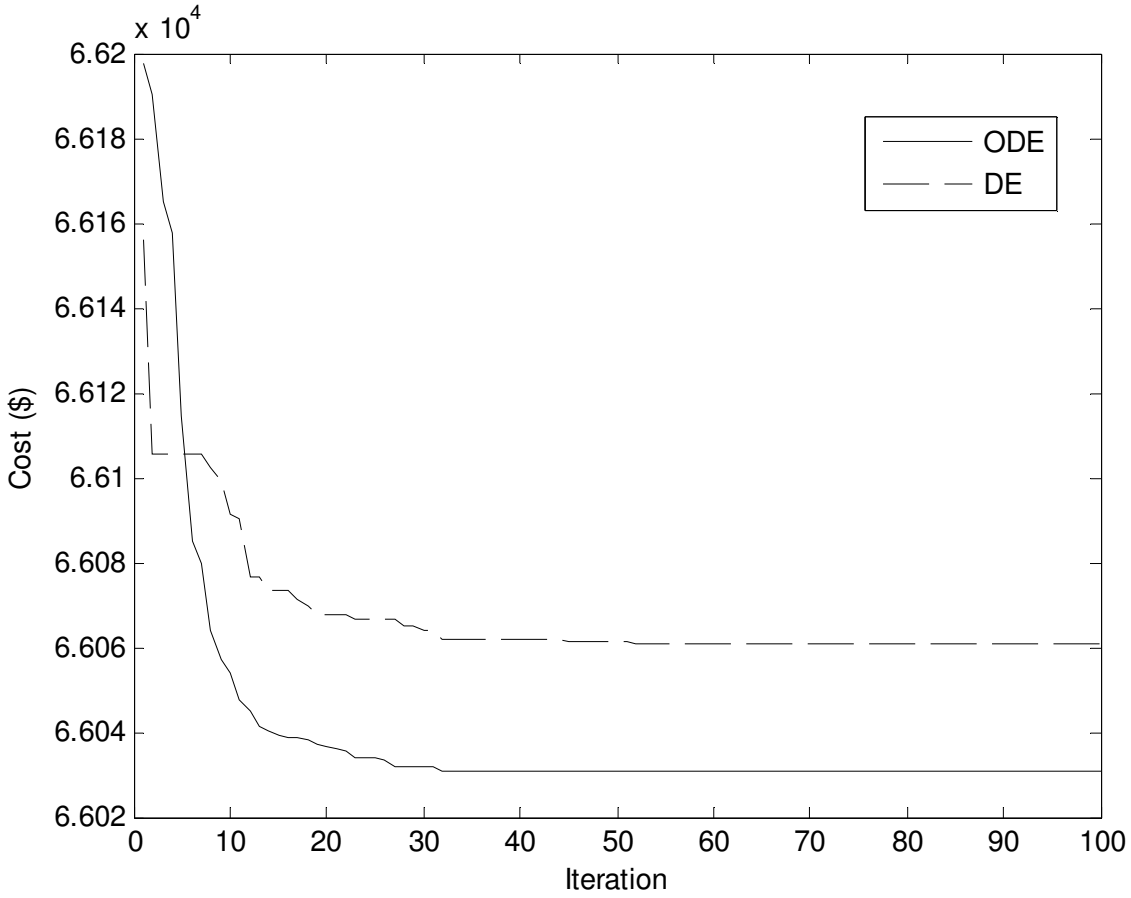

Fig. 5.4. Cost convergence of test system 1 of fixed head hydrothermal system

5.6.2. Test System 2

This system comprises of two hydro plants and four thermal plants whose characteristics and load demands are given in Table A-12, Table A-13 and Table A-14 respectively in ices. Transmission loss formula coefficients are also given in the appendices.

The problem is solved by using both the proposed ODE and DE. Here, the population size (N_P), scaling factor (F), crossover rate (C_R) and the maximum iteration number (N_{max}) have been selected as 100, 1.0, 1.0 and 200 respectively for the test system under consideration. The optimal hydrothermal generation obtained by the proposed ODE and DE are provided in Table 5.6 and Table 5.7 respectively. The best, average and worst cost and average CPU time among 100 runs of solutions obtained from proposed ODE and DE are summarized in Table 5.8. The cost obtained from artificial immune system (AIS) [76], particle swarm optimization (PSO) [76] and evolutionary programming (EP) [76] are also shown in Table 5.8. The cost convergence characteristic obtained from proposed ODE and DE is depicted in Fig. 5.5. It is seen from Table 8 that the cost found by using ODE is the lowest among all other methods

Table 5.6: Results obtained from ODE of test system 2 of fixed head hydrothermal system

Subin-terval	P_{h1} (MW)	P_{h2} (MW)	P_{s1} (MW)	P_{s2} (MW)	P_{s3} (MW)	P_{s4} (MW)
1	172.6478	317.8272	93.6207	174.7438	109.2596	50.3779
2	243.8370	411.3216	124.8716	174.6929	123.6025	50.1150
3	209.7780	351.8750	116.1764	174.7282	120.3243	50.0519
4	249.8641	499.8741	124.8642	174.9127	222.4536	68.0992

Table 5.7: Results obtained from DE of test system 2 of fixed head hydrothermal system

Subin-terval	P_{h1} (MW)	P_{h2} (MW)	P_{s1} (MW)	P_{s2} (MW)	P_{s3} (MW)	P_{s4} (MW)
1	184.4627	303.6346	88.3611	174.7233	116.2664	50.9170
2	241.0344	419.5791	117.4402	174.8712	124.7407	50.9397
3	201.9931	357.2371	123.3403	173.9739	115.3547	51.0280
4	249.3076	499.1428	124.0676	174.7184	221.4260	71.3501

Table 5.8: Comparison of performance for Test System 2 of fixed head hydrothermal system

Techniques	Best cost ($)	Average cost ($)	Worst cost ($)	CPU time (s)
ODE	92817.01	92819.81	92822.68	46.09
DE	93107.34	93110.45	93114.07	41.53
AIS [74]	93950	-	-	59.14
PSO [74]	94126	-	-	83.54
EP [74]	94250	-	-	67.82

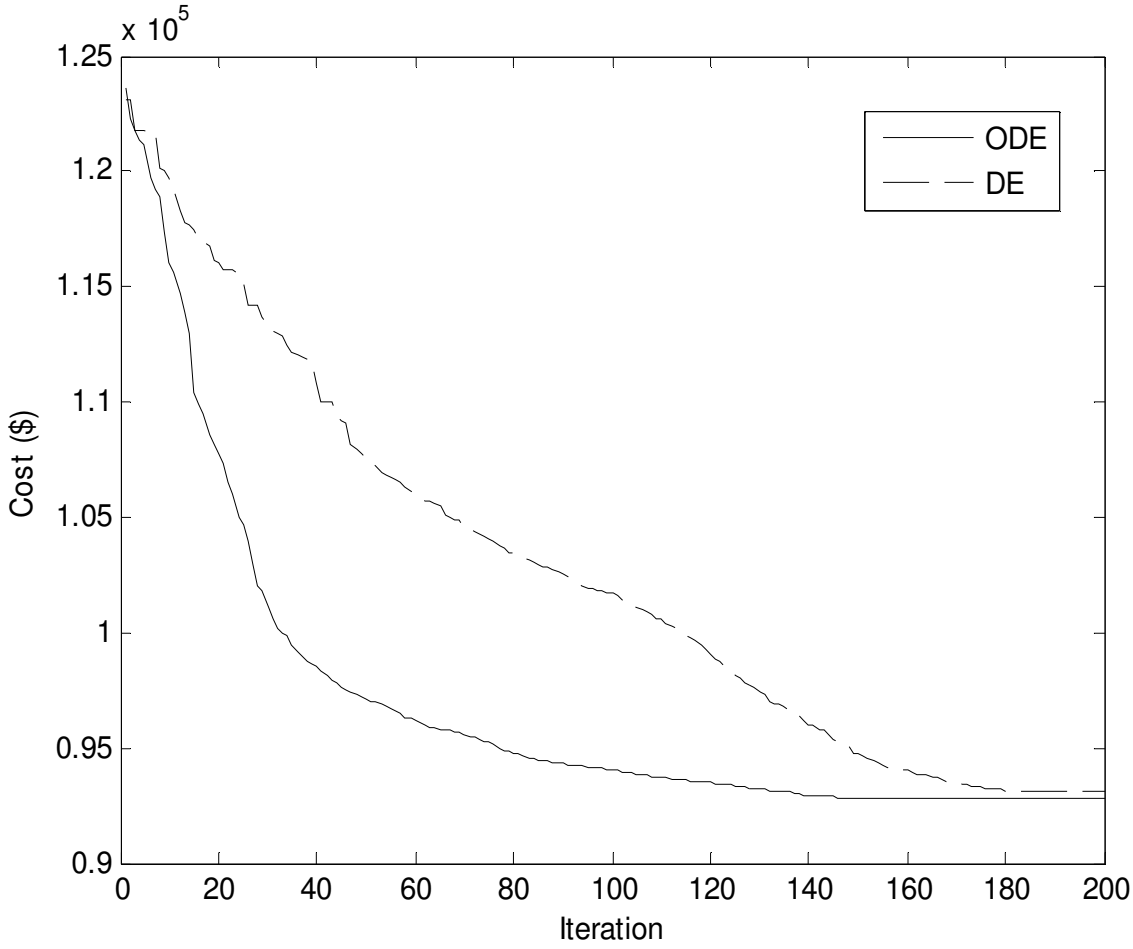

Fig. 5.5. Cost convergence of test system 2 of fixed head hydrothermal system

5.7. Overview of Improved Real Coded Genetic algorithm

The overview of Improved Real Coded Genetic algorithm described in Chapter 3.4.

5.8. Simulation Results of RCGA and IRCGA method

The developed improved real coded genetic algorithm (IRCGA) and real coded genetic algorithm (RCGA) have been pertained for solving two different test systems. IRCGA and RCGA techniques have been realized by using MATLAB 7.0 on a PC (Pentium-IV, 80 GB, 3.0 GHz).

5.8.1. Test System 1

Test system 1 consists of two hydro plants and two thermal plants whose characteristics and load demands are given in Table A-9, Table A-10 and Table A-11 respectively in appendices. Transmission loss formula coefficients are also given in the appendix Table A-11. Hydro plant data is taken from [64]. The problem is solved by using IRCGA and RCGA. Here, maximum number of iterations, population size, crossover and mutation probabilities have been chosen as 100, 50, 0.9 and 0.2, respectively for IRCGA and RCGA. Test results acquired from the best fuel cost among 100 runs of solutions by using developed IRCGA and RCGA are summed up in Table 5.9 and Table 5.10 respectively. The cost convergence characteristic acquired from developed IRCGA and RCGA has been portrayed in Fig. 5.6. It has been observed from Table 5.9 and Table 5.10 that the fuel cost acquired from IRCGA is the less than RCGA.

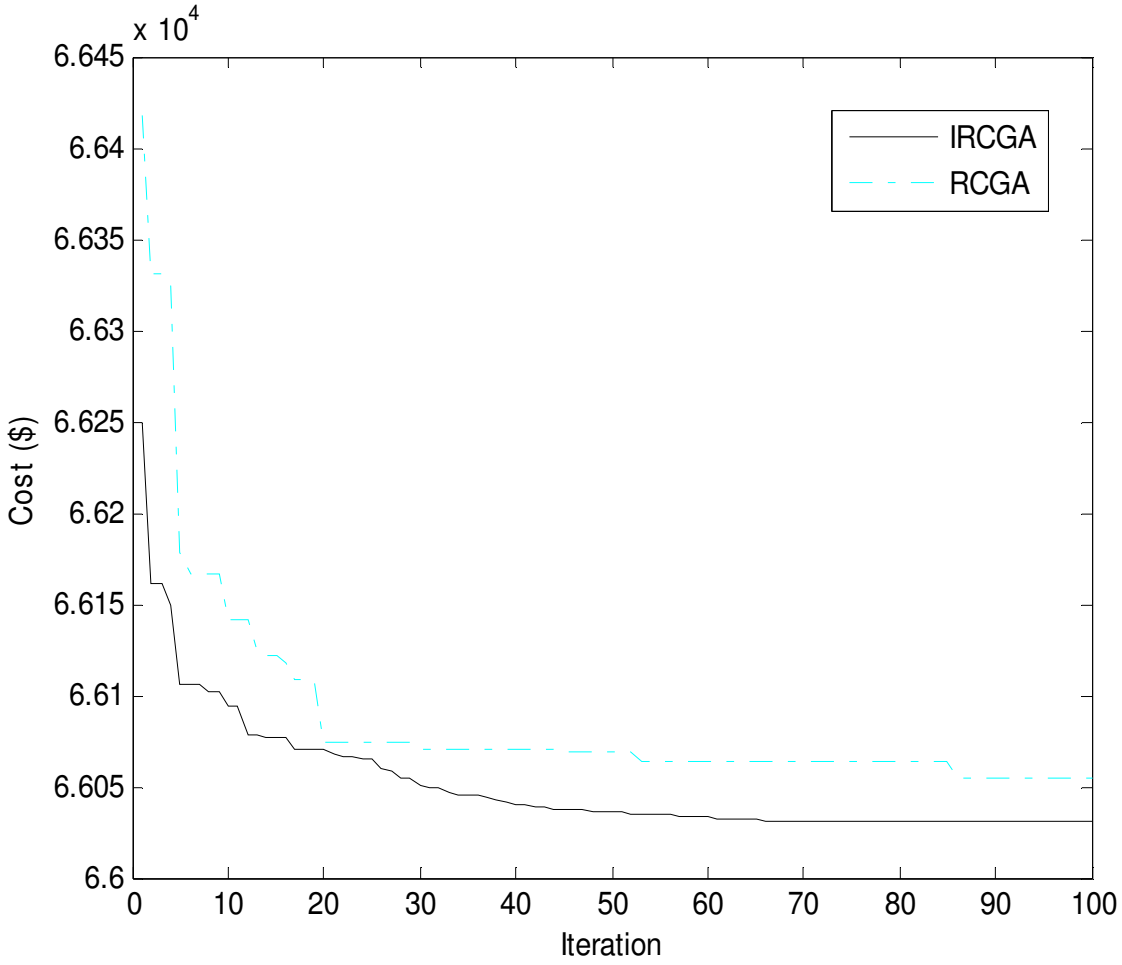

Fig. 5.6. Cost convergence of test system 1

Table 5.9: Results acquired from IRCGA of test system 1

Subin-terval	P_{h1} (MW)	P_{h2} (MW)	P_{s1} (MW)	P_{s2} (MW)	Cost ($)	CPU time (sec)
1	244.4824	91.7609	177.1186	426.4080	66031	55.03
2	306.6226	162.1315	226.9595	574.0518		
3	286.3345	139.5808	212.0984	520.5925		

Table 5.10: Results acquired from RCGA of test system 1

Subin-terval	P_{h1} (MW)	P_{h2} (MW)	P_{s1} (MW)	P_{s2} (MW)	Cost ($)	CPU time (sec)
1	237.6474	97.7308	183.3124	420.6857	66054	51.97
2	310.2027	170.4667	226.3238	562.0064		
3	289.1620	124.9021	212.3097	533.4285		

5.8.2. Test System 2

Test system 2 comprises of two hydro plants and four thermal plants whose characteristics and load demands are given in Table A-12, Table A-13 and Table A-14 respectively in appendices. Transmission loss formula coefficients are also given in the appendix Table A-14.

The problem is solved by using developed IRCGA and RCGA. Here, maximum number of iterations, population size, crossover and mutation probabilities have been chosen as 200, 50, 0.9 and 0.2, respectively for IRCGA and RCGA.

Test results acquired from the best fuel cost among 100 runs of solutions by using developed IRCGA and RCGA are summed up in Table 5.11 and Table 5.12 respectively.

The cost convergence characteristic acquired from developed IRCGA and RCGA has been portrayed in Fig. 5.7. It has been observed from Table 5.11 and Table 5.12 that the fuel cost acquired from IRCGA is the less than RCGA.

Table 5.11: Results acquired from IRCGA of test system 2

Subin-terval	P_{h1} (MW)	P_{h2} (MW)	P_{s1} (MW)	P_{s2} (MW)	P_{s3} (MW)	P_{s4} (MW)	Cost ($)	CPU time (sec)
1	177.1505	314.8073	89.4437	174.9074	111.9127	50.2581		
2	248.7030	408.1596	123.8875	174.9438	122.6685	50.0685	92773	77.78
3	200.2083	358.1134	116.9637	174.7650	122.8367	50.0770		
4	249.9786	499.9132	124.9163	174.9314	220.4093	69.8954		

Table 5.12: Results acquired from RCGA of test system 2

Subin-Terval	P_{h1} (MW)	P_{h2} (MW)	P_{s1} (MW)	P_{s2} (MW)	P_{s3} (MW)	P_{s4} (MW)	Cost ($)	CPU time (sec)
1	157.6372	307.7543	106.4287	175.0000	118.9544	52.4040		
2	247.5443	410.5934	125.0000	175.0000	117.1135	53.1834	93125	70.89
3	219.6215	362.0285	97.3968	171.6784	122.3066	50.2556		
4	250.0000	500.0000	125.0000	174.8682	217.2241	72.9124		

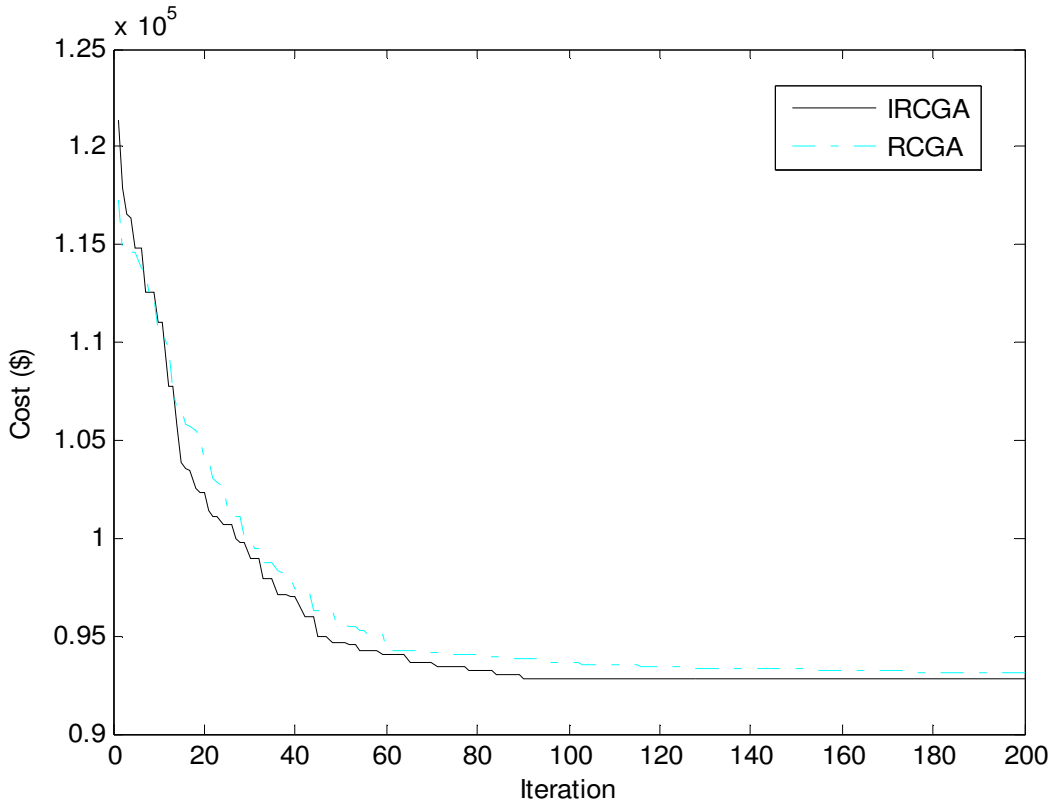

Fig. 5.7. Cost convergence of test system 2

5.9. Conclusion

Here, opposition-based differential evolution is demonstrated and presented to solve the hydrothermal scheduling problem. The proposed opposition-based differential evolution method has been successfully applied to two test problems, two fixed head hydrothermal test systems. The results have been compared with those obtained by other evolutionary algorithms reported in the literature. It is seen from the comparisons that the proposed opposition-based differential evolution method performs better than other evolutionary algorithms in the literature.

CHAPTER-6

Short-term Scheduling of Variable Head Hydrothermal Power System

6.1. Introduction

The hydro thermal generation scheduling problem is a nonlinear constrained dynamic optimization problem which plays an important role to electric utility systems. With the insignificant marginal cost of hydroelectric power, operational cost of a hydrothermal system essentially reduces to that of minimizing the fuel cost for thermal plants under the various constraints on the hydraulic, thermal and power system network.

The main constraints include: the time coupling effect of the hydro sub problem, where the water flow in an earlier time interval affects the discharge capability at a later period of time, the cascaded nature of the hydraulic network, the varying hourly reservoir inflows, the physical limitations on the reservoir storage and turbine flow rate, the varying system load demand and the loading limits of both thermal and hydro plants.

In this study, opposition-based differential evolution (ODE) for optimal scheduling of generation in a hydrothermal system has been applied to a variable head hydrothermal power system. Here, opposition-based differential evolution is applied to determine the optimal hourly schedule of power generation in a hydrothermal system. Differential evolution (DE) is a population-based stochastic parallel search evolutionary algorithm. Opposition-based differential evolution has been used here to improve the effectiveness and quality of the solution.

The proposed opposition-based differential evolution (ODE) employs opposition-based learning (OBL) for population initialization and also for generation jumping. The effectiveness of the proposed method has been verified on three hydrothermal multi-reservoir cascaded hydroelectric test systems having prohibited operating zones and thermal units with valve point loading.

6.2. Problem Formulation

The variable head hydrothermal scheduling problem is aimed to minimize the fuel cost of thermal plants, while making use of the availability of hydro power as much as possible. The objective function and associated constraints of the hydrothermal scheduling problem are formulated as follows.

6.2.1. Objective function

$$\text{Minimize } f_{VH} = \sum_{t=1}^{\mathrm{T}} \sum_{i=1}^{\mathrm{N}_s} \left[a_{si} + b_{si}\mathrm{P}_{sit} + c_{si}\mathrm{P}_{sit}^2 + \left| d_{si} \times \sin\left\{ e_{si} \times \left(\mathrm{P}_{si}^{\min} - \mathrm{P}_{sit} \right) \right\} \right| \right] \tag{6.1}$$

6.2.2. Constraints

(i) Power balance constraints:

The total active power generation must balance the predicted power demand and transmission loss, at each time interval over the scheduling horizon

$$\sum_{i=1}^{\mathrm{N}_s} \mathrm{P}_{sit} + \sum_{j=1}^{\mathrm{N}_h} \mathrm{P}_{hjt} - \mathrm{P}_{Dt} - \mathrm{P}_{Lt} = 0 \qquad t \in \mathrm{T} \tag{6.2}$$

The hydroelectric generation is a function of water discharge rate and reservoir water head, which in turn, is a function of storage.

$$\mathrm{P}_{hjt} = C_{1j}V_{hjt}^2 + C_{2j}Q_{hjt}^2 + C_{3j}V_{hjt}Q_{hjt} + C_4 V_{hjt} + C_{5j}Q_{hjt} + C_{6j} \quad j \in \mathrm{N}_h \qquad t \in \mathrm{T} \tag{6.3}$$

The transmission loss P_{Lt} is given by

$$\mathrm{P}_{Lt} = \sum_{i=1}^{\mathrm{N}_s+\mathrm{N}_h} \sum_{j=1}^{\mathrm{N}_s+\mathrm{N}_h} \mathrm{P}_{it}\mathrm{B}_{ij}\mathrm{P}_{jt} + \sum_{i=1}^{\mathrm{N}_s+\mathrm{N}_h} \mathrm{B}_{0i}\mathrm{P}_{it} + \mathrm{B}_{00} \tag{6.4}$$

(ii) Generation limits:

$$\mathrm{P}_{hj}^{\min} \le \mathrm{P}_{hjt} \le \mathrm{P}_{hj}^{\max} \qquad , \; j \in \mathrm{N}_h \; , \; t \in \mathrm{T} \tag{6.5}$$

and

$$\mathrm{P}_{si}^{\min} \le \mathrm{P}_{sit} \le \mathrm{P}_{si}^{\max} , \qquad i \in \mathrm{N}_s , \; t \in \mathrm{T} \tag{6.6}$$

(iii) Hydraulic network constraints

The hydraulic operational constraints comprise the water balance equations for each hydro unit as well as the bounds on reservoir storage and release targets. These bounds are determined by the physical reservoir and plant limitations as well as the multipurpose requirements of the hydro system. These constraints include:

(a) Physical limitations on reservoir storage volumes and discharge rates,

$$V_{hj}^{\min} \le V_{hjt} \le V_{hj}^{\max} , \qquad j \in \mathrm{N}_h , \ t \in \mathrm{T} \tag{6.7}$$

$$Q_{hj}^{\min} \le Q_{hjt} \le Q_{hj}^{\max} , \qquad j \in \mathrm{N}_h , \ t \in \mathrm{T} \tag{6.8}$$

b) The continuity equation for the hydro reservoir network

$$V_{hj(t+1)} = V_{hjt} + \mathrm{I}_{hjt} - Q_{hjt} - S_{hjt} + \sum_{l=1}^{R_{uj}} \left(Q_{hl(t-\tau_{lj})} + S_{hl(t-\tau_{lj})} \right) , \qquad j \in \mathrm{N}_h , \ t \in \mathrm{T} \tag{6.9}$$

(iv) Prohibited operating regions of water discharge- rates

$$Q_{hj} \in \begin{cases} Q_{hj}^{\min} \le Q_{hj} \le Q_{hj,1}^{L} \\ Q_{hj,k-1}^{U} \le Q_{hj} \le Q_{hj,k}^{L} , k = 2,\ldots n_j \\ Q_{hj,n_j}^{U} \le Q_{hj} \le Q_{hj}^{\max} \end{cases} \tag{6.10}$$

6.3. Overview of Opposition-based Differential Evolution method

The overview of Opposition based Differential Evolution (ODE) method has been described in Chapter 5 of subsection 5.4

6.4. Simulation Results of ODE and DE algorithm

Three variable head hydrothermal test systems are considered to inspect and verify the proposed Opposition-based Differential Evolution (ODE) method.

6.4.1. Test System 1

This test system considers a multi-chain cascade of four reservoir hydro plants and an equivalent thermal plant. The entire scheduling period is 1 day and divided into 24 intervals. Here, two cases are considered.

Case 1: Here fuel cost is considered as a quadratic function of the power from the composite thermal plant. The detailed parameters for this case come from [69].

The problem is solved by using both the proposed ODE and DE. Here, the population size (N_P), scaling factor (F), crossover constant (C_R) and maximum iteration number have been selected 100, 1, 1 and 300 respectively for this case.

The optimal hourly discharges and hydrothermal generation obtained by the proposed ODE method are provided in Table A-15 and Table A-16 in appendices respectively. Fig. 6.1 depicts the reservoir storage volumes of four hydro plants obtained from ODE. The best, average and worst cost and average CPU time among 100 runs of solutions obtained from proposed ODE and DE are summarized in Table 6.1. The cost obtained from modified differential evolution (MDE) [72], improved particle swarm optimization (IPSO) [75], teaching learning based optimization (TLBO) [78], improved fast evolutionary programming (IFEP) [71] and genetic algorithm (GA) [69] methods are also shown in Table 6.1. The cost convergence characteristic obtained from proposed ODE and DE is shown in Fig.6.2. It is seen from Table 6.1 that the cost found by using ODE is the lowest among all other methods.

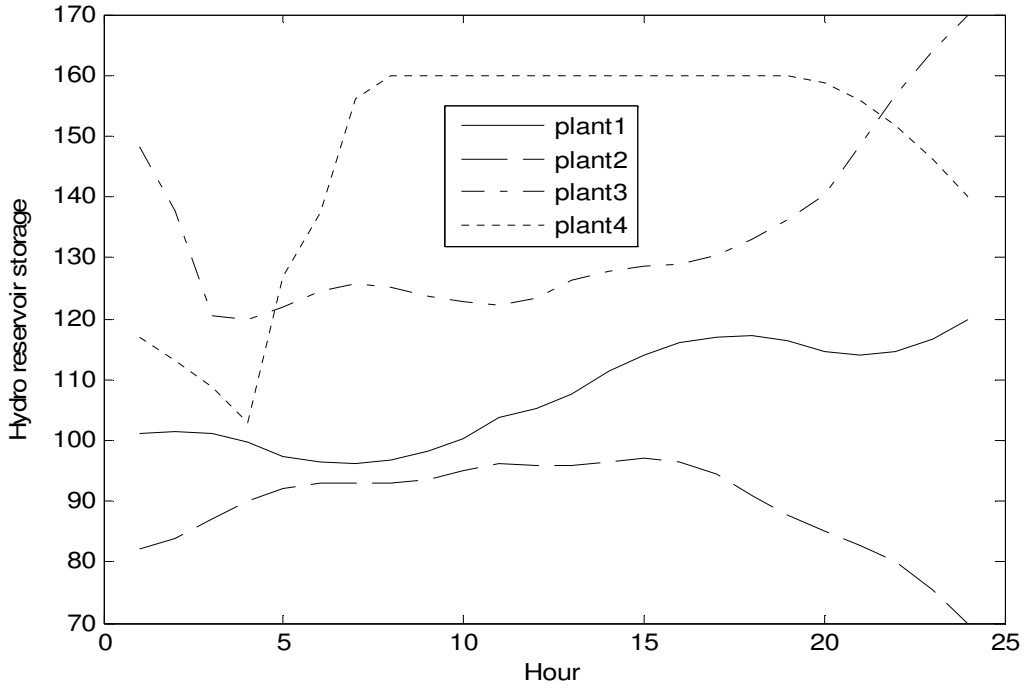

Fig. 6.1. Hydro reservoir storage volumes for case 1 of test system 1 of variable head hydrothermal system

Table 6.1: Comparison of performance for case 1 of Test System 1 of variable head hydrothermal system

Techniques	Best cost ($)	Average cost ($)	Worst cost ($)	CPU time (s)
ODE	917199.44	917208.56	917221.37	257.03
DE	918480.03	918494.37	918504.47	256.75
TLBO [78]	922373.39	922462.24	922873.81	-
IPSO [75]	922553.49	-	-	-
MDE [72]	922556.44	-	-	-
IFEP [71]	930129.82	930290.13	930881.92	1033.20
GA [69]	926707.00	-	-	-

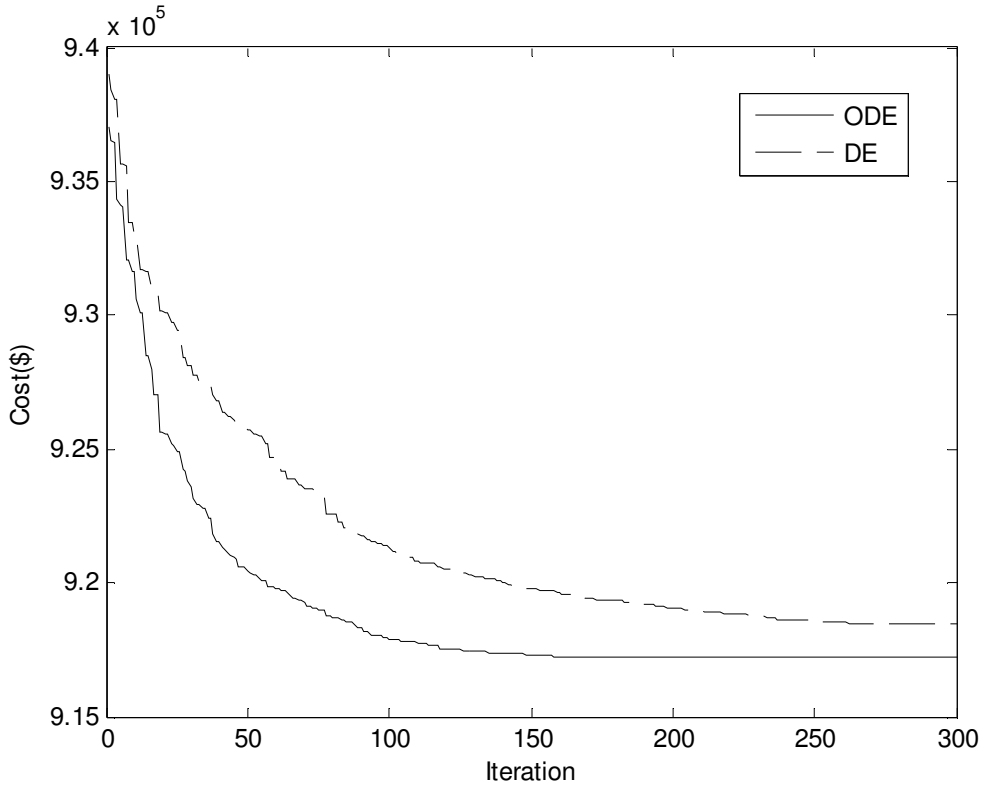

Fig. 6.2. Cost convergence characteristics for case 1 of test system 1 of variable head hydrothermal system

Case 2: Here prohibited operating zones of hydro plants and valve point loading of thermal generator are considered. The detailed parameters for this case come from [71].

The problem is solved by using both the proposed ODE and DE. Here, the population size (N_P),

scaling factor (F), crossover constant (C_R) and maximum iteration number have been selected 100, 1, 1 and 400 respectively for this case.

The optimal hourly discharges and hydrothermal generation obtained by the proposed ODE method are provided in Table A-17, Table A-18 respectively in appendices. Fig. 6.3 shows the reservoir storage volumes of four hydro plants obtained from ODE. The best, average and worst cost and average CPU time among 100 runs of solutions obtained from proposed ODE and DE are summarized in Table 6.4. The cost obtained from improved fast evolutionary programming (IFEP) [71], improved particle swarm optimization (IPSO) [75] and teaching learning based optimization (TLBO) [78] method is also shown in Table 6.4. The cost convergence characteristic obtained from proposed ODE and DE is shown in Fig. 6.4. It is seen from Table 6.4 that the cost found by using ODE is the lowest among all other methods.

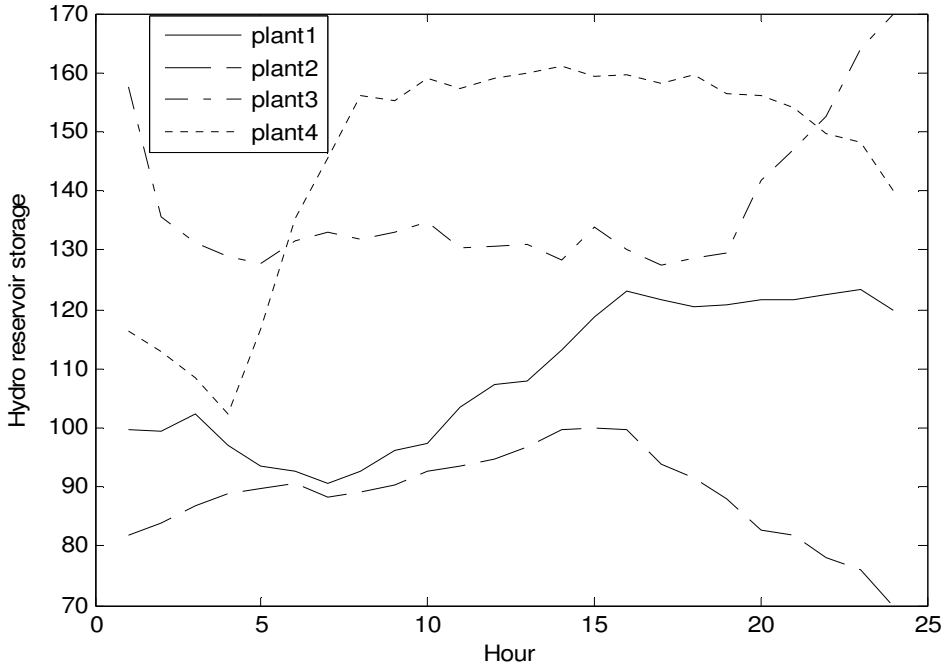

Fig. 6.3. Hydro reservoir storage volumes for case 2 of test system 1 of variable head hydrothermal system

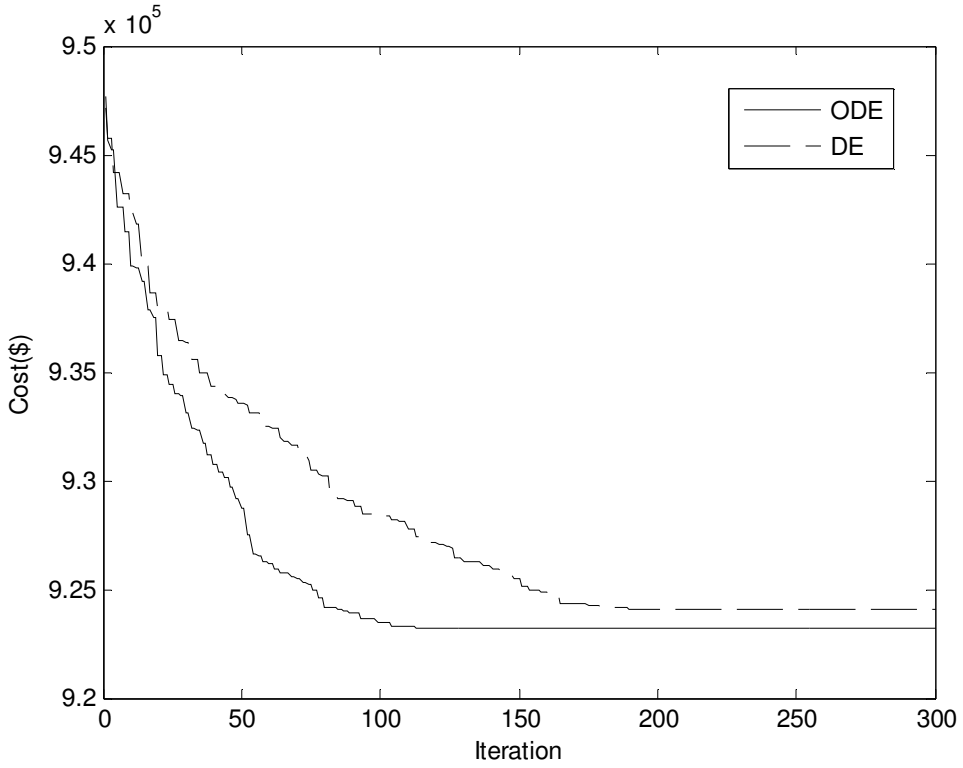

Fig. 6.4. Cost convergence characteristics for case 2 of test system 1 of variable head hydrothermal system

Table 6.2: Optimal Hydro Discharge ($\times 10^4 m^3$) for case 2 of test system 1 of variable head hydrothermal system

Hour	Q_{h1}	Q_{h2}	Q_{h3}	Q_{h4}
1	10.1845	6.1121	20.5536	6.3438
2	9.3545	6.0000	29.9857	6.0059
3	5.0934	6.0672	18.8188	6.0081
4	12.3025	6.9922	19.7814	6.0011
5	9.4396	6.9832	15.2970	6.3376
6	7.8835	6.3622	18.4255	11.1545
7	10.2721	8.2105	18.0212	8.7499
8	6.7694	6.0283	17.9212	9.3215
9	6.6014	6.9949	16.6465	15.9994
10	9.8394	6.6298	14.1732	14.6373
11	5.8365	8.0881	17.9684	19.8695
12	6.2467	6.7252	18.3894	15.9965
13	10.4311	6.0065	16.4035	15.9976
14	6.7118	6.0342	19.8262	13.0358
15	5.2117	8.9019	14.7661	19.6512
16	5.8669	8.0785	18.5218	18.0045
17	10.3436	13.0473	15.8221	18.0241
18	9.0289	8.2601	15.6486	18.1861
19	6.8068	10.6257	18.4059	18.1376
20	5.0351	13.1212	10.7805	18.6221
21	7.2673	9.9088	11.9574	18.0174
22	7.0480	12.8178	11.9622	20.0000
23	7.9655	10.0050	10.1140	19.8378
24	13.2600	13.2228	11.6386	19.6248

Table 6.3: Optimal Hydrothermal generation (MW) for case 2 of test system 1 of variable head hydrothermal system

Hour	P_{h1}	P_{h2}	P_{h3}	P_{h4}	P_s
1	86.8344	49.7921	42.4872	136.4915	1054.39
2	82.7927	50.0996	0	128.7959	1128.31
3	53.2023	51.7131	38.2060	125.5285	1091.35
4	95.3572	59.6889	32.3296	121.2998	981.32
5	82.2469	60.718	45.8186	119.8371	981.38
6	72.3219	57.0068	36.5382	189.8853	1054.25
7	84.3272	69.3217	39.5418	180.8054	1276.01
8	63.8671	53.8113	40.4187	196.2406	1645.66
9	63.4079	61.0171	43.8752	273.675	1798.02
10	83.8010	59.0764	48.8933	261.1712	1867.06
11	58.8915	69.7213	40.9075	304.3079	1756.17
12	63.6159	61.3895	37.7617	274.8044	1872.42
13	90.3650	56.9064	44.1043	276.5894	1762.03
14	68.1055	58.0340	32.0219	249.5939	1792.24
15	56.4505	78.0365	46.5805	304.8704	1644.06
16	62.7673	73.2219	38.5827	292.2578	1603.17
17	93.8183	96.3354	45.1644	292.7708	1601.91
18	86.3257	71.3305	44.6121	292.334	1645.39
19	70.6874	82.4647	36.9713	293.5957	1756.28
20	55.3803	89.5719	48.3725	293.5926	1793.08
21	74.3523	73.9104	52.4342	289.3438	1749.96
22	72.6529	84.7098	53.7410	299.7932	1609.10
23	79.4951	71.3102	53.2242	294.2187	1351.75
24	104.9608	81.7733	57.2461	291.4408	1054.58

Table 6.4: Comparison of performance for case 2 of test system 1 of variable head hydrothermal system

Techniques	ODE	DE	IFEP [71]	TLBO [78]	IPSO [75]
Best cost ($)	923230.63	924069.73	933949.25	924550.78	925978.84
Average cost($)	923242.45	924083.56	938508.87	924702.43	-
Worst cost ($)	923255.37	924096.28	942593.02	925149.06	-
CPU time (s)	264.73	258.65	1450.90	-	-

6.4.2. Test System 2

This system considers a multi-chain cascade of four reservoir hydro plants and three thermal plants. The entire scheduling period is 1 day and divided into 24 intervals. The effect of valve point loading is considered. Transmission loss is also considered. The detailed parameters for this case are taken from [72].

The problem is solved by using both the proposed ODE and DE. Here, the population size (N_P), scaling factor (F), crossover constant (C_R) and maximum iteration number have been selected 100, 1, 1 and 300 respectively for this case. The optimal hourly discharges and hydrothermal

generation obtained by the proposed ODE method are provided in Table A-19 Table A-20 respectively in appendices. Fig. 6.5. shows the reservoir storage volumes of four hydro plants obtained from ODE.

The best, average and worst cost and average CPU time among 100 runs of solutions obtained from proposed ODE and DE are shown in Table 6.7. The cost obtained from modified differential evolution (MDE) [72], clonal selection algorithm (CSA) [77] and teaching learning based optimization (TLBO) [78] is also shown in Table 6.7. The cost convergence characteristic obtained from proposed ODE and DE is shown in Fig. 6.6. It is seen from Table 6.7 that the cost found by using ODE is the lowest among all other methods.

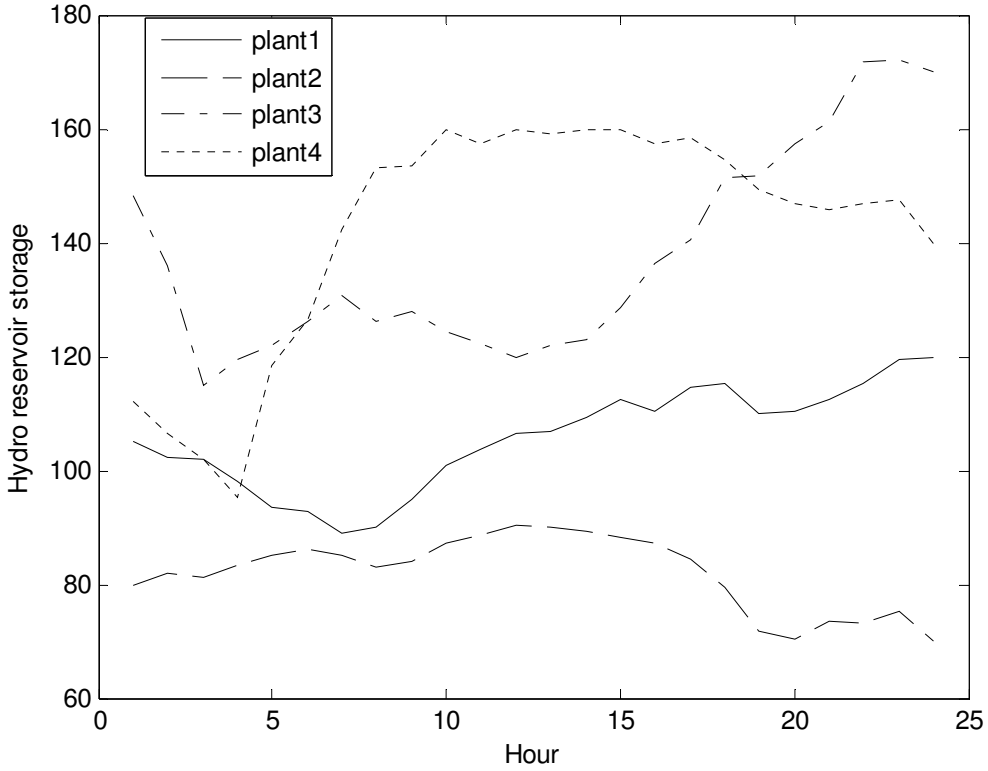

Fig. 6.5. Hydro reservoir storage volumes of test system 2
of variable head hydrothermal system

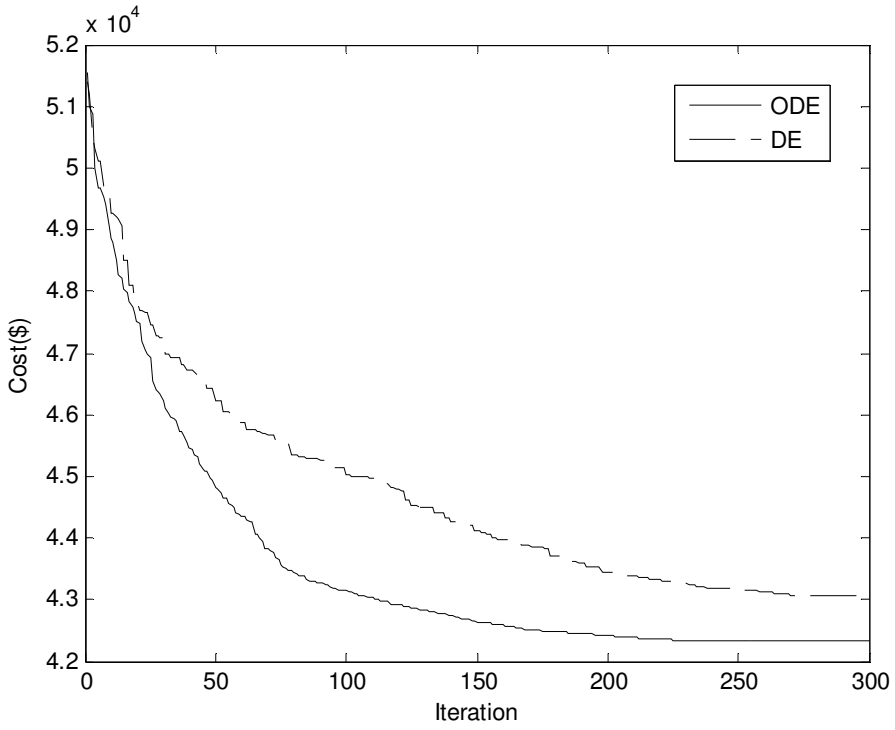

Fig. 6.6. Cost convergence characteristics of test system 2
of variable head hydrothermal system

Table 6.5: Optimal Hydro Discharge ($\times 10^4 m^3$) of test system 2 of variable head hydrothermal system

Hour	Q_{h1}	Q_{h2}	Q_{h3}	Q_{h4}
1	5.0000	8.1694	29.9825	10.6846
2	11.8249	6.0349	20.3834	8.1109
3	8.2756	9.3968	29.9993	6.0699
4	10.6764	7.1839	17.4356	6.5270
5	10.7913	6.1217	14.9166	7.0655
6	7.5122	6.0114	19.9168	12.2241
7	11.8929	7.1014	16.4236	14.2319
8	8.0364	8.9342	19.9639	6.3860
9	5.0000	7.0265	17.2913	14.8253
10	5.2012	6.0000	19.6801	13.3341
11	9.0382	7.4124	16.8647	18.8811
12	7.1895	6.0830	16.7021	17.6400
13	10.7560	8.4874	17.0601	18.0055
14	9.6444	9.6666	16.3546	18.8809
15	7.5333	10.1478	14.5476	16.8217
16	12.2331	9.0725	12.3182	19.4624
17	5.0001	9.8397	14.7639	16.0024
18	6.9996	10.8825	13.7793	20.0000
19	12.3816	14.8071	14.5850	20.0000
20	5.7002	9.2668	12.3534	14.4891
21	5.0013	6.0008	21.3704	15.8796
22	5.0078	9.1880	11.7756	12.9617
23	5.0002	6.0045	15.2021	13.6869
24	9.3038	13.1606	12.9722	19.9519

Table 6.6: Optimal Hydrothermal generation (MW) of test system 2 of variable head hydrothermal system

Hour	P_{h1}	P_{h2}	P_{h3}	P_{h4}	P_{s1}	P_{s2}	P_{s3}
1	52.5001	62.9911	0	188.4124	20.0000	40.0470	409.0353
2	94.9645	49.1472	36.0943	151.4483	20.0001	294.7080	139.9935
3	77.4693	70.7940	0	120.2516	174.9999	40.0626	229.7881
4	89.6264	57.8274	34.8294	121.7495	174.9999	40.0144	140.0427
5	88.6817	51.7208	43.1194	121.7213	20.0713	209.8746	139.7717
6	69.9013	51.9834	27.7926	202.2525	20.0027	294.7478	139.7384
7	90.0410	59.9969	42.2954	229.2022	102.8131	294.9635	140.0704
8	71.5381	70.3084	31.2740	155.4249	175.0000	294.7975	229.5029
9	49.9772	57.7790	39.9087	261.0326	174.9942	294.7360	229.4873
10	53.0657	51.3073	31.4504	247.0815	102.6427	294.7893	319.3190
11	81.4462	62.5231	40.4364	298.9633	20.0014	294.7375	319.3074
12	70.7288	54.3802	40.1454	287.9098	102.6722	294.7042	319.2878
13	91.5678	70.9632	38.1093	292.8062	20.0158	294.6822	319.3190
14	86.4941	77.0705	40.8922	298.1207	102.6981	294.7381	139.8472
15	74.3655	79.0482	45.0727	283.9845	102.6488	294.7742	139.7885
16	98.9002	72.9424	48.6283	302.6975	20.0008	298.7904	229.5013
17	54.2296	76.2645	49.2103	274.8114	174.9981	294.7637	139.6912
18	71.4333	79.2985	51.6777	304.2234	102.6951	294.7382	229.7389
19	100.2199	87.8464	53.8828	300.4273	102.7774	294.7563	140.0848
20	60.3478	63.3576	55.0328	254.1731	20.0000	294.7757	319.3300
21	54.2311	42.9424	34.5069	264.0216	175.0000	40.0042	319.0230
22	54.5201	64.1698	56.8181	236.6617	20.0000	294.7116	139.6709
23	54.7321	44.8122	58.1308	244.4422	20.0024	294.6434	139.7895
24	87.5753	80.9892	59.3598	292.6200	20.0004	125.0043	139.8794

Table 6.7: Comparison of performance of test system 2 of variable head hydrothermal system

Techniques	ODE	DE	MDE [72]	TLBO [79]	CSA [77]
Best cost ($)	42322.23	43068.01	43435.41	42385.88	42440.574
Averagecost ($)	42330.53	43079.52	-	42407.23	-
Worst cost ($)	42339.36	43083.05	-	42441.36	-
CPU time (s)	304.05	298.72	-	-	-

6.4.3. Test System 3

This system considers a multi-chain cascade of four reservoir hydro plants and ten thermal plants. The entire scheduling period is 1 day and divided into 24 intervals. The effect of valve point loading is taken into account. Here transmission loss is not considered. The detailed data for this system is taken from [74].

The problem is solved by using both the proposed ODE and DE. Here, the population size (N_P), scaling factor (F), crossover constant (C_R) and maximum iteration number have been selected 100, 1, 1 and 900 respectively for this case. The optimal hourly discharges and hydrothermal

generation obtained by the proposed ODE method are provided in Table A-21, Table A-22 respectively in appendices.

Fig. 6.7 shows the reservoir storage volumes of four hydro plants obtained from ODE. The best, average and worst cost and average CPU time among 100 runs of solutions obtained from proposed ODE and DE are summarized in Table 6.10. The cost obtained from differential evolution (DE) [74] method is also shown in Table 6.10. The cost convergence characteristic obtained from proposed ODE and DE is shown in Fig. 6.8. It is seen from Table 6.10 that the cost found by using ODE is the lowest among all other methods.

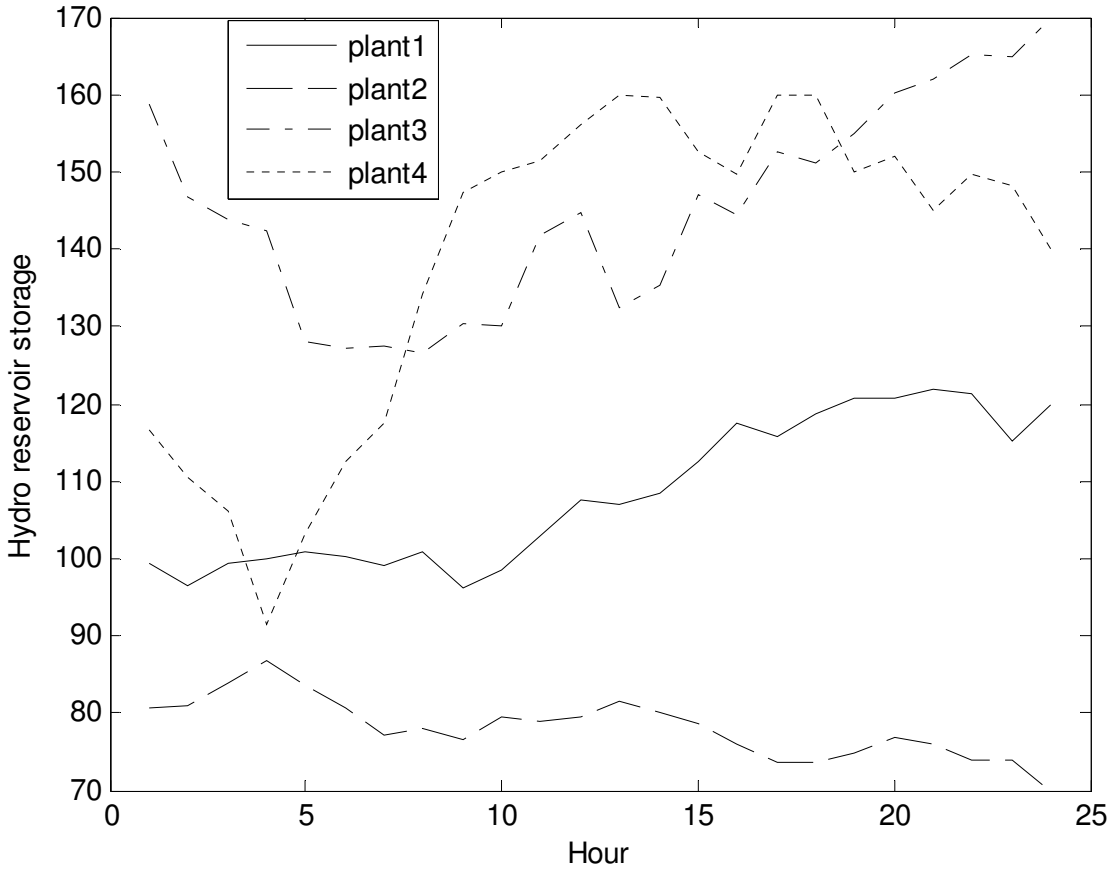

Fig. 6.7. Hydro reservoir storage volumes for test system 3 of variable head hydrothermal system

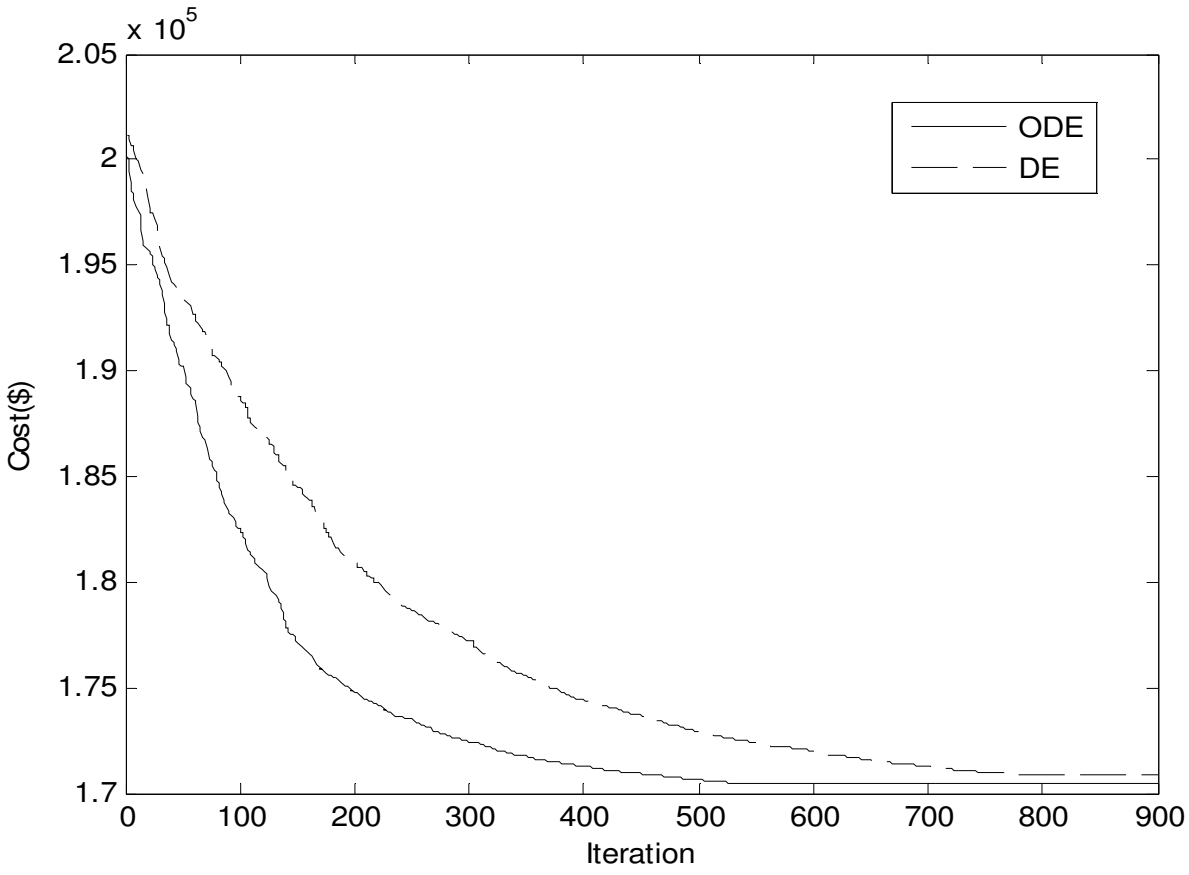

Fig. 6.8. Cost convergence characteristics for test system 3 of variable head hydrothermal system

Table 6.8: Optimal Hydro Discharge ($\times 10^4 m^3$) of test system 3 of variable head hydrothermal system

Hour	Q_{h1}	Q_{h2}	Q_{h3}	Q_{h4}
1	10.5900	7.2207	19.4370	6.0254
2	12.0523	7.7304	20.2455	8.5457
3	5.0001	6.0184	17.4557	6.0000
4	6.4478	6.3207	22.6585	14.8061
5	5.0000	11.1350	29.9287	7.6698
6	7.6269	9.9408	17.6070	10.8973
7	9.2146	9.5815	13.9492	12.4732
8	7.1216	6.0000	21.4589	6.0044
9	14.7220	9.4742	16.3758	16.8335
10	8.7003	6.0001	18.0804	15.0361
11	7.6528	9.7120	10.0203	12.3636
12	5.4338	7.2947	17.1649	16.8305
13	11.5460	6.0053	30.0000	12.6269
14	10.5001	10.4945	15.3613	18.1704
15	6.9555	10.5776	10.0003	17.1377
16	5.0000	10.6310	21.2541	19.9868
17	10.5398	9.0909	11.1185	19.9873
18	5.1753	6.0028	19.1245	15.2733
19	5.0000	6.0000	18.4536	19.9871
20	5.8448	6.0003	10.0100	19.2115
21	6.0854	9.8456	11.2876	17.9333
22	8.5236	11.1071	10.4763	14.4865
23	14.9775	7.8296	13.2974	19.9983
24	5.2899	11.9870	13.3435	18.2195

Table 6.9: Optimal Hydrothermal generation (MW) for test system 3 of variable head hydrothermal system

Hour	P_{h1}	P_{h2}	P_{h3}	P_{h4}	P_{s1}	P_{s2}	P_{s3}	P_{s4}	P_{s5}	P_{s6}	P_{s7}	P_{s8}	P_{s9}	P_{s10}
1	88.5676	57.2201	47.0843	132.2239	139.7462	199.5787	94.9554	119.9507	274.6901	139.7256	45.0047	134.5020	98.1889	178.5618
2	93.4214	60.8649	40.3432	161.1911	50.0010	350.6038	20.4259	20.0004	224.3871	239.4088	281.9108	85.1760	25.0195	127.2461
3	51.6806	49.7455	46.6711	123.3513	229.2817	124.0582	20.0000	119.8332	274.3626	89.8035	163.1392	134.3029	97.0795	176.6904
4	64.1960	53.5788	22.2002	210.9095	229.2333	124.6531	20.0501	119.5701	224.5807	139.8210	104.1674	134.6485	25.0013	177.3898
5	52.4810	81.8434	0	124.6475	140.1426	199.9715	95.3239	120.0332	175.6493	40.2031	222.6977	135.1454	103.3599	178.5014
6	72.9780	74.5900	39.6390	172.7592	228.4289	199.5966	20.1401	69.3630	174.6341	289.5033	222.8367	134.7805	25.0000	75.7505
7	82.2228	70.9868	47.2010	198.3559	318.9251	199.5684	94.6931	119.9201	174.6363	139.7735	45.0001	234.5971	97.7873	126.3325
8	69.0212	47.2262	22.2530	129.7342	229.4300	422.7929	95.4989	119.5967	273.9787	189.4554	102.8809	84.9181	97.3506	125.8631
9	98.8275	68.7802	42.6653	258.0113	319.3601	423.9171	20.3141	69.8048	25.0100	139.9045	163.4803	184.4494	98.0940	177.3813
10	78.0403	46.9347	38.9243	257.2106	319.8205	274.7959	95.2935	69.9514	224.6139	189.1829	163.6077	35.0485	159.9696	126.6063
11	72.4527	70.9485	47.7153	234.1379	319.2929	124.7317	94.8140	120.2192	224.5801	139.5221	341.3076	35.0054	98.2030	177.0697
12	56.8438	56.9932	45.9128	275.8907	230.0333	50.7516	20.1698	119.5267	379.1170	289.1176	104.2716	184.7861	159.9982	176.5876
13	94.8980	48.7840	0	242.2134	139.8324	274.4415	95.1403	69.8449	469.9935	89.6793	163.3926	84.8894	159.9984	176.8925
14	90.5802	75.8706	46.9657	293.9404	229.3965	274.4531	94.6048	20.0137	273.2281	139.8295	281.7942	35.0008	98.4802	75.8422
15	70.0608	75.2619	49.0555	286.2452	50.0001	424.0944	94.7114	129.9991	174.5623	40.0000	45.0649	284.1163	159.9975	126.8307
16	54.4620	74.4441	31.4282	298.2087	229.3469	199.3362	129.9942	70.0416	25.0000	188.9987	400.0086	134.4338	97.6077	126.6892
17	93.6431	65.3782	52.5869	295.1849	50.0097	273.9768	94.4723	69.8887	74.8041	289.2354	281.7366	184.3100	98.3925	126.3805
18	56.3901	45.1903	43.0147	270.9021	229.4754	423.8369	94.6491	69.8844	174.6510	189.6651	163.6530	184.4627	98.1968	76.0285
19	54.9594	45.1688	44.9555	305.7963	454.3275	274.4155	20.3014	69.5663	74.3859	239.4500	104.2637	184.7943	159.9911	37.6244
20	62.7075	45.8064	53.4968	290.7342	50.0001	274.6687	94.9396	119.5349	324.1705	90.0924	222.8150	134.4347	159.9665	126.6326
21	64.7903	69.7331	56.2031	284.4660	229.4512	349.3310	20.0004	20.0019	273.7897	139.5154	45.0000	184.7127	97.3568	75.6484
22	83.1783	74.6517	55.5310	250.3066	319.5464	349.2805	20.0039	119.7490	75.5053	40.0554	163.3451	84.7404	98.4503	125.6563
23	107.4231	57.0151	58.0351	295.2245	229.3402	199.7585	95.1532	119.6982	75.1793	140.3943	163.4162	84.8138	98.1993	126.3492
24	57.3775	76.5220	57.9827	282.6004	319.2834	274.0316	94.4750	69.6811	25.0002	139.5081	45.0000	134.7093	98.0004	125.8284

Table 6.10: Comparison of performance for test system 3 of variable head hydrothermal system

Techniques	ODE	DE	DE [74]
Best cost ($)	170452.35	170915.57	170964.15
Average cost ($)	170459.78	170924.41	-
Worst cost ($)	170468.52	170935.28	-
CPU time (s)	472.51	459.92	-

It is observed from in Table A-16, Table A-18, Table A-20 and Table A-22 respectively in appendices that the third hydro unit has no output during some time interval. This is because of the fact that output from a particular hydro unit during a specified time interval depends on the availability of water, reservoir storage volume limit, water transport delay between cascaded reservoirs and on the system configuration as a whole. Depending on the system configuration and constraints for the present problem, this has happened in case of the third hydro unit.

6.5. Conclusion

In this paper, opposition-based differential evolution is demonstrated and presented to solve the hydrothermal scheduling problem. The proposed opposition-based differential evolution method has been successfully applied to two test problems, two fixed head hydrothermal test systems and three hydrothermal multi-reservoir cascaded hydroelectric test systems having prohibited operating zones and thermal units with valve point loading. The results have been compared with those obtained by other evolutionary algorithms reported in the literature. It has been seen from the comparisons that the proposed opposition-based differential evolution method gives better result.

CHAPTER-7
Reactive Power Dispatch

7.1. Introduction

Reactive power dispatch (RPD) perks up power system economy and security. Reactive power generation has no production cost but in general it has an effect on the production cost related with active power transmission loss. RPD minimizes active power transmission loss and perks up voltage profile and voltage stability by adjusting control variables such as generator voltages, transformer tap settings, reactive power output of shunt VAR compensators etc. at the same time satisfying several equality and inequality constraints. The Reactive Power Dispatch (RPD) problem has a significant influence on secure and economic operation of power systems. It is one of the most complex problems, as it requires the minimization of the real power losses in a power system.

A variety of classical optimization techniques such as Newton method, linear programming, quadratic programming and interior point method have been pertained to solve RPD problem. RPD is a mixture of discrete and continuous variables with multiple local optima. So it is exigent to acquire global optima by using classical optimization techniques.

Here, improved real coded genetic algorithm (IRCGA) is applied to solve different types of reactive power dispatch problems. Genetic algorithm (GA) is a bunch of evolutionary algorithms root of the basic human heritable chromosome operation. GA has the ability to ascertain the global or close to the global optimal solutions. In this study, IRCGA has been suggested to heighten convergence speed and solution quality. The developed IRCGA has been exploited for acquiring the control variables settings such as generator terminal voltages, transformer taps and reactive power output of shunt VAR compensators to acquire minimum active power transmission loss, improved voltage profile and voltage stability. IRCGA has been tested on IEEE 30-bus, 57-bus and 118-bus test systems and 15 benchmark functions. Test results have been compared with those acquired from other stated evolutionary techniques.

7.2. Problem Formulation

The goal of RPD is to minimize active power transmission loss and to perk up voltage profile and stability at the same time fulfilling equality and inequality constraints. The objective functions and constraints can be stated as:

7.2.1. Objective functions

7.2.1.1. Minimization of active power transmission loss

The objective function [95] can be stated as:

$$\text{Minimize } F_1 = \mathrm{P}_{loss} = \sum_{k=1}^{\mathrm{NT}L} g_k \left[V_i^2 + V_j^2 - 2V_i V_j \cos\left(\delta_i - \delta_j\right) \right] \tag{7.1}$$

where P_{loss} signifies active power transmission loss, $\mathrm{NT}L$ is the number of transmission lines, g_k is the conductance of branch k connected between ith bus and jth bus, V_i and V_j are the magnitude voltage of ith and jth buses, δ_i and δ_j are the phase angle of voltages of the ith and jth buses.

7.2.1.2. Improvement of voltage profile

The objective is to minimize the voltage deviation of all load ($\mathrm{P}Q$) buses from 1 p.u to perk up power system security and service quality. The objective function [97] can be stated as:

$$\text{Minimize } F_2 = \sum_{i=1}^{\mathrm{NP}Q} \left| V_i - 1.0 \right| \tag{7.2}$$

where $\mathrm{NP}Q$ is the number of load buses.

7.2.1.3. Improvement of voltage stability

Voltage stability is the capacity of a power system to keep up suitable voltages at all bus bars beneath normal operating condition and even after disturbances such as change in load demand or system configuration. In recent times a number of major network collapses [103] have been taken place due to voltage instability. Improvement of voltage stability has been acquired by

minimizing voltage stability indicator i.e. $L-$index value at each bus which signifies voltage collapse condition of that bus. L_j of jth bus [104] can be stated as:

$$L_j = \left|1 - \sum_{i=1}^{\mathrm{NP}V} F_{ji} \frac{V_i}{V_j}\right| \quad \text{where } j = 1,2,....., \mathrm{NP}Q \tag{7.3}$$

$$F_{ji} = -[\mathrm{Y}_1]^{-1}[\mathrm{Y}_2] \tag{7.4}$$

where $\mathrm{NP}V$ is the number of PV bus and $\mathrm{NP}Q$ is the number of PQ bus. Y_1 and Y_2 are sub-matrices. YBUS acquired after segregating the PQ and PV bus parameters can be stated as:

$$\begin{bmatrix} \mathrm{I}_{\mathrm{PQ}} \\ \mathrm{I}_{\mathrm{PV}} \end{bmatrix} = \begin{bmatrix} \mathrm{Y}_1 \mathrm{Y}_2 \\ \mathrm{Y}_3 \mathrm{Y}_4 \end{bmatrix} \begin{bmatrix} V_{\mathrm{PQ}} \\ V_{\mathrm{PV}} \end{bmatrix} \tag{7.5}$$

$L-$index is computed for all PQ buses. L_j is zero or one depending upon no load condition or voltage collapse condition of jth bus. The objective function [97] can be stated as:

Minimize $F_3 = \max(L_j)$, where $j = 1,2,....., \mathrm{NP}Q$ (7.6)

7.2.2. Constraints

7.2.2.1. Equality constraints

$$\mathrm{P}_{Gi} - \mathrm{P}_{Di} - V_i \sum_{j=1}^{\mathrm{NB}} V_j \left[G_{ij} \cos(\delta_i - \delta_j) + \mathrm{B}_{ij} \sin(\delta_i - \delta_j)\right] = 0, \quad i = 1,2,.., \mathrm{NB} \tag{7.7}$$

$$Q_{Gi} - Q_{Di} - V_i \sum_{j=1}^{\mathrm{NB}} V_j \left[G_{ij} \sin(\delta_i - \delta_j) - \mathrm{B}_{ij} \cos(\delta_i - \delta_j)\right] = 0, \quad i = 1,2,.., \mathrm{NB} \tag{7.8}$$

where NB is the number of buses, P_{Gi} and Q_{Gi} are active and reactive power generation at the ith bus, P_{Di} and Q_{Di} are active and reactive power demands at the ith bus, G_{ij} and B_{ij} are the transfer conductance and susceptance between ith bus and jth bus respectively.

7.2.2.2. Inequality constraints

7.2.2.2.1. Generator constraints

The generator voltage magnitudes and reactive power outputs curbed by their minimum and maximum limits can be stated as:

$$V_{Gi}^{\min} \le V_{Gi} \le V_{Gi}^{\max},\ i = 1,2,...,\mathrm{N}G \tag{7.9}$$

$$Q_{Gi}^{\min} \le Q_{Gi} \le Q_{Gi}^{\max},\ i = 1,2,...,\mathrm{N}G \tag{7.10}$$

7.2.2.2.2. Shunt VAR compensator constraints

Reactive power output of shunt VAR compensators curbed by their minimum and maximum limits can be stated as:

$$Q_{ci}^{\min} \le Q_{ci} \le Q_{ci}^{\max},\ i = 1,2,....,\mathrm{N}C \tag{7.11}$$

7.2.2.2.3. Transformer constraints

Transformer tap settings curbed by their physical deliberation can be stated as:

$$\mathrm{T}_i^{\min} \le \mathrm{T}_i \le \mathrm{T}_i^{\max},\quad i = 1,2,...,\mathrm{NT} \tag{7.12}$$

7.2.2.2.4. Security constraints

The voltage magnitude of each PQ bus curbed by its minimum and maximum limits and transmission line flow curbed by its maximum limit can be stated as:

$$V_{Li}^{\min} \le V_{Li} \le V_{Li}^{\max},\ i = 1,2,..,\mathrm{NP}Q \tag{7.13}$$

$$S_{li} \le S_{li}^{\max},\ i = 1,2,...,\mathrm{NT}L \tag{7.14}$$

7.3. Overview of Improved Real Coded Genetic Algorithm

The overview of Improved Real Coded Genetic Algorithm (IRCGA) has been explained in Chapter 3 of subsection 3.4.

7.4. Simulation and Results of IRCGA and RCGA algorithm

The developed IRCGA and RCGA have been pertained to solve different types of RPD problems and three different test systems with three different objective functions and 15 benchmark functions have been tested to confirm its efficacy. Test results compared with those acquired from other stated evolutionary techniques. The developed IRCGA and RCGA programs have been executed in MATLAB 7.0 on a PC (Pentium-IV, 80 GB, 3.0 GHz).

7.4.1. IEEE 30-bus system

The line data, bus data, generator data and the minimum and maximum limits for the control variables have been adapted from [95]. The system has six generators at buses 1, 2, 5, 8, 11 and 13 and four transformers with off nominal tap ratio at lines 6-9, 6-10, 4-12, and 28-27 and shunt VAR compensators are connected at bus bars 10, 12, 15, 17, 20, 21, 23, 24 and 29. Total real power demand is 2.834 p.u. at 100 MVA base. 50 runs are carried out for each case.

7.4.1.1. Minimization of active power transmission loss

The developed IRCGA and RCGA have been pertained to minimize active power transmission loss. Here, maximum number of iterations, population size, crossover and mutation probabilities have been chosen as 100, 100, 0.9 and 0.2, respectively for IRCGA and RCGA.

The optimal control variables acquired from the developed IRCGA have been summed up in Table 7.1. The best, average and worst minimum active power transmission loss and average CPU time among 50 runs acquired from developed IRCGA and RCGA are summarized in Table 7.2. The minimum active power transmission loss acquired from PSO [101] and CLPSO [101], modified teaching learning algorithm and double differential evolution (MTLA-DDE) [102], novel teaching–learning-based optimization (NTLBO) [99] and quasi-oppositional differential evolution (QODE) [97] are also shown in Table 7.2. The convergence characteristic acquired from developed IRCGA and RCGA has been portrayed in Fig. 7.1. It has been observed from Table 7.2, that the minimum active power transmission loss acquired from IRCGA is the lowest among all other stated techniques.

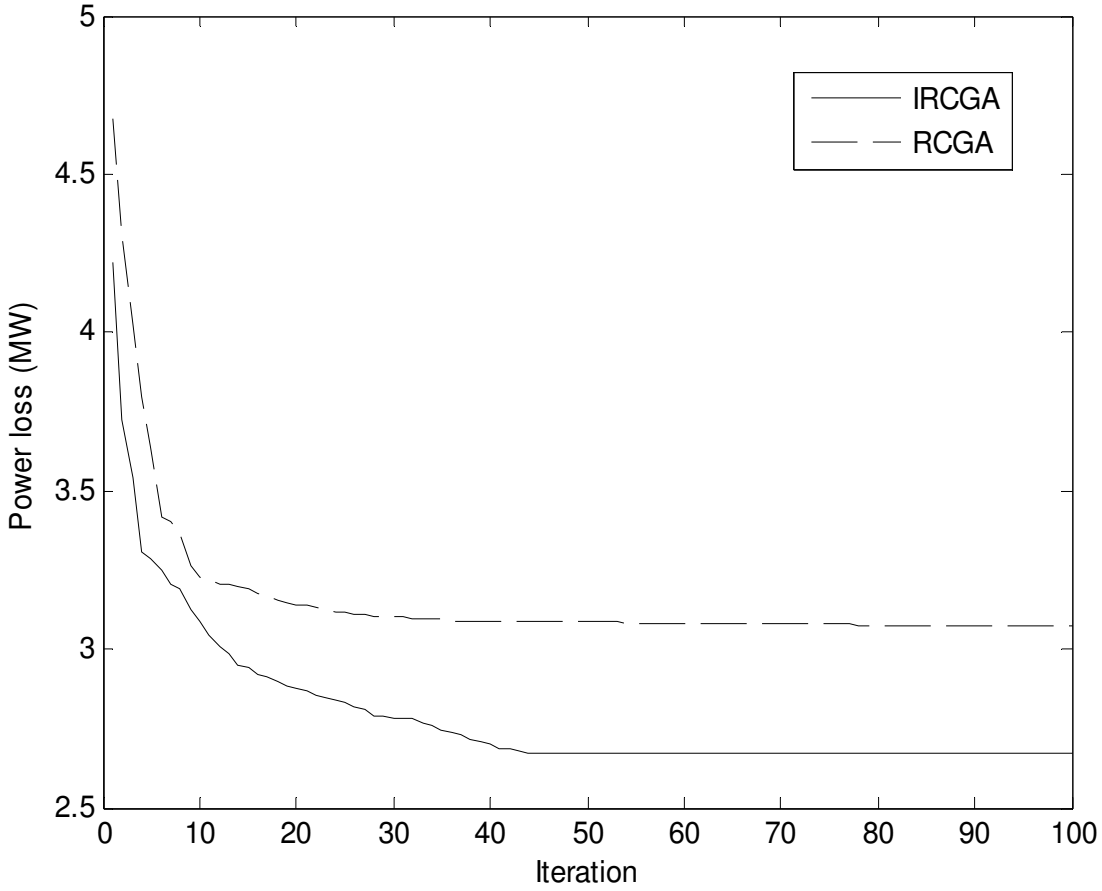

Fig. 7.1. Active power transmission loss minimization Convergence characteristics of IEEE 30 bus system

Table 7.1: Optimal control variables acquired from IRCGA of IEEE 30 bus system for three different cases

Variable	Active power loss minimization	Voltage stability improvement	Voltage profile improvement
V_1	1.0500	1.0500	1.0500
V_2	1.0337	1.0335	1.0341
V_5	1.0055	1.0054	1.0062
V_8	1.0229	1.0231	1.0237
V_{11}	1.0911	1.0912	1.0910
V_{13}	1.0398	1.0403	1.0393
T_{6-9}	0.9865	0.9911	1.0114
T_{6-10}	1.0150	1.0058	1.0203
T_{4-12}	0.9823	1.0248	1.0001
T_{28-27}	0.9805	0.9910	0.9961
Q_{c10}	0.0171	0.0273	0.0049
Q_{c12}	0.0436	0.0500	0.0000
Q_{c15}	0.0056	0.0103	0.0000
Q_{c17}	0.0442	0.0000	0.0158
Q_{c20}	0.0353	0.0346	0.0475
Q_{c21}	0.0280	0.0483	0.0395
Q_{c23}	0.0111	0.0407	0.0381
Q_{c24}	0.0407	0.0428	0.0065
Q_{c29}	0.0221	0.0500	0.0071
power loss (MW)	2.6699	9.0759	9.3400
voltage deviation	0.6902	0.9019	0.0612
$L_{\max}$	0.0489	0.0225	0.0535

Table 7.2: Comparison of active power transmission loss minimization of IEEE 30 bus system

Techniques	Best loss (MW)	Average loss (MW)	Worst loss (MW)	CPU time (S)
IRCGA	2.6699	2.6708	2.6804	60.57
RCGA	3.2437	3.2459	3.2505	57.67
PSO [101]	4.6282	-	-	130
CLPSO [101]	4.5615	-	-	138
MTLA-DE[102]	4.8596	-	-	-
NTLBO [99]	4.7802	-	-	-
QODE [97]	2.6867	2.6879	2.6895	82.074

7.4.1.2. Improvement of voltage stability

The developed IRCGA and RCGA have been pertained to perk up voltage stability. Here, maximum number of iterations, population size, crossover and mutation probabilities have been chosen as 50, 100, 0.9 and 0.2, respectively for IRCGA and RCGA. The optimal control variables acquired from the developed IRCGA are summed up in Table 7.1. The best, average and worst $L_{\max}$ value and average CPU time among 50 runs acquired from developed IRCGA and RCGA are shown in Table 7.3. The convergence characteristic acquired from developed IRCGA and RCGA has been portrayed in Fig. 7.2. It has been observed from Table 7.3 that $L_{\max}$ value acquired from the developed IRCGA is lower than RCGA.

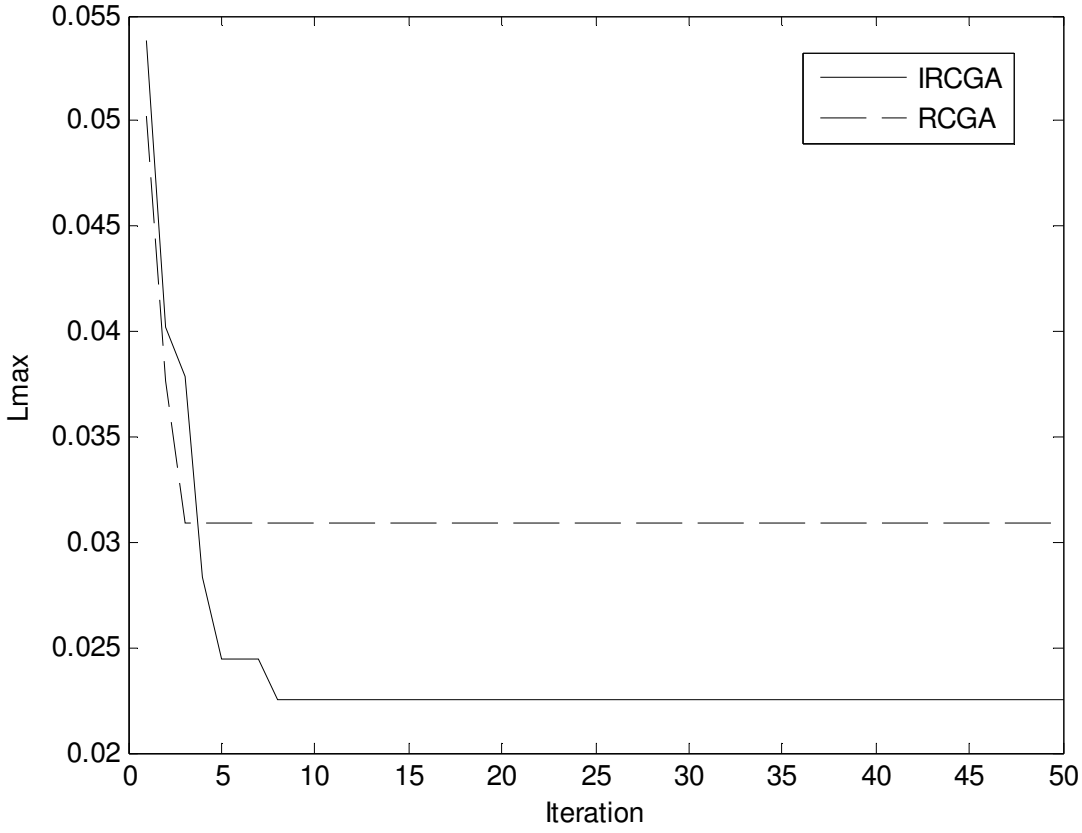

Fig. 7.2. L_{max} Convergence characteristics of IEEE 30 bus system

Table 7.3: Comparison of performance for L_{max} minimization of IEEE 30 bus system

Techniques	Best L_{max}	Average L_{max}	Worst L_{max}	CPU time (S)
IRCGA	0.0225	0.0236	0.0245	59.738
RCGA	0.0309	0.0310	0.0312	52.352

7.4.1.3. Improvement of voltage profile

The developed IRCGA and RCGA have been pertained to perk up voltage profile. Here, maximum number of iterations, population size, crossover and mutation probabilities have been chosen as 100, 100, 0.9 and 0.2, respectively for IRCGA and RCGA. The optimal control variables acquired from the developed IRCGA are summarized in Table 7.1. The best, average

and worst voltage deviation and average CPU time among 50 runs acquired from developed IRCGA and RCGA are summarized in Table 7.4. The convergence characteristic acquired from developed IRCGA and RCGA has portrayed in Fig. 7.3. It has been observed from Table 7.4 that voltage deviation acquired from the developed IRCGA is the lower than RCGA.

Table 7.4: Comparison of performance for voltage deviation of IEEE 30 bus system

Techniques	Best voltage deviation (p.u.)	Average voltage deviation (p.u.)	Worst voltage deviation (p.u.)	CPU time (S)
IRCGA	0.0612	0.0615	0.0620	63.10
RCGA	0.0627	0.0629	0.0633	58.06

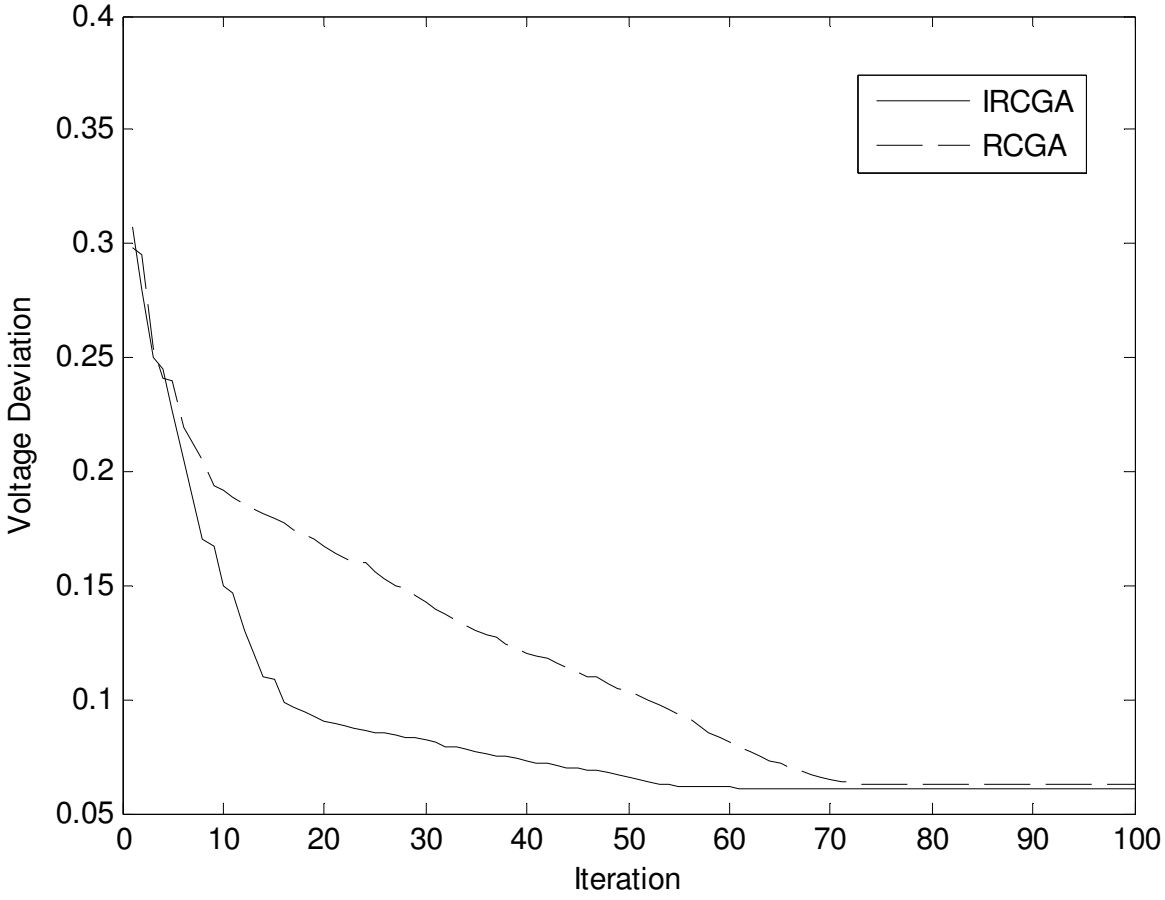

Fig. 7.3. Voltage deviation convergence characteristics of IEEE 30 bus system

7.4.2. IEEE 57-bus system

The IEEE 57-bus system comprises 80 transmission lines, seven generators at buses 1, 2, 3, 6, 8, 9, 12 and 15 branches with tap setting transformers. The reactive power sources are connected at buses 18, 25 and 53. The system line data, bus data, generator data and the minimum and maximum limits for the control variables have been adapted from [130]. Total active power demand is 12.508 p.u. and reactive power demand is 3.364 p.u. at 100 MVA base. Different types of RPD problem for this system have been solved by using developed OGSO and GSO. 50 test runs are carried out for each case.

7.4.2.1. Minimization of active power transmission loss

The developed IRCGA and RCGA have been pertained to minimize active power transmission loss. Here, maximum number of iterations, population size, crossover and mutation probabilities have been chosen as 100, 100, 0.9 and 0.2, respectively for IRCGA and RCGA. The optimal control variables obtained from the developed IRCGA are shown in Table 7.5. The best, average and worst minimum active power transmission loss and average CPU time among 50 runs of solutions obtained from developed IRCGA and RCGA are summarized in Table 7.6. The minimum active power transmission loss acquired from CLPSO [101] has been also shown in Table 7.6. The convergence characteristic acquired from developed IRCGA and RCGA for active power loss minimization is portrayed in Fig. 7.4. It has been observed from Table 7.6 that the active power transmission loss acquired from IRCGA is the lowest among all other stated techniques

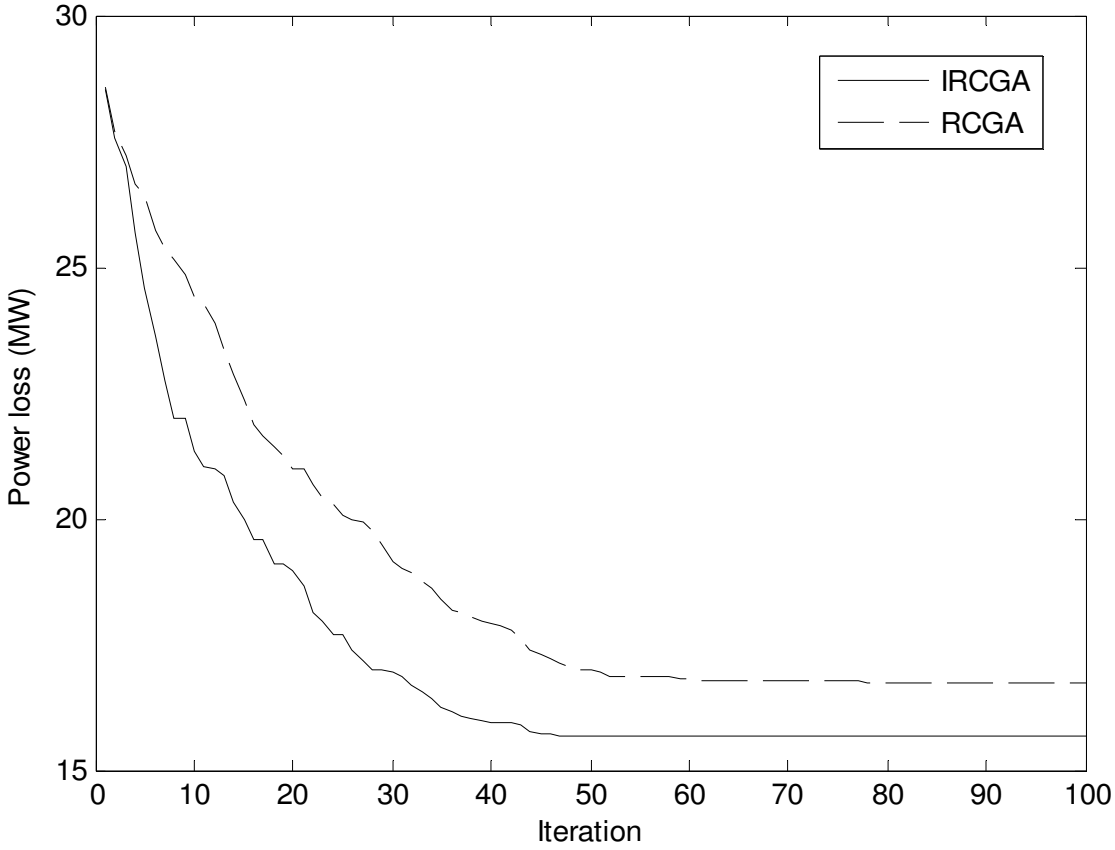

Fig. 7.4. Active power loss convergence characteristics of IEEE 57 bus system

Table 7.5: Optimal value of control variables acquired from IRCGA of IEEE 57 bus system for different cases

Control variable	Active power loss minimization	Improvement of voltage stability	Improvement of voltage profile
V_1	1.0400	1.0400	1.0400
V_2	1.0102	1.0104	1.0098
V_3	0.9848	0.9846	0.9853
V_6	0.9810	0.9799	0.9802
V_8	1.0055	1.0051	1.0044
V_9	0.9802	0.9809	0.9806
V_{12}	1.0152	1.0147	1.0149
T_{4-18}	1.0985	0.9803	0.9833
T_{4-18}	1.0821	0.9528	0.9508
T_{21-20}	0.9220	0.9505	0.9510
T_{24-26}	1.0173	1.0044	1.0045
T_{7-29}	0.9965	0.9779	0.9770
T_{34-32}	1.0998	0.9137	0.9138
T_{11-41}	1.0753	0.9466	0.9463
T_{15-45}	0.9542	0.9268	0.9259
T_{14-46}	0.9375	0.9961	0.9958
T_{10-51}	1.0162	1.0384	1.0377
T_{13-49}	1.0997	0.9053	0.9055
T_{11-43}	1.0982	0.9241	0.9227
T_{40-56}	0.9796	0.9874	0.9866
T_{39-57}	1.0243	1.0097	1.0094
T_{9-55}	1.0374	0.9374	0.9366
Q_{c18}	0.0876	0.0062	0.0121
Q_{c25}	0.0008	0.0440	0.0035
Q_{c53}	0.0073	0.0375	0.0427
power loss (MW)	15.6938	32.7760	31.7881
voltage deviation	3.7956	1.0811	0.6740
L_{max}	0.2242	0.1001	0.1371

Table 7.6: **Comparison of performance for active power transmission loss minimization of IEEE 57 bus system**

Techniques	Best loss (MW)	Average loss (MW)	Worst loss (MW)	CPU time (S)
IRCGA	15.6938	15.7054	15.7235	81.94
RCGA	16.7277	16.8380	16.9055	75.47
CLPSO[101]	24.5152	-	-	423

7.4.2.2 Improvement of voltage stability

The developed IRCGA and RCGA have been pertained to perk up voltage stability i.e. minimization of $L_{\max}$. Here, maximum number of iterations, population size, crossover and mutation probabilities have been chosen as 100, 100, 0.9 and 0.2, respectively for IRCGA and RCGA. The optimal values of control variables acquired from the developed IRCGA are summarized in Table 7.5. The best, average and worst $L_{\max}$ and average CPU time among 50 runs of solutions acquired from the developed IRCGA and RCGA are summarized in Table 7.7. The convergence characteristic acquired from the developed IRCGA and RCGA for minimization of $L_{\max}$ portrayed in Fig. 7.5. It has been observed from Table 7.7 that the value of $L_{\max}$ acquired from the developed IRCGA is lower than RCGA.

Table 7.7: Comparison of performance of $L_{\max}$ minimization of IEEE 57 bus system

Techniques	Best $L_{\max}$	Average $L_{\max}$	Worst $L_{\max}$	CPU time (S)
IRCGA	0.1001	0.1004	0.1008	84.01
RCGA	0.1032	0.1035	0.1040	76.95

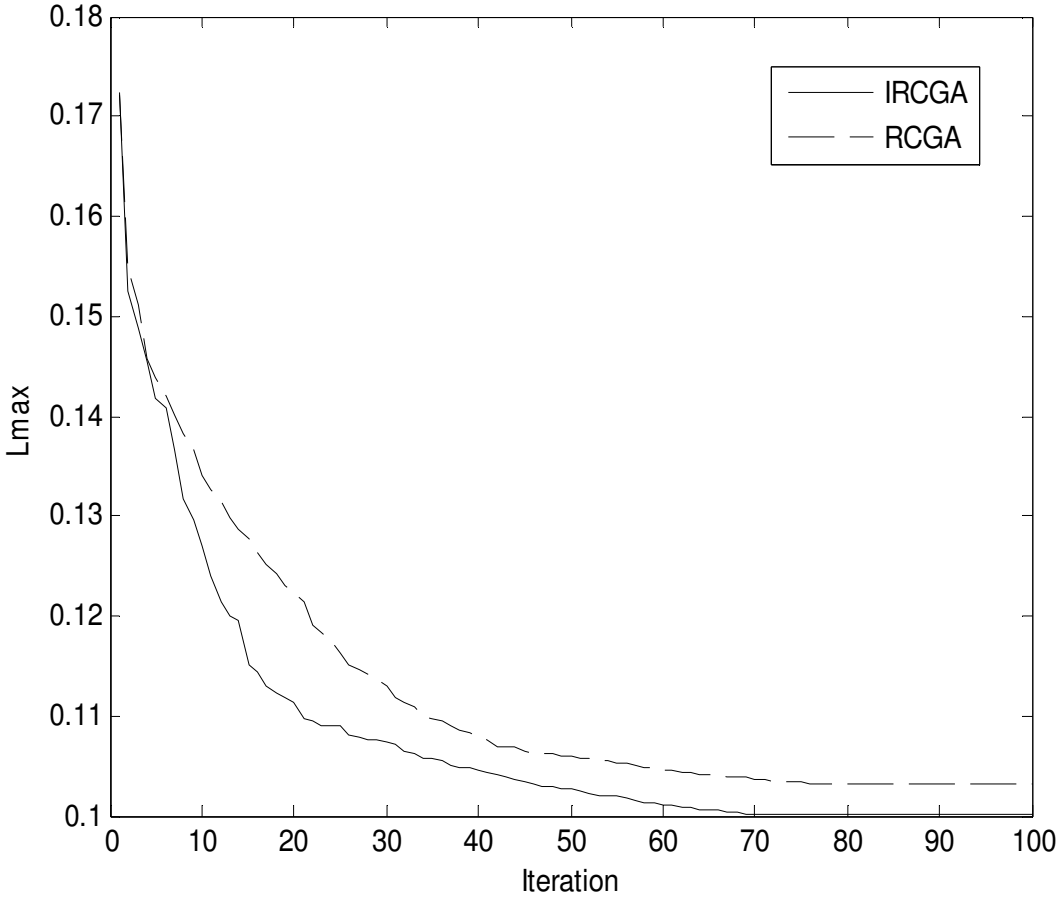

Fig. 7.5. $L_{\max}$ Convergence characteristics of IEEE 57 bus system

7.4.2.3 Improvement of voltage profile

The developed IRCGA and RCGA have been pertained to perk up voltage profile. Here, maximum number of iterations, population size, crossover and mutation probabilities have been chosen as 100, 100, 0.9 and 0.2, respectively for IRCGA and RCGA. The optimal values of control variables acquired from the developed IRCGA have been shown in Table 7.5. The best, average and worst voltage deviation and average CPU time among 50 runs of solutions acquired from developed IRCGA and RCGA are summarized in Table 7.8. The convergence characteristic acquired from the developed IRCGA and RCGA for voltage deviation is portrayed in Fig. 7.6. It has been observed from Table 7.8, that voltage deviation acquired from the developed IRCGA is lower than RCGA.

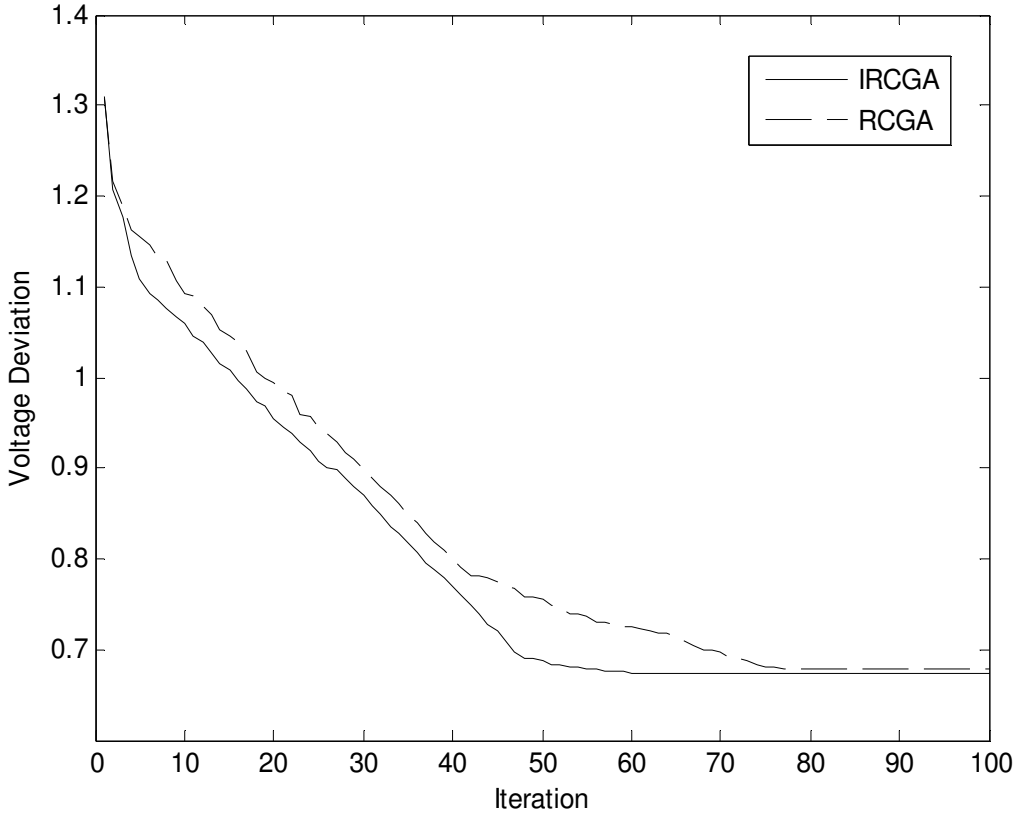

Fig. 7.6. Voltage deviation convergence characteristics of IEEE 57 bus system

Table 7.8: Comparison of performance of voltage deviation of IEEE 57 bus system

Techniques	Best voltage deviation (p.u.)	Average voltage deviation (p.u.)	Worst voltage deviation (p.u.)	CPU time (sec)
IRCGA	0.6740	0.6746	0.6750	83.05
RCGA	0.6775	0.6778	0.6784	77.98

7.4.3. IEEE 118-bus system

The standard IEEE 118-bus system comprises 186 transmission lines, 54 generator buses, 64 load buses, 9 branches with tap setting transformers and 14 reactive power sources. The system line data, bus data, generator data and the minimum and maximum limits for the control variables, the maximum and minimum limits of reactive power sources and transformer tap settings have been adapted from [131]. The total system active power demand is 42.4200 p.u.

and reactive power demand is 14.3800 p.u. at 100 MVA base. 50 runs are carried out by using the developed OGSO and GSO for solving different types of RPD problems.

7.4.3.1. Minimization of active power transmission loss

The developed IRCGA and RCGA have been pertained to minimize active power transmission loss. Here, maximum number of iterations, population size, crossover and mutation probabilities have been chosen as 100, 200, 0.9 and 0.2, respectively for IRCGA and RCGA. The optimal values of control variables acquired from the developed IRCGA are summarized in Table 7.9. The best, average and worst minimum active power transmission loss and average CPU time among 50 runs of solutions acquired from the developed IRCGA and RCGA are summarized in Table 7.10. The active power transmission loss acquired from comprehensive learning particle swarm optimization (CLPSO) [101] and particle swarm optimization (PSO) [101], MTLA-DDE [102] and QODE [97] have been shown in Table 7.10. The convergence characteristic acquired from the developed IRCGA and RCGA for minimization of active power transmission loss is portrayed in Fig. 7.7. It has been observed from Table 7.10 that active power transmission loss acquired from IRCGA is the lowest among all other stated techniques.

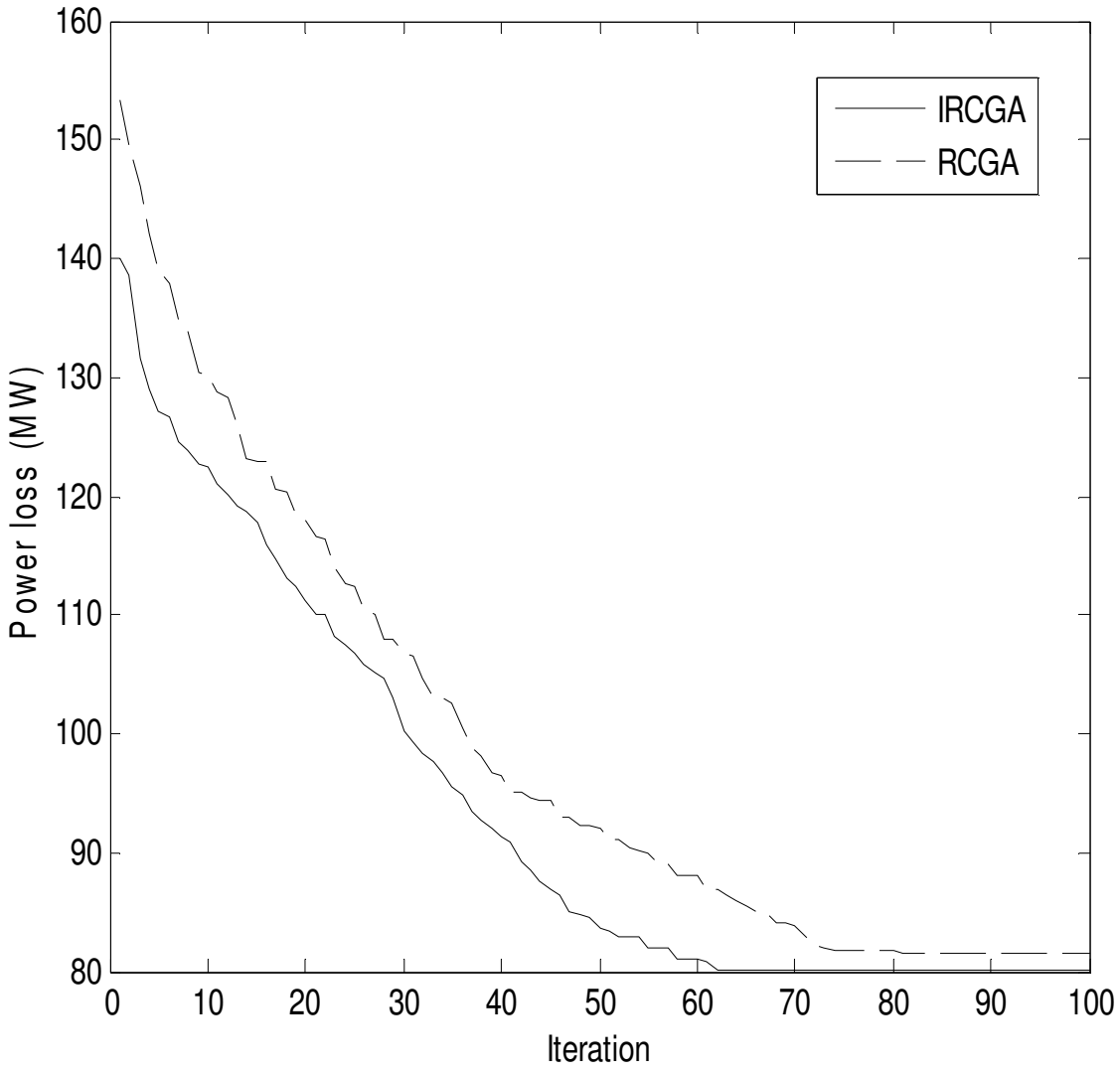

Fig. 7.7. Active power loss convergence characteristics of IEEE 118 bus system

Table 7.9: Optimal value of control variables acquired from IRCGA for IEEE 118 bus system of active power transmission loss minimization

Variable	IRCGA	Variable	IRCGA	Variable	IRCGA	Variable	IRCGA
V_1	0.9553	V_{49}	1.0253	V_{90}	0.9852	T_{65-66}	0.9347
V_4	0.9981	V_{54}	0.9551	V_{91}	0.9805	T_{68-69}	0.9353
V_6	0.9910	V_{55}	0.9519	V_{92}	0.9827	T_{81-82}	0.9358
V_8	1.0153	V_{56}	0.9547	V_{99}	1.0104	Q_{c5}	-0.0715
V_{10}	1.0500	V_{59}	0.9852	V_{100}	0.9697	Q_{c34}	0.0438
V_{12}	0.9908	V_{61}	0.9955	V_{103}	0.9549	Q_{c37}	-0.1016
V_{15}	0.9705	V_{62}	0.9986	V_{104}	0.9406	Q_{c44}	0.0002
V_{18}	0.9728	V_{65}	1.0052	V_{105}	0.9443	Q_{c45}	0.0622
V_{19}	0.9647	V_{66}	1.0500	V_{107}	0.9522	Q_{c46}	0.0000
V_{24}	0.9922	V_{69}	1.0350	V_{110}	0.9597	Q_{c48}	0.1271
V_{25}	1.0500	V_{70}	0.9847	V_{111}	0.9803	Q_{c74}	0.0285
V_{26}	1.0153	V_{72}	0.9802	V_{112}	0.9751	Q_{c79}	0.1358
V_{27}	0.9681	V_{73}	0.9914	V_{113}	0.9932	Q_{c82}	0.0378
V_{31}	0.9675	V_{74}	0.9637	V_{116}	1.0056	Q_{c83}	0.0979
V_{32}	0.9683	V_{76}	0.9416	T_{8-5}	0.9816	Q_{c105}	0.0628
V_{34}	0.9798	V_{77}	1.0062	T_{26-25}	0.9603	Q_{c107}	0.1890
V_{36}	0.9736	V_{80}	1.0403	T_{30-17}	0.9615	Q_{c110}	0.0007
V_{40}	0.9703	V_{85}	0.9837	T_{38-37}	0.9362	power loss (MW)	80.01
V_{42}	0.9851	V_{87}	1.0154	T_{63-59}	0.9596	voltage deviation	2.1978
V_{46}	1.0053	V_{89}	1.0051	T_{64-61}	0.9849	L_{max}	0.1125

Table 7.10: Comparison of performance of active power loss minimization of IEEE 118 bus system

Techniques	Best loss (MW)	Average loss (MW)	Worst loss (MW)	CPU time (sec)
IRCGA	80.01	80.98	82.27	102.49
RCGA	81.44	82.27	83.82	99.73
CLPSO [101]	130.96	-	-	1472
PSO [101]	131.99	-	-	1215

7.4.3.2. Improvement of voltage stability

The developed IRCGA and RCGA have been pertained to perk up voltage stability i.e. minimization of $L_{\max}$. Here, maximum number of iterations, population size, crossover and mutation probabilities have been chosen as 100, 200, 0.9 and 0.2, respectively for IRCGA and RCGA. The optimal values of control variables among 50 runs of solutions acquired from the developed IRCGA are shown in Table 7.11. The convergence characteristic acquired from the developed IRCGA and RCGA for $L_{\max}$ minimization is portrayed in Fig. 7.8.

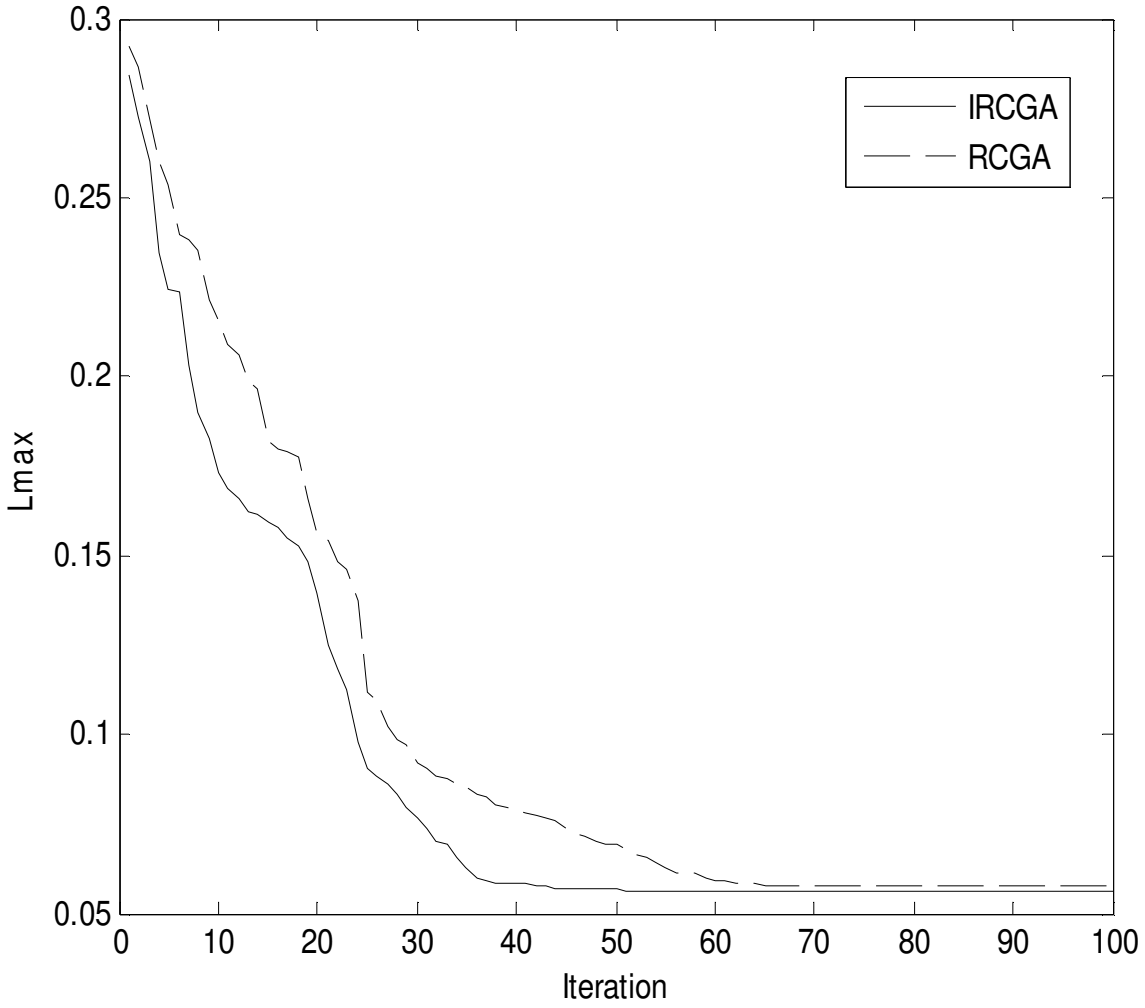

Fig. 7.8. $L_{\max}$ Convergence characteristics of IEEE 118 bus system

Table 7.11: Optimal value of control variables acquired from IRCGA of IEEE 118 bus system for voltage stability enhancement

Variable	IRCGA	Variable	IRCGA	Variable	IRCGA	Variable	IRCGA
V_1	0.9546	V_{49}	1.0255	V_{90}	0.9851	T_{65-66}	0.9349
V_4	0.9978	V_{54}	0.9552	V_{91}	0.9804	T_{68-69}	0.9348
V_6	0.9903	V_{55}	0.9527	V_{92}	0.9993	T_{81-82}	0.9351
V_8	1.0151	V_{56}	0.9549	V_{99}	1.0111	Q_{c5}	-0.1503
V_{10}	1.0500	V_{59}	0.9855	V_{100}	1.0173	Q_{c34}	0.0000
V_{12}	0.9904	V_{61}	0.9947	V_{103}	1.0069	Q_{c37}	-0.1434
V_{15}	0.9701	V_{62}	0.9981	V_{104}	0.9822	Q_{c44}	0.0 461
V_{18}	0.9727	V_{65}	1.0056	V_{105}	0.9773	Q_{c45}	0.0899
V_{19}	0.9653	V_{66}	1.0503	V_{107}	0.9524	Q_{c46}	0.0000
V_{24}	0.9926	V_{69}	1.0350	V_{110}	0.9738	Q_{c48}	0.1425
V_{25}	1.0481	V_{70}	0.9895	V_{111}	0.9806	Q_{c74}	0.0000
V_{26}	1.0155	V_{72}	0.9810	V_{112}	0.9755	Q_{c79}	0.0177
V_{27}	0.9687	V_{73}	0.9913	V_{113}	0.9931	Q_{c82}	0.0253
V_{31}	0.9672	V_{74}	0.9670	V_{116}	1.0047	Q_{c83}	0.1047
V_{32}	0.9697	V_{76}	0.9487	T_{8-5}	0.9801	Q_{c105}	0.0000
V_{34}	0.9873	V_{77}	1.0065	T_{26-25}	0.9601	Q_{c107}	0.0000
V_{36}	0.9832	V_{80}	1.0403	T_{30-17}	0.9603	Q_{c110}	0.0000
V_{40}	0.9708	V_{85}	0.9865	T_{38-37}	0.9352	power loss (MW)	99.52
V_{42}	0.9856	V_{87}	1.0152	T_{63-59}	0.9599	voltage deviation	1.6499
V_{46}	1.0057	V_{89}	1.0057	T_{64-61}	0.9847	L_{max}	0.0561

7.4.3.3. Improvement of voltage profile

The developed IRCGA and RCGA have been pertained to perk up voltage profile. Here, maximum number of iterations, population size, crossover and mutation probabilities have been chosen as 100, 200, 0.9 and 0.2, respectively for IRCGA and RCGA. The optimal values of control variables among 50 runs of solutions acquired from the developed IRCGA are shown in Table 7.12. The convergence characteristic acquired from the developed IRCGA and RCGA for voltage deviation is portrayed in Fig. 7.9.

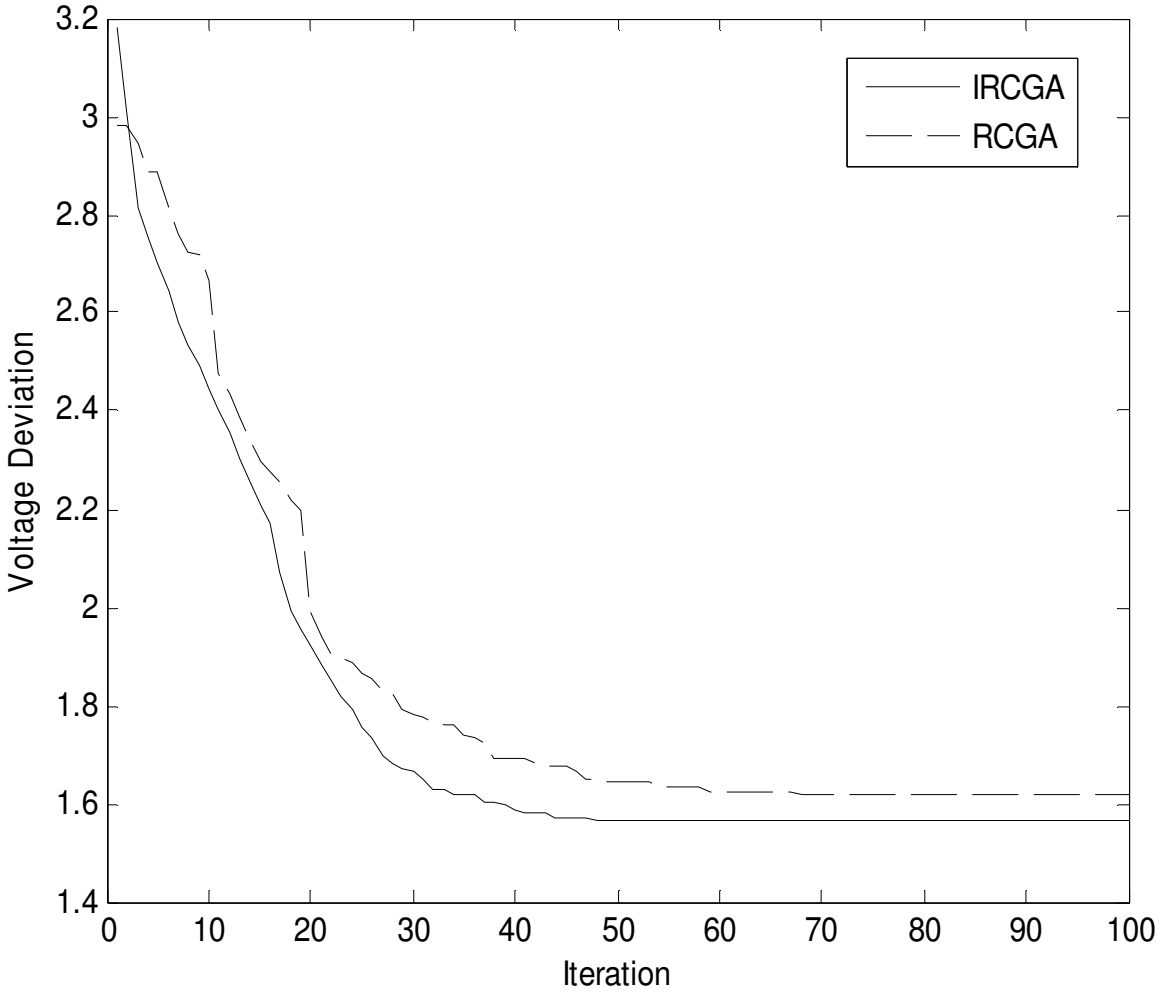

Fig. 7.9. Voltage deviation convergence characteristics of IEEE 118 bus system

Table 7.12: Optimal value of control variables acquired from IRCGA of IEEE 118 bus system for improvement of voltage profile

Variable	IRCGA	Variable	IRCGA	Variable	IRCGA	Variable	IRCGA
V_1	0.9553	V_{49}	1.0251	V_{90}	0.9853	T_{65-66}	0.9347
V_4	0.9981	V_{54}	0.9554	V_{91}	0.9801	T_{68-69}	0.9344
V_6	0.9905	V_{55}	0.9520	V_{92}	1.0002	T_{81-82}	0.9358
V_8	1.0152	V_{56}	0.9548	V_{99}	1.0105	Q_{c5}	-0.2610
V_{10}	1.0497	V_{59}	0.9850	V_{100}	1.0173	Q_{c34}	0.0000
V_{12}	0.9903	V_{61}	0.9952	V_{103}	1.0048	Q_{c37}	-0.0871
V_{15}	0.9705	V_{62}	0.9981	V_{104}	0.9806	Q_{c44}	0.0202
V_{18}	0.9731	V_{65}	1.0053	V_{105}	0.9749	Q_{c45}	0.0849
V_{19}	0.9654	V_{66}	1.0500	V_{107}	0.9521	Q_{c46}	0.0000
V_{24}	0.9923	V_{69}	1.0350	V_{110}	0.9732	Q_{c48}	0.0541
V_{25}	1.0495	V_{70}	0.9854	V_{111}	0.9804	Q_{c74}	0.0000
V_{26}	1.0152	V_{72}	0.9801	V_{112}	0.9755	Q_{c79}	0.1644
V_{27}	0.9684	V_{73}	0.9912	V_{113}	0.9929	Q_{c82}	0.0052
V_{31}	0.9673	V_{74}	0.9628	V_{116}	1.0051	Q_{c83}	0.1976
V_{32}	0.9721	V_{76}	0.9431	T_{8-5}	0.9815	Q_{c105}	0.0000
V_{34}	0.9860	V_{77}	1.0064	T_{26-25}	0.9602	Q_{c107}	0.0000
V_{36}	0.9828	V_{80}	1.0403	T_{30-17}	0.9610	Q_{c110}	0.0317
V_{40}	0.9701	V_{85}	0.9889	T_{38-37}	0.9359	power loss (MW)	100.2234
V_{42}	0.9854	V_{87}	1.0151	T_{63-59}	0.9596	voltage deviation	1.5644
V_{46}	1.0052	V_{89}	1.0054	T_{64-61}	0.9847	L_{max}	0.0597

7.5. Benchmark Functions

The developed IRCGA and RCGA have been pertained for solving 15 benchmark functions [29]. These test functions are revealed in Table 7.13. All other data is taken from [29]. The population size, crossover and mutation probabilities have been chosen as 100, 0.9 and 0.2 respectively for IRCGA and RCGA.

To verify the performance of the proposed IRCGA technique, these 15 test functions are repeatedly tested by using the IRCGA. Each test is repeated 100 times. Mean results of 15 test

functions acquired from 100 runs are summarized in Table 7.14 and Table 7.15 summarizes best optimum values and the variables corresponding to the best optimum value, number of iterations and CPU time of all 15 benchmark functions in 100 runs acquired from IRCGA. These 15 test functions are also tested by using RCGA technique. Table 7.16 shows best optimum values, number of iterations and CPU time acquired from RCGA.

Table 7.15: Best Optimum value, the variables corresponding to the best optimum value, number of iterations and CPU time acquired from IRCGA

Function	x^*	$f(x^*)$	Number of Iterations	CPU time (sec)
f_1	[0,0,…….,0]	1.6701e-24	200	25.5788
f_2	[0,0,…….,0]	7.7935e-18	200	26.9347
f_3	[0,0,…….,0]	5.8031e-17	300	37.7409
f_4	[0,0,…….,0]	1.3135e-17	300	36.7092
f_5	[1,1,…….,1]	2.6149e-17	300	37.5872
f_6	[0,0,…….,0]	8.9901e-18	300	40.8805
f_7	[0,0,…….,0]	2.1067e-17	300	37.7943
f_8	[0,0,…….,0]	6.3568e-18	300	39.9052
f_9	[4.8581, 5.4829] , [-7.0835, -7.7083], [-0.8003, -7.7083]	-186.7309	100	1.6325
f_{10}	[0.1928, 0.1909, 0.1231, 0.1358]	0.0003075	200	5.8807
f_{11}	[0.089842, -0.712654], [-0.089842, 0.712655],	-1.0316285	50	0.6183
f_{12}	[-3.1416, 12.272], [3.1416, 2.276]	0.397725	50	0.5996
f_{13}	[0, -1]	3	50	0.6074
f_{14}	[0.1146, 0.5556, 0.8525]	-3.86	50	0.8807
f_{15}	[0.2017, 0.1468, 0.4767, 0.2753, 0.3117, 0.6573]	-3.32	50	1.6038

Table 7.13: Test Functions

Mathematical representation	Domain	Optimum
$f_1(x)=\sum_{i=1}^{30} x_i^2$	[-100,100]	0
$f_2(x)=\sum_{i=1}^{30} \lvert x_i \rvert + \prod_{i=1}^{30} \lvert x_i \rvert$	[-10,10]	0
$f_3(x)=\sum_{i=1}^{30} \left(\sum_{j=1}^{i} x_j \right)^2$	[-100,100]	0
$f_4(x)=\max_i \{ \lvert x_i \rvert, 1 \le i \le 30 \}$	[-100,100]	0
$f_5(x)=\sum_{i=1}^{29} \left[100\left(x_{i+1}-x_i^2\right)^2 + \left(x_i-1\right)^2 \right]$	[-30,30]	0
$f_6(x)=\sum_{i=1}^{30} \left[x_i^2 - 10\cos\left(2\pi x_i\right) + 10 \right]$	[-5.12,5.12]	0
$f_7(x)=-20\exp\left(-0.2\sqrt{\frac{1}{30}\sum_{i=1}^{30} x_i^2} \right) - \exp\left(\frac{1}{30}\sum_{i=1}^{30} \cos 2\pi x_i \right) + 20 + e$	[-32,32]	0
$f_8(x)=\frac{1}{4000}\sum_{i=1}^{30} x_i^2 - \prod_{i=1}^{30} \cos\left(\frac{x_i}{\sqrt{i}} \right) + 1$	[-600,600]	0
$f_9(x)=\sum_{i=1}^{5} i\cos\left[(i+1)x_1 + i \right] \sum_{i=1}^{5} i\cos\left[(i+1)x_2 + i \right]$	[-10,10]	-186.73
$f_{10}(x)=\sum_{i=1}^{11} \left[a_i - \frac{x_1\left(b_i^2 + b_i x_2\right)}{b_i^2 + b_i x_3 + x_4} \right]$	[-5,5]	0.0003075
$f_{11}(x)=4x_1^2 - 2.1x_1^4 + \frac{1}{3}x_1^6 + x_1x_2 - 4x_2^2 + 4x_2^4$	[-5,5]	-1.0316285
$f_{12}(x)=\left(x_2 - \frac{5.1}{4\pi^2}x_1^2 + \frac{5}{\pi}x_1 - 6 \right)^2 + 10\left(1 - \frac{1}{8\pi} \right)\cos x_1 + 10$	[-5,10] ,[0,15]	0.398
$f_{13}(x)=[1+(x_1+x_2+1)^2(19-14x_1+3x_1^2-14x_2+6x_1x_2+3x_2^2)]$ $\times[30+(2x_1-3x_2)^2\times(18-32x_1+12x_1^2+48x_2-36x_1x_2+27x_2^2)]$	[-2,2]	3
$f_{14}(x)=-\sum_{i=1}^{4} c_i \exp\left[-\sum_{j=1}^{3} a_{ij}\left(x_j - p_{ij}\right)^2 \right]$	[0,1]	-3.86
$f_{15}(x)=-\sum_{i=1}^{4} c_i \exp\left[-\sum_{j=1}^{6} a_{ij}\left(x_j - p_{ij}\right)^2 \right]$	[0,1]	-3.32

Table 7.14: Mean optimum value, number of iterations and mean CPU time acquired from IRCGA

Function	Mean Optimum Value	Number of Iterations	Mean CPU time (sec)
f_1	1.6703e-22	200	27.5631
f_2	8.6875e-18	200	28.6573
f_3	7.0153e-17	300	38.9348
f_4	1.2035e-17	300	37.9738
f_5	3.0151e-17	300	39.0571
f_6	9.4572e-18	300	41.3401
f_7	22.324e-17	300	38.0479
f_8	6.8957e-18	300	40.9752
f_9	-186.7307	100	1.5042
f_{10}	0.00030763	200	5.9033
f_{11}	-1.031642	50	0.7047
f_{12}	0.397733	50	0.6981
f_{13}	3	50	0.6348
f_{14}	-3.8626	50	0.9015
f_{15}	-3.319	50	1.7748

Table 7.16: Best optimum value, number of iterations and CPU time acquired from RCGA

Function	RCGA		
	$f(x^*)$	Number of Iterations	CPU time (sec)
f_1	6.0739e-019	200	25.7905
f_2	1.6857e-005	300	39.6358
f_3	0.26796	500	62.7043
f_4	0.05389	500	64.9351
f_5	71.7808	400	54.9532
f_6	33.8247	300	40.8562
f_7	1.5308e-005	300	37.7794
f_8	4.9494	300	39.8093
f_9	-186.7308	100	1.3835
f_{10}	0.0003077	200	5.8774
f_{11}	-1.0316273	50	0.6058
f_{12}	0.397728	50	0.5495
f_{13}	3	50	0.6015
f_{14}	-3.8621	50	0.8795
f_{15}	-3.3214	50	1.49752

7.6. Conclusion

Improved real coded genetic algorithm (IRCGA) has been developed and validated for solving different types of RPD problems such as minimization of active power transmission loss and improvement of voltage profile and stability and 15 benchmark functions. The developed IRCGA is experimented on IEEE 30-bus, 57-bus and 118-bus test systems to reveal its efficacy. It has been examined that test results acquired from the developed IRCGA is superior compared to those acquired from other stated evolutionary techniques.

CHAPTER-8

Optimal Power Flow

8.1. Introduction

Optimal power flow (OPF) is an important tool for power system operators both in power system planning and operation for many years. The main purpose of an OPF is to determine the settings of control variables for economic and secure operation of a power system. The OPF minimizes the power system operating objective function while satisfying a set of equality and inequality constraints. The equality constraints are power flow equations and inequality constraints are the limits on control variables and functional operating constraints. The OPF is a highly non-linear, non-convex, large scale static optimization problem. Optimal power flow (OPF) is a nonlinear programming problem which optimizes a certain objective function while satisfying a set of physical and operational constraints imposed by equipment limitations and security requirements. Over the last three decades, several successful methods have been developed such as, generalized reduced gradient method, successive linear programming, successive quadratic programming, Newton method, P-Q decomposition, interior point method (IPM), genetic algorithm (GA), evolutionary programming (EP).

In this Chapter, two different algorithms have been applied to solve Optimal Power Flow Problems.

1. Heat transfer search (HTS) algorithm
2. Quasi-oppositional differential evolution (QODE) algorithm

The effectiveness of the above proposed algorithm is tested on IEEE 30-bus, 57-bus and 118-bus test systems for four objective problems. These are (i) fuel cost minimization, (ii) emission minimization, (iii) voltage deviation minimization and (iv) enhancement of voltage stability. It has been seen that performance of the proposed HTS and QODE algorithm is better compared to other evolutionary methods.

8.2. Problem Formulation

The OPF problem optimizes the steady state performance of power system with respect to specified objective function subject to various equality and inequality constraints. Here, four different objectives i.e. (i) fuel cost minimization, (ii) emission minimization, (iii) reduction of voltage deviation and (iv) improvement of voltage stability are considered. Four objective functions and constraints are formulated as follows.

8.2.1. Objective Functions

8.2.1.1. Minimization of fuel cost

The fuel cost function of each thermal generating unit, considering the valve-point effects [22], is expressed as the sum of a quadratic and a sinusoidal function. The total fuel cost in terms of active power output can be expressed as

$$F_1 = \sum_{i=1}^{\mathrm{N}_G} \left[a_i + b_i \mathrm{P}_{Gi} + c_i \mathrm{P}_{Gi}^2 + \left| d_i \times \sin\left\{ e_i \times \left(\mathrm{P}_{Gi}^{\min} - \mathrm{P}_{Gi} \right) \right\} \right| \right] \tag{8.1}$$

where a_i, b_i, c_i are the fuel cost coefficients of the ith generator; d_i and e_i are the coefficients of the ith generator reflecting valve-point effect; P_{Gi} is the active power generation of the ith generator; $\mathrm{P}_{Gi}^{\min}$ is the minimum active power generation limit of the ith generator. N_G is the number of committed generators.

The vector of dependent variables x may be represented as

$$x^{\mathrm{T}} = \left[\mathrm{P}_{Gslack}, V_{L1}, ..., V_{L\mathrm{N}_{PQ}}, Q_{G1}, .., Q_{G\mathrm{N}_{PV}}, S_{l1}, ..., S_{l\mathrm{N}_{TL}} \right] \tag{8.2}$$

where P_{Gslack} denotes the slack bus power; V_L is the $\mathrm{P}Q$ bus voltage; Q_G is the reactive power output of the generator; S_l is the transmission line flow; N_{PV} is the number of generator bus; N_{PQ} is the number of $\mathrm{P}Q$ bus; N_{TL} is the number of transmission lines.

The vector of control variables u may be represented as

$$u^{\mathrm{T}} = \left[V_{G1},..,V_{G\mathrm{N}_{PV}},\mathrm{P}_{G2},..,\mathrm{P}_{G\mathrm{N}_{PV}},Q_{c1},..,Q_{c\mathrm{N}_C},\mathrm{T}_1,..,\mathrm{T}_{\mathrm{N}_\mathrm{T}}\right] \tag{8.3}$$

where N_C and N_T are the number of shunt VAR compensators and the number of tap changing transformers, V_G is the terminal voltage at the generator bus, Q_c is the output of shunt VAR compensator and T is the tap setting of the tap changing transformer.

8.2.1.2. Minimization of emission

The atmospheric pollutants such as sulfur oxides (SO_x) and nitrogen oxides (NO_x) caused by thermal generating units can be modeled separately. However, for comparison purposes, the total emission of these pollutants which is the sum of a quadratic and an exponential function [126] can be expressed as

$$F_2 = \sum_{i=1}^{\mathrm{N}_G}\left[\alpha_i + \beta_i \mathrm{P}_{Gi} + \gamma_i \mathrm{P}_{Gi}^2 + \eta_i \exp(\lambda_i \mathrm{P}_{Gi})\right] \tag{8.4}$$

where $\alpha_i, \beta_i, \gamma_i, \eta_i, \lambda_i$ are the emission coefficients of the i th generator.

8.2.1.3. Minimization of voltage deviation

The objective is to minimize the voltage deviation of all load ($\mathrm{P}Q$) buses from 1 p.u. As a result the power system operates more securely and service quality is also improved. The objective function can be formulated as follows

$$\text{Minimize } F_3 = \sum_{i=1}^{\mathrm{N}_{PQ}} \left|V_i - 1.0\right| \tag{8.5}$$

where N_{PQ} is the number of load buses in the power system.

8.2.1.4. Voltage stability enhancement

Voltage stability problem is the ability of a power system to maintain acceptable voltages at all bus bars in the system under normal operating condition. A system experiences a state of voltage instability when the system is being subjected to a disturbance, increase in load demand or change in system configuration which causes a progressive and uncontrollable decrease in

voltage. Weak system, system with long transmission lines and heavily loaded system are much prone to voltage instability problem. In recent years, several major network collapses [103] have taken place due to voltage instability. Enhancement of voltage stability of a system is an important parameter of power system planning and operation. Voltage stability enhancement can be done by minimizing the voltage stability indicator i.e. $L-$index value at each bus of a power system. The $L-$index of a bus indicates the proximity of voltage collapse condition of that bus. $L-$index L_j of jth bus is defined as follows [104]

$$L_j = \left| 1 - \sum_{i=1}^{\mathrm{NP}V} F_{ji} \frac{V_i}{V_j} \right| \quad \text{where } j = 1,2,.....,\mathrm{NP}Q \tag{8.6}$$

$$\text{where } F_{ji} = -[\mathrm{Y}_1]^{-1}[\mathrm{Y}_2] \tag{8.7}$$

where $\mathrm{N}_{\mathrm{P}V}$ is the number of $\mathrm{P}V$ bus and $\mathrm{N}_{\mathrm{P}Q}$ is the number of PQ bus. Y_1 and Y_2 are the sub-matrices of the system YBUS obtained after segregating the PQ and PV bus bar parameters as described in (8).

$$\begin{bmatrix} \mathrm{I}_{\mathrm{P}Q} \\ \mathrm{I}_{\mathrm{P}V} \end{bmatrix} = \begin{bmatrix} \mathrm{Y}_1 \mathrm{Y}_2 \\ \mathrm{Y}_3 \mathrm{Y}_4 \end{bmatrix} \begin{bmatrix} V_{\mathrm{P}Q} \\ V_{\mathrm{P}V} \end{bmatrix} \tag{8.8}$$

$L-$index is calculated for all the PQ buses. L_j represents no load case and voltage collapse case of bus j in the range of 0 and 1 respectively. Hence, a global system indicator L describing the stability of a complete system is given as follows

$$L = \max(L_j), \quad \text{where } j = 1,2,.....,\mathrm{N}_{\mathrm{P}Q} \tag{8.9}$$

Lower value of L represents a more stable system. In order to improve voltage stability and to move the system far from the voltage collapse point, the objective function can be defined as follows

$$\text{Minimize } F_4 = L_{\max} \tag{8.10}$$

where $L_{\max}$ is the maximum value of $L-$index.

8.2.2. Constraints

The objective functions are subjected to the equality constraints imposed by the physical laws governing the transmission system as well as the inequality constraints imposed by the equipment ratings given below:

8.2.2.1. Equality constraints

These constraints are load flow equations as described below

$$\mathrm{P}_{Gi} - \mathrm{P}_{Di} - V_i \sum_{j=1}^{\mathrm{N_B}} V_j \left[G_{ij} \cos\left(\delta_i - \delta_j\right) + \mathrm{B}_{ij} \sin\left(\delta_i - \delta_j\right) \right] = 0 , \quad i = 1,2,..,\mathrm{N_B} \tag{8.11}$$

$$Q_{Gi} - Q_{Di} - V_i \sum_{j=1}^{\mathrm{N_B}} V_j \left[G_{ij} \sin\left(\delta_i - \delta_j\right) - \mathrm{B}_{ij} \cos\left(\delta_i - \delta_j\right) \right] = 0 , \quad i = 1,2,..,\mathrm{N_B} \tag{8.12}$$

where $\mathrm{N_B}$ is the number of buses, P_{Gi} and Q_{Gi} are active and reactive power generation at the i th bus, P_{Di} and Q_{Di} are active and reactive power demand at the i th bus, G_{ij} and B_{ij} are the transfer conductance and susceptance between i th bus and j th bus respectively.

8.2.2.2. Inequality constraints

8.2.2.2.1 Generator constraints*:* The generator voltage magnitudes and reactive power outputs are constrained by design specifications. The lower and upper limits of generator voltage magnitude and reactive power output are given below:

$$V_{Gi}^{\min} \le V_{Gi} \le V_{Gi}^{\max} , \; i = 1,2,..., \mathrm{N_{PV}} \tag{8.13}$$

$$\mathrm{P}_{Gi}^{\min} \le \mathrm{P}_{Gi} \le \mathrm{P}_{Gi}^{\max} , \; i = 1,2,..., \mathrm{N_{PV}} \tag{8.14}$$

$$Q_{Gi}^{\min} \le Q_{Gi} \le Q_{Gi}^{\max} , \; i = 1,2,..., \mathrm{N_{PV}} \tag{8.15}$$

8.2.2.2.2 Shunt VAR compensator constraints: Reactive power output of shunt VAR compensators must be restricted within their lower and upper limits as follows:

$$Q_{ci}^{\min} \le Q_{ci} \le Q_{ci}^{\max},\ i = 1,2,....,\mathrm{N}_C \tag{8.16}$$

8.2.2.2.3 Transformer constraints: The upper and lower values for the transformer tap settings are limited by physical considerations and these are given below:

$$\mathrm{T}_i^{\min} \le \mathrm{T}_i \le \mathrm{T}_i^{\max},\quad i = 1,2,...,\mathrm{N}_\mathrm{T} \tag{8.17}$$

8.2.2.2.4 Security constraints: These include the constraints on voltage magnitudes at PQ buses and transmission line loadings. Voltage of each PQ bus must be within its lower and operating limits. Line flow through each transmission line must be within its capacity limits. These are described as follows:

$$V_{Li}^{\min} \le V_{Li} \le V_{Li}^{\max},\ i = 1,2,..,\mathrm{N}_{PQ} \tag{8.18}$$

$$S_{li} \le S_{li}^{\max},\ i = 1,2,...,\mathrm{N}_{TL} \tag{8.19}$$

8.3. Overview of Heat Transfer Search Algorithm

The overview of HTS algorithm has been explained in Chapter 4 of subsection 4.7

8.4. Simulation and Results of HTS algorithm

To verify the effectiveness and performance of the proposed HTS algorithm by solving four objectives OPF problems, IEEE 30-bus, 57-bus and 118-bus test systems have been considered. Programs have been written in MATLAB-7 language and executed on a 3.0 GHz Pentium-IV personal computer. The results obtained from proposed HTS algorithm are compared with those obtained from other evolutionary methods reported in the literature.

8.4.1. IEEE 30-bus system:

The line data, bus data, generator data and the minimum and maximum limits for the control variables have been adapted from [128]. The system has six generators at buses 1, 2, 5, 8, 11 and 13 and four transformers with off nominal tap ratio at lines 6-9, 6-10, 4-12, and 28-27. In addition, shunt VAR compensating devices are assumed to be connected at bus bars 10, 12, 15, 17, 20, 21, 23, 24 and 29. as in [129]. The total system active power demand is 2.834 p.u. at 100

MVA base. In this study, 50 test runs are performed to solve the OPF problem for different objective functions.

8.4.1.1. Minimization of fuel cost

The proposed HTS algorithm has been applied for minimization of fuel cost as the objective function. Here, the population size (N_P), elite size(N_E) and the maximum iteration number (N_{max}) have been selected as 50, 5 and 100 respectively for this test system. The optimal values of control variables obtained from the proposed HTS algorithm are given in Table 8.1. The best, average and worst fuel cost and average CPU time among 50 runs of solutions obtained from proposed HTS algorithm are summarized in Table 8.2. The minimum fuel cost obtained from biogeography based optimization (BBO) [118], differential evolution (DE) [117], particle swarm optimization (PSO) [129], improved genetic algorithm (IGA) [113] and improved particle swarm optimization (IPSO) [115] are also shown in Table 8.2. The convergence characteristic obtained from proposed HTS algorithm for cost minimization is shown in Fig. 8.1. It is seen from Table 8.2, that minimum cost obtained from HTS algorithm is the lowest among all other methods.

Table 8.1: Optimal value of control variables obtained from HTS for IEEE 30 bus system for different cases

Control variable	Fuel cost minimization	Emission minimization	Voltage stability enhancement	Improvement of voltage profile
P_{G1} (MW)	190.31	115.68	113.20	158.60
P_{G2} (MW)	47.90	72.43	62.13	52.56
P_{G5} (MW)	19.61	38.75	47.17	39.84
P_{G8} (MW)	11.25	32.96	35.00	14.51
P_{G11} (MW)	10.000	29.53	19.10	10.00
P_{G13} (MW)	12.000	0	12.00	14.50
V_1 (p.u.)	1.0500	1.0500	1.0500	1.0500
V_2 (p.u.)	1.0338	1.0334	1.0337	1.0339
V_5 (p.u.)	1.0058	1.0053	1.0059	1.0060
V_8 (p.u.)	1.0230	1.0227	1.0233	1.0231
V_{11} (p.u.)	1.0913	1.0908	1.0914	1.0911
V_{13} (p.u.)	1.0400	1.0404	1.0398	1.0399
T_{6-9}	1.0155	0.9946	1.0069	1.0157
T_{6-10}	0.9629	0.9953	0.9820	1.0274
T_{4-12}	1.0129	0.9844	0.9913	1.0087
T_{28-27}	0.9581	1.0044	1.0095	0.9817
Q_{c10} (Mvar)	4.12	0.5914	5.0000	0.95
Q_{c12} (Mvar)	1.15	0.9519	5.0000	0.68
Q_{c15} (Mvar)	4.99	1.7289	2.4663	3.01
Q_{c17} (Mvar)	4.80	2.9142	0	0
Q_{c20} (Mvar)	0.08	3.5631	5.0000	5.0000
Q_{c21} (Mvar)	4.93	0.8467	5.0000	5.0000
Q_{c23} (Mvar)	0.38	1.4583	2.1800	2.1800
Q_{c24} (Mvar)	1.06	2.8836	3.7715	3.7715
Q_{c29} (Mvar)	4.85	2.5745	5.0000	5.0000
Fuel Cost ($/h)	793.79	859.26	866.98	821.07
Emission (ton/h)	0.4080	0.1961	0.2476	0.3201
Loss (MW)	7.67	5.94	5.20	6.61
Voltage deviation (p.u.)	0.5405	0.3535	0.8706	0.0615
L_{max}	0.0489	0.0729	0.0202	0.0641

Table 8.2: Comparison of performance for cost minimization of IEEE 30 bus system

Techniques	Best cost ($/h)	Average cost ($/h)	Worst cost ($/h)	CPU time (S)
HTS	793.79	793.84	793.91	18.25
BBO [118]	799.11	-	-	-
DE [117]	799.28	-	-	-
PSO [129]	800.41	-	-	-
IGA [113]	800.80	-	-	-
IPSO [115]	801.97	-	-	-

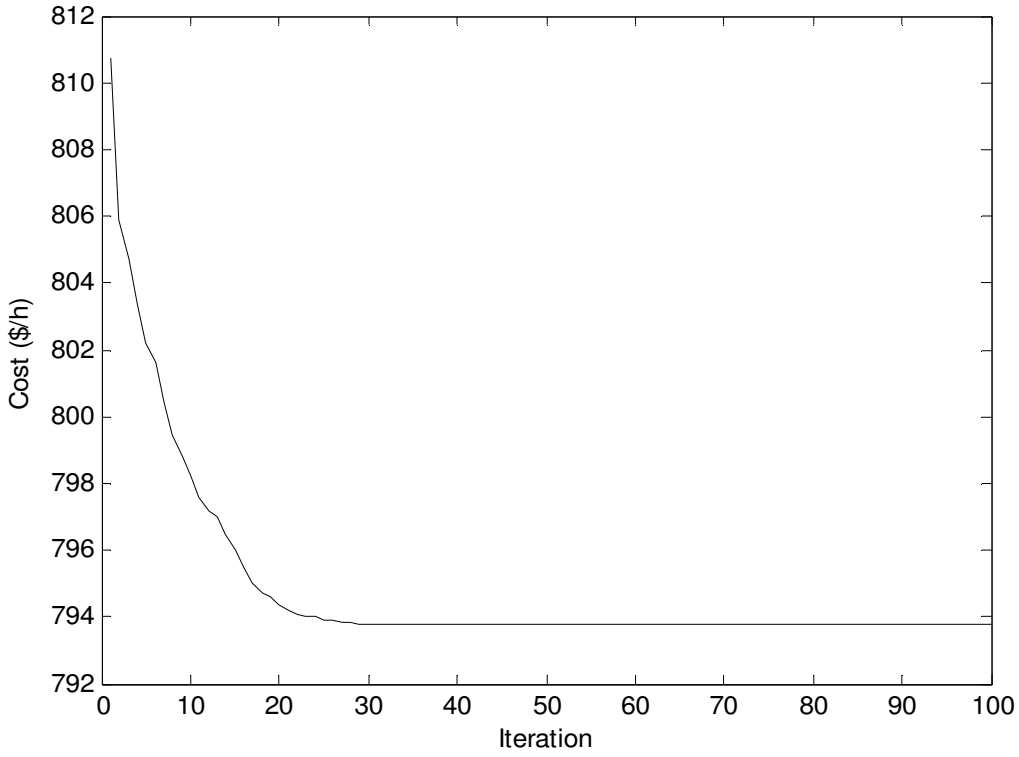

Fig. 8.1. Cost convergence characteristics for IEEE 30 bus system

8.4.1.2. Minimization of emission

The proposed HTS algorithm has been applied for minimization of emission as the objective function. Here, the population size (N_P), elite size(N_E) and the maximum iteration number (N_{max}) have been selected as 50, 5 and 100 respectively for this test system. The optimal values

of control variables obtained from the proposed HTS algorithm are given in Table 8.1. The best, average and worst emission and average CPU time among 50 runs of solutions obtained from proposed HTS algorithm are summarized in Table 8.3. The minimum emission obtained from improved particle swarm optimization (IPSO) [115] is also shown in Table 8.3. The convergence characteristic obtained from proposed HTS algorithm for emission minimization is shown in Fig. 8.2. It is seen from Table 8.3, that minimum emission obtained from HTS algorithm is the lowest among all other methods.

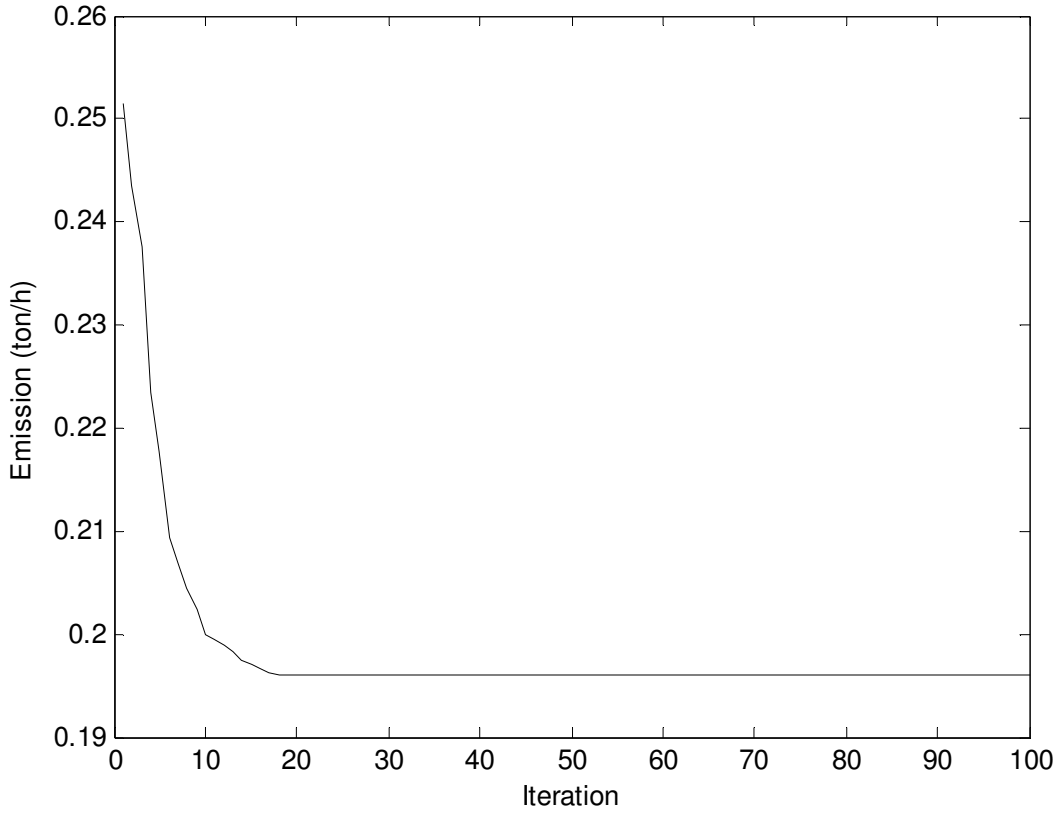

Fig. 8.2. Emission convergence characteristics for IEEE 30 bus system

Table 8.3: Comparison of performance for emission minimization of IEEE 30 bus system

Techniques	Best emission (ton/h)	Average emission (ton/h)	Worst emission (ton/h)	CPU time (S)
HTS	0.1961	0.1964	0.1969	20.57
IPSO [115]	0.2058	-	-	-

8.4.1.3. Enhancement of voltage stability

In this case, the proposed HTS algorithm has been applied for enhancement of voltage stability i.e. minimization of $L_{\max}$. Here, the population size (N_P), elite size(N_E) and the maximum iteration number ($N_{\max}$) have been selected as 50, 5 and 100 respectively for this test system. The optimal values of control variables obtained from the proposed HTS algorithm are shown in Table 1. The best, average and worst $L_{\max}$ and average CPU time among 50 runs of solutions obtained from proposed HTS algorithm are summarized in Table 8.4. The $L_{\max}$ obtained from BBO [118] and improved particle swarm optimization (IPSO) [115] are also shown in Table 8.4. The convergence characteristic obtained from proposed HTS algorithm for $L_{\max}$ minimization is shown in Fig. 8.3. It is seen from Table 8.4 that the value of $L_{\max}$ obtained from HTS algorithm is the lowest among all other methods.

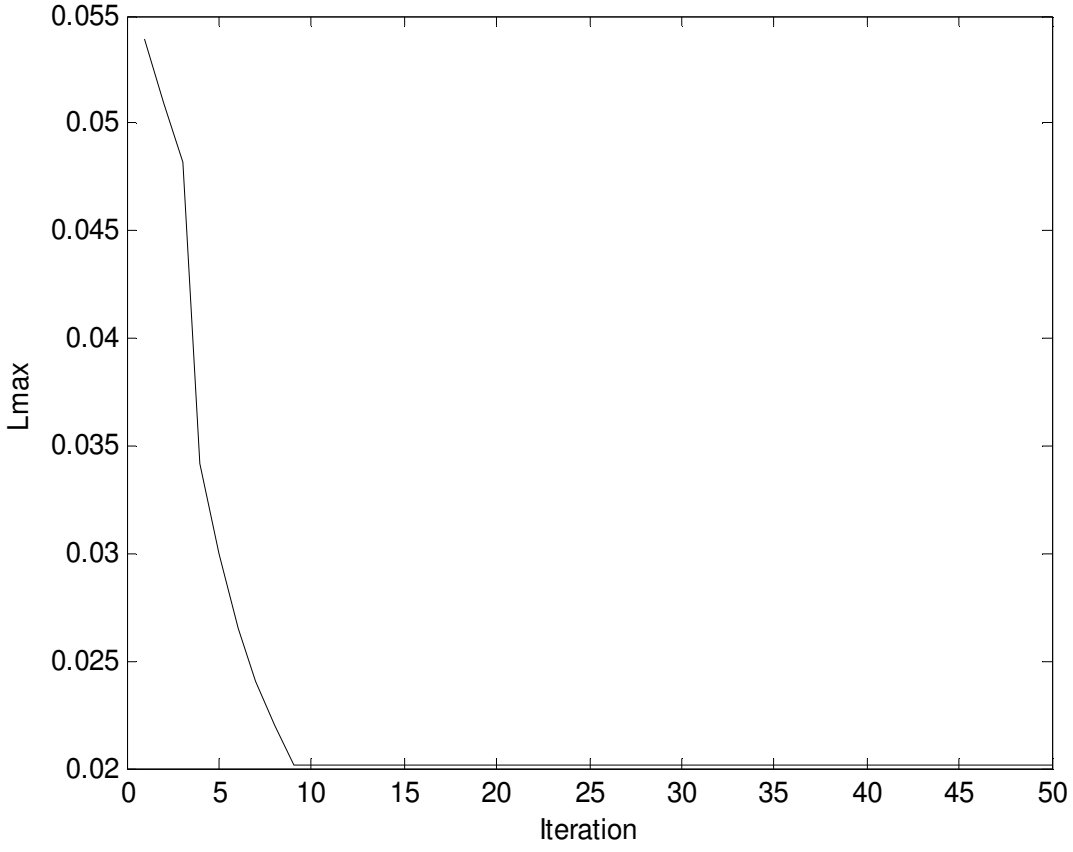

Fig. 8.3. $L_{\max}$ convergence characteristics for IEEE 30 bus system

Table 8.4: Comparison of performance for L_{max} minimization of IEEE 30 bus system

Techniques	Best L_{max}	Average L_{max}	Worst L_{max}	CPU time (S)
HTS	0.0202	0.0205	0.0209	19.23
BBO [118]	0.0980	-	-	-
IPSO [115]	0.1037	-	-	-

8.4.1.4. Improvement of voltage profile

In this case, the proposed HTS algorithm applied for improvement of voltage profile. Here, the population size (N_P), elite size(N_E) and the maximum iteration number (N_{max}) have been selected as 50, 5 and 100 respectively for this test system. The optimal values of control variables obtained from the proposed HTS algorithm are given in Table 8.1. The best, average and worst voltage deviation and average CPU time among 50 runs of solutions obtained from proposed HTS algorithm are summarized in Table 5. The voltage deviation obtained from BBO [118] and faster evolutionary algorithm (FEA) [119] is also shown in Table 8.5. The convergence characteristic obtained from proposed HTS algorithm for voltage deviation is shown in Fig. 8.4. It is seen from Table 8.5, that voltage deviation obtained from HTS algorithm is the lowest among all other methods.

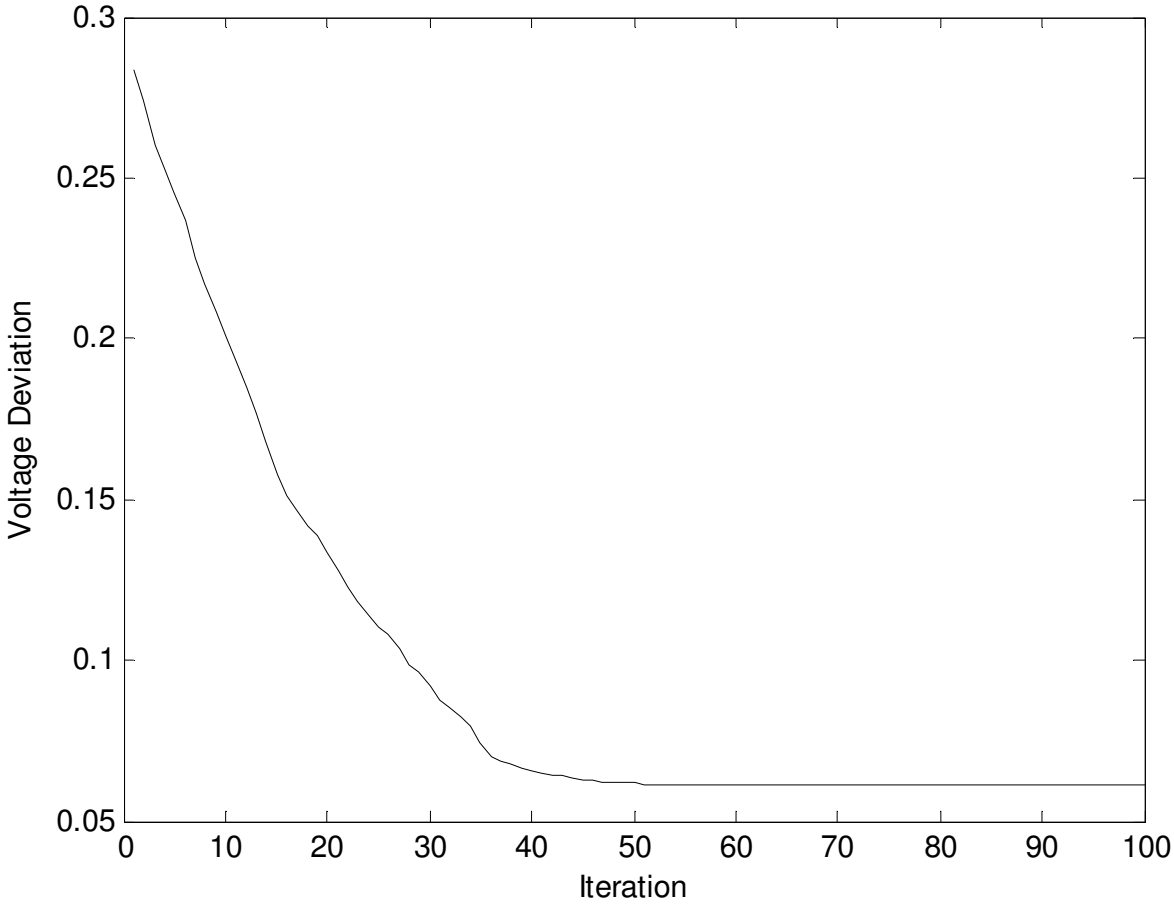

Fig. 8.4. Voltage deviation convergence characteristics for IEEE 30 bus system

Table 8.5: Comparison of performance for voltage deviation of IEEE 30 bus system

Techniques	Best voltage deviation	Average voltage deviation	Worst voltage deviation	CPU time (S)
HTS	0.0615	0.0617	0.0621	26.99
BBO [118]	0.0951	-	-	-
FEA [119]	0.1052	-	-	-

8.4.2. IEEE 57-bus system

The standard IEEE 57-bus system consists of 80 transmission lines, seven generators at buses 1, 2, 3, 6, 8, 9, 12 and 15 branches under load tap setting transformer branches. The reactive power sources are considered at buses 18, 25 and 53. The system line data, bus data, generator data and the minimum and maximum limits for the control variables have been adapted from [127] and [130]. The upper and lower limits of reactive power sources and transformer tap settings are taken from [128]. The total system active power demand is 12.508 p.u. and reactive power demand is 3.364 p.u. at 100 MVA base. In this study, 50 test runs are performed to solve the OPF problem for different objective functions.

8.4.2.1. Minimization of fuel cost

The proposed HTS algorithm has been applied for minimization of fuel cost as the objective function. Here, the population size (N_P), elite size(N_E) and the maximum iteration number (N_{max}) have been selected as 50, 5 and 100 respectively for this test system. The optimal values of control variables obtained from the proposed HTS are given in Table 8.6. The best, average and worst fuel cost and average CPU time among 50 runs of solutions obtained from proposed HTS algorithm are summarized in Table 8.7. The convergence characteristic obtained from proposed HTS algorithm for minimum fuel cost solution is shown in Fig. 8.5.

Table 8.7: Comparison of performance for cost minimization of IEEE 57 bus system

Technique	Best cost ($/h)	Average cost ($/h)	Worst cost ($/h)	CPU time (S)
HTS	7640.00	7642.03	7644.83	37.87

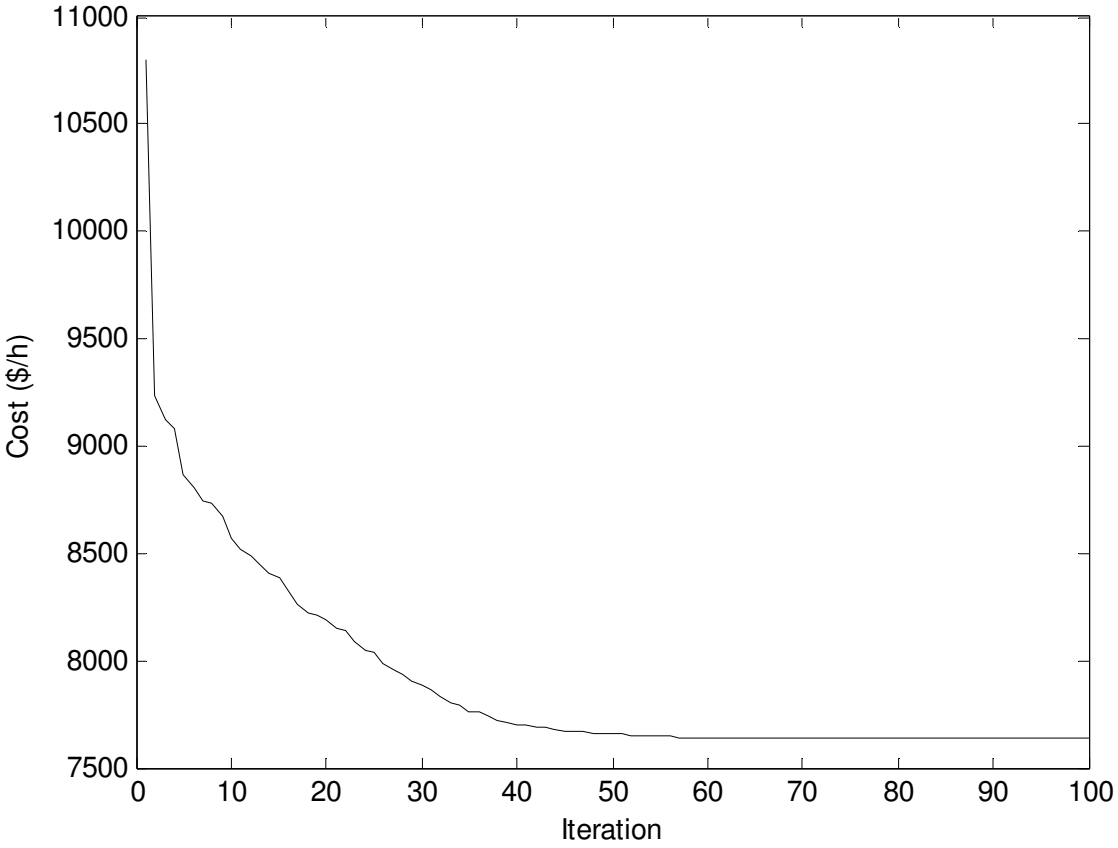

Fig. 8.5. Cost convergence characteristics for IEEE 57 bus system

Table 8.6: Optimal value of control variables obtained from HTS for IEEE 57 bus system for different cases

Control variable minimization	Fuel cost	Emission minimization	Voltage Stability enhancement	Improvement of voltage profile
P_{G1} (MW)	592.76	304.02	522.37	589.66
P_{G2} (MW)	0	0	0	0
P_{G3} (MW)	97.62	172.65	35.73	16.35
P_{G6} (MW)	0	0	0	0
P_{G8} (MW)	136.25	341.89	523.20	482.32
P_{G9} (MW)	0	0	0	0
P_{G12} (MW)	460.61	461.89	201.67	196.53
V_1 (p.u.)	1.0400	1.0400	1.0400	1.0400
V_2 (p.u.)	1.0100	1.0104	1.0103	1.0107
V_3 (p.u.)	0.9850	0.9855	0.9853	0.9856
V_6 (p.u.)	0.9801	0.9806	0.9801	0.9804
V_8 (p.u.)	1.0052	1.0057	1.0049	1.0055
V_9 (p.u.)	0.9800	0.9804	0.9805	0.9806
V_{12} (p.u.)	1.0153	1.0148	1.0151	1.0153
T_{4-18}	0.9700	1.0987	0.9801	0.9831
T_{4-18}	0.9780	1.0820	0.9526	0.9510
T_{21-20}	1.0430	0.9221	0.9501	0.9507
T_{24-26}	1.0430	1.0171	1.0045	1.0043
T_{7-29}	0.9670	0.9960	0.9777	0.9769
T_{34-32}	0.9750	1.0999	0.9138	0.9139
T_{11-41}	0.9550	1.0750	0.9465	0.9461
T_{15-45}	0.9550	0.9541	0.9269	0.9258
T_{14-46}	0.9000	0.9370	0.9962	0.9957
T_{10-51}	0.9300	1.0160	1.0385	1.0379
T_{13-49}	0.8950	1.0998	0.9052	0.9053
T_{11-43}	0.9580	1.0980	0.9240	0.9229
T_{40-56}	0.9580	0.9799	0.9875	0.9868
T_{39-57}	0.9800	1.0246	1.0098	1.0095
T_{9-55}	0.9400	1.0371	0.9373	0.9367
Q_{c18} (Mvar)	4.0117	0.2339	3.5236	5.7907

Q_{c25} (Mvar)	4.0184	2.8458	4.0004	0.6058
Q_{c53} (Mvar)	1.7637	1.2245	3.1840	5.8095
Cost ($/h)	7640.00	13181.08	20833.36	18556.16
Emission (ton/h)	2.8086	1.7003	2.8134	3.0945
power loss (MW)	36.4534	29.6432	32.1714	34.0597
Voltage deviation (p.u.)	1.1486	5.3719	1.1228	0.6725
$L_{\max}$	0.1129	0.4161	0.0987	0.1362

8.4.2.2. Minimization of emission

The proposed HTS algorithm has been applied for minimization of emission as the objective function. Here, the population size (N_P), elite size(N_E) and the maximum iteration number (N_{max}) have been selected as 50, 5 and 100 respectively for this test system. The optimal values of control variables obtained from the proposed HTS algorithm are given in Table 8.6. The best, average and worst emission and average CPU time among 50 runs of solutions obtained from proposed HTS are summarized in Table 8.8. The convergence characteristic obtained from proposed HTS for emission minimization is shown in Fig. 8.6.

Table 8.8: Comparison of performance for emission minimization of IEEE 57 bus system

Technique	Best emission (ton/h)	Average emission (ton/h)	Worst emission (ton/h)	CPU time (S)
HTS	1.7003	1.7006	1.7011	38.01

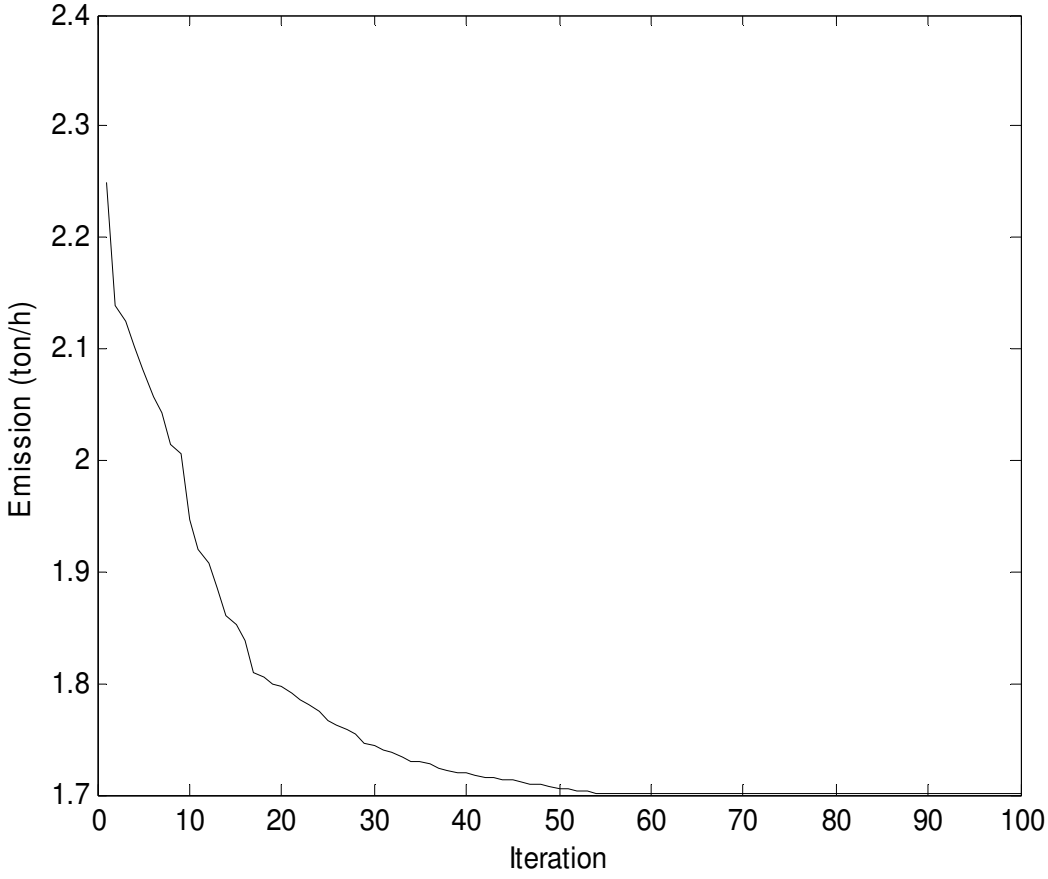

Fig. 8.6. Emission convergence characteristics for IEEE 57 bus system

8.4.2.3. Enhancement of voltage stability

In this case, the proposed HTS algorithm has been applied for enhancement of voltage stability i.e. minimization of $L_{\max}$. Here, the population size (N_P), elite size(N_E) and the maximum iteration number (N_{max}) have been selected as 50, 5 and 100 respectively for this test system. The optimal values of control variables obtained from the proposed HTS algorithm are given in Table 8.6. The best, average and worst $L_{\max}$ and average CPU time among 50 runs of solutions obtained from proposed HTS algorithm are summarized in Table 8.9. The convergence characteristic obtained from proposed HTS algorithm for $L_{\max}$ minimization is shown in Fig. 8.7.

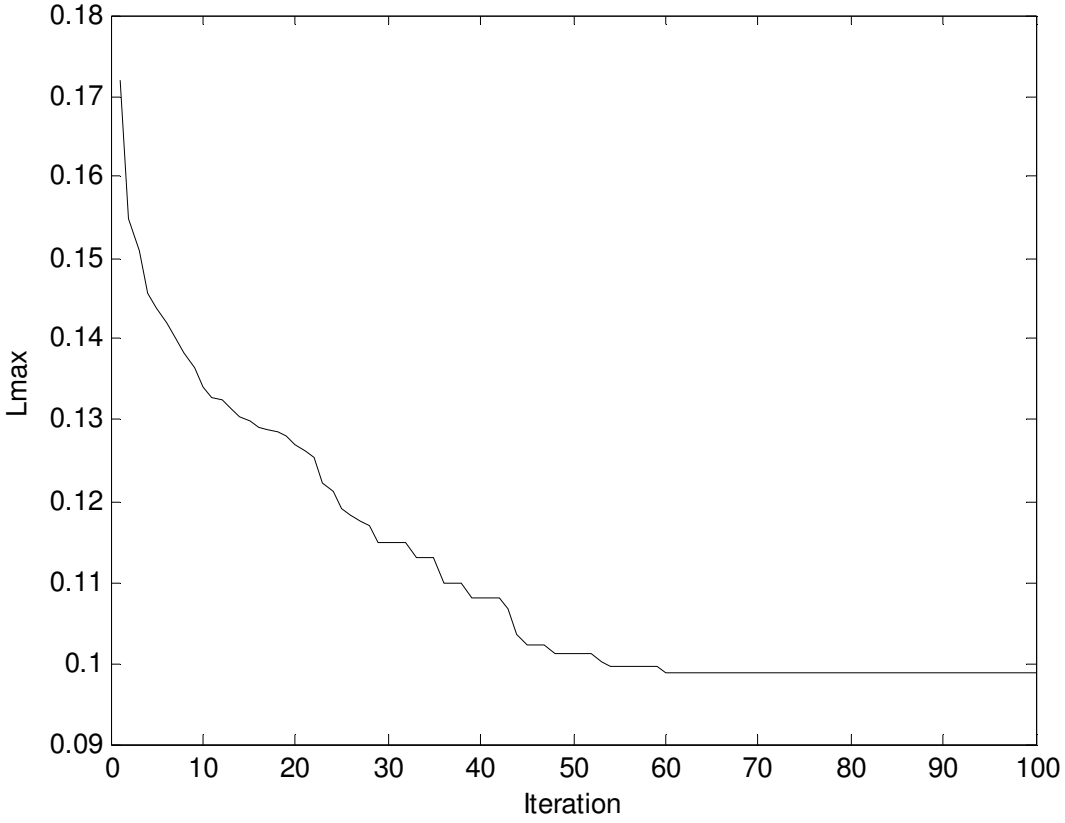

Fig. 8.7. $L_{\max}$ convergence characteristics for IEEE 57 bus system

Table 8.9: Comparison of performance for $L_{\max}$ minimization of IEEE 57 bus system

Technique	Best $L_{\max}$	Average $L_{\max}$	Worst $L_{\max}$	CPU time (S)
HTS	0.0987	0.0989	0.0992	33.6524

8.4.2.4. Improvement of voltage profile

In this case, the proposed HTS algorithm has been applied for improvement of voltage profile. Here, the population size (N_P), elite size(N_E) and the maximum iteration number (N_{max}) have been selected as 50, 5 and 100 respectively for this test system. The optimal values of control variables obtained from the proposed HTS algorithm are given in Table 8.6. The best, average and worst voltage deviation and average CPU time among 50 runs of solutions obtained from

proposed HTS algorithm are summarized in Table 8.10. The convergence characteristic obtained from proposed HTS for voltage deviation is shown in Fig. 8.8.

Table 8.10: Comparison of performance for voltage deviation of IEEE 57 bus system

Technique	Best voltage deviation	Average voltage deviation	Worst voltage deviation	CPU time (S)
HTS	0.6725	0.6728	0.6732	38.93

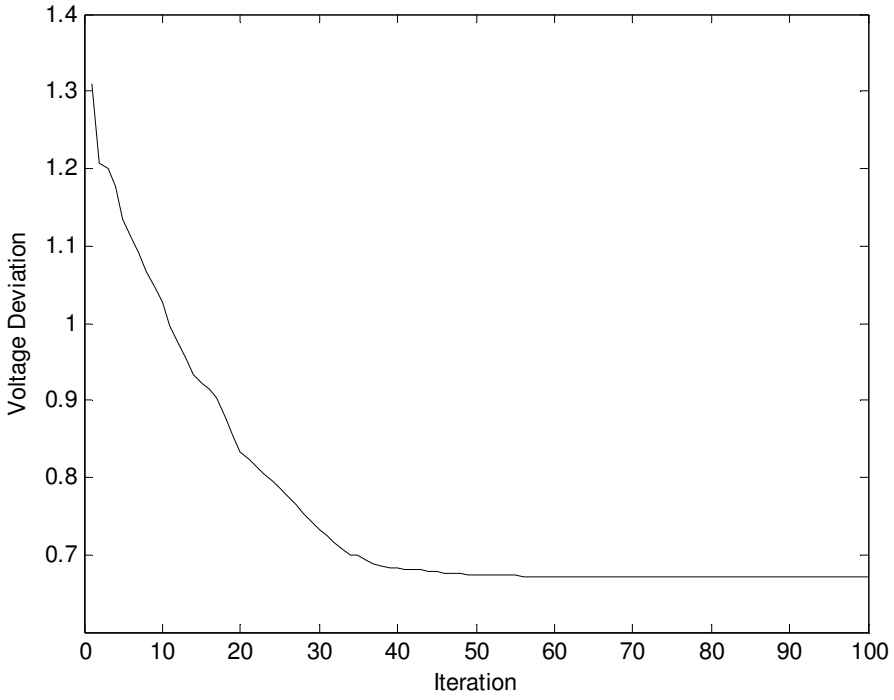

Fig. 8.8. Voltage deviation convergence characteristics for IEEE 57 bus system

8.4.3. IEEE 118-bus system

The standard IEEE 118-bus system consists of 186 transmission lines, 54 generator buses, 64 load buses, 9 branches under load tap setting transformer and 14 reactive power sources. The system line data, bus data, generator data and the minimum and maximum limits for the control variables have been adapted from [101] and [131]. The upper and lower limits of reactive power sources and transformer tap settings are taken from [101]. The generator data has been taken

from [132]. The total system active power demand is 42.4200 p.u. and reactive power demand is 14.3800 p.u. at 100 MVA base. In this study, 50 test runs are performed to solve different OPF problems by using HTS algorithm. Here, Due to brevity, only comparison tables obtained from different objective functions are given here.

8.4.3.1. Minimization of fuel cost

The proposed HTS algorithm has been applied for minimization of fuel cost as the objective function. Here, the population size (N_P), elite size(N_E) and the maximum iteration number (N_{max}) have been selected as 100, 10, and 100 respectively for this test system. The optimal values of control variables obtained from the proposed HTS algorithm are given in Table 8.11. The best, average and worst fuel cost and average CPU time among 50 runs of solutions obtained from proposed HTS algorithm are summarized in Table 8.12. The convergence characteristic obtained from proposed HTS algorithm for minimum fuel cost solution is shown in Fig. 8.9.

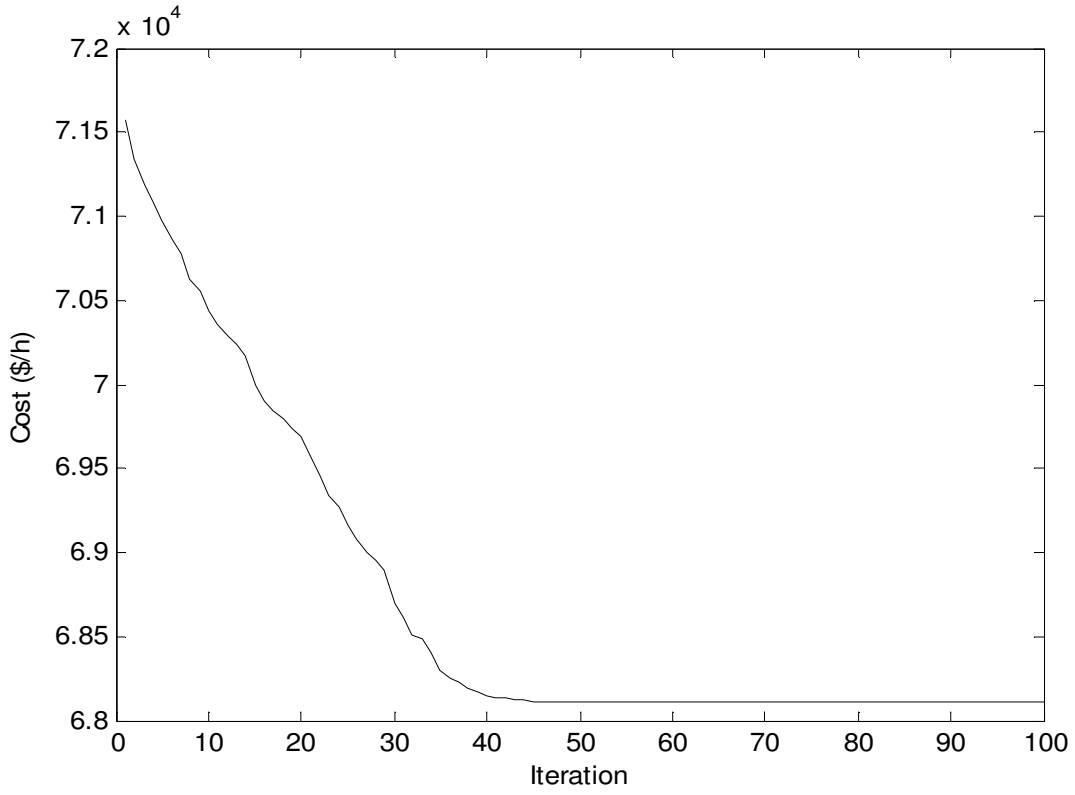

Fig. 8.9. Cost convergence characteristics for IEEE 118 bus system

Table 8.11: Optimal value of control variables obtained from HTS for IEEE 118 bus system for cost minimization

Variable		Variable		Variable		Variable		Variable	
P_{G1} (MW)	29.2109	P_{G66} (MW)	381.8617	V_6	0.9903	V_{70}	0.9854	T_{63-59}	0.9597
P_{G4} (MW)	27.7608	P_{G69} (MW)	332.5110	V_8	1.0151	V_{72}	0.9801	T_{64-61}	0.9846
P_{G6} (MW)	12.7737	P_{G70} (MW)	0	V_{10}	1.0500	V_{73}	0.9909	T_{65-66}	0.9351
P_{G8} (MW)	14.1875	P_{G72} (MW)	11.2969	V_{12}	0.9904	V_{74}	0.9663	T_{68-69}	0.9347
P_{G10} (MW)	422.6864	P_{G73} (MW)	15.7119	V_{15}	0.9692	V_{76}	0.9430	T_{81-82}	0.9356
P_{G12} (MW)	110.9571	P_{G74} (MW)	0	V_{18}	0.9733	V_{77}	1.0071	Q_{c5} (Mvar)	36.6145
P_{G15} (MW)	11.3817	P_{G76} (MW)	0	V_{19}	0.9648	V_{80}	1.0403	Q_{c34} (Mvar)	13.5245
P_{G18} (MW)	59.5803	P_{G77} (MW)	55.6755	V_{24}	0.9921	V_{85}	0.9565	Q_{c37} (Mvar)	-12.7591
P_{G19} (MW)	0	P_{G80} (MW)	232.4882	V_{25}	1.0500	V_{87}	1.0151	Q_{c44} (Mvar)	2.8039
P_{G24} (MW)	28.1248	P_{G85} (MW)	0	V_{26}	1.0151	V_{89}	1.0048	Q_{c45} (Mvar)	0.5621
P_{G25} (MW)	198.2669	P_{G87} (MW)	163.8951	V_{27}	0.9683	V_{90}	0.9853	Q_{c46} (Mvar)	-17.1541
P_{G26} (MW)	291.1758	P_{G89} (MW)	210.0919	V_{31}	0.9672	V_{91}	0.9801	Q_{c48} (Mvar)	3.9863
P_{G27} (MW)	12.7930	P_{G90} (MW)	11.1843	V_{32}	0.9678	V_{92}	0.9837	Q_{c74} (Mvar)	11.1285
P_{G31} (MW)	20.0211	P_{G91} (MW)	24.6972	V_{34}	0.9815	V_{99}	1.0102	Q_{c79} (Mvar)	2.4003
P_{G32} (MW)	0	P_{G92} (MW)	0	V_{36}	0.9754	V_{100}	0.9710	Q_{c82} (Mvar)	37.9876
P_{G34} (MW)	0	P_{G99} (MW)	176.6940	V_{40}	0.9701	V_{103}	0.9557	Q_{c83} (Mvar)	9.1203
P_{G36} (MW)	0	P_{G100} (MW)	180.4911	V_{42}	0.9853	V_{104}	0.9411	Q_{c105} (Mvar)	4.0877
P_{G40} (MW)	12.1452	P_{G103} (MW)	0	V_{46}	1.0049	V_{105}	0.9443	Q_{c107} (Mvar)	-5.7172
P_{G42} (MW)	21.9355	P_{G104} (MW)	0	V_{49}	1.0247	V_{107}	0.9521	Q_{c110} (Mvar)	18.2214
P_{G46} (MW)	49.4955	P_{G105} (MW)	0	V_{54}	0.9553	V_{110}	0.9588	Cost ($/h)	68110.35
P_{G49} (MW)	70.0794	P_{G107} (MW)	16.8557	V_{55}	0.9517	V_{111}	0.9802	Emission(lb/h)	405.9932
P_{G54} (MW)	241.5004	P_{G110} (MW)	28.6788	V_{56}	0.9545	V_{112}	0.9753	power loss(MW)	104.8402
P_{G55} (MW)	0	P_{G111} (MW)	81.7905	V_{59}	0.9851	V_{113}	0.9931	Voltage deviation (p.u.)	1.8182
P_{G56} (MW)	0	P_{G112} (MW)	59.7296	V_{61}	0.9953	V_{116}	1.0054	L_{max}	0.1046
P_{G59} (MW)	129.0256	P_{G113} (MW)	57.3315	V_{62}	0.9975	T_{8-5}	0.9816		
P_{G61} (MW)	140.2808	P_{G116} (MW)	25.0041	V_{65}	1.0051	T_{26-25}	0.9605		
P_{G62} (MW)	51.2464	V_1 (p.u.)	0.9563	V_{66}	1.0500	T_{30-17}	0.9614		
P_{G65} (MW)	381.8979	V_4 (p.u.)	0.9981	V_{69}	1.0350	T_{38-37}	0.9367		

Table 8.12: Comparison of performance for cost minimization of IEEE 118 bus system

Technique	Best cost ($/h)	Average cost ($/h)	Worst cost ($/h)	CPU time (S)
HTS	68110.35	68111.84	68114.16	288.6257

8.4.3.2. Minimization of emission

The proposed HTS algorithm has been applied for minimization of emission as the objective function. Here, the population size (N_P), elite size(N_E) and the maximum iteration number (N_{max}) have been selected as 100, 10 and 100 respectively for this test system. The optimal values of control variables obtained from the proposed HTS are given in Table 8.13. The best, average and worst emission and average CPU time among 50 runs of solutions obtained from proposed HTS are summarized in Table 8.14. The convergence characteristic obtained from proposed HTS algorithm for minimum emission solution is shown in Fig. 8.10.

Table 8.13: Optimal value of control variables obtained from HTS for IEEE 118 bus system for emission minimization

Variable		Variable		Variable		Variable		Variable	
P_{G1} (MW)	5.1743	P_{G66} (MW)	388.5257	V_6	0.9905	V_{70}	0.9857	T_{63-59}	0.9596
P_{G4} (MW)	25.8042	P_{G69} (MW)	43.0101	V_8	1.0147	V_{72}	0.9808	T_{64-61}	0.9855
P_{G6} (MW)	7.5464	P_{G70} (MW)	0	V_{10}	1.0500	V_{73}	0.9915	T_{65-66}	0.9357
P_{G8} (MW)	11.9135	P_{G72} (MW)	28.3154	V_{12}	0.9906	V_{74}	0.9667	T_{68-69}	0.9348
P_{G10} (MW)	401.9364	P_{G73} (MW)	17.2548	V_{15}	0.9698	V_{76}	0.9433	T_{81-82}	0.9356
P_{G12} (MW)	121.5883	P_{G74} (MW)	0	V_{18}	0.9735	V_{77}	1.0072	Q_{c5} (Mvar)	-17.7742
P_{G15} (MW)	22.5734	P_{G76} (MW)	0	V_{19}	0.9647	V_{80}	1.0401	Q_{c34} (Mvar)	3.1362
P_{G18} (MW)	82.5876	P_{G77} (MW)	0	V_{24}	0.9929	V_{85}	0.9568	Q_{c37} (Mvar)	-8.2974
P_{G19} (MW)	0	P_{G80} (MW)	175.0243	V_{25}	1.0500	V_{87}	1.0155	Q_{c44} (Mvar)	6.9876
P_{G24} (MW)	20.3710	P_{G85} (MW)	0	V_{26}	1.0147	V_{89}	1.0054	Q_{c45} (Mvar)	5.8355
P_{G25} (MW)	105.9800	P_{G87} (MW)	227.5886	V_{27}	0.9686	V_{90}	0.9857	Q_{c46} (Mvar)	-35.4268
P_{G26} (MW)	303.1171	P_{G89} (MW)	297.4263	V_{31}	0.9678	V_{91}	0.9806	Q_{c48} (Mvar)	10.0909
P_{G27} (MW)	8.5042	P_{G90} (MW)	14.8003	V_{32}	0.9677	V_{92}	0.9838	Q_{c74} (Mvar)	8.0010
P_{G31} (MW)	13.8602	P_{G91} (MW)	43.6077	V_{34}	0.9816	V_{99}	1.0107	Q_{c79} (Mvar)	15.6264
P_{G32} (MW)	0	P_{G92} (MW)	0	V_{36}	0.9755	V_{100}	0.9713	Q_{c82} (Mvar)	95.1279
P_{G34} (MW)	0	P_{G99} (MW)	151.7637	V_{40}	0.9707	V_{103}	0.9567	Q_{c83} (Mvar)	6.7833
P_{G36} (MW)	0	P_{G100} (MW)	287.3936	V_{42}	0.9853	V_{104}	0.9414	Q_{c105} (Mvar)	13.0101
P_{G40} (MW)	16.2087	P_{G103} (MW)	0	V_{46}	1.0055	V_{105}	0.9445	Q_{c107} (Mvar)	-4.5025
P_{G42} (MW)	15.0353	P_{G104} (MW)	0	V_{49}	1.0254	V_{107}	0.9529	Q_{c110} (Mvar)	20.6641
P_{G46} (MW)	99.6463	P_{G105} (MW)	0	V_{54}	0.9559	V_{110}	0.9583	Cost ($/h)	70467.71
P_{G49} (MW)	224.6444	P_{G107} (MW)	10.1385	V_{55}	0.9517	V_{111}	0.9805	Emission (lb/h)	298.6965
P_{G54} (MW	207.6887	P_{G110} (MW)	45.3030	V_{56}	0.9545	V_{112}	0.9752	power loss (MW)	162.2439
P_{G55} (MW)	0	P_{G111} (MW)	97.4258	V_{59}	0.9858	V_{113}	0.9937	Voltage deviation (p.u.)	2.0173
P_{G56} (MW)	0	P_{G112} (MW)	80.5707	V_{61}	0.9956	V_{116}	1.0055	L_{max}	0.1075
P_{G59} (MW)	72.7896	P_{G113} (MW)	94.4714	V_{62}	0.9977	T_{8-5}	0.9819		
P_{G61} (MW)	191.9093	P_{G116} (MW)	30.7140	V_{65}	1.0053	T_{26-25}	0.9625		
P_{G62} (MW)	67.9450	V_1 (p.u.)	0.9564	V_{66}	1.0500	T_{30-17}	0.9607		
P_{G65} (MW)	389.3891	V_4 (p.u.)	0.9987	V_{69}	1.0350	T_{38-37}	0.9369		

Table 8.14: Comparison of performance for emission minimization of IEEE 118 bus system

Technique	Best emission (lb/h)	Average emission (lb/h)	Worst emission (lb/h)	CPU time (S)
HTS	298.6965	300.4253	302.0186	287.8752

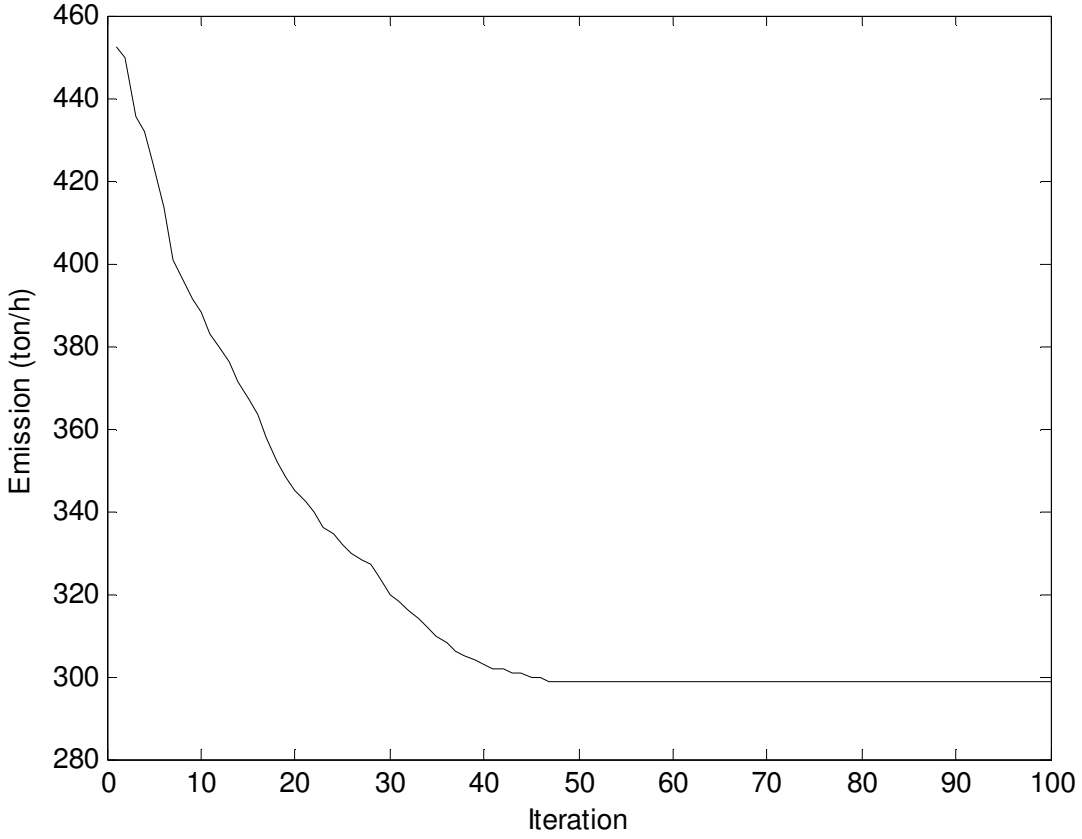

Fig. 8.10. Emission convergence characteristics for IEEE 118 bus system

8.4.3.3. Enhancement of voltage stability

In this case, the proposed HTS algorithm has been applied for enhancement of voltage stability i.e. minimization of $L_{\max}$. Here, the population size (N_P), elite size(N_E) and the maximum iteration number (N_{max}) have been selected as 100, 10 and 100 respectively for this test system. The optimal values of control variables obtained from the proposed HTS are given in Table 8.15. The best, average and worst $L_{\max}$ and average CPU time among 50 runs of solutions obtained from proposed HTS are summarized in Table 8.16. The convergence characteristic obtained from proposed HTS algorithm for $L_{\max}$ minimization is shown in Fig. 8.11.

Table 8.15: Optimal value of control variables obtained from HTS for IEEE 118 bus system for voltage stability enhancement

Variable		Variable		Variable		Variable		Variable	
P_{G1} (MW)	15.1000	P_{G66} (MW)	382.4401	V_6	0.9903	V_{70}	0.9856	T_{63-59}	0.9596
P_{G4} (MW)	26.7207	P_{G69} (MW)	362.3144	V_8	1.0151	V_{72}	0.9805	T_{64-61}	0.9848
P_{G6} (MW)	14.9317	P_{G70} (MW)	70.9164	V_{10}	1.0500	V_{73}	0.9911	T_{65-66}	0.9345
P_{G8} (MW)	20.3994	P_{G72} (MW)	12.4464	V_{12}	0.9904	V_{74}	0.9667	T_{68-69}	0.9343
P_{G10} (MW)	404.2671	P_{G73} (MW)	9.3132	V_{15}	0.9693	V_{76}	0.9426	T_{81-82}	0.9366
P_{G12} (MW)	262.3616	P_{G74} (MW)	19.9994	V_{18}	0.9736	V_{77}	1.0071	Q_{c5} (Mvar)	-24.0515
P_{G15} (MW)	27.5909	P_{G76} (MW)	30.7464	V_{19}	0.9648	V_{80}	1.0403	Q_{c34} (Mvar)	0
P_{G18} (MW)	91.2769	P_{G77} (MW)	84.0866	V_{24}	0.9925	V_{85}	0.9569	Q_{c37} (Mvar)	-17.9176
P_{G19} (MW)	14.3799	P_{G80} (MW)	293.6501	V_{25}	1.0500	V_{87}	1.0152	Q_{c44} (Mvar)	0.0290
P_{G24} (MW)	17.4469	P_{G85} (MW)	12.2924	V_{26}	1.0146	V_{89}	1.0054	Q_{c45} (Mvar)	5.4166
P_{G25} (MW)	148.8825	P_{G87} (MW)	132.3614	V_{27}	0.9682	V_{90}	0.9853	Q_{c46} (Mvar)	-27.6219
P_{G26} (MW)	303.1802	P_{G89} (MW)	299.9668	V_{31}	0.9678	V_{91}	0.9806	Q_{c48} (Mvar)	11.3379
P_{G27} (MW)	15.0559	P_{G90} (MW)	16.7316	V_{32}	0.9676	V_{92}	0.9833	Q_{c74} (Mvar)	0
P_{G31} (MW)	27.2856	P_{G91} (MW)	44.3270	V_{34}	0.9814	V_{99}	1.0106	Q_{c79} (Mvar)	2.2228
P_{G32} (MW)	90.4919	P_{G92} (MW)	196.5727	V_{36}	0.9755	V_{100}	0.9712	Q_{c82} (Mvar)	110.8863
P_{G34} (MW)	25.5560	P_{G99} (MW)	133.9130	V_{40}	0.9702	V_{103}	0.9558	Q_{c83} (Mvar)	0.0138
P_{G36} (MW)	45.1288	P_{G100} (MW)	267.0140	V_{42}	0.9853	V_{104}	0.9416	Q_{c105} (Mvar)	0
P_{G40} (MW)	9.0982	P_{G103} (MW)	9.8975	V_{46}	1.0057	V_{105}	0.9444	Q_{c107} (Mvar)	-14.6412
P_{G42} (MW)	19.9417	P_{G104} (MW)	52.2055	V_{49}	1.0255	V_{107}	0.9526	Q_{c110} (Mvar)	5.3472
P_{G46} (MW)	57.8948	P_{G105} (MW)	87.4796	V_{54}	0.9559	V_{110}	0.9587	Cost ($/h)	72213.61
P_{G49} (MW)	90.3132	P_{G107} (MW)	17.3746	V_{55}	0.9514	V_{111}	0.9803	Emission (lb/h)	398.4442
P_{G54} (MW)	61.5296	P_{G110} (MW)	43.0175	V_{56}	0.9545	V_{112}	0.9754	power loss (MW)	182.4603
P_{G55} (MW)	56.8374	P_{G111} (MW)	58.5205	V_{59}	0.9857	V_{113}	0.9932	Voltagem deviation (p.u)	1.7401
P_{G56} (MW)	37.4630	P_{G112} (MW)	79.7727	V_{61}	0.9956	V_{116}	1.0053	L_{max}	0.0506
P_{G59} (MW)	167.2125	P_{G113} (MW)	55.7530	V_{62}	0.9975	T_{8-5}	0.9806		
P_{G61} (MW)	73.5977	P_{G116} (MW)	30.6073	V_{65}	1.0053	T_{26-25}	0.9614		
P_{G62} (MW)	69.7190	V_1 (p.u.)	0.9567	V_{66}	1.0500	T_{30-17}	0.9608		
P_{G65} (MW)	394.8187	V_4 (p.u.)	0.9984	V_{69}	1.0350	T_{38-37}	0.9367		

Table 8.16: Comparison of performance for L_{max} minimization of IEEE 118 bus system

Technique	Best L_{max}	Average L_{max}	Worst L_{max}	CPU time (S)
HTS	0.0506	0.0507	0.0510	288.8312

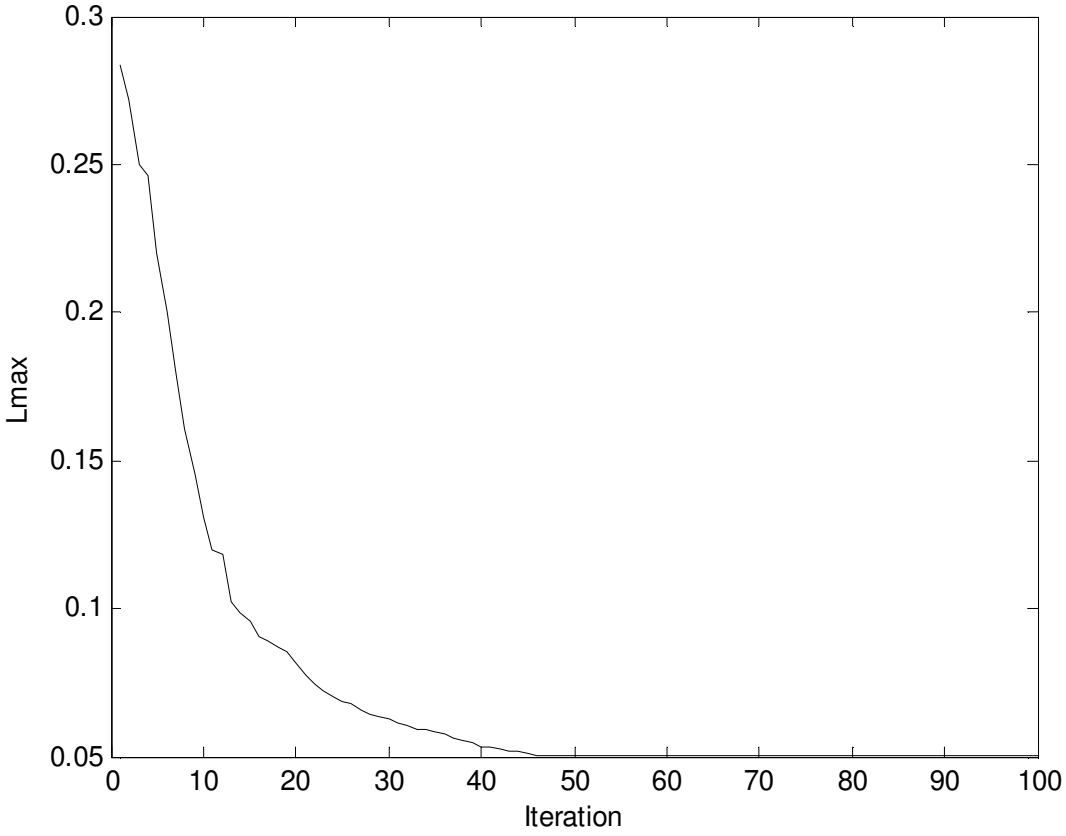

Fig. 8.11. L_{max} convergence characteristics for IEEE 118 bus system

8.4.3.4. Improvement of voltage profile

In this case, the proposed HTS algorithm has been applied for improvement of voltage profile. Here, the population size (N_P), elite size (N_E) and the maximum iteration number (N_{max}) have been selected as 100, 10 and 100 respectively for this test system. The optimal values of control variables obtained from the proposed HTS algorithm are given in Table 8.17. The best, average and worst voltage deviation and average CPU time among 50 runs of solutions obtained from

proposed HTS algorithm are summarized in Table 8.18. The convergence characteristic obtained from proposed HTS algorithm for voltage deviation is shown in Fig. 8.12.

Table 8.17: Optimal value of control variables obtained from HTS for IEEE 118 bus system for improvement of voltage profile

Variable		Variable		Variable		Variable		Variable	
P_{G1} (MW)	24.8354	P_{G66} (MW)	386.8658	V_6	0.9908	V_{70}	0.9855	$T_{63–59}$	0.9593
P_{G4} (MW)	27.3774	P_{G69} (MW)	431.2400	V_8	1.0155	V_{72}	0.9803	$T_{64–61}$	0.9845
P_{G6} (MW)	7.4553	P_{G70} (MW)	47.0490	V_{10}	1.0500	V_{73}	0.9911	$T_{65–66}$	0.9348
P_{G8} (MW)	23.1324	P_{G72} (MW)	27.1003	V_{12}	0.9912	V_{74}	0.9664	$T_{68–69}$	0.9346
P_{G10} (MW)	406.4214	P_{G73} (MW)	14.1555	V_{15}	0.9697	V_{76}	0.9435	$T_{81–82}$	0.9357
P_{G12} (MW)	188.1378	P_{G74} (MW)	19.9808	V_{18}	0.9734	V_{77}	1.0077	Q_{c5} (Mvar)	-10.2461
P_{G15} (MW)	14.8522	P_{G76} (MW)	69.3648	V_{19}	0.9647	V_{80}	1.0402	Q_{c34} (Mvar)	0
P_{G18} (MW)	36.5888	P_{G77} (MW)	87.9338	V_{24}	0.9924	V_{85}	0.9568	Q_{c37} (Mvar)	-15.0288
P_{G19} (MW)	19.6471	P_{G80} (MW)	220.4790	V_{25}	1.0500	V_{87}	1.0154	Q_{c44} (Mvar)	7.9582
P_{G24} (MW)	6.0058	P_{G85} (MW)	26.1360	V_{26}	1.0147	V_{89}	1.0047	Q_{c45} (Mvar)	1.7116
P_{G25} (MW)	240.1806	P_{G87} (MW)	53.1162	V_{27}	0.9685	V_{90}	0.9855	Q_{c46} (Mvar)	-33.5173
P_{G26} (MW)	301.7679	P_{G89} (MW)	173.7364	V_{31}	0.9678	V_{91}	0.9806	Q_{c48} (Mvar)	7.6346
P_{G27} (MW)	12.2519	P_{G90} (MW)	17.8891	V_{32}	0.9676	V_{92}	0.9838	Q_{c74} (Mvar)	0
P_{G31} (MW)	22.1487	P_{G91} (MW)	22.0689	V_{34}	0.9818	V_{99}	1.0106	Q_{c79} (Mvar)	19.3213
P_{G32} (MW)	56.7973	P_{G92} (MW)	242.4305	V_{36}	0.9754	V_{100}	0.9717	Q_{c82} (Mvar)	33.4421
P_{G34} (MW)	14.9005	P_{G99} (MW)	172.2366	V_{40}	0.9705	V_{103}	0.9556	Q_{c83} (Mvar)	13.4003
P_{G36} (MW)	44.6387	P_{G100} (MW)	111.5876	V_{42}	0.9853	V_{104}	0.9413	Q_{c105} (Mvar)	0
P_{G40} (MW)	21.6357	P_{G103} (MW)	11.6736	V_{46}	1.0055	V_{105}	0.9452	Q_{c107} (Mvar)	-12.4021
P_{G42} (MW)	15.6677	P_{G104} (MW)	77.6202	V_{49}	1.0251	V_{107}	0.9525	Q_{c110} (Mvar)	7.4332
P_{G46} (MW)	80.0593	P_{G105} (MW)	6 0.1407	V_{54}	0.9558	V_{110}	0.9587	Cost($/h)	70904.50

P_{G49} (MW)	179.8429	P_{G107} (MW)	12.8669	V_{55}	0.9517	V_{111}	0.9805	Emission (lb /h)	451.7620
P_{G54} (MW)	50.4990	P_{G110} (MW)	40.6254	V_{56}	0.9548	V_{112}	0.9755	powerloss (MW)	110.3291
P_{G55} (MW)	32.2701	P_{G111} (MW)	68.1610	V_{59}	0.9855	V_{113}	0.9934	Voltage deviation (p.u.)	1.5955
P_{G56} (MW)	39.2898	P_{G112} (MW)	78.7837	V_{61}	0.9951	V_{116}	1.0053	L_{max}	0.0894
P_{G59} (MW)	92.3657	P_{G113} (MW)	43.0954	V_{62}	0.9973	T_{8-5}	0.9805		
P_{G61} (MW)	142.8751	P_{G116} (MW)	31.0410	V_{65}	1.0054	T_{26-25}	0.9616		
P_{G62} (MW)	81.2074	V_1 (p.u.)	0.9566	V_{66}	1.0500	T_{30-17}	0.9625		
P_{G65} (MW)	395.0630	V_4 (p.u.)	0.9984	V_{69}	1.0350	T_{38-37}	0.9369		

Table 8.18: Comparison of performance for voltage deviation of IEEE 118 bus system

Technique	Best voltage deviation	Average voltage deviation	Worst voltage deviation	CPU time (S)
HTS	1.5955	1.5957	1.5961	287.3169

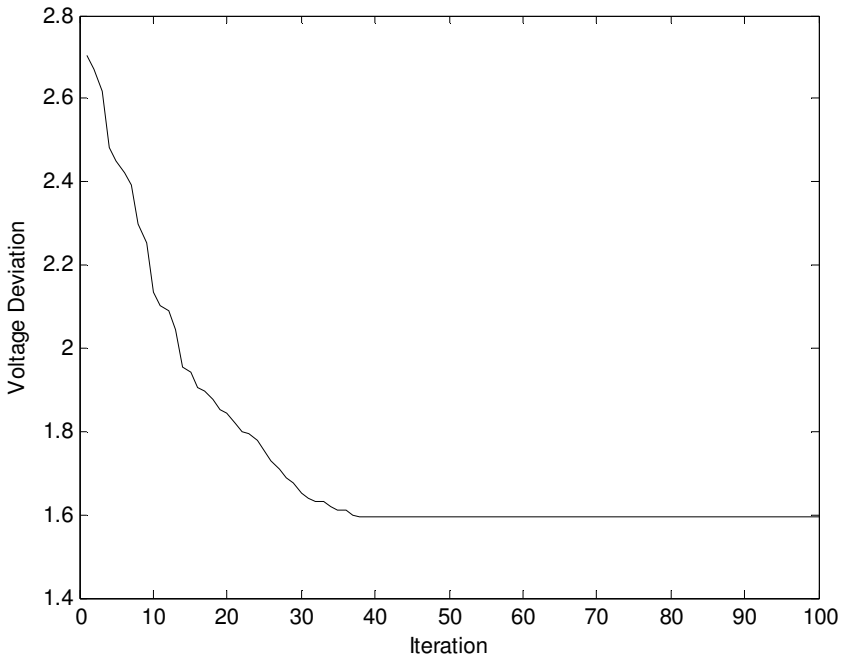

Fig. 8.12. Voltage deviation convergence characteristics for IEEE 118 bus system

8.5. Overview of Quasi-oppositional Differential Evolution algorithm

Quasi-opposition-based learning was introduced by Rahnamayan et al [106] to improve candidate solution by considering current population as well as its quasi-opposite population at the same time.

The process can be improved by starting with a closer i.e. fitter solution by simultaneously checking the quasi-opposite solution. By doing this, the fitter one (guess or quasi-opposite guess) may be chosen as an initial solution. The process starts with the closer of the two guesses. The same approach can be applied not only to the initial solution but also continuously to each solution in the current population. It is proved that a quasi-opposite number is usually closer than an opposite number to the solution. [106]

8.5.1. Definition of opposite number and quasi-opposite number

If x be a real number between $[lb, ub]$, its opposite number (x_o) and its quasi-opposite number (x_{qo}) are defined as

$$x_o = lb + lu - x \tag{8.20}$$

and

$$x_{qo} = rand\left[\left(\frac{lb+lu}{2}\right), (lb+lu-x)\right] \tag{8.21}$$

Similarly, this definition can be extended to higher dimensions [105] as stated in the next sub-section.

8.5.2. Definition of opposite point and quasi-opposite point

Let $X = (x_1, x_2, ..., x_n)$ be a point in n- dimensional space where $x_i \in [lb_i, ub_i]$ and $i \in 1,2,...,n$. The opposite point $X_o = (x_{o1}, x_{o2}, ..., x_{on})$ is completely defined by its components as in (8.22)

$$x_{oi} = lb_i + ub_i - x_i \tag{8.22}$$

The quasi-opposite point $X_{qo} = (x_{qo1}, x_{qo2}, ..., x_{qon})$ is completely defined by its components as in (8.23)

$$x_{qoi} = rand\left[\left(\frac{lb_i + lu_i}{2}\right), (lb_i + lu_i - x_i)\right] \tag{8.23}$$

By employing the definition of quasi-opposite point, the quasi-opposition-based optimization is defined in the following sub-section.

8.5.3. Quasi-Opposition based optimization

Let $X = (x_1, x_2, ..., x_n)$ be a point in n- dimensional space i.e. a candidate solution. Assume $f = (\bullet)$ is a fitness function which is used to measure the candidate's fitness. According to the definition of the quasi-opposite point, $X_{qo} = (x_{qo1}, x_{qo2}, ..., x_{qon})$ is the quasi-opposite of $X = (x_1, x_2, ..., x_n)$. Now, if $f(X_{qo}) < f(X)$ (for a minimization problem), then point X can be replaced with X_{qo}; otherwise, the process is continued with X. Hence, the point and its quasi-opposite point are evaluated simultaneously in order to continue with the fitter one.

8.5.4. Quasi-oppositional Differential evolution

Here, the concept of the quasi-opposition-based learning [106] is incorporated in differential evolution. The original DE is chosen as a parent algorithm and the quasi-opposition-based ideas are embedded in DE. Fig. 2.3 shows the flowchart of QODE algorithm.

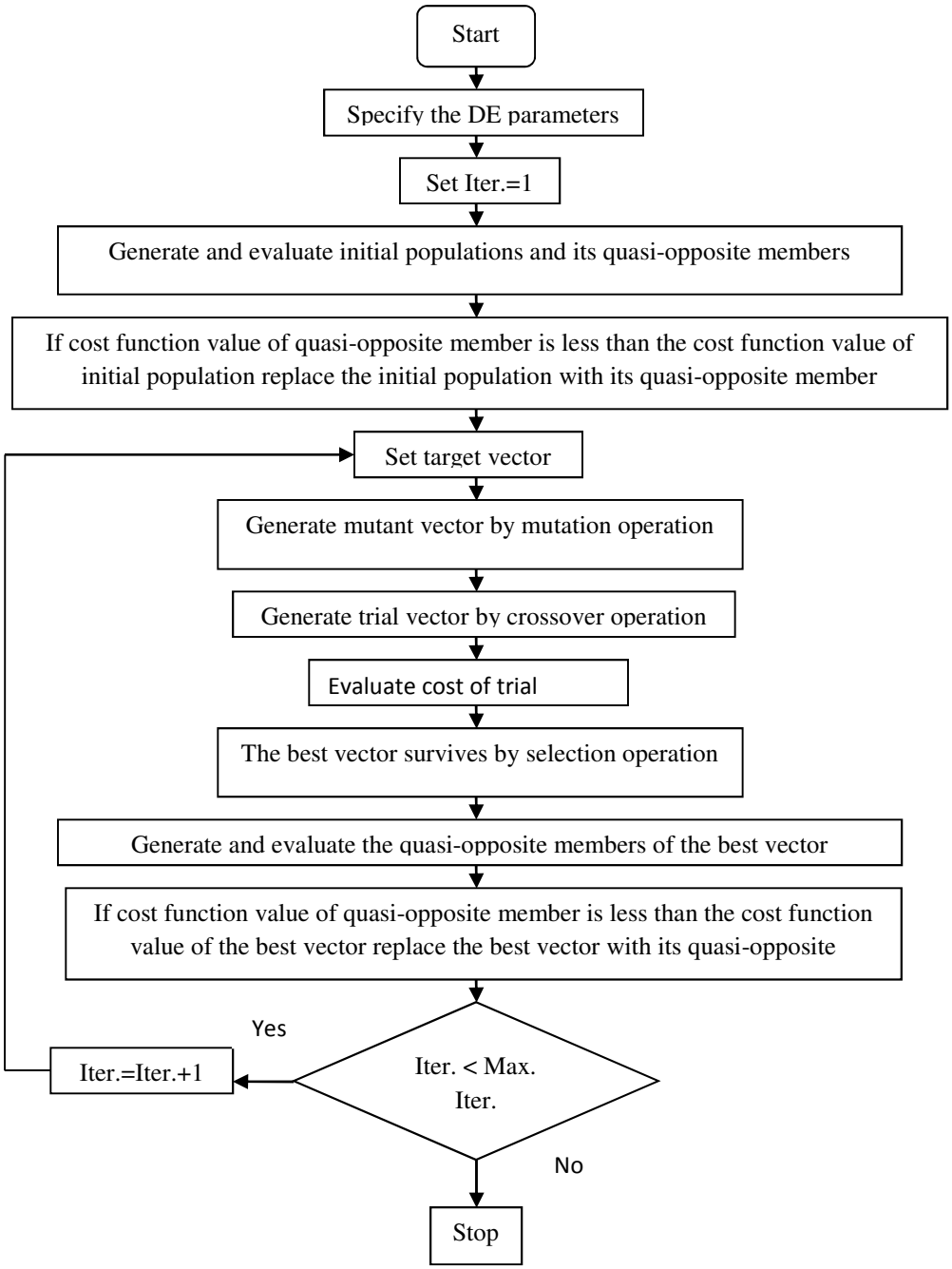

Fig. 8.13. Flowchart of QODE

8.6. Simulation and Results of QODE and DE algorithm

To verify the effectiveness and performance of the proposed QODE and DE for solving four objectives OPF problems, IEEE 30-bus, 57-bus and 118-bus test systems have been considered. Programs have been written in MATLAB-7 language and executed on a 3.0 GHz Pentium-IV personal computer. The results obtained from proposed QODE and DE method are compared with those obtained from other evolutionary methods reported in the literature.

8.6.1. IEEE 30-bus system

The line data, bus data, generator data and the minimum and maximum limits for the control variables have been adapted from [122]. The system has six generators at buses 1, 2, 5, 8, 11 and 13 and four transformers with off nominal tap ratio at lines 6-9, 6-10, 4-12, and 28-27. In addition, shunt VAR compensating devices are assumed to be connected at bus bars 10, 12, 15, 17, 20, 21, 23, 24 and 29. as in [129]. The generator characteristics are given in Table A-23 in the appendix. The total system active power demand is 2.834 p.u. at 100 MVA base. In this study, 50 test runs are performed to solve the OPF problem for different single objective and multi-objective functions.

8.6.1.1.Minimization of fuel cost

The proposed QODE and DE approach are applied for minimization of fuel cost as the objective function. Here, the population size (N_P), scaling factor (S_F), crossover rate (C_R) and the maximum iteration number (N_{max}) have been selected as 100, 1.0, 1.0 and 100 respectively for this test system. The optimal values of control variables obtained from the proposed QODE are given in Table 19. The best, average and worst fuel cost and average CPU time among 50 runs of solutions obtained from proposed QODE and DE are summarized in Table 20. The minimum fuel cost obtained from biogeography based optimization (BBO) [118], differential evolution (DE) [117], particle swarm optimization (PSO) [129], improved genetic algorithm (IGA) [113], improved particle swarm optimization (IPSO) [115] and modified differential evolution (MDE) [125] are also shown in Table 20. The convergence characteristic obtained from proposed QODE and DE for cost minimization is shown in Fig. 8.14. It is seen from Table 20, that minimum cost obtained from QODE is the lowest among all other methods.

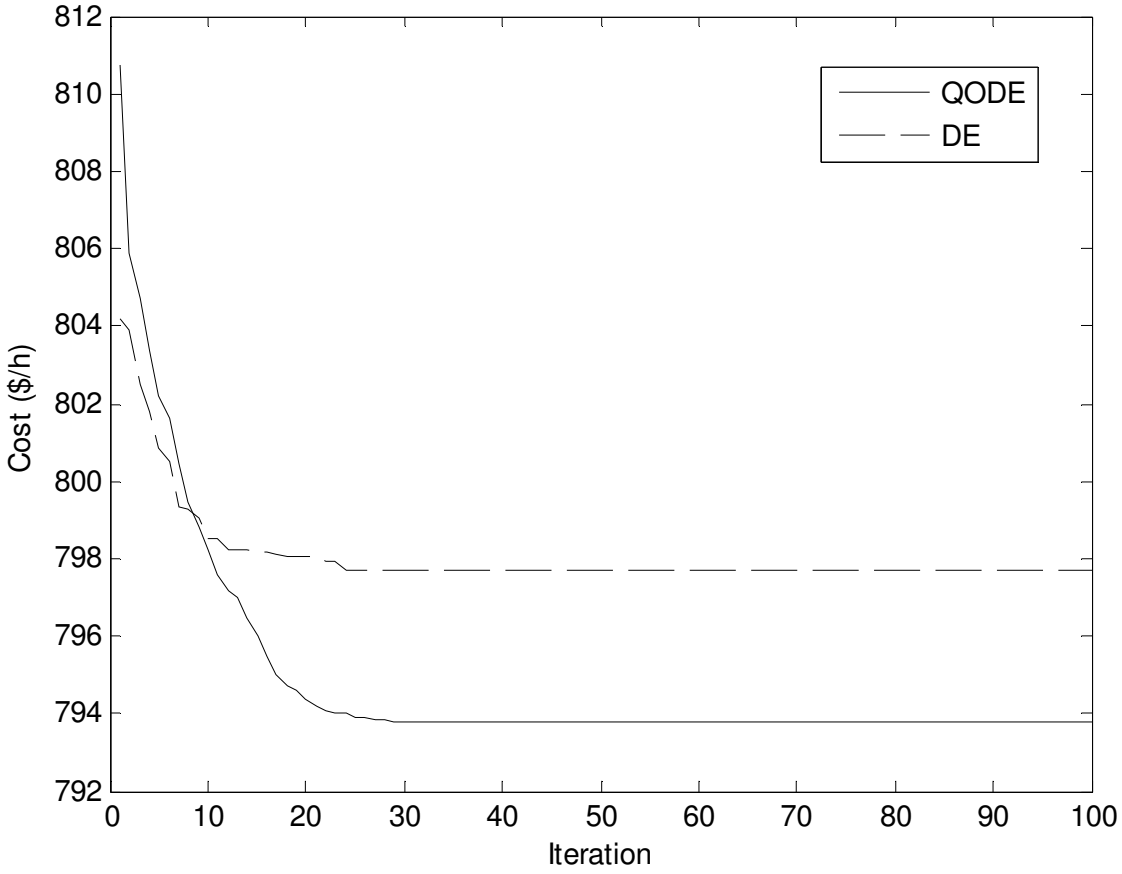

Fig. 8.14. Cost convergence characteristics for IEEE 30 bus system

Table 8.19: Optimal value of control variables obtained from QODE for IEEE 30 bus system for different cases

Control Variable	Fuel cost minimization	Emission minimization	Voltage stability enhancement	Improvement of Voltage Profile
P_{G1} (MW)	190.31	115.68	113.20	158.60
P_{G2} (MW)	47.90	72.43	62.13	52.56
P_{G5} (MW)	19.61	38.75	47.17	39.84
P_{G8} (MW)	11.25	32.96	35.00	14.51
P_{G11} (MW)	10.000	29.53	19.10	10.00
P_{G13} (MW)	12.000	0	12.00	14.50
V_1 (p.u.)	1.0500	1.0500	1.0500	1.0500
V_2 (p.u.)	1.0338	1.0334	1.0337	1.0339
V_5 (p.u.)	1.0058	1.0053	1.0059	1.0060
V_8 (p.u.)	1.0230	1.0227	1.0233	1.0231
V_{11} (p.u.)	1.0913	1.0908	1.0914	1.0911
V_{13} (p.u.)	1.0400	1.0404	1.0398	1.0399
T_{6-9}	1.0155	0.9946	1.0069	1.0157
T_{6-10}	0.9629	0.9953	0.9820	1.0274
T_{4-12}	1.0129	0.9844	0.9913	1.0087
T_{28-27}	0.9581	1.0044	1.0095	0.9817
Q_{c10} (Mvar)	4.12	0.5914	5.0000	0.95
Q_{c12} (Mvar)	1.15	0.9519	5.0000	0.68
Q_{c15} (Mvar)	4.99	1.7289	2.4663	3.01
Q_{c17} (Mvar)	4.80	2.9142	0	0
Q_{c20} (Mvar)	0.08	3.5631	5.0000	5.0000
Q_{c21} (Mvar)	4.93	0.8467	5.0000	5.0000
Q_{c23} (Mvar)	0.38	1.4583	2.1800	2.1800
Q_{c24} (Mvar)	1.06	2.8836	3.7715	3.7715
Q_{c29} (Mvar)	4.85	2.5745	5.0000	5.0000
FuelCost ($/h)	793.79	859.26	866.98	821.07
Emission(ton/h)	0.4080	0.1961	0.2476	0.3201
Loss Voltage(MW)	7.67	5.94	5.20	6.61
Voltage deviation (p.u.)	0.5405	0.3535	0.8706	0.0615
$L_{\max}$	0.0489	0.0729	0.0202	0.0641

Table 8.20: Comparison of performance for cost minimization of IEEE 30 bus system

Techniques	Best cost ($/h)	Average cost ($/h)	Worst cost ($/h)	CPU time (S)
QODE	793.79	793.84	793.91	38.2537
DE	797.07	796.81	796.93	36.0264
BBO [118]	799.11	-	-	-
DE [117]	799.28	-	-	-
PSO [129]	800.41	-	-	-
IGA [113]	800.80	-	-	-
IPSO [115]	801.97	-	-	-
MDE [125]	802.37	-	-	-

8.6.1.2.Minimization of emission

The proposed QODE and DE approach are applied for minimization of emission as the objective function. Here, the population size (N_P), scaling factor (S_F), crossover rate (C_R) and the maximum iteration number (N_{max}) have been selected as 100, 1.0, 1.0 and 100 respectively for this test system. The optimal values of control variables obtained from the proposed QODE are given in Table 8.19. The best, average and worst emission and average CPU time among 50 runs of solutions obtained from proposed QODE and DE are summarized in Table 8.21. The minimum emission obtained from improved particle swarm optimization (IPSO) [115] is also shown in Table 8.21. The convergence characteristic obtained from proposed QODE and DE for emission minimization is shown in Fig. 8.15. It is seen from Table 8.21, that minimum emission obtained from QODE is the lowest among all other methods.

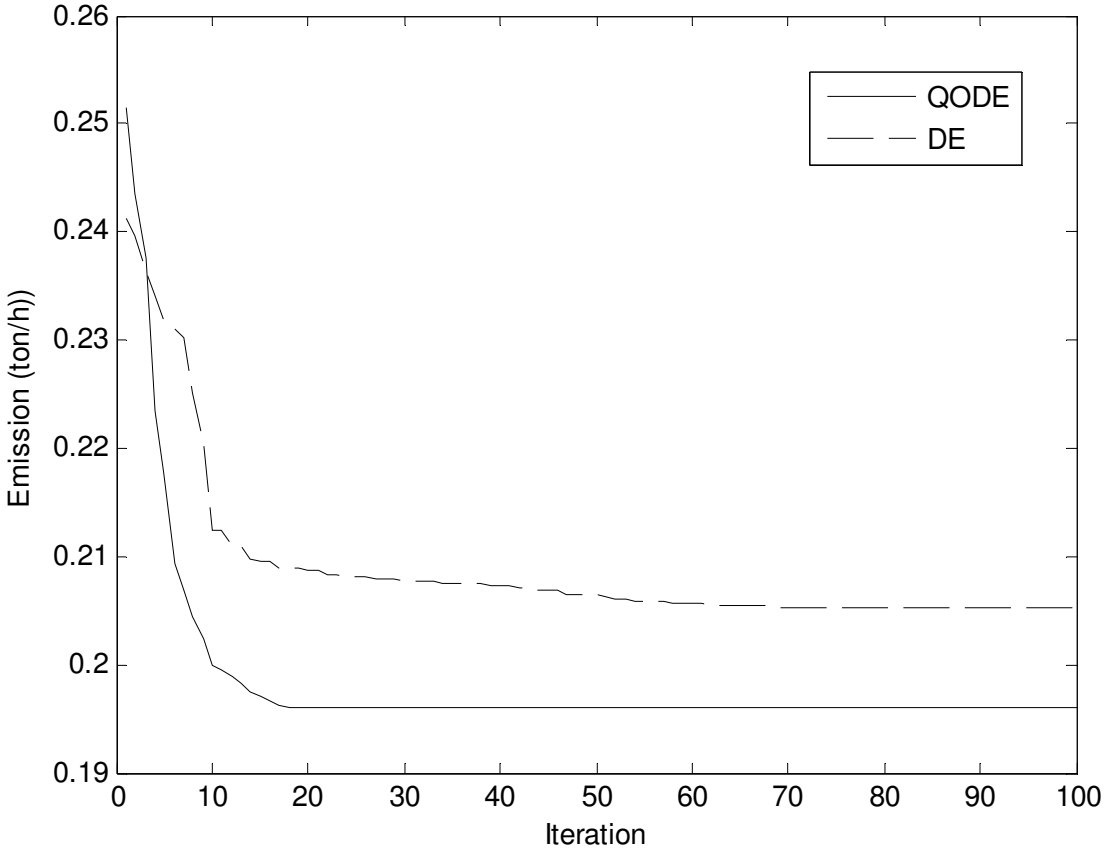

Fig. 8.15. Emission convergence characteristics for IEEE 30 bus system

Table 8.21: Comparison of performance for emission minimization of IEEE 30 bus system

Techniques	Best emission (ton/h)	Average emission (ton/h)	Worst emission (ton/h)	CPU time (S)
QODE	0.1961	0.1965	0.1971	40.5756
DE	0.2053	0.2058	0.2064	37.9302
IPSO [115]	0.2058	-	-	-

8.6.1.3. Enhancement of voltage stability

In this case, the proposed QODE and DE approach are applied for enhancement of voltage stability i.e. minimization of $L_{\max}$. Here, the population size (N_P), scaling factor (S_F), crossover rate (C_R) and the maximum iteration number ($N_{\max}$) have been selected as 100, 1.0, 1.0 and 100 respectively for this test system. The optimal values of control variables obtained from the

proposed QODE are shown in Table 8.19. The best, average and worst L_{max} and average CPU time among 50 runs of solutions obtained from proposed QODE and DE are summarized in Table 8.22. The L_{max} obtained from BBO [118] and improved particle swarm optimization (IPSO) [115] are also shown in Table 8.22. The convergence characteristic obtained from proposed QODE and DE for L_{max} minimization is shown in Fig. 8.16. It is seen from Table 8.22 that the value of L_{max} obtained from QODE is the lowest among all other methods.

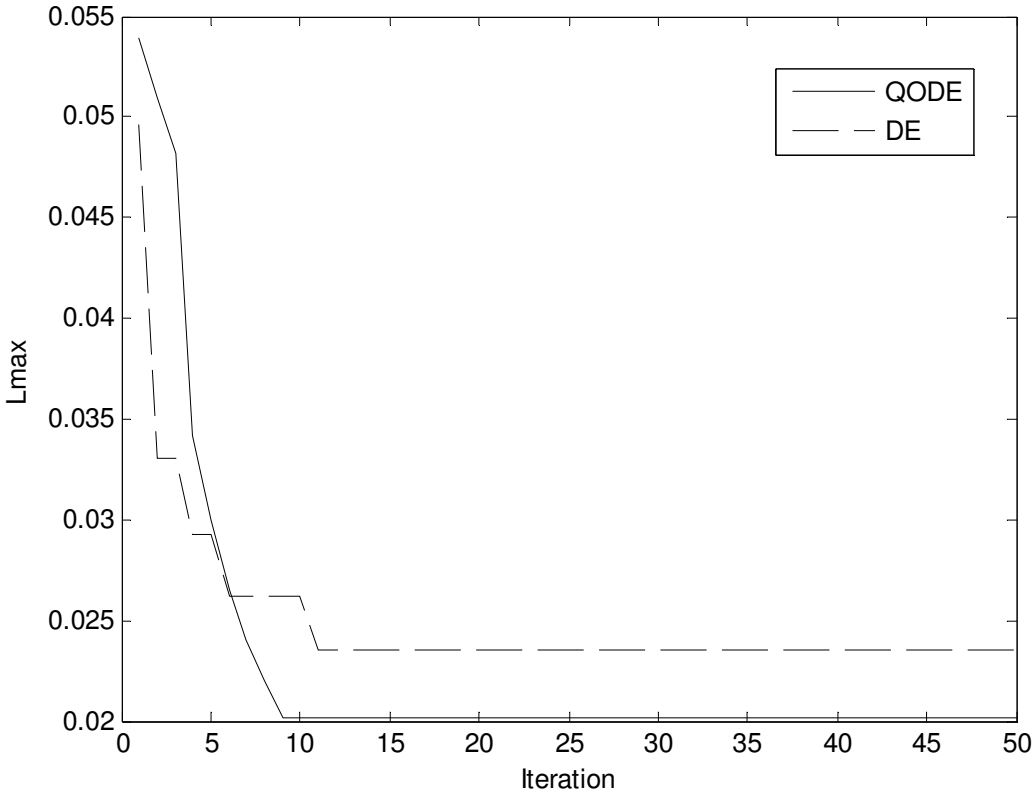

Fig. 8.16. L_{max} convergence characteristics for IEEE 30 bus system

Table 8.22: Comparison of performance for L_{max} minimization of IEEE 30 bus system

Techniques	Best L_{max}	Average L_{max}	Worst L_{max}	CPU time (S)
QODE	0.0202	0.0206	0.02012	39.2357
DE	0.0235	0.0238	0.0243	37.4235
BBO [118]	0.09803	-	-	-
IPSO [115]	0.1037	-	-	-

8.6.1.4.Improvement of voltage profile

In this case, the proposed QODE and DE approach are applied for improvement of voltage profile. Here, the population size (N_P), scaling factor (S_F), crossover rate (C_R) and the maximum iteration number (N_{max}) have been selected as 100, 1.0, 1.0 and 100 respectively for this test system. The optimal values of control variables obtained from the proposed QODE are given in Table 8.19. The best, average and worst voltage deviation and average CPU time among 50 runs of solutions obtained from proposed QODE and DE are summarized in Table 8.23. The voltage deviation obtained from BBO [118] and faster evolutionary algorithm (FEA) [119] is also shown in Table 8.23. The convergence characteristic obtained from proposed QODE and DE for voltage deviation is shown in Fig. 8.17. It is seen from Table 8.23, that voltage deviation obtained from QODE is the lowest among all other methods.

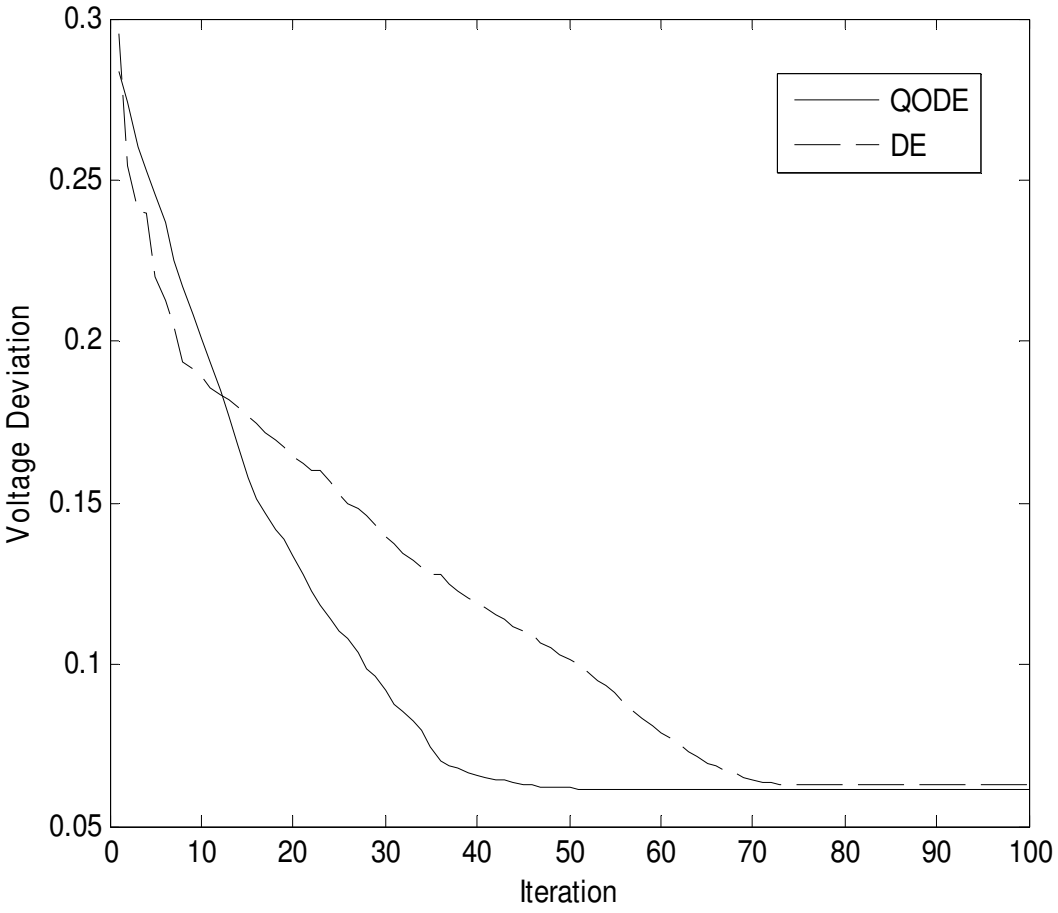

Fig. 8.17. Voltage deviation convergence characteristics for IEEE 30 bus system

Table 8.23: Comparison of performance for voltage deviation of IEEE 30 bus system

Techniques	Best voltage deviation	Average voltage deviation	Worst voltage deviation	CPU time (S)
QODE	0.0615	0.0618	0.0625	46.9973
DE	0.0627	0.0629	0.0633	45.0637
BBO [118]	0.0951	-	-	-
FEA [119]	0.1052	-	-	-

8.6.2. IEEE 57-bus system

The standard IEEE 57-bus system consists of 80 transmission lines, seven generators at buses 1, 2, 3, 6, 8, 9, 12 and 15 branches under load tap setting transformer branches. The reactive power sources are considered at buses 18, 25 and 53. The system line data, bus data, generator data and the minimum and maximum limits for the control variables have been adapted from [127] and [130]. The upper and lower limits of reactive power sources and transformer tap settings are taken from [128]. The generator characteristics are given in Table A-24 in the appendix. The total system active power demand is 12.508 p.u. and reactive power demand is 3.364 p.u. at 100 MVA base. In this study, 50 test runs are performed to solve the OPF problem for different single objective and multi-objective functions.

8.6.2.1.Minimization of fuel cost

The proposed QODE and DE are applied for minimization of fuel cost as the objective function. Here, the population size (N_P), scaling factor (S_F), crossover rate (C_R) and the maximum iteration number (N_{max}) have been selected as 100, 1.0, 1.0 and 100 respectively for this test system. The optimal values of control variables obtained from the proposed QODE are given in Table 8.24. The best, average and worst fuel cost and average CPU time among 50 runs of solutions obtained from proposed QODE and DE are summarized in Table 8.25. The convergence characteristic obtained from proposed QODE and DE for minimum fuel cost solution is shown in Fig. 8.18.

Table 8.24: Optimal value of control variables obtained from QODE for IEEE 57 bus system for different cases

Control variable	Fuel Cost Minimization	Emission Minimization	Voltage stability enhancement	Improvement of voltage profile	Minimization of F_5	Minimization of F_6
P_{G1} (MW)	592.76	304.02	522.37	589.66	417.72	418.87
P_{G2} (MW)	0	0	0	0	0	0
P_{G3} (MW)	97.62	172.65	35.73	16.35	112.00	85.56
P_{G6} (MW)	0	0	0	0	0	0
P_{G8} (MW)	136.25	341.89	523.20	482.32	270.71	284.92
P_{G9} (MW)	0	0	0	0	0	0
P_{G12} (MW)	460.61	461.89	201.67	196.53	479.25	488.58
V_1 (p.u.)	1.0400	1.0400	1.0400	1.0400	1.0400	1.0400
V_2 (p.u.)	1.0100	1.0104	1.0103	1.0107	1.0103	1.0102
V_3 (p.u.)	0.9850	0.9855	0.9853	0.9856	0.9852	0.9854
V_6 (p.u.)	0.9801	0.9806	0.9801	0.9804	0.9804	0.9802
V_8 (p.u.)	1.0052	1.0057	1.0049	1.0055	1.0053	1.0051
V_9 (p.u.)	0.9800	0.9804	0.9805	0.9806	0.9801	0.9802
V_{12} (p.u.)	1.0153	1.0148	1.0151	1.0153	1.0149	1.0151
T_{4-18}	0.9700	1.0987	0.9801	0.9831	1.0975	1.0983
T_{4-18}	0.9780	1.0820	0.9526	0.9510	1.0810	1.0816
T_{21-20}	1.0430	0.9221	0.9501	0.9507	0.9212	0.9215
T_{24-26}	1.0430	1.0171	1.0045	1.0043	1.0172	1.0170
T_{7-29}	0.9670	0.9960	0.9777	0.9769	0.9954	0.9953
T_{34-32}	0 .9750	1.0999	0.9138	0.9139	1.0993	1.0995
T_{11-41}	0.9550	1.0750	0.9465	0.9461	1.0761	1.0757
T_{15-45}	0.9550	0.9541	0.9269	0.9258	0.9543	0.9542
T_{14-46}	0.9000	0.9370	0.9962	0.9957	0.9367	0.9365
T_{10-51}	0.9300	1.0160	1.0385	1.0379	1.0158	1.0161
T_{13-49}	0.8950	1.0998	0.9052	0.9053	1.0996	1.0994
T_{11-43}	0.9580	1.0980	0.9240	0.9229	1.0974	1.0981
T_{40-56}	0.9580	0.9799	0.9875	0.9868	0.9796	0.9787
T_{39-57}	0.9800	1.0246	1 .0098	1.0095	1.0244	1.0243
T_{9-55}	0.9400	1.0371	0.9373	0.9367	1.0374	1.0369
Q_{c18} (Mvar)	4.0117	0.2339	3.523	5.7907	0	10.0000
Q_{c25} (Mvar)	4.0184	2.8458	4.0004	0.6058	0.0361	0.6325

Q_{c53} (Mvar)	1.7637	1.2245	3.1840	5.8095	0	5.2532
Cost ($/h)	7640.00	13181.08	20833.36	18556.16	10509.89	10910.29
Emission (ton/h)	2.8086	1.7003	2.8134	3.0945	2.0003	2.0499
power loss (MW)	36.4534	29.6432	32.1714	34.0597	28.8854	27.1294
voltage deviation (p.u.)	1.1486	5.3719	1.1228	0.6725	4.3066	3.8625
$L_{\max}$	0.1129	0.4161	0.0987	0.1362	0.2828	0.2209

Table 8.25: Comparison of performance for cost minimization of IEEE 57 bus system

Techniques	Best cost ($/h)	Average cost ($/h)	Worst cost ($/h)	CPU time (S)
QODE	7640.00	7642.03	7644.83	47.8745
DE	7680.42	7681.75	76883.67	45.6595

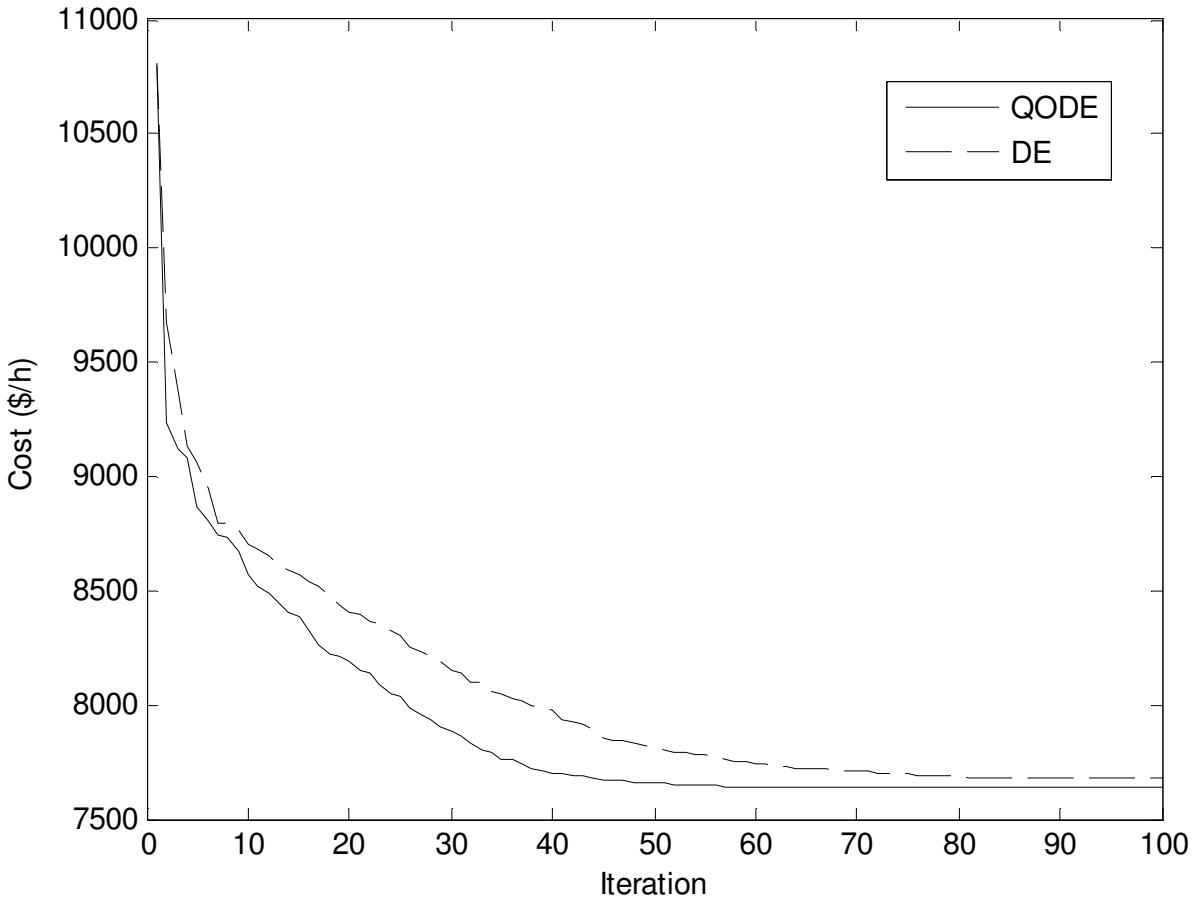

Fig. 8.18. Cost convergence characteristics for IEEE 57 bus system

8.6.2.2.Minimization of emission

The proposed QODE and DE are applied for minimization of emission as the objective function. Here, the population size (N_P), scaling factor (S_F), crossover rate (C_R) and the maximum iteration number (N_{max}) have been selected as 100, 1.0, 1.0 and 100 respectively for this test system. The optimal values of control variables obtained from the proposed QODE are given in Table 8.24. The best, average and worst emission and average CPU time among 50 runs of solutions obtained from proposed QODE and DE are summarized in Table 8.26. The convergence characteristic obtained from proposed QODE and DE for emission minimization is shown in Fig. 8.19.

Table 8.26: Comparison of performance for emission minimization of IEEE 57 bus system

Techniques	Best emission (ton/h)	Average emission (ton/h)	Worst emission (ton/h)	CPU time (S)
QODE	1.7003	1.7006	1.7011	98.0136
DE	1.7187	1.7191	1.7195	95.3025

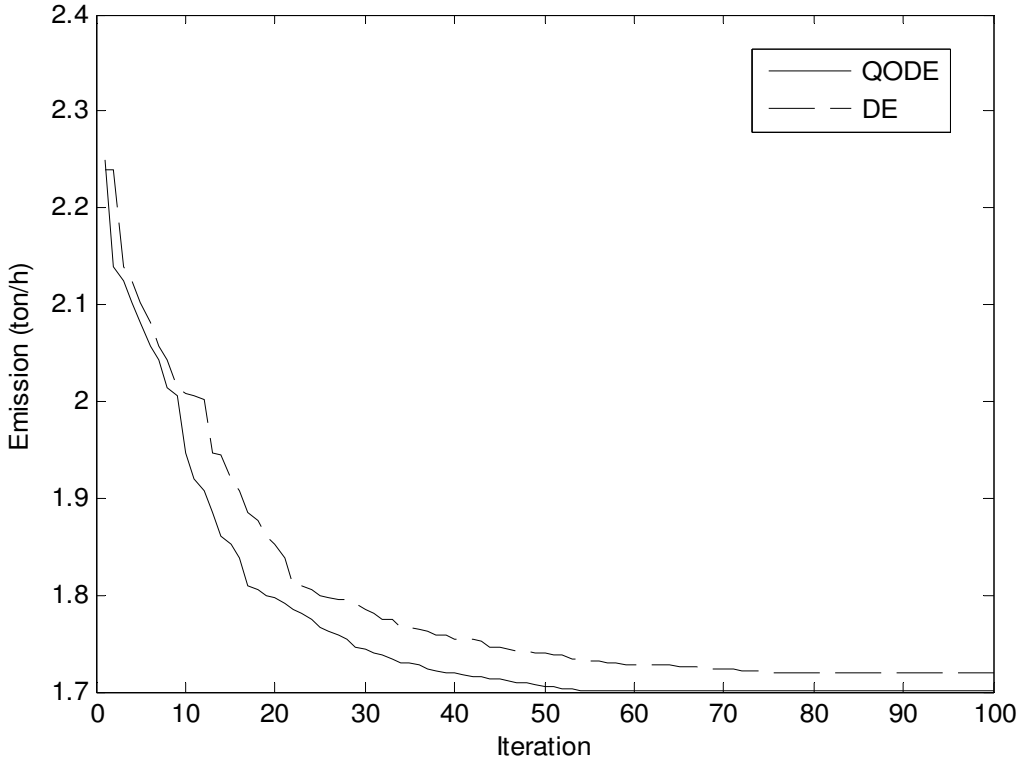

Fig. 8.19. Emission convergence characteristics for IEEE 57 bus system

8.6.2.3.Enhancement of voltage stability

In this case, the proposed QODE and DE are applied for enhancement of voltage stability i.e. minimization of $L_{\max}$. Here, the population size (N_P), scaling factor (S_F), crossover rate (C_R) and the maximum iteration number (N_{max}) have been selected as 100, 1.0, 1.0 and 100 respectively for this test system. The optimal values of control variables obtained from the proposed QODE are given in Table 8.24. The best, average and worst $L_{\max}$ and average CPU time among 50 runs of solutions obtained from proposed QODE and DE are summarized in Table 8.27. The convergence characteristic obtained from proposed QODE and DE for $L_{\max}$ minimization is shown in Fig. 8.20.

Table 8.27: Comparison of performance for $L_{\max}$ minimization of IEEE 57 bus system

Techniques	Best $L_{\max}$	Average $L_{\max}$	Worst $L_{\max}$	CPU time (S)
QODE	0.0987	0.0989	0.0992	103.6524
DE	0.1036	0.1038	0.1041	101.4525

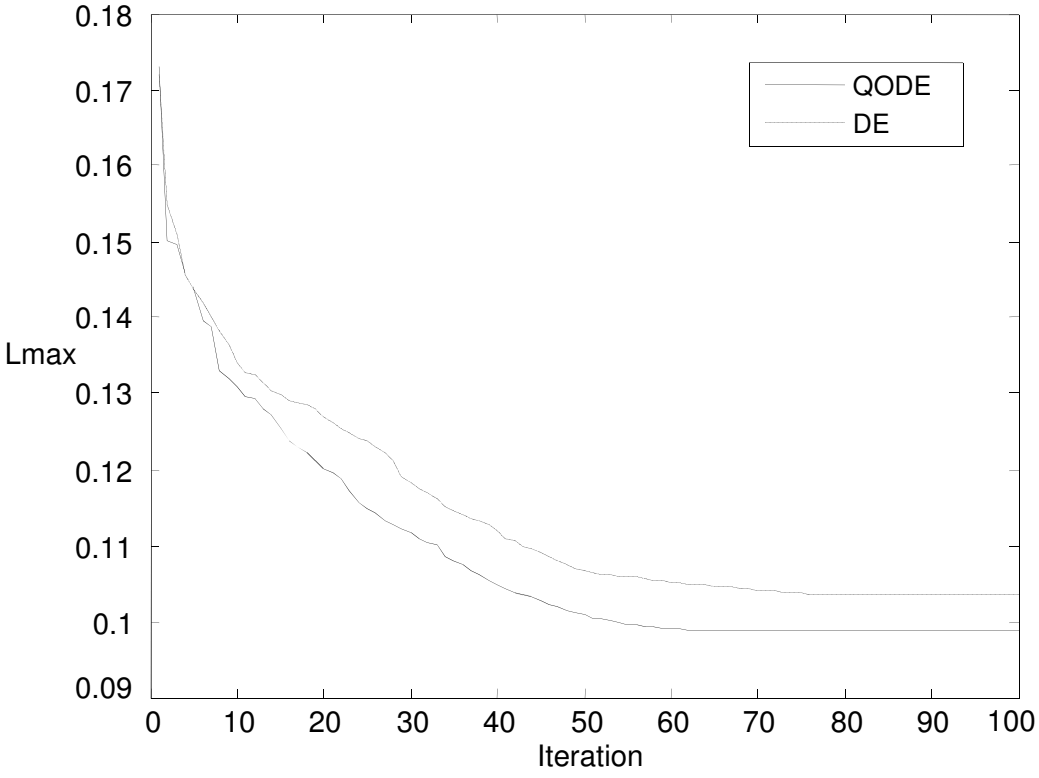

Fig. 8.20. $L_{\max}$ convergence characteristics for IEEE 57 bus system

8.6.2.4.Improvement of voltage profile

In this case, the proposed QODE and DE approach are applied for improvement of voltage profile. Here, the population size (N_P), scaling factor (S_F), crossover rate (C_R) and the maximum iteration number (N_{max}) have been selected as 100, 1.0, 1.0 and 100 respectively for this test system. The optimal values of control variables obtained from the proposed QODE are given in Table 8.24. The best, average and worst voltage deviation and average CPU time among 50 runs of solutions obtained from proposed QODE and DE are summarized in Table 8.28. The convergence characteristic obtained from proposed QODE and DE for voltage deviation is shown in Fig. 8.21.

Table 8.28: Comparison of performance for voltage deviation of IEEE 57 bus system

Techniques	Best voltage deviation	Average voltage deviation	Worst voltage deviation	CPU time (S)
QODE	0.6725	0.6728	0.6732	98.9354
DE	0.7041	0.7044	0.7047	96.0439

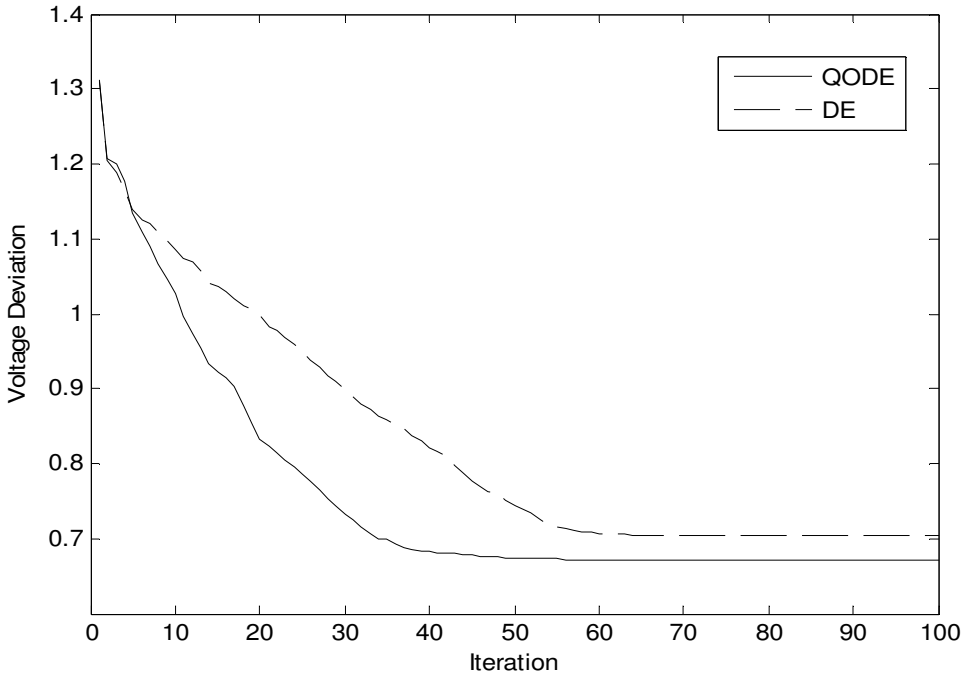

Fig. 8.21. Voltage deviation convergence characteristics for IEEE 57 bus system

8.6.3. IEEE 118-bus system

The standard IEEE 118-bus system consists of 186 transmission lines, 54 generator buses, 64 load buses, 9 branches under load tap setting transformer and 14 reactive power sources. The system line data, bus data, generator data and the minimum and maximum limits for the control variables have been adapted from [101] and [132]. The upper and lower limits of reactive power sources and transformer tap settings are taken from [101]. The generator data has been taken from [132]. The total system active power demand is 42.4200 p.u. and reactive power demand is 14.3800 p.u. at 100 MVA base. In this study, 50 test runs are performed to solve different single objective and multi-objective OPF problems by using QODE.

8.6.3.1.Minimization of fuel cost

The proposed QODE and DE are applied for minimization of fuel cost as the objective function. Here, the population size (N_P), scaling factor (S_F), crossover rate (C_R) and the maximum iteration number (N_{max}) have been selected as 200, 1.0, 1.0 and 100 respectively for this test system. The optimal values of control variables obtained from the proposed QODE are given in Table 8.29. The best, average and worst fuel cost and average CPU time among 50 runs of solutions obtained from proposed QODE and DE are summarized in Table 8.30. The convergence characteristic obtained from proposed QODE and DE for minimum fuel cost solution is shown in Fig. 8.22.

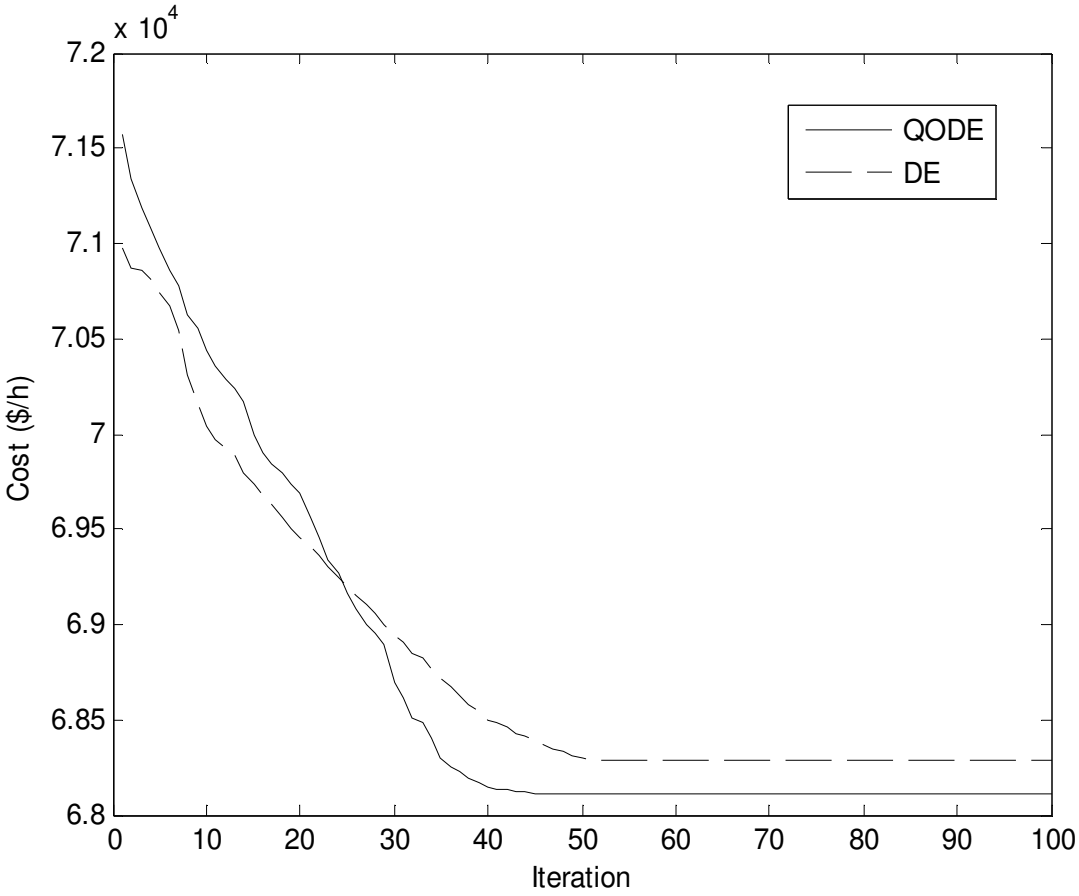

Fig. 8.22. Cost convergence characteristics for IEEE 118 bus system

Table 8.30: Comparison of performance for cost minimization of IEEE 118 bus system

Techniques	Best cost ($/h)	Average cost ($/h)	Worst cost ($/h)	CPU time (S)
QODE	68110.35	68111.84	68114.16	288.6257
DE	68292.79	68294.27	68297.02	286.0725

Table 8.29: Optimal value of control variables obtained from QODE for IEEE 118 bus system for cost minimization

Variable		Variable		Variable		Variable		Variable	
P_{G1} (MW)	29.2109	P_{G66} (MW)	381.8617	V_6	0.9903	V_{70}	0.9854	T_{63-59}	0.9597
P_{G4} (MW)	27.7608	P_{G69} (MW)	332.5110	V_8	1.0151	V_{72}	0.9801	T_{64-61}	0.9846
P_{G6} (MW)	12.7737	P_{G70} (MW)	0	V_{10}	1.0500	V_{73}	0.9909	T_{65-66}	0.9351
P_{G8} (MW)	14.1875	P_{G72} (MW)	11.2969	V_{12}	0.9904	V_{74}	0.9663	T_{68-69}	0.9347
P_{G10} (MW)	422.6864	P_{G73} (MW)	15.7119	V_{15}	0.9692	V_{76}	0.9430	T_{81-82}	0.9356
P_{G12} (MW)	110.9571	P_{G74} (MW)	0	V_{18}	0.9733	V_{77}	1.0071	Q_{c5} (Mvar)	36.6145
P_{G15} (MW)	11.3817	P_{G76} (MW)	0	V_{19}	0.9648	V_{80}	1.0403	Q_{c34} (Mvar)	13.5245
P_{G18} (MW)	59.5803	P_{G77} (MW)	55.6755	V_{24}	0.9921	V_{85}	0.9565	Q_{c37} (Mvar)	-12.7591
P_{G19} (MW)	0	P_{G80} (MW)	232.4882	V_{25}	1.0500	V_{87}	1.0151	Q_{c44} (Mvar)	2.8039
P_{G24} (MW)	28.1248	P_{G85} (MW)	0	V_{26}	1.0151	V_{89}	1.0048	Q_{c45} (Mvar)	0.5621
P_{G25} (MW)	198.2669	P_{G87} (MW)	163.8951	V_{27}	0.9683	V_{90}	0.9853	Q_{c46} (Mvar)	-17.1541
P_{G26} (MW)	291.1758	P_{G89} (MW)	210.0919	V_{31}	0.9672	V_{91}	0.9801	Q_{c48} (Mvar)	3.9863
P_{G27} (MW)	12.7930	P_{G90} (MW)	11.1843	V_{32}	0.9678	V_{92}	0.9837	Q_{c74} (Mvar)	11.1285
P_{G31} (MW)	20.0211	P_{G91} (MW)	24.6972	V_{34}	0.9815	V_{99}	1.0102	Q_{c79} (Mvar)	2.4003
P_{G32} (MW)	0	P_{G92} (MW)	0	V_{36}	0.9754	V_{100}	0.9710	Q_{c82} (Mvar)	37.9876
P_{G34} (MW)	0	P_{G99} (MW)	176.6940	V_{40}	0.9701	V_{103}	0.9557	Q_{c83} (Mvar)	9.1203
P_{G36} (MW)	0	P_{G100} (MW)	180.4911	V_{42}	0.9853	V_{104}	0.9411	Q_{c105} (Mvar)	4.0877
P_{G40} (MW)	12.1452	P_{G103} (MW)	0	V_{46}	1.0049	V_{105}	0.9443	Q_{c107} (Mvar)	5.7172
P_{G42} (MW)	21.9355	P_{G104} (MW)	0	V_{49}	1.0247	V_{107}	0.9521	Q_{c110} (Mvar)	18.2214
P_{G46} (MW)	49.4955	P_{G105} (MW)	0	V_{54}	0.9553	V_{110}	0.9588	Cost ($/h)	68110.35
P_{G49} (MW)	70.0794	P_{G107} (MW)	16.8557	V_{55}	0.9517	V_{111}	0.9802	Emission (lb/h)	405.9932
P_{G54} (MW)	241.5004	P_{G110} (MW)	28.6788	V_{56}	0.9545	V_{112}	0.9753	power loss (MW)	104.8402

P_{G55} (MW)	0	P_{G111} (MW)	81.7905	V_{59}	0.9851	V_{113}	0.9931	voltagedeviation (p.u.)	1.8182
P_{G56} (MW)	0	P_{G112} (MW)	59.7296	V_{61}	0.9953	V_{116}	1.0054	L_{max}	0.1046
P_{G59} (MW)	129.0256	P_{G113} (MW)	57.3315	V_{62}	0.9975	T_{8-5}	0.9816		
P_{G61} (MW)	140.2808	P_{G116} (MW)	25.0041	V_{65}	1.0051	T_{26-25}	0.9605		
P_{G62} (MW)	51.2464	V_1 (p.u.)	0.9563	V_{66}	1.0500	T_{30-17}	0.9614		
P_{G65} (MW)	381.8979	V_4 (p.u.)	0.9981	V_{69}	1.0350	T_{38-37}	0.9367		

8.6.3.2.Minimization of emission

The proposed QODE and DE are applied for minimization of emission as the objective function. Here, the population size (N_P), scaling factor (S_F), crossover rate (C_R) and the maximum iteration number (N_{max}) have been selected as 200, 1.0, 1.0 and 100 respectively for this test system. The optimal values of control variables obtained from the proposed QODE are given in Table 8.31. The best, average and worst emission and average CPU time among 50 runs of solutions obtained from proposed QODE and DE are summarized in Table 8.32. The convergence characteristic obtained from proposed QODE and DE for minimum emission solution is shown in Fig. 8.23.

Table 8.31: Optimal value of control variables obtained from QODE for IEEE 118 bus system for emission minimization

Variable		Variable		Variable		Variable		Variable	
P_{G1} (MW)	5.1743	P_{G66} (MW)	388.5257	V_6	0.9905	V_{70}	0.9857	T_{63-59}	0.9596
P_{G4} (MW)	25.8042	P_{G69} (MW)	43.0101	V_8	1.0147	V_{72}	0.9808	T_{64-61}	0.9855
P_{G6} (MW)	7.5464	P_{G70} (MW)	0	V_{10}	1.0500	V_{73}	0.9915	T_{65-66}	0.9357
P_{G8} (MW)	11.9135	P_{G72} (MW)	28.3154	V_{12}	0.9906	V_{74}	0.9667	T_{68-69}	0.9348
P_{G10} (MW)	401.9364	P_{G73} (MW)	17.2548	V_{15}	0.9698	V_{76}	0.9433	T_{81-82}	0.9356
P_{G12} (MW)	121.5883	P_{G74} (MW)	0	V_{18}	0.9735	V_{77}	1.0072	Q_{c5} (Mvar)	-17.7742
P_{G15} (MW)	22.5734	P_{G76} (MW)	0	V_{19}	0.9647	V_{80}	1.0401	Q_{c34} (Mvar)	3.1362
P_{G18} (MW)	82.5876	P_{G77} (MW)	0	V_{24}	0.9929	V_{85}	0.9568	Q_{c37} (Mvar)	-8.2974
P_{G19} (MW)	0	P_{G80} (MW)	175.0243	V_{25}	1.0500	V_{87}	1.0155	Q_{c44} (Mvar)	6.9876

P_{G24} (MW)	20.3710	P_{G85} (MW)	0	V_{26}	1.0147	V_{89}	1.0054	Q_{c45} (Mvar)	5.8355
P_{G25} (MW)	105.9800	P_{G87} (MW)	227.5886	V_{27}	0.9686	V_{90}	0.9857	Q_{c46} (Mvar)	-35.4268
P_{G26} (MW)	303.1171	P_{G89} (MW)	297.4263	V_{31}	0.9678	V_{91}	0.9806	Q_{c48} (Mvar)	10.0909
P_{G27} (MW)	8.5042	P_{G90} (MW)	14.8003	V_{32}	0.9677	V_{92}	0.9838	Q_{c74} (Mvar)	8.0010
P_{G31} (MW)	13.8602	P_{G91} (MW)	43.6077	V_{34}	0.9816	V_{99}	1.0107	Q_{c79} (Mvar)	15.6264
P_{G32} (MW)	0	P_{G92} (MW)	0	V_{36}	0.9755	V_{100}	0.9713	Q_{c82} (Mvar)	95.1279
P_{G34} (MW)	0	P_{G99} (MW)	151.7637	V_{40}	0.9707	V_{103}	0.9567	Q_{c83} (Mvar)	6.7833
P_{G36} (MW)	0	P_{G100} (MW)	287.3936	V_{42}	0.9853	V_{104}	0.9414	Q_{c105} (Mvar)	13.0101
P_{G40} (MW)	16.2087	P_{G103} (MW)	0	V_{46}	1.0055	V_{105}	0.9445	Q_{c107} (Mvar)	-4.5025
P_{G42} (MW)	15.0353	P_{G104} (MW)	0	V_{49}	1.0254	V_{107}	0.9529	Q_{c110} (Mvar)	20.6641
P_{G46} (MW)	99.6463	P_{G105} (MW)	0	V_{54}	0.9559	V_{110}	0.9583	Cost ($/h)	70467.71
P_{G49} (MW)	224.6444	P_{G107} (MW)	10.1385	V_{55}	0.9517	V_{111}	0.9805	Emission (lb/h)	298.6965
P_{G54} (MW)	207.6887	P_{G110} (MW)	45.3030	V_{56}	0.9545	V_{112}	0.9752	power loss (MW)	162.2439
P_{G55} (MW)	0	P_{G111} (MW)	97.4258	V_{59}	0.9858	V_{113}	0.9937	Voltage deviation (p.u.)	2.0173
P_{G56} (MW)	0	P_{G112} (MW)	80.5707	V_{61}	0.9956	V_{116}	1.0055	$L_{\max}$	0.1075
P_{G59} (MW)	72.7896	P_{G113} (MW)	94.4714	V_{62}	0.9977	T_{8-5}	0.9819		
P_{G61} (MW)	191.9093	P_{G116} (MW)	30.7140	V_{65}	1.0053	T_{26-25}	0.9625		
P_{G62} (MW)	67.9450	V_1 (p.u.)	0.9564	V_{66}	1.0500	T_{30-17}	0.9607		
P_{G65} (MW)	389.3891	V_4 (p.u.)	0.9987	V_{69}	1.0350	T_{38-37}	0.9369		

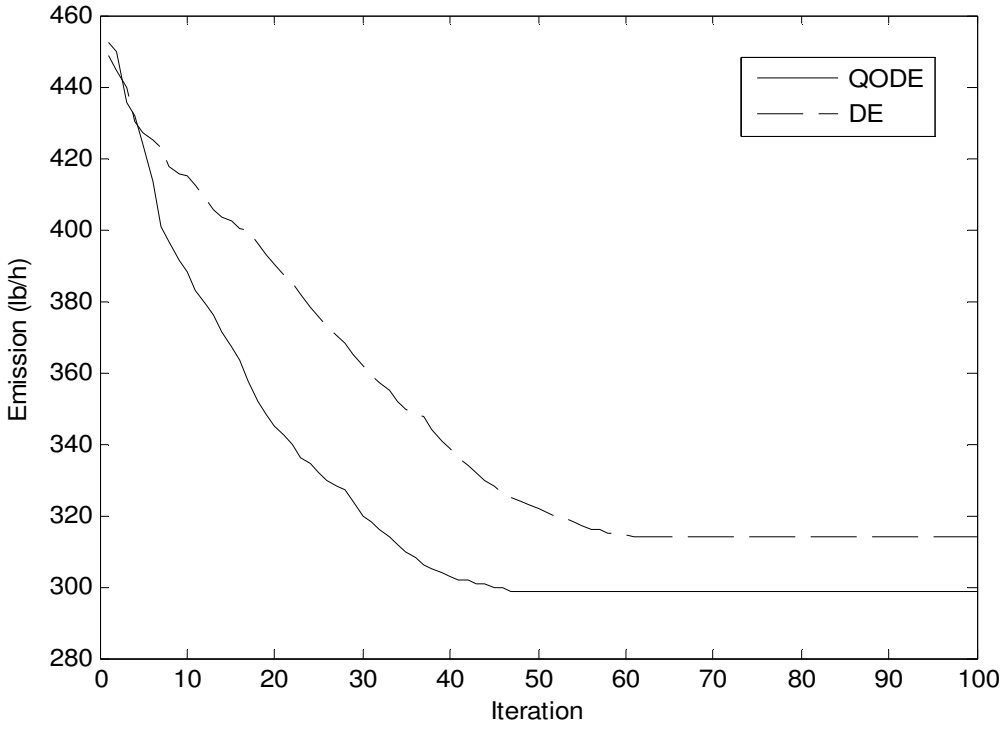

Fig. 8.23. Emission convergence characteristics for IEEE 118 bus system

Table 8.32: Comparison of performance for emission minimization of IEEE 118 bus system

Techniques	Best emission (lb/h)	Average emission (lb/h)	Worst emission (lb/h)	CPU time (S)
QODE	298.6965	300.4253	302.0186	287.8752
DE	314.0861	316.9684	318.7568	285.3085

8.6.3.3.Enhancement of voltage stability

In this case, the proposed QODE and DE are applied for enhancement of voltage stability i.e. minimization of $L_{\max}$. Here, the population size ($\mathrm{N_P}$), scaling factor (S_F), crossover rate (C_R) and the maximum iteration number ($\mathrm{N_{max}}$) have been selected as 200, 1.0, 1.0 and 100 respectively for this test system. The optimal values of control variables obtained from the proposed QODE are given in Table 8.33. The best, average and worst $L_{\max}$ and average CPU time among 50 runs of solutions obtained from proposed QODE and DE are summarized in Table 8.34. The convergence characteristic obtained from proposed QODE and DE for $L_{\max}$ minimization is shown in Fig. 8.24.

Table 8.33: Optimal value of control variables obtained from QODE for IEEE 118 bus system for voltage stability enhancement

Variable		Variable		Variable		Variable		Variable	
P_{G1} (MW)	15.1000	P_{G66} (MW)	382.4401	V_6	0.9903	V_{70}	0.9856	T_{63-59}	0.9596
P_{G4} (MW)	26.7207	P_{G69} (MW)	362.3144	V_8	1.0151	V_{72}	0.9805	T_{64-61}	0.9848
P_{G6} (MW)	14.9317	P_{G70} (MW)	70.9164	V_{10}	1.0500	V_{73}	0.9911	T_{65-66}	0.9345
P_{G8} (MW)	20.3994	P_{G72} (MW)	12.4464	V_{12}	0.9904	V_{74}	0.9667	T_{68-69}	0.9343
P_{G10} (MW)	404.2671	P_{G73} (MW)	9.3132	V_{15}	0.9693	V_{76}	0.9426	T_{81-82}	0.9366
P_{G12} (MW)	262.3616	P_{G74} (MW)	19.9994	V_{18}	0.9736	V_{77}	1.0071	Q_{c5} (Mvar)	-24.0515
P_{G15} (MW)	27.5909	P_{G76} (MW)	30.7464	V_{19}	0.9648	V_{80}	1.0403	Q_{c34} (Mvar)	0
P_{G18} (MW)	91.2769	P_{G77} (MW)	84.0866	V_{24}	0.9925	V_{85}	0.9569	Q_{c37} (Mvar)	-17.9176
P_{G19} (MW)	14.3799	P_{G80} (MW)	293.6501	V_{25}	1.0500	V_{87}	1.0152	Q_{c44} (Mvar)	0.0290
P_{G24} (MW)	17.4469	P_{G85} (MW)	12.2924	V_{26}	1.0146	V_{89}	1.0054	Q_{c45} (Mvar)	5.4166
P_{G25} (MW)	148.8825	P_{G87} (MW)	132.3614	V_{27}	0.9682	V_{90}	0.9853	Q_{c46} (Mvar)	-27.6219
P_{G26} (MW)	303.1802	P_{G89} (MW)	299.9668	V_{31}	0.9678	V_{91}	0.9806	Q_{c48} (Mvar)	11.3379
P_{G27} (MW)	15.0559	P_{G90} (MW)	16.7316	V_{32}	0.9676	V_{92}	0.9833	Q_{c74} (Mvar)	0
P_{G31} (MW)	27.2856	P_{G91} (MW)	44.3270	V_{34}	09814	V_{99}	1.0106	Q_{c79} (Mvar)	2.2228
P_{G32} (MW)	90.4919	P_{G92} (MW)	196.5727	V_{36}	0.9755	V_{100}	0.9712	Q_{c82} (Mvar)	110.8863
P_{G34} (MW)	25.5560	P_{G99} (MW)	133.9130	V_{40}	0.9702	V_{103}	0.9558	Q_{c83} (Mvar)	0.0138
P_{G36} (MW)	45.1288	P_{G100} (MW)	267.0140	V_{42}	0.9853	V_{104}	0.9416	Q_{c105} (Mvar)	0
P_{G40} (MW)	9.0982	P_{G103} (MW)	9.8975	V_{46}	1.0057	V_{105}	0.9444	Q_{c107} (Mvar)	-14.6412
P_{G42} (MW)	19.9417	P_{G104} (MW)	52.2055	V_{49}	1.0255	V_{107}	0.9526	Q_{c110} (Mvar)	5.3472

P_{G46} (MW)	57.8948	P_{G105} (MW)	87.4796	V_{54}	0.9559	0.9587	V_{110}	Cost ($/h)	72213.61
P_{G49} (MW)	90.3132	P_{G107} (MW)	17.3746	V_{55}	0.9514	V_{111}	0.9803	Emission(lb /h)	398.4442
P_{G54} (MW)	61.5296	P_{G110} (MW)	43.0175	V_{56}	0.9545	V_{112}	0.9754	Power loss (MW)	182.4603
P_{G55} (MW)	56.8374	P_{G111} (MW)	58.5205	V_{59}	0.9857	V_{113}	0.9932	voltage deviation (p.u.)	1.7401
P_{G56} (MW)	37.4630	P_{G112} (MW)	79.7727	V_{61}	0.9956	V_{116}	1.0053	$L_{\max}$	0.0506
P_{G59} (MW)	167.2125	P_{G113} (MW)	55.7530	V_{62}	0.9975	T_{8-5}	0.9806		
P_{G61} (MW)	73.5977	P_{G116} (MW)	30.6073	V_{65}	1.0053	T_{26-25}	0.9614		
P_{G62} (MW)	69.7190	V_1 (p.u.)	0.9567	V_{66}	1.0500	T_{30-17}	0.9608		
P_{G65} (MW)	394.8187	V_4 (p.u.)	0.9984	V_{69}	1.0350	T_{38-37}	0.9367		

Table 8.34: Comparison of performance for $L_{\max}$ minimization of IEEE 118 bus system

Techniques	Best $L_{\max}$	Average $L_{\max}$	Worst $L_{\max}$	CPU time (S)
QODE	0.0506	0.0507	0.0510	288.8312
DE	0.0587	0.0591	0.0593	287.0318

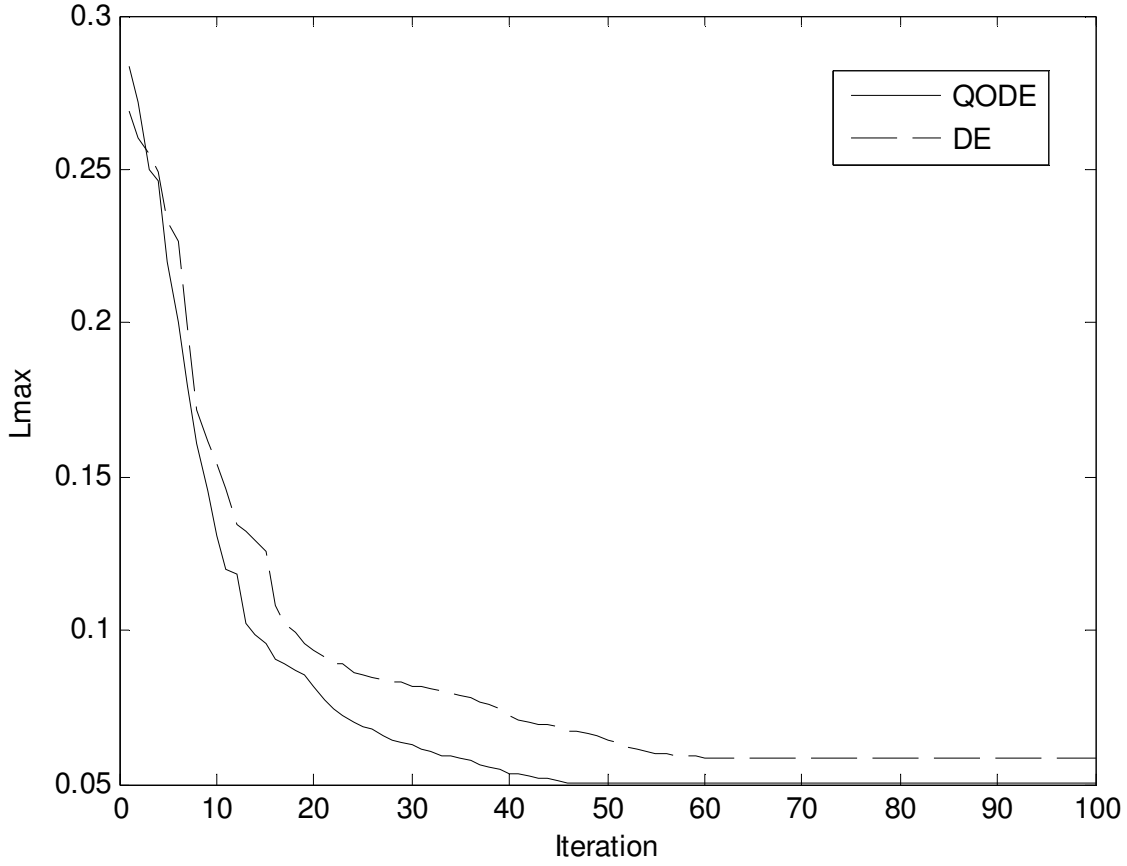

Fig. 8.24. $L_{\max}$ convergence characteristics for IEEE 118 bus system

8.6.3.4.Improvement of voltage profile

In this case, the proposed QODE and DE approach are applied for improvement of voltage profile. Here, the population size (N_P), scaling factor(S_F), crossover rate (C_R) and the maximum iteration number (N_{max}) have been selected as 200, 1.0, 1.0 and 100 respectively for this test system. The optimal values of control variables obtained from the proposed QODE are given in Table 8.35. The best, average and worst voltage deviation and average CPU time among 50 runs of solutions obtained from proposed QODE and DE are summarized in Table 8.36. The convergence characteristic obtained from proposed QODE and DE for voltage deviation is shown in Fig. 8.25.

Table 8.35: Optimal value of control variables obtained from QODE for IEEE 118 bus system for improvement of voltage profile

Variable		Variable		Variable		Variable		Variable	
P_{G1} (MW)	24.8354	P_{G66} (MW)	386.8658	V_6	0.9908	V_{70}	0.9855	T_{63-59}	0.9593
P_{G4} (MW)	27.3774	P_{G69} (MW)	431.2400	V_8	1.0155	V_{72}	0.9803	T_{64-61}	0.9845
P_{G6} (MW)	7.4553	P_{G70} (MW)	47.0490	V_{10}	1.0500	V_{73}	0.9911	T_{65-66}	0.9348
P_{G8} (MW)	23.1324	P_{G72} (MW)	27.1003	V_{12}	0.9912	V_{74}	0.9664	T_{68-69}	0.9346
P_{G10} (MW)	406.4214	P_{G73} (MW)	14.1555	V_{15}	0.9697	V_{76}	0.9435	T_{81-82}	0.9357
P_{G12} (MW)	188.1378	P_{G74} (MW)	19.9808	V_{18}	0.9734	V_{77}	1.0077	Q_{c5} (Mvar)	-10.2461
P_{G15} (MW)	14.8522	P_{G76} (MW)	69.3648	V_{19}	0.9647	V_{80}	1.0402	Q_{c34} (Mvar)	0
P_{G18} (MW)	36.5888	P_{G77} (MW)	87.9338	V_{24}	0.9924	V_{85}	0.9568	Q_{c37} (Mvar)	-15.0288
P_{G19} (MW)	19.6471	P_{G80} (MW)	220.4790	V_{25}	1.0500	V_{87}	1.0154	Q_{c44} (Mvar)	7.9582
P_{G24} (MW)	6.0058	P_{G85} (MW)	26.1360	V_{26}	1.0147	V_{89}	1.0047	Q_{c45} (Mvar)	1.7116
P_{G25} (MW)	240.1806	P_{G87} (MW)	53.1162	V_{27}	0.9685	V_{90}	0.9855	Q_{c46} (Mvar)	-33.5173
P_{G26} (MW)	301.7679	P_{G89} (MW)	173.7364	V_{31}	0.9678	V_{91}	0.9806	Q_{c48} (Mvar)	7.6346
P_{G27} (MW)	12.2519	P_{G90} (MW)	17.8891	V_{32}	0.9676	V_{92}	0.9838	Q_{c74} (Mvar)	0
P_{G31} (MW)	22.1487	P_{G91} (MW)	22.0689	V_{34}	0.9818	V_{99}	1.0106	Q_{c79} (Mvar)	19.3213
P_{G32} (MW)	56.7973	P_{G92} (MW)	242.4305	V_{36}	0.9754	V_{100}	0.9717	Q_{c82} (Mvar)	33.4421
P_{G34} (MW)	14.9005	P_{G99} (MW)	172.2366	V_{40}	0.9705	V_{103}	0.9556	Q_{c83} (Mvar)	13.4003
P_{G36} (MW)	44.6387	P_{G100} (MW)	111.5876	V_{42}	0.9853	V_{104}	0.9413	Q_{c105} (Mvar)	0
P_{G40} (MW)	21.6357	P_{G103} (MW)	11.6736	V_{46}	1.0055	V_{105}	0.9452	Q_{c107} (Mvar)	-12.4021
P_{G42} (MW)	15.6677	P_{G104} (MW)	77.6202	V_{49}	1.0251	V_{107}	0.9525	Q_{c110} (Mvar)	7.4332
P_{G46} (MW)	80.0593	P_{G105} (MW)	60.1407	V_{54}	0.9558	V_{110}	0.9587	Cost ($/h)	70904.50
P_{G49} (MW)	179.8429	P_{G107} (MW)	12.8669	V_{55}	0.9517	V_{111}	0.9805	Emission (lb/h)	451.7620
P_{G54} (MW)	50.4990	P_{G110} (MW)	40.6254	V_{56}	0.9548	V_{112}	0.9755	power loss (MW)	110.3291

P_{G55}(MW)	32.2701	P_{G111}(MW)	68.1610	V_{59}	0.9855	V_{113}	0.9934	voltage deviation (p.u.)	1.5955
P_{G56}(MW)	39.2898	P_{G112}(MW)	78.7837	V_{61}	0.9951	V_{116}	1.0053	L_{max}	0.0894
P_{G59}(MW)	92.3657	P_{G113}(MW)	43.0954	V_{62}	0.9973	T_{8-5}	0.9805		
P_{G61}(MW)	142.8751	P_{G116}(MW)	31.0410	V_{65}	1.0054	T_{26-25}	0.9616		
P_{G62} (MW)	81.2074	V_1 (p.u.)	0.9566	V_{66}	1.0500	T_{30-17}	0.9625		
P_{G65}(MW)	395.0630	V_4 (p.u.)	0.9984	V_{69}	1.0350	T_{38-37}	0.9369		

Table 8.36: Comparison of performance for voltage deviation of IEEE 118 bus system

Techniques	Best voltage deviation	Average voltage deviation	Worst voltage deviation	CPU time (S)
QODE	1.5955	1.5957	1.5961	287.3169
DE	1.6317	1.6320	1.6323	285.3158

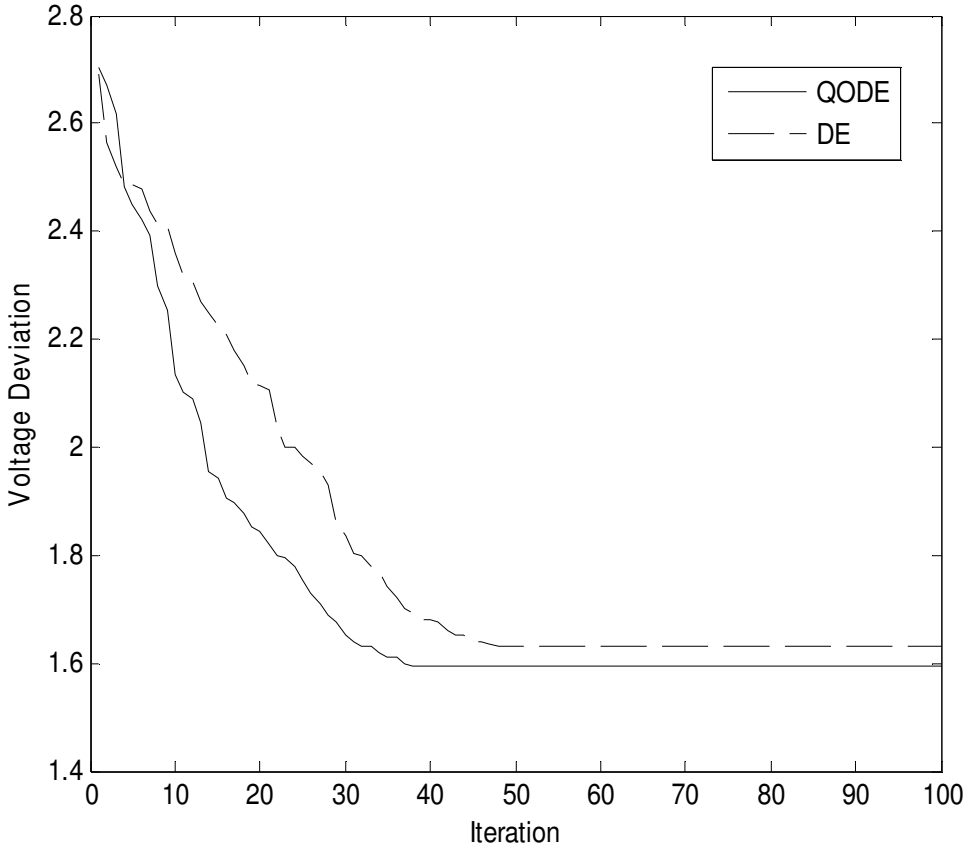

Fig. 8.25. Voltage deviation convergence characteristics for IEEE 118 bus system

8.6.3.5.Minimization of fuel cost and emission

The value of ψ in this case is chosen as 1000. The problem is solved by using QODE. Here, the population size (N_P), scaling factor (S_F), crossover rate (C_R) and the maximum iteration number (N_{max}) have been selected as 200, 1.0, 1.0 and 100 respectively for this test system. The results obtained from proposed QODE for optimal values of control variables are shown in Table 8.37.

Table 8.37: Optimal value of control variables obtained from QODE for IEEE 118 bus system for fuel cost and emission minimization

Variable		Variable		Variable		Variable		Variable	
P_{G1} (MW)	24.4411	P_{G66} (MW)	390.2885	V_6	0.9907	V_{70}	0.9855	T_{63-59}	0.9596
P_{G4} (MW)	29.9011	P_{G69} (MW)	32.8835	V_8	1.0151	V_{72}	0.9803	T_{64-61}	0.9847
P_{G6} (MW)	23.7663	P_{G70} (MW)	0	V_{10}	1.0500	V_{73}	0.9906	T_{65-66}	0.9349
P_{G8} (MW)	11.8135	P_{G72} (MW)	11.1104	V_{12}	0.9904	V_{74}	0.9664	T_{68-69}	0.9344
P_{G10} (MW)	466.7529	P_{G73} (MW)	17.1720	V_{15}	0.9698	V_{76}	0.9433	T_{81-82}	0.9356
P_{G12} (MW)	290.7476	P_{G74} (MW)	0	V_{18}	0.9735	V_{77}	1.0072	Q_{c5} (Mvar)	-39.4989
P_{G15} (MW)	15.4058	P_{G76} (MW)	0	V_{19}	0.9646	V_{80}	1.0401	Q_{c34} (Mvar)	1.1773
P_{G18} (MW)	59.9337	P_{G77} (MW)	91.2272	V_{24}	0.9921	V_{85}	0.9563	Q_{c37} (Mvar)	-13.2530
P_{G19} (MW)	0	P_{G80} (MW)	294.2445	V_{25}	1.0500	V_{87}	1.0152	Q_{c44} (Mvar)	4.9713
P_{G24} (MW)	6.1776	P_{G85} (MW)	0	V_{26}	1.0153	V_{89}	1.0055	Q_{c45} (Mvar)	4.0560
P_{G25} (MW)	111.4086	P_{G87} (MW)	179.6139	V_{27}	0.9682	V_{90}	0.9851	Q_{c46} (Mvar)	-25.9087
P_{G26} (MW)	250.1633	P_{G89} (MW)	239.7910	V_{31}	0.9671	V_{91}	0.9804	Q_{c48} (Mvar)	4.8949
P_{G27} (MW)	14.4614	P_{G90} (MW)	12.0063	V_{32}	0.9677	V_{92}	0.9836	Q_{c74} (Mvar)	5.3109
P_{G31} (MW)	9.3482	P_{G91} (MW)	25.9256	V_{34}	0.9815	V_{99}	1.0103	Q_{c79} (Mvar)	3.3505
P_{G32} (MW)	0	P_{G92} (MW)	0	V_{36}	0.9753	V_{100}	0.9705	Q_{c82} (Mvar)	38.2120
P_{G34} (MW)	0	P_{G99} (MW)	161.6689	V_{40}	0.9701	V_{103}	0.955	Q_{c83} (Mvar)	14.2517
P_{G36} (MW)	40.7704	P_{G100} (MW)	180.0080	V_{42}	0.9855	V_{104}	0.940	Q_{c105} (Mvar)	12.2687

P_{G40} (MW)	11.3385	P_{G103} (MW)	0	V_{46}	1.0053	V_{105}	0.9446	Q_{c107} (Mva)	-9.8406
P_{G42} (MW)	28.1754	P_{G104} (MW)	0	V_{49}	1.0252	V_{107}	0.952	Q_{c110} (Mvar)	9.3443
P_{G46} (MW)	57.7918	P_{G105} (MW)	0	V_{54}	0.9554	V_{110}	0.9583	Cost ($/h)	69167.10
P_{G49} (MW)	115.0737	P_{G107} (MW)	18.4037	V_{55}	0.9517	V_{111}	0.9804	Emission (lb\h)	323.6974
P_{G54} (MW)	165.7851	P_{G110} (MW)	25.2177	V_{56}	0.9546	V_{112}	0.9754	power loss (MW)	100.2088
P_{G55} (MW)	0	P_{G111} (MW)	54.6984	V_{59}	0.9853	V_{113}	0.9933	voltage deviation(p.u.)	1.7728
P_{G56} (MW)	0	P_{G112} (MW)	47.0741	V_{61}	0.9955	V_{116}	1.0052	$L_{\max}$	0.1054
P_{G59} (MW)	149.3231	P_{G113} (MW)	85.2145	V_{62}	0.9971	T_{8-5}	0.9806		
P_{G61} (MW)	180.2244	P_{G116} (MW)	32.0288	V_{65}	1.0053	T_{26-25}	0.9604		
P_{G62} (MW)	88.3819	V_1 (p.u.)	0.9563	V_{66}	1.0500	T_{30-17}	0.9617		
P_{G65} (MW)	383.6734	V_4 (p.u.)	0.9981	V_{69}	1.0350	T_{38-37}	0.9365		

8.6.3.6. Minimization of fuel cost, emission and voltage deviation and enhancement of voltage stability

The value of ψ, ρ and σ in this case are chosen as 1000, 10000 and 100000 respectively. The problem is solved by using QODE. Here, the population size (N_P), scaling factor(S_F), crossover rate (C_R) and the maximum iteration number (N_{max}) have been selected as 200, 1.0, 1.0 and 100 respectively for this test system. The results obtained from proposed QODE for optimal values of control variables are shown in Table 8.38.

Table 8.38: Optimal value of control variables obtained from QODE for IEEE 118 bus system for minimization of fuel cost, emission and voltage deviation and enhancement of voltage stability

Variable		Variable		Variable		Variable		Variable	
P_{G1} (MW)	23.0088	P_{G66} (MW)	395.1631	V_6	0.9905	V_{70}	0.9855	T_{63-59}	0.9594
P_{G4} (MW)	6.9193	P_{G69} (MW)	206.0957	V_8	1.0153	V_{72}	0.9803	T_{64-61}	0.9849
P_{G6} (MW)	24.4549	P_{G70} (MW)	79.2383	V_{10}	1.0500	V_{73}	0.9911	T_{65-66}	0.9346
P_{G8} (MW)	5.2956	P_{G72} (MW)	23.8707	V_{12}	0.990	V_{74}	0.9663	T_{68-69}	0.9343
P_{G10} (MW)	437.1753	P_{G73} (MW)	18.7049	V_{15}	0.9693	V_{76}	0.9427	T_{81-82}	0.9355
P_{G12} (MW)	294.6273	P_{G74} (MW)	10.5942	V_{18}	0.9727	V_{77}	1.0072	Q_{c5} (Mvar)	-8.0943
P_{G15} (MW)	27.5509	P_{G76} (MW)	93.1198	V_{19}	0.9645	V_{80}	1.0405	Q_{c34} (Mvar)	0
P_{G18} (MW)	76.3999	P_{G77} (MW)	44.3106	V_{24}	0.9916	V_{85}	0.9563	Q_{c37} (Mvar)	-1.2401
P_{G19} (MW)	18.8869	P_{G80} (MW)	263.0722	V_{25}	1.0500	V_{87}	1.0154	Q_{c44} (Mvar)	5.6484
P_{G24} (MW)	28.5297	P_{G85} (MW)	17.4067	V_{26}	1.0147	V_{89}	1.0052	Q_{c45} (Mvar)	4.3767
P_{G25} (MW)	114.7655	P_{G87} (MW)	103.1024	V_{27}	0.9684	V_{90}	0.9853	Q_{c46} (Mvar)	-20.6662
P_{G26} (MW)	253.3012	P_{G89} (MW)	157.3679	V_{31}	0.9673	V_{91}	0.9804	Q_{c48} (Mvar)	11.6488
P_{G27} (MW)	16.7096	P_{G90} (MW)	8.8590	V_{32}	0.9677	V_{92}	0.9833	Q_{c74} (Mvar)	0
P_{G31} (MW)	9.3482	P_{G91} (MW)	25.9256	V_{34}	0.9815	V_{99}	1.0103	Q_{c79} (Mvar)	3.3505
P_{G32} (MW)	27.5363	P_{G92} (MW)	234.1465	V_{36}	0.9751	V_{100}	0.9706	Q_{c82} (Mvar)	57.0130
P_{G34} (MW)	14.7008	P_{G99} (MW)	193.7836	V_{40}	0.9704	V_{103}	0.9558	Q_{c83} (Mvar)	4.9391
P_{G36} (MW)	54.1406	P_{G100} (MW)	206.1550	V_{42}	0.9853	V_{104}	0.9409	Q_{c105} (Mvar)	0
P_{G40} (MW)	18.3070	P_{G103} (MW)	17.3832	V_{46}	1.0047	V_{105}	0.9445	Q_{c107} (Mvar)	11.7700
P_{G42} (MW)	8.0693	P_{G104} (MW)	30.4592	V_{49}	1.0253	V_{107}	0.9523	Q_{c110} (Mvar)	2.1827
P_{G46} (MW)	34.7227	P_{G105} (MW)	74.3720	V_{54}	0.9554	V_{110}	0.9587	Cost ($/h)	69709.99
P_{G49} (MW)	190.5395	P_{G107} (MW)	10.6044	V_{55}	0.9516	V_{111}	0.9801	Emission (lb/h)	354.4841

P_{G54}(MW)	178.0808	P_{G110}(MW)	32.6684	V_{56}	0.9544	V_{112}	0.9753	power loss (MW)	117.1778
P_{G55}(MW)	32.0726	P_{G111}(MW)	50.3478	V_{59}	0.9853	V_{113}	0.9935	voltage deviation (p.u.)	1.6489
P_{G56}(MW)	94.9690	P_{G112}(MW)	66.0932	V_{61}	0.9955	V_{116}	1.0053	L_{max}	0.0666
P_{G59}(MW)	135.2936	P_{G113}(MW)	57.0389	V_{62}	0.9976	T_{8-5}	0.9817		
P_{G61}(MW)	127.9625	P_{G116}(MW)	30.5116	V_{65}	1.0053	T_{26-25}	0.9605		
P_{G62} (MW)	57.9078	V_1 (p.u.)	0.9561	V_{66}	1.0500	T_{30-17}	0.9609		
P_{G65}(MW)	387.0729	V_4 (p.u.)	0.9976	V_{69}	1.0350	T_{38-37}	0.9365		

8.7. Conclusion

Here, HTS algorithm has been successfully applied to solve optimal power flow problems. The optimal power flow problem is formulated as a nonlinear optimization problem with equality and inequality constraints of power system. In this study, different objective functions such as fuel cost minimization, emission minimization, improvement of voltage profile and enhancement of voltage stability are considered. The proposed HTS algorithm is tested on IEEE 30-bus, 57-bus and 118-bus test systems to demonstrate its effectiveness.

Also QODE is demonstrated and successfully applied to solve single-objective and multi-objective optimal power flow problems. The optimal power flow problem is formulated as a nonlinear optimization problem with equality and inequality constraints of power system. In this study, different single objective functions such as fuel cost minimization, emission minimization and improvement of voltage profile and enhancement of voltage stability and multi-objective functions such as minimization of fuel cost, emission and minimization of fuel cost, emission, voltage deviation and enhancement of voltage stability are considered. The proposed QODE approach is tested on IEEE 30-bus, 57-bus and 118-bus test systems to demonstrate its effectiveness. The results obtained from proposed QODE approach is better than the results obtained from other evolutionary methods reported in the literature.

CHAPTER-9

Conclusion & Future Scope

(a) Overall Conclusion

In this thesis intelligent techniques like differential evolution, opposition based differential evolution, quasi-oppositional differential evolution, evolutionary algorithm, genetic algorithm, improved real coded genetic algorithm, simulated annealing, teaching-learning based optimization, modified teaching-learning based optimization, heat transfer search algorithm, meta-heuristic techniques have been applied to solve different complex power system optimization problems such as multi area economic dispatch, dynamic economic dispatch, reactive power dispatch, combined heat and power economic dispatch, short-term hydrothermal scheduling problem of fixed head and variable head hydrothermal power systems. Results obtained from all the techniques were compared with the results obtained from other computational intelligent technique from the literature. It has been found that here the results are competitive and quite encouraging.

Chapter wise conclusion has been presented below.

Chapter-2

Here, four different metaheuristic techniques viz., differential evolution, evolutionary programming, real coded genetic algorithm and simulated annealing technique for multi-area economic dispatch problem considering transmission losses, multiple fuels, valve-point loading and prohibited operating zones with respect to minimum cost and CPU time. Differential evolution achieves the lowest minimum cost and SA requires least CPU time amongst the four metaheuristic techniques.

Chapter-3

Here, improved real coded genetic algorithm (IRCGA) has been developed and pertained for solving dynamic economic dispatch problem with non-smooth fuel cost function and 15

benchmark functions. Test results have been matched up to those acquired from real coded genetic algorithm. It has been observed from the comparison that the developed improved real coded genetic algorithm has the capability to offer superior solution and quick convergence. Due to these properties, improved real coded genetic algorithm can be utilized for solving complicated power system problems.

Chapter -4

Modified teaching-learning-based optimization (MTLBO) has been developed and pertained to solve three different complex combined heat and power economic dispatch test systems and 15 benchmark functions. Test results acquired from three different complex combined heat and power economic dispatch problems have been compared with those acquired by other evolutionary techniques suggested in the literature.

Heat transfer search (HTS) algorithm has been pertained to solve four different complex combined heat and power economic dispatch test systems. Test results have been matched up to those acquired by other evolutionary techniques suggested in the literature. The results obtained using the proposed algorithm is compared with the results of other optimization algorithm.

Chapter -5

Here, opposition-based differential evolution is demonstrated and presented to solve the hydrothermal scheduling problem. The proposed opposition-based differential evolution method has been successfully applied to two test problems, two fixed head hydrothermal test systems. The results have been compared with those obtained by other evolutionary algorithms reported in the literature. It is seen from the comparisons that the proposed opposition-based differential evolution method performs better than other evolutionary algorithms in the literature.

Chapter -6

In this chapter, opposition-based differential evolution is demonstrated and presented to solve the hydrothermal scheduling problem. The proposed opposition-based differential evolution method has been successfully applied to two fixed head hydrothermal test systems and three hydrothermal multi-reservoir cascaded hydroelectric test systems having prohibited operating zones and thermal units with valve point loading. The results have been compared with those obtained by other evolutionary algorithms reported in the literature. It is seen from the

comparisons that the proposed opposition-based differential evolution method performs better than other evolutionary algorithms in the literature.

Chapter-7

Improved real coded genetic algorithm (IRCGA) has been developed and validated for solving different types of reactive power dispatch (RPD) problems such as minimization of active power transmission loss and improvement of voltage profile and stability. The developed IRCGA is experimented on IEEE 30-bus, 57-bus and 118-bus test systems to reveal its efficacy. It has been examined that test results acquired from the developed IRCGA is superior compared to those acquired from other stated evolutionary techniques.

Chapter -8

Here, heat transfer search (HTS) algorithm has been successfully applied to solve optimal power flow problems. The optimal power flow problem is formulated as a nonlinear optimization problem with equality and inequality constraints of power system. In this study, different objective functions such as fuel cost minimization, emission minimization, improvement of voltage profile and enhancement of voltage stability are considered. The performance of the proposed algorithm has been assessed on IEEE 30-bus, 57-bus and 118-bus test systems to demonstrate its effectiveness.

Also quasi-oppositional differential evolution (QODE) is demonstrated and successfully applied to solve single-objective and multi-objective optimal power flow problems. The optimal power flow problem is formulated as a nonlinear optimization problem with equality and inequality constraints of power system. In this study, different single objective functions such as fuel cost minimization, emission minimization and improvement of voltage profile and enhancement of voltage stability and multi-objective functions such as minimization of fuel cost, emission and minimization of fuel cost, emission, voltage deviation and enhancement of voltage stability are considered. The proposed QODE approach is tested on IEEE 30-bus, 57-bus and 118-bus test systems to demonstrate its effectiveness. The results obtained from proposed QODE approach is better than the results obtained from other evolutionary methods reported in the literature.

(b) Future Scope

Metaheuristic techniques for multi area economic dispatch (MAED) are applied to 2 area, 3 area and 4 area system. Future work can be carried out with other optimization technique for multi-area system and compare the result with metaheuristic method.

Improved real coded genetic algorithm (IRCGA) has been developed and pertained for solving dynamic economic dispatch problem with non-smooth fuel cost function and 15 benchmark functions. Further study can be carried out with other intelligent control method and compare the result with IRCGA.

Here, HTS and TLBO methods are applied in CHEPD problems. Further study can be carried out with other intelligent control method and compare with this method.

Opposition-based differential evolution is presented to solve the hydrothermal scheduling problem and has been successfully applied to two test problems, two fixed head hydrothermal test systems. Further work can be carried out on more test systems and compare with the cost value.

IRCGA has been developed and validated for solving different types of RPD problems such as minimization of active power transmission loss and improvement of voltage profile and voltage stability have been assessed by testing on IEEE 30-bus, 57-bus and 118-bus test systems to reveal its efficacy. Future work can be carried out on more test bus system and check the voltage deviation with this.

HTS and QODE algorithm has been successfully applied to solve optimal power flow problems tested on IEEE 30-bus, 57-bus and 118-bus test systems to demonstrate its effectiveness. Future work can be carried out on more test bus system and check the fuel cost minimization, emission minimization and improvement of voltage profile.

CHAPTER-10

References

[1] L. J. Fogel, A. J. Owens, M. J. Walsh, “Artificial Intelligence Through simulated Evolution”, John Wiley, 1966.

[2] J. H. Holland, “Adaptation in Natural and Artificial Systems”, Ann Arbor: University of Michigan Press, 1975.

[3] D. E. Goldberg, “Genetic Algorithms in Search, Optimization, and Machine Learning, Addison-Wesley, 1989.

[4] D. B. Fogel, Evolutionary Computation: towards a new philosophy of machine intelligence. IEEE Press, New York, NY, 1995.

[5] K. V. Price, R. Storn and J. Lampinen. Differential Evolution: A Practical Approach to Global Optimization. Springer-Verlag, Berlin, 2005.

[6] S. Kirkpatrick, C. Gelatt, and M. Vecchi, “Optimization by simulated annealing,” Science, vol. 22, pp. 671–680, 1983.

[7] R. R. Shoults, S. K. Chang, S. Helmick and W. M. Grady, “A practical approach to unit commitment, economic dispatch and savings allocation for multiple-area pool operation with import/export constraints”, IEEE Trans Power Apparatus Syst. Vol. 99, no. 2, pp. 625-635, 1980.

[8] R. Romano, V. H. Quintana, R. Lopez and V. Valadez, “Constrained economic dispatch of multi-area systems using the Dantzig–Wolfe decomposition principle”, IEEE Trans. Power Apparatus Syst., vol. 100, no. 4, pp. 2127-2137, 1981.

[9] A. L. Desell, E. C. McClelland, K. Tammar and P. R.Van Horne, “Transmission constrained production cost analysis in power system planning”, IEEE Trans Power Apparatus Syst., vol. 103, no. 8, pp. 2192-2198, 1984.

[10] S. D. Helmick and R. R. Shoults, “A practical approach to an interim multi-area economic dispatch using limited computer resources”, IEEE Trans Power Apparatus Syst., vol. 104, no. 6, pp. 1400-1404, 1985.

[11] C. Wang and S. M. Shahidehpour, “A decomposition approach to non-linear multi area generation scheduling with tie-line constraints using expert systems”, IEEE Trans Power Syst., vol. 7, no. 4, pp. 1409-1418, 1992.

[12] D. Streiffert, “Multi-area economic dispatch with tie line constraints”, IEEE Trans. Power Syst. Vol. 10, no. 4, pp. 1946-1951, 1995.

[13] J. Wernerus and L. Soder, “Area price based multi-area economic dispatch with tie line losses and constraints”, In: IEEE/KTH Stockholm power tech conference, Sweden,. pp. 710–715, 1995.

[14] T. Yalcinoz and M. J. Short, “Neural networks approach for solving economic dispatch problem with transmission capacity constraints”, IEEE Trans Power Syst., vol. 13, no. 2, pp. 307-313, 1998.

[15] T. Jayabarathi, G. Sadasivam and V. Ramachandran, “Evolutionary programming based multi-area economic dispatch with tie line constraints”, Electric Machine and Power System, vol. 28, pp. 1165-1176, 2000.

[16] C. L. Chen, N. Chen, “Direct Search Method for solving Economic Dispatch Problem Considering Transmission Capacity Constraints”, IEEE Trans. Power Syst., Vol. 16, no. 4, pp. 764-769, Nov. 2001.

[17] C.-L. Chiang, “Improved genetic algorithm for power economic dispatch of units with valve-point effects and multiple fuels,” IEEE Trans. Power Syst., vol. 20, no. 4, pp. 1690–1699, Nov. 2005.

[18] H. T. Yang, P. C. Yang and C. L. Huang, “Evolutionary Programming based economic dispatch for units with non-smooth fuel cost functions”, IEEE Trans. on PWRS, Vol. 11, No. 1, February 1996, pp. 112-118.

[19] Z-L Gaing, “Particle Swarm Optimization to Solving the Economic Dispatch Considering the Generator Constraints”, IEEE Transactions on Power Systems, vol. 18, no.3, pp. 1187-1195, August 2003.

[20] K. P. Wong, C. C. Fung, “Simulated annealing based economic dispatch algorithm”, IEE Proceedings Generation Transmission and Distribution, vol. 140, No. 6, pp. 509-515, 1993.

[21] N. Sinha, R. Chakrabarti, and P. K. Chattopadhyay, "Evolutionary programming techniques for economic load dispatch", IEEE Trans. Evol. Comput., vol. 7, no. 1, pp. 83–94, Feb. 2003.

[22] D. C. Walter, G. B. Sheble, "Genetic algorithm solution of economic dispatch with valve point loading", IEEE Transactions on Power Systems, vol.8, no. 3, pp. 1325-1332, August 1993.

[23] D. W. Ross, S. Kim, "Dynamic Economic Dispatch of Generation", IEEE Transactions on Power Apparatus and Systems, vol. PAS-99, no. 6, pp. 2060-2068, 1980.

[24] P. P. J. Van Den Bosch, "Optimal Dynamic Dispatch owing to Spinning-Reserve and Power-Rate Limits", IEEE Transactions on Power Apparatus and Systems, vol. PAS-104, no. 12, pp. 3395-3401, 1985.

[25] G. P. Granelli, P. Marannino, M. Montagna and A. Silvestri, "Fast and efficient gradient projection algorithm for dynamic generation dispatching", IEE Proceedings Generation Transmission and Distribution, 1989, vol. 136, no. 5, pp. 295-302.

[26] K. S. Hindi and M.R. Ab Ghani, "Dynamic economic dispatch for large scale power systems; a Lagrangian relaxation approach", Electric Power System Research, vol.13, no. 1, 1991, pp. 51-56.

[27] D. L. Travers, R. J. Kaye, "Dynamic Dispatch by constructive Dynamic programming", IEEE Transactions on Power Systems, vol. 13, no. 1, pp. 72-78, February 1998.

[28] X. S. Han, H. B. Gooi and D. S. Kirschen, "Dynamic Economic Dispatch: Feasible and Optimal Solutions", IEEE Transactions on Power Systems, vol. 16, no. 1, pp. 22-28, February 2001.

[29] X. Yao, Y. Liu and G. Lin, "Evolutionary programming made faster", IEEE Trans. on Evol. Comput., vol. 3, pp. 82-102, 1999

[30] C, K. Panigrahi, P. K. Chattopadhyay, R. N. Chakrabatri, M. Basu, "Simulated annealing technique for dynamic economic dispatch", Electr. Power Comp. Syst. 2006; 34(5):577-586.

[31] P. Saravuth, N. Issarachai, K. Waree, "Application of multiple tabu search algorithm to solve dynamic economic dispatch considering generator constraints", Energy Conversion and Management 9 (4) (2007) 506–516.

[32] Y. L. Lu, J. Z. Zhou, Q. Hui, Y. Wang, Y. C. Zhang, "Chaotic differential evolution methods for dynamic economic dispatch with valve-point effects", Engineering Applications of Artificial Intelligence 4 (4) (2011) 378–387.

[33] R. Arul, G. Ravi, S. Velusami, "Chaotic self-adaptive differential harmony search algorithm based dynamic economic dispatch", Int J Electr Power Energy Syst 2013;50:85–96.

[34] B. K. Panigrahi, V. Ravikumar Pandi, S. Das, "Adaptive particle swarm optimization approach for static and dynamic economic load dispatch", Energy Conversion and Management 9 (6) (2008) 1407–1415.

[35] X. H. Yuan, L. Wang, Y. Zhang, Y. B. Yuan, "A hybrid differential evolution method for dynamic economic dispatch with valve-point effects", Expert Systems with Applications 6 (2) (2009) 4042–4048.

[36] K. Deb and R. B. Agrawal, "Simulated binary crossover for continuous search space", Complex Systems, vol. 9, no. 2, pp. 115-148, 1995.

[37] F. Herrera, M. Lozano, and J. L. Verdegay, "Tackling real-coded genetic algorithms: Operators and tools for behavioral analysis", Artif. Intell. Rev., vol.12, no. 4, pp. 265-319, 1998

[38] F. J. Rooijers, R.A.M. van Amerongen, "Static economic dispatch for co-generation systems", IEEE Transactions on Power Systems 9 (3) (1994) 1392-1398.

[39] Tao Guo, M.I. Henwood, M. van Ooijen, An algorithm for heat and power dispatch, IEEE Transactions on Power Systems 11 (4) (1996) 1778-/1784.

[40] A. M. Jubril, A. O. Adediji, O. A. Olaniyan, "Solving the combined heat and power dispatch problem: A semi-definite programming approach", Electric Power Components and Systems, Volume 40, 2012, pp. 1362 - 1376.

[41] Y. H. Song, C. S. Chou, T. J. Stonham, "Combined heat and power dispatch by improved ant colony search algorithm", Electric Power System Research (52) (1999) 115-121.

[42] K. P. Wong, C. Algie, "Evolutionary programming approach for combined heat and power dispatch", Electric Power Systems Research (61) (2002) 227–232.

[43] C. T. Su, C. L. Chiang, "An incorporated algorithm for combined heat and power economic dispatch", Electric Power System Research 2004, 69 (2-3) 187-195.

[44] A. Vasebi, M. Fesanghary, S. M. T. Bathaee, “Combined heat and power economic dispatch by harmony search algorithm”, Electric Power and Energy Systems, (29) (2007) 713–719.

[45] H. Karami, M. J. Sanjari, A, Tavakoli, G. B. Gharehpetian, “Optimal scheduling of residential energy system including combined heat and power system and storage device”, Electric Power Components and Systems, Volume 41, 2013, pp. 765 – 781.

[46] L. Wang, C. Singh, “Stochastic combined heat and power dispatch based on multi-objective particle swarm optimization”, Electric Power and Energy Systems (30) (2008) 226–234.

[47] P. Subbaraj, R. Rengaraj, S. Salivahanan, “Enhancement of combined heat and power economic dispatch using self adaptive real-coded genetic algorithm”, Applied Energy 86 (2009) 915–921.

[48] V. Ramesh, T. Jayabaratchi, N. Shrivastava, A. Baska, “A novel selective particle swarm optimization approach for combined heat and power economic dispatch”, Electric Power Components and Systems 37 (2009) 1231–1240.

[49] S. S. Sadat Hosseini, A. Jafarnejad, A. H. Behrooz, A. H. Gandomi, “Combined heat and power economic dispatch by mesh adaptive direct search algorithm”, Expert Systems with Applications 38 (2011) 6556–6564.

[50] Behnam Mohammadi-Ivatloo, Mohammad Moradi-Dalvand and Abbas Rabiee, “Combined heat and power economic dispatch problem solution using particle swarm optimization with time varying acceleration coefficients”, Electric Power System Research 2013, 95 9-18.

[51] P. K. Roy, C. Paul and S. Sultana, “Oppositional teaching learning based optimization approach for combined heat and power dispatch”, Electric Power and Energy Systems, (57) (2014) 392–403.

[52] R. V. Rao, V. J. Savsani and D. P. Vakharia, “Teaching-learning-based optimization: A novel method for constrained mechanical design optimization problems”, Computer-Aided Design, 43 (3)(2011), pp. 303-315.

[53] R. V. Rao, V. J. Savsani and D. P. Vakharia, “Teaching-learning-based optimization: A novel optimization method for continuous non-linear large scale problems”, Information Sciences, 183 (1) (2012), pp.1-15.

[54] R.V. Rao, V. Patel, “An elitist teaching–learning-based optimization algorithm for solving complex constrained optimization problems”, International Journal of Industrial Engineering Computations, 3 (2012), pp. 535–560.

[55] M. S. Javadi, A. E. Nezhad, and S. Sabramooz," Economic heat and power dispatch in modern power system harmony search algorithm versus analytical solution", Scientia Iranica D, Vol. 19, no. 6, pp. 1820–1828. 2012.

[56] Y. H. Song, and Y. Q. Xuan, "Combined heat and power economic dispatch using genetic algorithm based penalty function method", Electr Mach Pow Syst, Vol.26, no.4, pp.363-372, 1998.

[57] M. Basu, "Combined heat and power economic dispatch using opposition-based group search optimization", International Journal of Electrical Power and Energy Systems, Vol. 73, pp. 819-829, Dec 2015.

[58] M. Basu, “Group search optimization for combined heat and power economic dispatch”, International Journal of Electrical Power & Energy Systems, Vol. 78, pp. 138–147, June 2016.

[59] T. T. Nguyen, D. N. Vo, and B. H. Dinh, "Cuckoo search algorithm for combined heat and power economic dispatch", International Journal of Electrical Power & Energy Systems, Vol. 81, pp. 204-214, Oct. 2016.

[60] N. Narang, E. Sharma, and J.S. Dhillon, "Combined heat and power economic dispatch using integrated civilized swarm optimization and Powell’s pattern search method", Applied Soft Computing, Vol. 52, pp. 190-202, Mar. 2017.

[61] V. K. Patel, and V. J. Savsani, “Heat transfer search (HTS): a novel optimization algorithm”, Information Sciences, Vol. 324, pp. 217–246, 2015.

[62] A. Pereira-Neto, C. Unsihuary, and O. R. Saavedra, “Efficient evolutionary strategy optimization procedure to solve the nonconvex economic dispatch problem with generator constraints”, IEE Proc. Gen., Trans., Distrib., vol. 152, No. 5, pp. 653-660, 2005.

[63] M.F. Zaghlool, F. C. Trutt, “Efficient methods for optimal scheduling of fixed head hydrothermal power systems”, IEEE Transactions on Power Systems, vol.3, no. 1, 1988.

[64] A. H. A. Rashid and K. M. Nor, “An efficient method for optimal scheduling of fixed head hydro and thermal plants”, IEEE Transactions on Power Systems, Vol. 6, No. 2, pp. 632-636, May 1991.

[65] O. Nilsson, D. Sjelvgren, “Mixed-integer programming applied to short-term planning of a hydro-thermal system”, Proceedings of the 1995, IEEE PICA, Salt Lake City, UT, USA, May 1995, pp. 158-163.

[66] L. Engles, R. E. Larson, J. Peschon, K. N. Stanton, “Dynamic programming applied to hydro and thermal generation scheduling”, IEEE tutorial course text, 76CH1107-2-PWR, IEEE, New York, 1976.

[67] K. P. Wong, Y. W. Wong, “Short-term hydrothermal scheduling part 1: simulated annealing approach”, IEE Proceedings Generation, Transmission and Distribution, 1994, Vol. 141, No.5, pp. 497-501.

[68] P. C. Yang, H. T. Yang, C. L. Huang, “Scheduling short-term hydrothermal generation using evolutionary Programming techniques”, IEE Proceedings Generation Transmission and Distribution, vol. 143, No. 4, July 1996, pp. 371-376.

[69] S. O. Orero, M. R. Irving, “A genetic algorithm modeling framework and solution technique for short term optimal hydrothermal scheduling”, IEEE Trans. on PWRS, Vol. 13, No. 2, May 1998.

[70] E. Gil, J. Bustos, H. Rudnick, “Short-term hydrothermal generation scheduling model using a genetic algorithm”, IEEE Trans. on PWRS, Vol. 18, No. 4, Nov. 2003, pp. 1256-1264.

[71] N. Sinha, R. Chakrabarti and P. K. Chattopadhyay, “Fast evolutionary programming techniques for short-term hydrothermal scheduling”, IEEE Trans. on PWRS, Vol. 18, No. 1, Feb. 2003, pp. 214-220.

[72] L. Lakshminarasimman, S. Subramanian, “Short-term scheduling of hydrothermal power system with cascaded reservoirs by using modified differential evolution”, IEE Proceedings – Generation, Transmission and Distribution, Volume 153, No. 6, November 2006, pp.693-700.

[73] X. Yuan, B. Cao, B. Yang, Y. Yuan, “Hydrothermal scheduling using chaotic hybrid differential evolution”, Energy Conversion and Management, 49 (12), pp. 3627–33, 2008.

[74] K. K. Mandal and N. Chakraborty, “Differential evolution technique-based short-term economic generation scheduling of hydrothermal systems”, Electric Power System Research, vol. 78, no. 11, pp. 1972-1979, November 2008.

[75] P. K. Hota, A. K. Barisal, R. Chakrabarti, “An improved PSO technique for short-term optimal hydrothermal scheduling”, Electric Power System Research, vol. 79, no. 7, pp. 1047-1053, July 2009.

[76] M. Basu, "Artificial immune system for fixed head hydrothermal power system", Energy 36 (2011) pp. 608-612.

[77] R. K. Swain, A. K. Barisal, P. K. Hota, R. Chakrabarti, “Short-term hydrothermal scheduling using clonal selection algorithm”, International Journal of Electric Power and Energy Systems, Vol-33, pp. 647–56, 2011.

[78] P. K. Roy, “Teaching learning based optimization for short-term hydrothermal scheduling problem considering valve point effect and prohibited discharge constraint”, International Journal of Electric Power and Energy Systems, Vol.-53, pp. 10-19, 2013.

[79] Jiangtao Jia, “Mixed-integer linear programming formulation for short-term scheduling of cascaded hydroelectric plants with pumped-storage units”, Electric Power Components and Systems, vol. 41, pp. 1456-1468, 2013.

[80] R. Storn, K. Price, “Minimizing the real functions of the ICEC’96 contest by differential evolution”, in Proc. 1996 IEEE Int. Conf. Evolutionary Computation, ICEC’96, 1996.

[81] R. Storn, K. Price, Differential evolution – A Simple and Efficient Adaptive Scheme for Global Optimization Over Continuous Spaces, Berkeley, CA, 1995,Tech. Rep.TR-95-012.

[82] R. Storn, K. V. Price, “Differential evolution- a simple and efficient heuristic for global optimization over continuous spaces”, Journal of Global Optimization 11 (4) (1997) 341-359.

[83] H. Wang, Y. Liu, S. Zeng, H. Li, C. Li, “Opposition-based particle swarm algorithm with Cauchy mutation”, IEEE Congress Evol. Comput. Singapore 2007, 4750–4756.

[84] H. R. Tizhoosh, “Opposition-based learning: a new scheme for machine intelligence”, In Proc int conf comput intell modeling control and autom, vol. 1, 2005, pp. 695-701.

[85] H. R. Tizhoosh, “Reinforcement learning based on actions and opposite actions”, In Proc. ICGST int conf artif intell mach learn, Cairo, Egypt, 2005.

[86] H. R. Tizhoosh, "Opposition-based reinforcement learning", J. Adv. Comput. Intell. Intelligent Inform 2006, 10(3), pp. 578-585.

[87] M. Ventresca, H. R. Tizhoosh, "Improving the convergence of back propagation by opposite transfer functions", In Proc IEEE world congr. comput. intell., Vancouver, BC, Canada, 2006, pp. 9527–9534.

[88] S. Rahnamayan, H. R. Tizhoosh, M. M. A. Salama, "Opposition-based differential evolution", IEEE Transactions on Evolutionary Computation, 12(1), 2008, pp.64–79.

[89] A. R. Malisia, Investigating the application of opposition-based ideas to ant algorithm, Master's thesis. Ontario, Canada: University of Waterloo, Waterloo, 2007.

[90] A. Chatterjee, S. P. Ghoshal, V. Mukherjee, "Solution of combined economic and emission dispatch problems of power systems by an opposition-based harmony search algorithm", International Journal of Electric Power and Energy Systems (39) (2012), pp. 9–20.

[91] K. Bhattacharjee, A. Bhattacharya, S. Halder nee Dey, "Oppositional real coded chemical reaction optimization for different economic dispatch problems", International Journal of Electric Power and Energy Systems (55) (2014), pp. 378–391.

[92] Michalewicz Z., "Genetic algorithms + data structures =evolution programs" (New York, 1999, 3rd edn.)

[93] H. Dommel , W. Tinny, "Optimal power flow solution", IEEE Trans. Power Appar. Syst., 1968, PAS-87, (10), pp. 1866-1876.

[94] J. A. Momoh, M. E. El-Hawary and R. Adapa, "A review of selected optimal power flow literature to 1993 part I & II", IEEE Trans Power Syst. 1999, 14(1), pp. 96–111.

[95] Lee, K., Park, Y., Ortiz, J., "A united approach to optimal real and reactive power dispatch", IEEE Trans. Power Appar. Syst., 1985, PAS-104, (5), pp. 1147-1153.

[96] V. H. Quintana and M. Santos-Nieto, "Reactive power-dispatch by successive quadratic programming", IEEE Trans. Energy Conver. 1989, 4(3), pp. 425-435.

[97] M. Basu, "Quasi-oppositional differential evolution for optimal reactive power dispatch", International Journal of Electrical Power & Energy Systems, Volume 78, June 2016, pp. 29-40.

[98] Q. H. Wu and J. T. Ma, “Power system optimal reactive power dispatch using evolutionary programming”, IEEE Trans Power Syst. 1995, 10(3), pp.1243–1249.

[99] M. Ghasemi, M. Taghizadeh, S. Ghavidel, J. Aghaei, A. Abbasian, "Solving optimal reactive power dispatch problem using a novel teaching–learning-based optimization algorithm", Engineering Applications of Artificial Intelligence 39 (2015), pp. 100–108

[100] J. G. Vlachogiannis and K. Y. Lee, “Quantum-inspired evolutionary algorithm for real and reactive power dispatch”, IEEE Trans Power Syst. 2008, 23(4), pp. 1627–1636.

[101] K. Mahadevan and P. S. Kannan, “Comprehensive learning particle swarm optimization for reactive power dispatch”, Applied Soft Computing 10 (2010), pp. 641-652.

[102] M. Ghasemi, M. M. Ghanbarian, S. Ghavidel, S. Rahmani, E. M. Moghaddam, "Modified teaching learning algorithm and double differential evolution algorithm for optimal reactive power dispatch problem: A comparative study", Information Sciences 278 (2014) pp. 231–249.

[103] IEEE Working Group: “Voltage stability of power systems: concepts, analytical tools and industry experience”, IEEE Special Publication 90TH0358-2-PWR, 1990.

[104] P. Kessel, H. Glavitsch, “Estimating the voltage stability of a power system”, IEEE Transaction on Power Delivery, 1986, 1 (3), pp. 346-354.

[105] N. Metropolis, A. W. Rosenbluth, M. N. Rosenbluth, A. H. Teller, and E. Teller, “Equations of state calculations by fast computing machines”, J. Chem. Phys., vol. 21, pp. 1087–1092, Jun. 1953.

[106] S. Rahnamayan, H. R. Tizhoosh and M. M. A. Salama, “Quasi Oppositional differential evolution”, In proceeding of IEEE congress on evolu. Comput. CEC 2007, 25th-28th September, 2007, pp. 2229-2236.

[107] J. Carpentier, “Contribution a l’Etude du Dispatching Economique”, Bulletin de la Societe Francaise des Electriciens, 1962, 3, pp. 431–474

[108] R. C. Burchett, H. H. Happ, D. R. Vierath, “Quadratically convergent optimal power flow”, IEEE Transaction on Power Apparatus and Systems, 1984, PAS-103, (11), pp. 3267–3276.

[109] D. I. Sun, B. Ashley, B. Brewer, A. Hughes, W. F. Tinney, “Optimal power flow by Newton approach”, IEEE Transaction on Power Apparatus and Systems, 1984, PAS-103, (10), pp. 2864–2875.

[110] R. Mota-Palomino, V. H. Quintana, “Sparse reactive power scheduling by a penalty-function linear programming technique”, IEEE Transaction on Power Systems, 1986, 1, (3), pp. 31–39.

[111] X. Yan, V. H. Quintana, “Improving an interior point based OPF by dynamic adjustments of step sizes and tolerances”, IEEE Transaction on Power Systems, 1999, 14, (2), pp.709–717.

[112] W. Yan, J. Yu, D. C. Yu, K. Bhattarai, “A new optimal reactive power flow model in rectangular form and its solution by predictor corrector primal dual interior point method”, IEEE Transaction on Power Systems, 2006, 21, (1), pp. 61–67.

[113] L. L. Lai, J. T. Ma, “Improved genetic algorithms for optimal power flow under both normal and contingent operation states”, Electric Power and Energy Systems, 1997, 19, (5), pp. 287–292.

[114] J. Yuryevich, K. P. Wong, “Evolutionary programming based optimal power flow algorithm”, IEEE Transaction on Power Systems, 1999, 14, (4), pp. 1245–1250.

[115] T. Niknam, M. R. Narimani, J. Aghaei, R. Azizipanah-Abarghooee, “Improved particle swarm optimization for multi-objective optimal power flow considering cost, loss, emission and voltage stability index”, IET Generation Transmission Distribution 2012, vol. 6, pp. 515-527.

[116] C. A. Roa-Sepulveda, B. J. Pavez-Lazo, “A solution to the optimal power flow using simulated annealing”, Electric Power and Energy Systems, 2003, 25, (1), pp. 47–57.

[117] A. A. Abou El Ela, M. A. Abido, S. R. Spea, “Optimal power flow using differential evolution algorithm”, Electric Power System Research, 2010, 80, (7), pp. 878–885.

[118] A. Bhattacharya, P. K. Chattopadhyay, “Application of biogeography-based optimization to solve different optimal power flow problems”, IET Generation Transmission Distribution 2011, vol. 5, pp. 70-80.

[119] S. Surender Reddy, P.R. Bijwe, A. R. Abhyankar, “Faster evolutionary algorithm based optimal power flow using incremental variables”, Electric Power and Energy Systems, 2014, 54, pp. 198–210.

[120] P. E. Yumbla Onate, J. M. Ramirez, C. A. Coello Coello, “Optimal power flow subject to security constraints solved with a particle swarm optimizer”, IEEE Trans. Power Syst., 2008, 23, (1), pp. 33–40.

[121] W. F. Tinney, C. E. Hart, “Power flow solution by Newton’s method” IEEE Trans. Power Appar. Syst., 1967, PAS-86, (11), pp. 1449–1460.

[122] O. Alsac, B. Stott, ‘Optimal load flow with steady-state security’, IEEE Transaction on Power Apparatus and Systems, 1974, PAS-93, (3), pp. 745–751.

[123] W. Ongsakul, T. Tantimaporn, “Optimal powers flow by improved evolutionary programming”, Electr. Power Comp. Syst., 2006, 34, (1), pp. 79–95.

[124] A. G. Bakirtzis, P. N. Biskas, C. E. Zoumas, V. Petridis, “Optimal power flow by enhanced genetic algorithm”, IEEE Trans. Power Syst., 2002, 17, (2), pp. 229–236.

[125] M. Varadarajan, K. S. Swarup, “Solving multi-objective optimal power flow using differential evolution”, IET Generation Transmission Distribution 2008, vol. 2, pp. 720-730.

[126] R. Yokoyama, S. H. Bae, T. Morita, H. Sasaki, “Multi-objective Optimal generation dispatch based on probability security criteria”, IEEE Transaction on Power Systems, vol. 3, no. 1 (1988) 317-324.

[127] C. Dai, W. Chen, Y. Zhu, X. Zhang, “Seeker optimization algorithm for optimal reactive power dispatch”, IEEE Transaction on Power Systems, 2009, 24(3), pp.1218–1231.

[128] S. Duman, Y. Sonmez, U. Guvenc and N. Yorukeren, “Optimal reactive power dispatch using a gravitational search algorithm”, IET Gen Trans. Distrib 2012, 6(6), pp. 563–576.

[129] M. A. Abido, “Optimal power flow using particle swarm optimization”, Int. J. Electric Power and Energy Systems, 2002, 24, (7), pp. 563–571.

[130] The IEEE 57-bus test system [online], available at
http://www.ee.washington.edu/research/pstca/pf57/pg_tca57bus.

[131] The IEEE 118-bus test system [online], available at
http://www.ee.washington.edu/research/pstca/pf118/ pg_ tca118bus.htm

[132] http://motor.ece.iit.edu/data

CHAPTER-11

Appendices

Chapter: 2
Table A.1: Data for 2 area system

Generator ij	a_{ij} \$/h	b_{ij} \$/MWh	c_{ij} \$/(MW)	P_{ij}^{min} MW	P_{ij}^{max} MW	Prohibited zones MW
$G_{1,1}$	550	8.10	0.00028	100	500	[210 240] [350 380]
$G_{1,2}$	350	7.50	0.00056	50	200	[90 110] [140 160]
$G_{1,3}$	310	8.10	0.00056	50	150	[80 90] [110 120]
$G_{2,1}$	240	7.74	0.00324	80	300	[150 170] [210 240]
$G_{2,2}$	200	8.00	0.00254	50	200	[90 110] [140 150]
$G_{2,3}$	126	8.60	0.00284	50	120	[75 85] [100 105]

The transmission loss formula coefficients of two-area system are:

$$B_1 = \begin{bmatrix} 17 & 12 & 7 \\ 12 & 14 & 9 \\ 7 & 9 & 31 \end{bmatrix} X10^{-6}$$

$$B_{01} = \begin{bmatrix} -0.3908 & -0.1297 & 0.7047 \end{bmatrix} X10^{-3}$$

$$B_{001} = 0.045$$

$$B_2 = \begin{bmatrix} 24 & -6 & -8 \\ -6 & 129 & -2 \\ -8 & -2 & 150 \end{bmatrix} X10^{-6}$$

$$B_{02}= \begin{bmatrix} 0.0591 & 0.2161 & -0.6635 \end{bmatrix} X10^{-3}$$

$B_{002} = 0.056$

Table A.2: The transmission loss formula coefficients of three-area system are:

$$B_1 = \begin{bmatrix} 8.70 & 0.43 & -4.61 & 0.36 \\ 0.43 & 8.30 & -0.97 & 0.22 \\ -4.61 & -0.97 & 9.00 & -2.00 \\ 0.36 & 0.22 & -2.00 & 5.30 \end{bmatrix} X10^{-5}$$

$$B_{01}= \begin{bmatrix} -0.3908 & -0.1297 & 0.7047 & 0.0591 \end{bmatrix} X10^{-3}$$

$B_{001} = 0.056$

$$B_2 = \begin{bmatrix} 8.60 & -0.80 & 0.37 \\ -0.80 & 9.08 & -4.90 \\ 0.37 & -4.90 & 8.24 \end{bmatrix} X10^{-5}$$

$$B_{02}= \begin{bmatrix} 0.2161 & -0.6635 & 0.5034 \end{bmatrix} X10^{-3}$$

$B_{002} = 0.045$

$$B_3 = \begin{bmatrix} 1.20 & -0.96 & 0.56 \\ -0.96 & 4.93 & -0.30 \\ 0.56 & -0.30 & 5.99 \end{bmatrix} X10^{-5}$$

$$B_{03}= \begin{bmatrix} -0.3216 & 0.4635 & 0.3503 \end{bmatrix} X10^{-3}$$

$B_{003} = 0.055$

Chapter:3

Table A.3: Data for test system 1

Unit	P^{min} MW	P^{max} MW	*a* $/h	*b* $/MWh	*c* $/ MW^2h	*d* $/h	*e* rad/MW	*UR* MW/h	*DR* MW/h
1	10	75	25	2.0	0.0080	100	0.042	30	30
2	20	125	60	1.8	0.0030	140	0.040	30	30
3	30	175	100	2.1	0.0012	160	0.038	40	40
4	40	250	120	2.0	0.0010	180	0.037	50	50
5	50	300	40	1.8	0.0015	200	0.035	50	50

Table A.4: Load Demand for 24h for test system 1

Hour	Load (MW)	Hour	Load (MW)	Hour	Load (MW)
1	410	9	690	17	558
2	435	10	704	18	608
3	475	11	720	19	654
4	530	12	740	20	704
5	558	13	704	21	680
6	608	14	690	22	605
7	626	15	654	23	527
8	654	16	580	24	463

The transmission loss formula coefficients for test system 1 are:

$$\begin{bmatrix} 0.000049 & 0.000014 & 0.000015 & 0.000015 & 0.000020 \\ 0.000014 & 0.000045 & 0.000016 & 0.000020 & 0.000018 \\ 0.000015 & 0.000016 & 0.000039 & 0.000010 & 0.000012 \\ 0.000015 & 0.000020 & 0.000010 & 0.000040 & 0.000014 \\ 0.000020 & 0.000018 & 0.000012 & 0.000014 & 0.000035 \end{bmatrix}$$

Table.A.5: Data for test system 2

Unit	P^{min} MW	P^{max} MW	*a* $/h	*b* $/MWh	*c* $/ MW^2h	*d* $/h	*e* rad/MW	*UR* MW/h	*DR* MW/h
1	150	470	786.7988	38.53973	0.15241	450	0.041	100	100
2	135	470	451.3251	46.15916	0.10587	600	0.036	100	100
3	73	340	1049.9977	40.39655	0.02803	320	0.028	100	100
4	60	300	1243.5311	38.30553	0.03546	260	0.052	80	80
5	73	243	1658.5696	36.32782	0.02111	280	0.063	60	60
6	57	160	1356.6592	38.27041	0.01799	310	0.048	50	50
7	20	130	1450.7045	36.51045	0.01211	300	0.086	30	30
8	47	120	1450.7045	36.51045	0.01211	340	0.082	30	30
9	20	80	1455.6056	39.58042	0.10908	270	0.098	30	30
10	10	55	1469.4026	40.54074	0.12951	380	0.094	30	30

Table.A.6: Load Demand for 24h for test system 2

Hour	Load (MW)	Hour	Load (MW)	Hour	Load (MW)
1	1036	9	1924	17	1480
2	1110	10	2072	18	1628
3	1258	11	2106	19	1776
4	1406	12	2150	20	1972
5	1480	13	2072	21	1924
6	1628	14	1924	22	1628
7	1702	15	1776	23	1332
8	1776	16	1554	24	1184

The transmission loss formula coefficients for test system 2 are:

$$B = \begin{bmatrix} 0.000049 & 0.000014 & 0.000015 & 0.000015 & 0.000016 & 0.000017 & 0.000017 & 0.000018 & 0.000019 & 0.000020 \\ 0.000014 & 0.000045 & 0.000016 & 0.000016 & 0.000017 & 0.000015 & 0.000015 & 0.000016 & 0.000018 & 0.000018 \\ 0.000015 & 0.000016 & 0.000039 & 0.000010 & 0.000012 & 0.000012 & 0.000014 & 0.000014 & 0.000016 & 0.000016 \\ 0.000015 & 0.000016 & 0.000010 & 0.000040 & 0.000014 & 0.000010 & 0.000011 & 0.000012 & 0.000014 & 0.000015 \\ 0.000016 & 0.000017 & 0.000012 & 0.000014 & 0.000035 & 0.000011 & 0.000013 & 0.000013 & 0.000015 & 0.000016 \\ 0.000017 & 0.000015 & 0.000012 & 0.000010 & 0.000011 & 0.000036 & 0.000012 & 0.000012 & 0.000014 & 0.000015 \\ 0.000017 & 0.000015 & 0.000014 & 0.000011 & 0.000013 & 0.000012 & 0.000038 & 0.000016 & 0.000016 & 0.000018 \\ 0.000018 & 0.000016 & 0.000014 & 0.000012 & 0.000013 & 0.000012 & 0.000016 & 0.000040 & 0.000015 & 0.000016 \\ 0.000019 & 0.000018 & 0.000016 & 0.000014 & 0.000015 & 0.000014 & 0.000016 & 0.000015 & 0.000042 & 0.000019 \\ 0.000020 & 0.000018 & 0.000016 & 0.000015 & 0.000016 & 0.000015 & 0.000018 & 0.000016 & 0.000019 & 0.000044 \end{bmatrix}$$

Chapter: 4 :

4.1. Data of test system 1

(a) Conventional thermal generators

$$C_{t1}(P_1) = 25 + 2P_1 + 0.008P_1^2 + \left|100\sin\left\{0.042\left(P_1^{\min} - P_1\right)\right\}\right| \ \$ \qquad 0 \le P_1 \le 150\,\mathbf{MW}$$

$$C_{t2}(P_2) = 60 + 1.8P_2 + 0.003P_2^2 + \left|140\sin\left\{0.04\left(P_2^{\min} - P_2\right)\right\}\right| \ \$ \qquad 20 \le P_2 \le 125\,\mathbf{MW}$$

$$C_{t3}(P_3) = 100 + 2.1P_3 + 0.0012P_3^2 + \left|160\sin\left\{0.038\left(P_3^{\min} - P_3\right)\right\}\right| \ \$ \qquad 30 \le P_2 \le 175\,\mathbf{MW}$$

$$C_{t4}(P_4) = 120 + 2P_4 + 0.001P_4^2 + \left|180\sin\left\{0.037\left(P_4^{\min} - P_4\right)\right\}\right| \ \$ \qquad 40 \le P_2 \le 250\,\mathbf{MW}$$

Table A.7: Prohibited zones of Conventional Thermal generator for test system 1

Unit	Zone 1, MW	Zone 2, MW
1	[20, 30]	[50, 60]
2	[40, 50]	[90, 100]
3	[50, 70]	[120, 140]
4	[70, 90]	[180, 200]

(b) Cogeneration units

$$C_{c5}(P_5, H_5) = 2650 + 14.5P_5 + 0.0345P_5^2 + 4.2H_5 + 0.03H_5^2 + 0.031P_5H_5 \ \$$

$$C_{c6}(P_6, H_6) = 1250 + 36P_6 + 0.0435P_6^2 + 0.6H_6 + 0.027H_6^2 + 0.011P_6H_6 \ \$$

(c) Heat-only unit

$$C_{h7}(H_7) = 950 + 2.0109H_7 + 0.038H_7^2 \ \$ \qquad 0 \le H_7 \le 60 \ \text{MWth}$$

Network loss coefficients: These are given below.

$$B = \begin{bmatrix} 49 & 14 & 15 & 15 & 20 & 25 \\ 14 & 45 & 16 & 20 & 18 & 19 \\ 15 & 16 & 39 & 10 & 12 & 15 \\ 15 & 20 & 10 & 40 & 14 & 11 \\ 20 & 18 & 12 & 14 & 35 & 17 \\ 25 & 19 & 15 & 11 & 17 & 39 \end{bmatrix} X10^{-6}$$

4.2. Data of test system 2

(a) Conventional thermal generators

$$C_{t1}(P_1) = 550 + 8.1P_1 + 0.000288P_1^2 + \left|300\sin\left\{0.035\left(P_1^{min} - P_1\right)\right\}\right| \ \$ \qquad 0 \le P_1 \le 680\,\mathbf{MW}$$

$$C_{t2}(P_2) = 309 + 8.1P_2 + 0.00056P_2^2 + \left|200\sin\left\{0.042\left(P_2^{min} - P_2\right)\right\}\right| \ \$ \qquad 0 \le P_2 \le 360\,\mathbf{MW}$$

$$C_{t3}(P_3) = 309 + 8.1P_3 + 0.00056P_3^2 + \left|200\sin\left\{0.042\left(P_3^{min} - P_3\right)\right\}\right| \ \$ \qquad 0 \le P_3 \le 360\,\mathbf{MW}$$

$$C_{t4}(P_4) = 240 + 7.74P_4 + 0.00324P_4^2 + \left|150\sin\left\{0.063\left(P_4^{min} - P_4\right)\right\}\right| \ \$ \qquad 60 \le P_4 \le 180\,\mathbf{MW}$$

$$C_{t5}(P_5) = 240 + 7.74P_5 + 0.00324P_5^2 + \left|150\sin\left\{0.063\left(P_5^{min} - P_5\right)\right\}\right| \ \$ \qquad 60 \le P_5 \le 180\,\mathbf{MW}$$

$$C_{t6}(P_6) = 240 + 7.74P_6 + 0.00324P_6^2 + \left|150\sin\left\{0.063\left(P_6^{min} - P_6\right)\right\}\right| \ \$ \qquad 60 \le P_6 \le 180\,\mathbf{MW}$$

$$C_{t7}(P_7) = 240 + 7.74P_7 + 0.00324P_7^2 + \left|150\sin\left\{0.063\left(P_7^{min} - P_7\right)\right\}\right| \ \$ \qquad 60 \le P_7 \le 180\,\mathbf{MW}$$

$$C_{t8}(P_8) = 240 + 7.74P_8 + 0.00324P_8^2 + \left|150\sin\left\{0.063\left(P_8^{min} - P_8\right)\right\}\right| \ \$ \qquad 60 \le P_8 \le 180\,\mathbf{MW}$$

$$C_{t9}(P_9) = 240 + 7.74P_9 + 0.00324P_9^2 + \left|150\sin\left\{0.063\left(P_9^{min} - P_9\right)\right\}\right| \ \$ \qquad 60 \le P_9 \le 180\,\mathbf{MW}$$

$$C_{t10}(P_{10}) = 126 + 8.6P_{10} + 0.00284P_{10}^2 + \left|100\sin\left\{0.084\left(P_{10}^{min} - P_{10}\right)\right\}\right| \ \$ \qquad 40 \le P_{10} \le 120\,\mathbf{MW}$$

$$C_{t11}(P_{11}) = 126 + 8.6P_{11} + 0.00284P_{11}^2 + \left|100\sin\left\{0.084\left(P_{11}^{min} - P_{11}\right)\right\}\right| \ \$ \qquad 40 \le P_{11} \le 120\,\mathbf{MW}$$

$$C_{t12}(P_{12}) = 126 + 8.6P_{12} + 0.00284P_{12}^2 + \left|100\sin\left\{0.084\left(P_{12}^{min} - P_{12}\right)\right\}\right| \ \$ \qquad 55 \le P_{12} \le 120\,\mathbf{MW}$$

$$C_{t13}(P_{13}) = 126 + 8.6P_{13} + 0.00284P_{13}^2 + \left|100\sin\left\{0.084\left(P_{13}^{min} - P_{13}\right)\right\}\right| \ \$ \qquad 55 \le P_{13} \le 120\,\mathbf{MW}$$

Table A.8: Prohibited zones of Conventional thermal generators for test system 2

Unit	Zone 1, MW	Zone 2, MW	Zone 3, MW
1	[180, 200]	[260, 335]	[390, 420]
2	[30, 40]	[180, 220]	[305, 335]
3	[30, 45]	[180, 225]	[305, 335]
10	[45, 55]	[65, 75]	-
11	[45, 55]	[65, 75]	-

(b) Cogeneration units

$$C_{c14}(P_{14}, H_{14}) = 2650 + 14.5P_{14} + 0.0345P_{14}^2 + 4.2H_{14} + 0.03H_{14}^2 + 0.031P_{14}H_{14} \ \$$$

$$C_{c15}(P_{15}, H_{15}) = 1250 + 36P_{15} + 0.0435P_{15}^2 + 0.6H_{15} + 0.027H_{15}^2 + 0.011P_{15}H_{15} \ \$$$

$$C_{c16}(P_{16}, H_{16}) = 2650 + 14.5P_{16} + 0.0345P_{16}^2 + 4.2H_{16} + 0.03H_{16}^2 + 0.031P_{16}H_{16} \ \$$$

$$C_{c17}(P_{17}, H_{17}) = 1250 + 36P_{17} + 0.0435P_{17}^2 + 0.6H_{17} + 0.027H_{17}^2 + 0.011P_{17}H_{17} \ \$$$

$$C_{c18}(P_{18}, H_{18}) = 2650 + 34.5P_{18} + 0.1035P_{18}^2 + 2.203H_{18} + 0.025H_{18}^2 + 0.051P_{18}H_{18} \ \$$$

$$C_{c19}(P_{19}, H_{19}) = 1565 + 20P_{19} + 0.072P_{19}^2 + 2.34H_{19} + 0.02H_{19}^2 + 0.04P_{19}H_{19} \ \$$$

(c) Heat-only units

$$C_{h20}(H_{20}) = 950 + 2.0109H_{20} + 0.038H_{20}^2 \ \$ \qquad 0 \le H_{20} \le 60 \text{ MWth}$$

$$C_{h21}(H_{21}) = 950 + 2.0109H_{21} + 0.038H_{21}^2 \ \$ \qquad 0 \le H_{21} \le 60 \text{ MWth}$$

$$C_{h22}(H_{22}) = 480 + 3.0651H_{22} + 0.052H_{22}^2 \ \$ \qquad 0 \le H_{22} \le 120 \text{ MWth}$$

$$C_{h23}(H_{23}) = 480 + 3.0651H_{23} + 0.052H_{23}^2 \ \$ \qquad 0 \le H_{23} \le 120 \text{ MWth}$$

$$C_{h24}(H_{24}) = 950 + 2.0109H_{24} + 0.038H_{24}^2 \ \$ \qquad 0 \le H_{24} \le 2695.2 \text{ MWth}$$

4.3. Operation limits:

The heat-power feasible regions of the cogeneration units are illustrated in Fig. 1, Fig. 2, Fig.3 and Fig. 4.

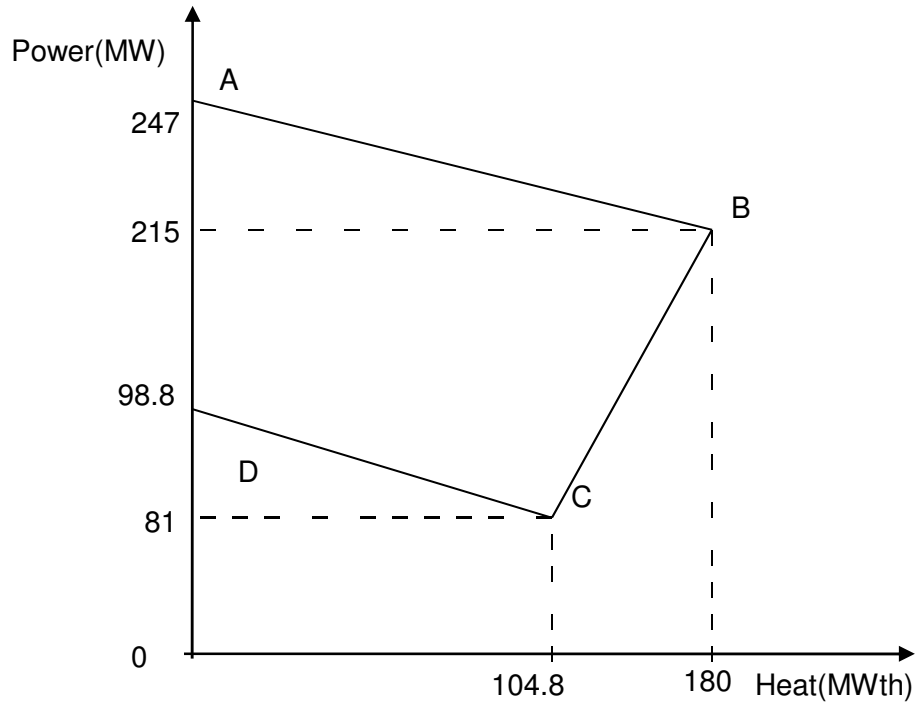

Fig. 1. Heat-Power Feasible Operation Region for the cogeneration unit 1 of test system 1 and cogeneration unit 1 and unit 3 of test system 2

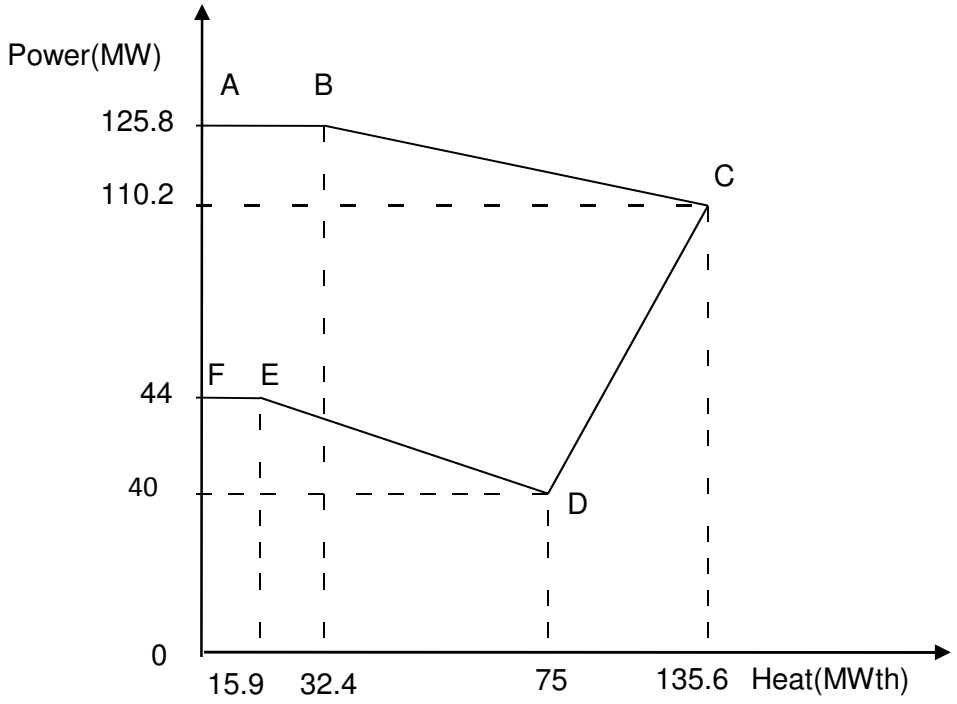

Fig. 2. Heat-Power Feasible Operation Region for the cogeneration unit 2 of test system 1 and cogeneration unit 2 and cogeneration unit 4 of test system 2

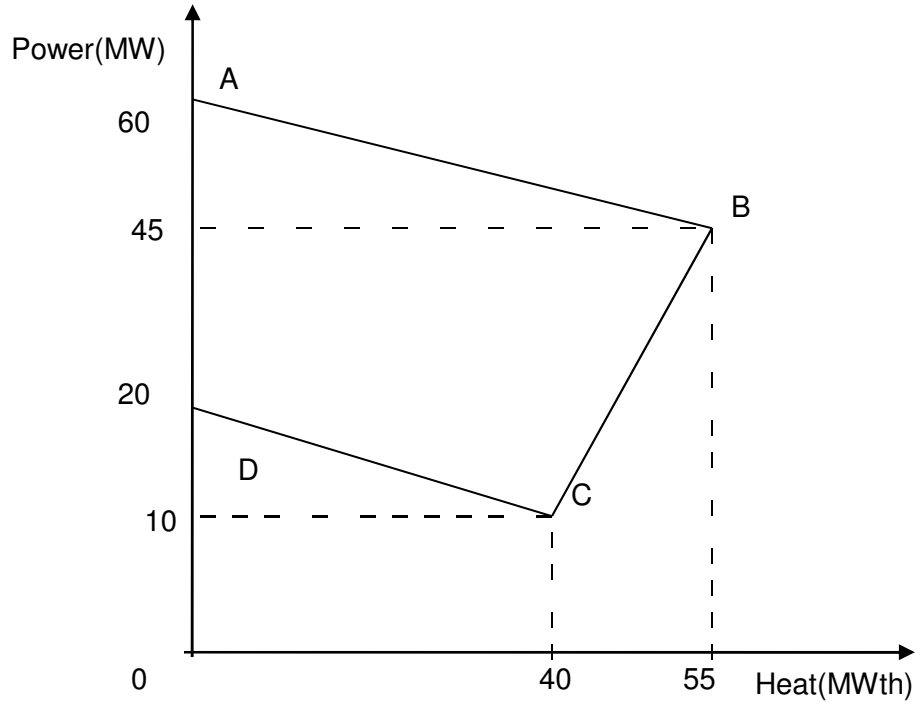

Fig. 3. Heat-Power Feasible Operation Region for the Cogeneration unit 5 of test system 2

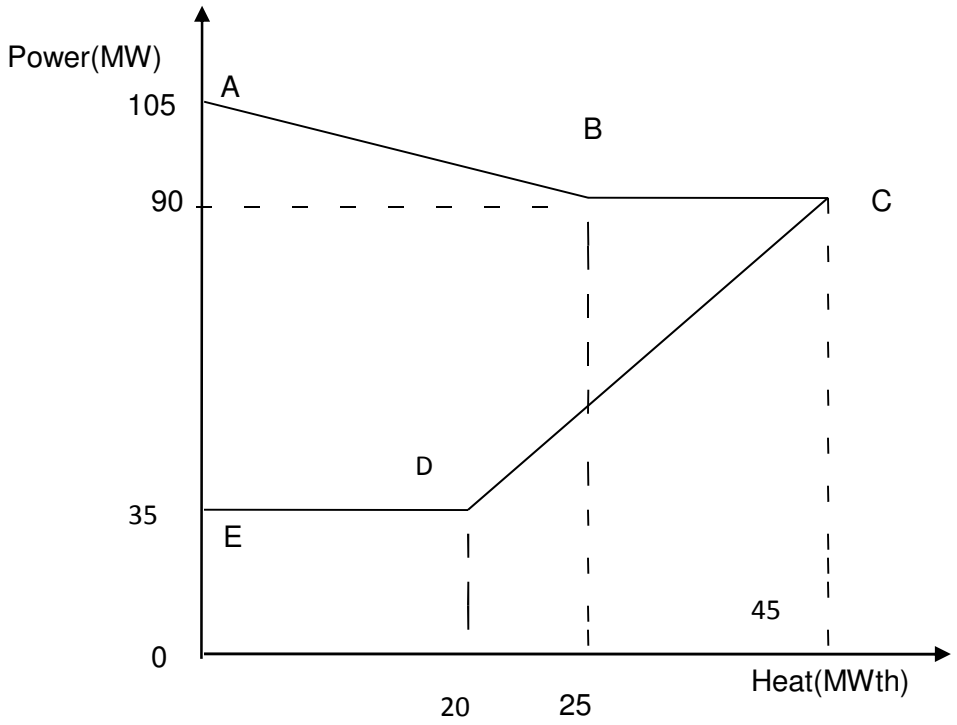

Fig. 4. Heat-Power Feasible Operation Region for the Cogeneration unit 6 of test system 2

Chapter:5 :

Table A-9: Hydro system data of test system 1

Unit	a_{0h}	a_{1h}	a_{2h}	W_h	P_h^{min}	P_h^{max}
	MCF/h	MCF/MWh	MCF/(MW)2h	MCF	MW	MW
1	1.980	0.306	0.000216	2500	0	400
2	0.936	0.612	0.000360	2100	0	300

Table A-10: Thermal generator data of test system 1

Unit	P_s^{min}	P_s^{max}	a_s	b_s	c_s	d_s	e_s
	MW	MW	$/h	$/MWh	$/(MW)2h	$/h	1/MW
1	50	300	25	3.2	0.0025	0	0
2	50	700	30	3.4	0.0008	0	0

Table A-11: Load demands of test system 1

Sub-interval	Duration (hr)	PD (MW)
1	8	900
2	8	1200
3	8	1100

The transmission loss formula coefficients of test system 1 are

$$B = \begin{bmatrix} 0.000015 & 0.000140 & 0.000010 & 0.000015 \\ 0.000010 & 0.000060 & 0.000010 & 0.000013 \\ 0.000015 & 0.000010 & 0.000068 & 0.000065 \\ 0.000015 & 0.000013 & 0.000065 & 0.000070 \end{bmatrix} \text{ per MW}$$

Table A-12: Hydro system data of test system 2

Unit	a_{0h} acre-ft/h	a_{1h} acre-ft/MWh	a_{2h} acre-ft/(MW)2h	W_h acre-ft	P_h^{min} MW	P_h^{max} MW
1	260	8.5	0.00986	125000	0	250
2	250	9.8	0.01140	286000	0	500

Table A-13: Thermal generator data of test system 2

Unit	P_s^{min} MW	P_s^{max} MW	a_s $/h	b_s $/MWh	c_s $/(MW)2h	d_s $/h	e_s rad/MW
3	20	125	10	3.25	0.0083	12	0.0450
4	30	175	10	2.00	0.0037	18	0.0370
5	40	250	20	1.75	0.0175	16	0.0380
6	50	300	20	1.00	0.0625	14	0.0400

Table A-14: Load demands of test system 2

Sub-interval	Duration (hr)	PD (MW)
1	12	900
2	12	1100
3	12	1000
4	12	1200

The transmission loss formula coefficients are of test system 2

$$B = \begin{bmatrix} 0.000049 & 0.000014 & 0.000015 & 0.000015 & 0.000020 & 0.000017 \\ 0.000014 & 0.000045 & 0.000016 & 0.000020 & 0.000018 & 0.000015 \\ 0.000015 & 0.000016 & 0.000039 & 0.000010 & 0.000012 & 0.000012 \\ 0.000015 & 0.000020 & 0.000010 & 0.000040 & 0.000014 & 0.000010 \\ 0.000020 & 0.000018 & 0.000012 & 0.000014 & 0.000035 & 0.000011 \\ 0.000017 & 0.000015 & 0.000012 & 0.000010 & 0.000011 & 0.000036 \end{bmatrix} \text{ per MW}$$

Chapter:6 :

Table A-15: **Optimal Hydro Discharge** ($\times 10^4 m^3$) **for case 1 of Test System 1 of variable head hydrothermal system**

Hour	Q_{h1}	Q_{h2}	Q_{h3}	Q_{h4}
1	8.7861	6.0009	30.0000	6.0000
2	8.6477	6.0001	18.5747	6.0000
3	8.5682	6.0000	29.9998	6.0000
4	8.3775	6.0006	17.3534	6.0008
5	8.1550	6.0000	15.4229	6.0005
6	8.0533	6.0030	15.9130	7.9993
7	8.1591	6.0910	15.9792	11.1179
8	8.4589	6.8847	16.5977	13.6690
9	8.6193	7.4527	16.4652	15.3635
10	8.7715	7.6903	16.5940	16.1257
11	8.5801	7.7683	17.1467	15.7670
12	8.6525	8.1049	16.8463	16.5977
13	8.5011	8.2039	17.4470	16.4653
14	8.3269	8.3350	17.8223	16.5934
15	8.2464	8.4235	18.7109	17.1544
16	8.0697	8.7110	18.4832	16.8390
17	8.0004	9.0106	16.9627	17.4464
18	7.8467	9.4610	15.9095	17.8224
19	7.8246	10.1045	14.5644	18.8539
20	7.7368	10.6701	13.8283	19.6055
21	7.5925	11.2530	11.0169	19.9997
22	7.3682	11.7971	11.5735	19.9999
23	6.9536	12.6091	12.0326	19.9999
24	6.7040	13.4245	12.5674	19.9998

Table A-16: Optimal Hydrothermal generation (MW) for case 1 of test system 1 of variable head hydrothermal system

Hour	P_{h1}	P_{h2}	P_{h3}	P_{h4}	P_s
1	79.7973	49.0061	0	131.8801	1109.32
2	79.3927	50.1639	43.5292	129.0270	1087.89
3	79.0387	51.2957	0	125.7437	1103.92
4	77.7373	52.9380	37.4242	121.6365	1000.26
5	75.9674	54.4995	42.2628	115.8283	1001.44
6	74.6619	55.5248	42.0011	163.8960	1073.92
7	74.9610	56.6535	42.7802	209.7731	1265.83
8	76.6787	62.1650	41.6644	252.8746	1566.62
9	77.7838	65.9683	41.8104	271.8340	1782.60
10	79.1114	67.7564	40.9661	278.4111	1853.75
11	78.7489	68.9033	38.9557	275.1930	1768.19
12	80.1994	71.5905	39.5975	282.2694	1836.34
13	79.6781	72.1369	38.3010	281.2003	1758.68
14	79.2573	72.8195	38.1722	282.2342	1727.52
15	79.5884	73.6734	35.5391	286.6439	1654.55
16	78.9796	75.6289	36.7765	284.1818	1594.43
17	78.8516	76.9618	41.8592	288.8606	1643.46
18	77.9593	78.3512	45.1334	291.6388	1646.92
19	77.8291	79.6915	48.4354	298.8079	1735.23
20	77.0919	80.4924	50.2710	303.4720	1768.67
21	75.8005	81.3147	51.4605	304.7025	1726.72
22	74.1001	81.9619	53.9109	301.5554	1608.47
23	71.1238	82.8437	56.0420	297.2275	1342.77
24	69.4655	81.8843	57.7491	291.3201	1089.58

Table A-17: Optimal Hydro Discharge ($\times 10^4 m^3$) for case 2 of test system 1 of variable head hydrothermal system

Hour	Q_{h1}	Q_{h2}	Q_{h3}	Q_{h4}
1	10.1845	6.1121	20.5536	6.3438
2	9.3545	6.0000	29.9857	6.0059
3	5.0934	6.0672	18.8188	6.0081
4	12.3025	6.9922	19.7814	6.0011
5	9.4396	6.9832	15.2970	6.3376
6	7.8835	6.3622	18.4255	11.1545
7	10.2721	8.2105	18.0212	8.7499
8	6.7694	6.0283	17.9212	9.3215
9	6.6014	6.9949	16.6465	15.9994
10	9.8394	6.6298	14.1732	14.6373
11	5.8365	8.0881	17.9684	19.8695
12	6.2467	6.7252	18.3894	15.9965
13	10.4311	6.0065	16.4035	15.9976
14	6.7118	6.0342	19.8262	13.0358
15	5.2117	8.9019	14.7661	19.6512
16	5.8669	8.0785	18.5218	18.0045
17	10.3436	13.0473	15.8221	18.0241
18	9.0289	8.2601	15.6486	18.1861
19	6.8068	10.6257	18.4059	18.1376
20	5.0351	13.1212	10.7805	18.6221
21	7.2673	9.9088	11.9574	18.0174
22	7.0480	12.8178	11.9622	20.0000
23	7.9655	10.0050	10.1140	19.8378
24	13.2600	13.2228	11.6386	19.6248

Table A-18: Optimal Hydrothermal generation (MW) for case 2 of test system 1 of variable head hydrothermal system

Hour	P_{h1}	P_{h2}	P_{h3}	P_{h4}	P_s
1	86.8344	49.7921	42.4872	136.4915	1054.39
2	82.7927	50.0996	0	128.7959	1128.31
3	53.2023	51.7131	38.2060	125.5285	1091.35
4	95.3572	59.6889	32.3296	121.2998	981.32
5	82.2469	60.718	45.8186	119.8371	981.38
6	72.3219	57.0068	36.5382	189.8853	1054.25
7	84.3272	69.3217	39.5418	180.8054	1276.01
8	63.8671	53.8113	40.4187	196.2406	1645.66
9	63.4079	61.0171	43.8752	273.675	1798.02
10	83.8010	59.0764	48.8933	261.1712	1867.06
11	58.8915	69.7213	40.9075	304.3079	1756.17
12	63.6159	61.3895	37.7617	274.8044	1872.42
13	90.3650	56.9064	44.1043	276.5894	1762.03
14	68.1055	58.0340	32.0219	249.5939	1792.24
15	56.4505	78.0365	46.5805	292.2578	1603.17
17	93.8183	96.3354	45.1644	292.7708	1601.91
18	86.3257	71.3305	44.6121	292.334	1645.39
19	70.6874	82.4647	36.9713	293.5957	1756.28
20	55.3803	89.5719	48.3725	293.5926	1793.08
21	74.3523	73.9104	52.4342	289.3438	1749.96
22	72.6529	84.7098	53.7410	299.7932	1609.10
23	79.4951	71.3102	53.2242	294.2187	1351.75
24	104.9608	81.7733	57.2461	291.4408	1054.58

Table A-19: Optimal Hydro Discharge ($\times 10^4 m^3$) of test system 2 of variable head hydrothermal system

Hour	Q_{h1}	Q_{h2}	Q_{h3}	Q_{h4}
1	5.0000	8.1694	29.9825	10.6846
2	11.8249	6.0349	20.3834	8.1109
3	8.2756	9.3968	29.9993	6.0699
4	10.6764	7.1839	17.4356	6.5270
5	10.7913	6.1217	14.9166	7.0655
6	7.5122	6.0114	19.9168	12.2241
7	11.8929	7.1014	16.4236	14.2319
8	8.0364	8.9342	19.9639	6.3860
9	5.0000	7.0265	17.2913	14.8253
10	5.2012	6.0000	19.6801	13.3341
11	9.0382	7.4124	16.8647	18.8811
12	7.1895	6.0830	16.7021	17.6400
13	10.7560	8.4874	17.0601	18.0055
14	9.6444	9.6666	16.3546	18.8809
15	7.5333	10.1478	14.5476	16.8217
16	12.2331	9.0725	12.3182	19.4624
17	5.0001	9.8397	14.7639	16.0024
18	6.9996	10.8825	13.7793	20.0000
19	12.3816	14.8071	14.5850	20.0000
20	5.7002	9.2668	12.3534	14.4891
21	5.0013	6.0008	21.3704	15.8796
22	5.0078	9.1880	11.7756	12.9617
23	5.0002	6.0045	15.2021	13.6869
24	9.3038	13.1606	12.9722	19.9519

Table A-20: Optimal Hydrothermal generation (MW) of test system 2 of variable head hydrothermal system

Hour	P_{h1}	P_{h2}	P_{h3}	P_{h4}	P_{s1}	P_{s2}	P_{s3}
1	52.5001	62.9911	0	188.4124	20.0000	40.0470	409.0353
2	94.9645	49.1472	36.0943	151.4483	20.0001	294.7080	139.9935
3	77.4693	70.7940	0	120.2516	174.9999	40.0626	229.7881
4	89.6264	57.8274	34.8294	121.7495	174.9999	40.0144	140.0427
5	88.6817	51.7208	43.1194	121.7213	20.0713	209.8746	139.7717
6	69.9013	51.9834	27.7926	202.2525	20.0027	294.7478	139.7384
7	90.0410	59.9969	42.2954	229.2022	102.8131	294.9635	140.0704
8	71.5381	70.3084	31.2740	155.4249	175.0000	294.7975	229.5029
9	49.9772	57.7790	39.9087	261.0326	174.9942	294.7360	229.4873
10	53.0657	51.3073	31.4504	247.0815	102.6427	294.7893	319.3190
11	81.4462	62.5231	40.4364	298.9633	20.0014	294.7375	319.3074
12	70.7288	54.3802	40.1454	287.9098	102.6722	294.7042	319.2878
13	91.5678	70.9632	38.1093	292.8062	20.0158	294.6822	319.3190
14	86.4941	77.0705	40.8922	298.1207	102.6981	294.7381	139.8472
15	74.3655	79.0482	45.0727	83.9845	102.6488	294.7742	139.7885
16	98.9002	72.9424	48.6283	302.6975	20.0008	298.7904	229.5013
17	54.2296	76.2645	49.2103	274.8114	174.9981	294.7637	139.6912
18	71.4333	79.2985	51.6777	304.2234	102.6951	294.7382	229.7389
19	100.2199	87.8464	53.8828	300.4273	102.7774	294.7563	140.0848
20	60.3478	63.3576	55.0328	254.1731	20.0000	294.7757	319.3300
21	54.2311	42.9424	34.5069	264.0216	175.0000	40.0042	319.0230
22	54.5201	64.1698	56.8181	236.6617	20.0000	294.7116	139.6709
23	54.7321	44.8122	58.1308	244.4422	20.0024	294.6434	139.7895
24	87.5753	80.9892	59.3598	292.6200	20.0004	125.0043	139.8794

Table A-21: Optimal Hydro Discharge ($\times 10^4 m^3$) of test system 3 of variable head hydrothermal system

Hour	Q_{h1}	Q_{h2}	Q_{h3}	Q_{h4}
1	10.5900	7.2207	19.4370	6.0254
2	12.0523	7.7304	20.2455	8.5457
3	5.0001	6.0184	17.4557	6.0000
4	6.4478	6.3207	22.6585	14.8061
5	5.0000	11.1350	29.9287	7.6698
6	7.6269	9.9408	17.6070	10.8973
7	9.2146	9.5815	13.9492	12.4732
8	7.1216	6.0000	21.4589	6.0044
9	14.7220	9.4742	16.3758	16.8335
10	8.7003	6.0001	18.0804	15.0361
11	7.6528	9.7120	10.0203	12.3636
12	5.4338	7.2947	17.1649	16.8305
13	11.5460	6.0053	30.0000	12.6269
14	10.5001	10.4945	15.3613	18.1704
15	6.9555	10.5776	10.0003	17.1377
16	5.0000	10.6310	21.2541	19.9868
17	10.5398	9.0909	11.1185	19.9873
18	5.1753	6.0028	19.1245	15.2733
19	5.0000	6.0000	18.4536	19.9871
20	5.8448	6.0003	10.0100	19.2115
21	6.0854	9.8456	11.2876	17.9333
22	8.5236	11.1071	10.4763	14.4865
23	14.9775	7.8296	13.2974	19.9983
24	5.2899	11.9870	13.3435	18.2195

Table A-22: Optimal Hydrothermal generation (MW) for test system 3 of variable head hydrothermal system

Hour	P_{h1}	P_{h2}	P_{h3}	P_{h4}	P_{s1}	P_{s2}	P_{s3}	P_{s4}	P_{s5}	P_{s6}	P_{s7}	P_{s8}	P_{s9}	P_{s10}
1	88.5676	57.2201	47.0843	132.2239	139.7462	199.5787	94.9554	119.9507	274.6901	139.7256	45.0047	134.5020	98.1889	178.5618
2	93.4214	60.8649	40.3432	161.1911	50.0010	350.6038	20.4259	20.0004	224.3871	239.4088	281.9108	85.1760	25.0195	127.2461
3	51.6806	49.7455	46.6711	123.3513	229.2817	124.0582	20.0000	119.8332	274.3626	89.8035	163.1392	134.3029	97.0795	176.6904
4	64.1960	53.5788	22.2002	210.9095	229.2333	124.6531	20.0501	119.5701	224.5807	139.8210	104.1674	134.6485	25.0013	177.3898
5	52.4810	81.8434	0	124.6475	140.1426	199.9715	95.3239	120.0332	175.6493	40.2031	222.6977	135.1454	103.3599	178.5014
6	72.9780	74.5900	39.6390	172.7592	228.4289	199.5966	20.1401	69.3630	174.6341	289.5033	222.8367	134.7805	25.0000	75.7505
7	82.2228	70.9868	47.2010	198.3559	318.9251	199.5684	94.6931	119.9201	174.6363	139.7735	45.0001	234.5971	97.7873	126.3325
8	69.0212	47.2262	22.2530	129.7342	229.4300	422.7929	95.4989	119.5967	273.9787	189.4554	102.8809	84.9181	97.3506	125.8631
9	98.8275	68.7802	42.6653	258.0113	319.3601	423.9171	20.3141	69.8048	25.0100	139.9045	163.4803	184.4494	98.0940	177.3813
10	78.0403	46.9347	38.9243	257.2106	319.8205	274.7959	95.2935	69.9514	224.6139	189.1829	163.6077	35.0485	159.9696	126.6063
11	72.4527	70.9485	47.7153	234.1379	319.2929	124.7317	94.8140	120.2192	224.5801	139.5221	341.3076	35.0054	98.2030	177.0697
12	56.8438	56.9932	45.9128	275.8907	230.0333	50.7516	20.1698	119.5267	379.1170	289.1176	104.2716	184.7861	159.9982	176.5876
13	94.8980	48.7840	0	242.2134	139.8324	274.4415	95.1403	69.8449	469.9935	89.6793	163.3926	84.8894	159.9984	176.8925
14	90.5802	75.8706	46.9657	293.9404	229.3965	274.4531	94.6048	20.0137	273.2281	139.8295	281.7942	35.0008	98.4802	75.8422
15	70.0608	75.2619	49.0555	286.2452	50.0001	424.0944	94.7114	129.9991	174.5623	40.0000	45.0649	284.1163	159.9975	126.8307
16	54.4620	74.4441	31.4282	298.2087	229.3469	199.3362	129.9942	70.0416	25.0000	188.9987	400.0086	134.4338	97.6077	126.6892
17	93.6431	65.3782	52.5869	295.1849	50.0097	273.9768	94.4723	69.8887	74.8041	289.2354	281.7366	184.3100	98.3925	126.3805
18	56.3901	45.1903	43.0147	270.9021	229.4754	423.8369	94.6491	69.8844	174.6510	189.6651	163.6530	184.4627	98.1968	76.0285
19	54.9594	45.1688	44.9555	305.7963	454.3275	274.4155	20.3014	69.5663	74.3859	239.4500	104.2637	184.7943	159.9911	37.6244
20	62.7075	45.8064	53.4968	290.7342	50.0001	274.6687	94.9396	119.5349	324.1705	90.0924	222.8150	134.4347	159.9665	126.6326
21	64.7903	69.7331	56.2031	284.4660	229.4512	349.3310	20.0004	20.0019	273.7897	139.5154	45.0000	184.7127	97.3568	75.6484
22	83.1783	74.6517	55.5310	250.3066	319.5464	349.2805	20.0039	119.7490	75.5053	40.0554	163.3451	84.7404	98.4503	125.6563
23	107.4231	57.0151	58.0351	295.2245	229.3402	199.7585	95.1532	119.6982	75.1793	140.3943	163.4162	84.8138	98.1993	126.3492
24	57.3775	76.5220	57.9827	282.6004	319.2834	274.0316	94.4750	69.6811	25.0002	139.5081	45.0000	134.7093	98.0004	125.8284

Chapter: 7: NA

Chapter: 8

Table A-23: Generator data of IEEE 30-bus system

Bus No.	P_G^{min} (MW)	P_G^{max} (MW)	a ($/h)	b ($/MWh)	c ($/MW2h	α (ton/h)	β (ton/MWh)	γ (ton/MW2h)	η (ton/h)	λ (1/MW)
1	50	200	0	2.00	0.00375	4.091E-2	-5.554E-4	6.490E-6	2.0E-4	2.857E-2
2	20	80	0	1.75	0.01750	2.543E-2	-6.047E-4	5.638E-6	5.0E-4	3.333E-2
5	15	50	0	1.00	0.06250	4.258E-2	-5.094E-4	4.586E-6	1.0E-6	8.000E-2
8	10	35	0	3.25	0.00834	5.326E-2	-3.550E-4	3.380E-6	2.0E-3	2.000E-2
11	10	30	0	3.00	0.02500	4.258E-2	-5.094E-4	4.586E-6	1.0E-6	8.000E-2
13	12	40	0	3.00	0.02500	6.131E-2	-5.555E-4	5.151E-6	1.0E-5	6.667E-2

Table A-24: Generator data of IEEE 57-bus system

Bus No.	P_G^{min} (MW)	P_G^{max} (MW)	a ($/h)	b ($/MWh)	c ($/MW^{2}h)	d ($/h)	e (rad/MW)	α (ton/h)	β (ton/MWh)	γ (ton/MW^{2}h)	η (ton/h)	λ (1/MW)
1	0	600	0	2.00	0.00375	18.00	0.0370	4.091E-2	-5.554E-4	6.490E-6	2.0E-4	2.857E-3
2	0	500	0	1.75	0.01750	16.00	0.0380	2.543E-2	-6.047E-4	5.638E-6	5.0E-4	3.333E-3
3	0	500	0	3.00	0.02500	13.50	0.0410	6.131E-2	-5.555E-4	5.151E-6	1.0E-5	6.667E-3
6	0	500	0	2.00	0.00375	18.00	0.0370	3.491E-2	-5.754E-4	6.390E-6	3.0E-4	2.657E-3
8	0	650	0	1.00	0.06250	14.00	0.0400	4.258E-2	-5.094E-4	4.586E-6	1.0E-6	8.000E-3
9	0	500	0	1.75	0.01950	15.00	0.0390	2.754E-2	-5.847E-4	5.238E-6	4.0E-4	2.875E-3
12	0	500	0	3.25	0.00834	12.00	0.0450	5.326E-2	-3.555E-4	3.380E-6	2.0E-3	2.000E-3